BIO-ELECTROCHEMICAL SYSTEMS FOR THE REMEDIATION OF METAL-ION EFFLUENTS

Jeet Varia

Thesis submitted in accordance with the regulations of Newcastle University for the degree of Doctorate of Philosophy

School of Chemical Engineering and Advanced Materials
University of Newcastle upon Tyne
August 2012

Abstract

The roots of this study stem from the applied sciences of microbiology and electrochemistry to form the exciting new field of bio-electrochemistry. Our aim here being the application of bioelectrochemical processes for social and environmental value in toxic metal ion remediation and recovery from the discharge of aqueous mine and industrial effluents. This within a broader vision of reducing the present burden caused by industrial and mining anthropogenic activity on the planet we inhabit. These processes we have explored within a green chemistry philosophy with the application of chemical engineering principles. Our aims being (i) to further the scientific state of art and (ii) conceptualize the feasible engineering of novel metal remediation strategies, with the lucrative application of bacterial cells as green "nanofactories" and recovery of metallic biogenic nanoparticles with application in the ever growing field of nanotechnology.

The proof of principle has been evaluated with a systematic study of Au^{3+}, Co^{2+} and Fe^{3+} metallic cationic species (C_o < 500 ppm) dissolved in acidic (pH < 3) aqueous electrolytes and their removal by microbiological (chapter 3) and bioelectrochemical (chapter 4) processes.

Electrochemical remediation as described by electronation charge transfer at an electrified interface for various potentials causes the electrodeposition of metal ions upon electrode surfaces and hence separation by phase transformation. Of note, base cations such Co^{2+} and Fe^{3+} co-deposited with the evolution of hydrogen gas could be applied as electron donors for chemolithotrophic bacteria as part of dissimilatory respiration.

Microbial biosorption of metal ions by means of ionized groups located on the outer membrane of the outer lipopolysaccharide leaf of gram negative bacteria, with some evidence of bio-reduction via dissimilatory and redox resistance mechanisms, with biogenic nanoparticles produced as a consequence.

Bio-electrochemistry formed by the collaboration of these two processes where electroactive bacteria such as that of the *Shewanella* genus are known to respire by the application of cathodic currents directly via bio-nanowires or indirectly using in-situ electron mediators or in-situ hydrogen production. The effects of bacteria on electronation thermodynamics were investigated in chapter 4 with observed positive shifts in reversible potentials (E_r) for $AuCl_3^-$ electrodeposition.

Declaration

I hereby declare that this thesis has been composed by myself and has not been accepted in any previous application for a degree. The work has been performed by me unless otherwise stated. All sources of information have been appropriately acknowledged by means of reference.

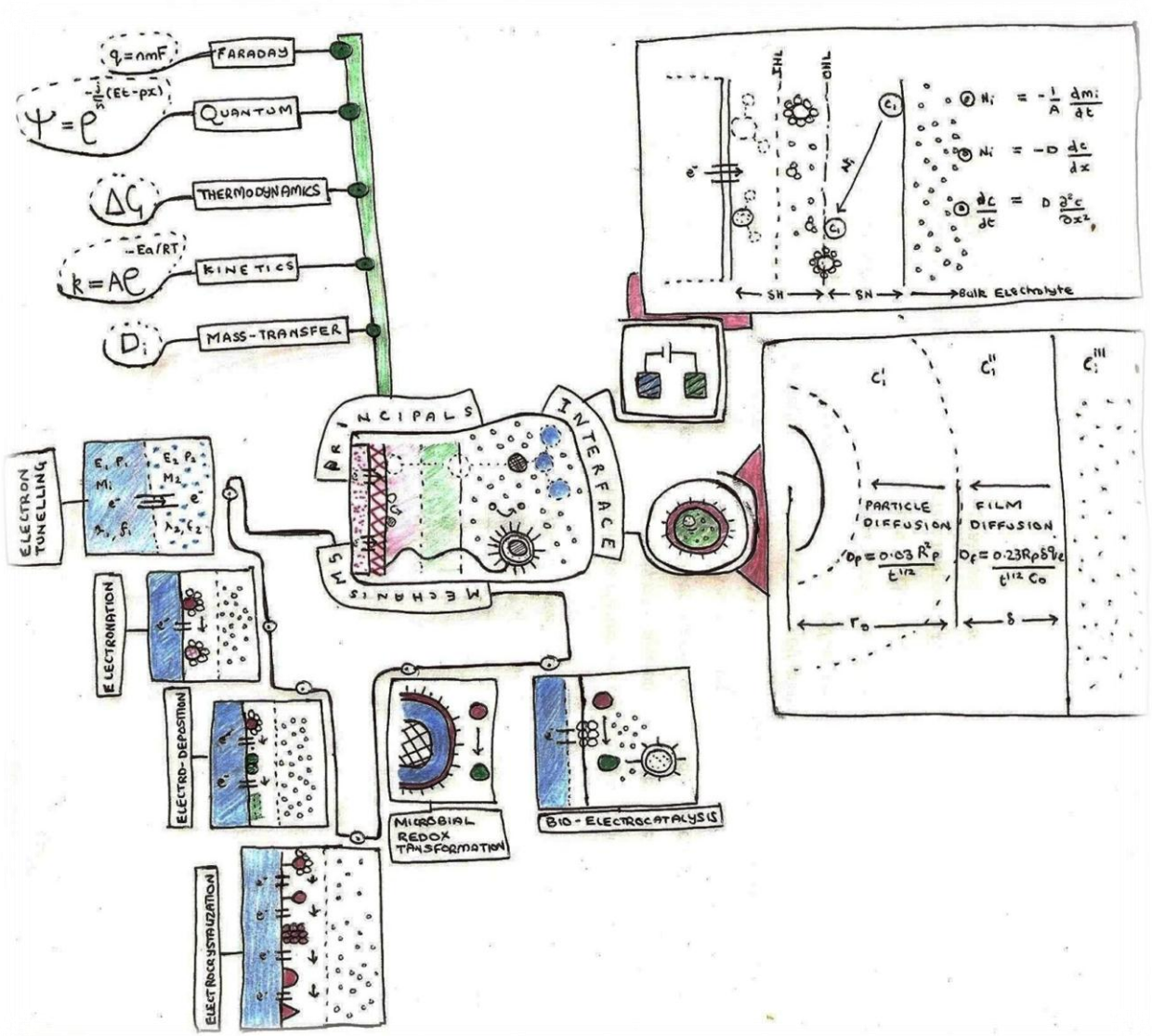
FARADAY
QUANTUM
THERMODYNAMICS
KINETICS
MASS-TRANSFER
PRINCIPALS
INTERFACE
MECHANISMS
ELECTRON TUNNELLING
ELECTRONATION
ELECTRO-DEPOSITION
MICROBIAL REDOX TRANSFORMATION
BIO-ELECTROCATALYSIS
ELECTROCRYSTALLIZATION
IHL
OHL
SH
SN
Bulk Electrolyte
PARTICLE DIFFUSION
FILM DIFFUSION

Dedicated to Ba, Mum and Dad

My living definitions of the altruistic principal…

"My desire [was] to escape from trade, which I thought vicious and selfish, and to enter into the service of science, which I imagined made its pursuers amiable and liberal…"

Michel Faraday, 1829

A Calling
{Zero five, zero four, twenty eleven}

I'm looking for a vocation
A place to baptize as my second home
A calling I must find
As without a goal...
I forget where and what I am
...and why and where it is I must go
The ego was long lost and the self has become lonesome...
The boats will leave soon but I fear not as I am of the enduring

In the streets
They shout in their thousands
"God is dead!!!!"
They scream of the herd
The rebellion of the collective adolescent
In journey to becoming mature chest beating adults

In truth not knowing what their words even mean
A metamorphosis manifesto will soon written
The deity of guilt will soon be forgiven

A new paradigm we seek
Us the fuzzy-logical minus one's now speak
Now we live our life on this earth for today
Not for the promised land of milk and honey…

Despise we, of those that speak
Of other worldly things
In this ambiguity
Meaning is what I find
...in a comrades beautiful biologically reflective human eyes

We look to embrace one and all
An exchange of energy
The giving of the spirit and soul
Enthalpy and entropy
Work and heat
The movement of knowledge and intelligence
A symbiotic relationship
Described by the laws of thermodynamic equilibrium
...and the dynamics of one's life's departure
From this safe sate
...of bliss-full serenity

We look for new sheltered walls
Where we can create and collaborate
In the modern cosmopolitan capitalist state

A place which make our whole being vibrate
To higher and higher
...and higher and human states
The freedom to be idle and intense
Where time no longer exists

As guardians we were born
A garden we must now protect and watch grow
Where we plant our magix bean stork seeds
The cycle as the season comes will once again repeat

In rich natural soils the roots will form
Remember that a little water
And lots and lots of love
Is all that is required from us
...the humble persons who protect the fragile soil

The gentle touch of a father hand
The love sent to all from the mother's womb
The call of the unconditional

ACKNOWLEDGEMENT

The author would like to express his deepest gratitude to the following people:

Professor Sudipta Roy
Professor Steve Bull
Professor Ian Head, Professor Tom Curtis
Professor Susana Silva Martinez

Tanja Fiegel

Rob Dixon, Brian E Grover, Paul Sterling, Stewart Latimer, Ian Banks, Ian Strong
Dr. Aslaf Zegue, Sani Yahaya, Dr. Sharon Velasquez Orta, Dr. Beate Christgen, Jane Davis, Vivian Thompson, Tracy Davie

David Hughes, Saskia Redman, Teresa Gooch, Megan Clancy
Bhavisha Balraj, Sanjiv Balraj, Kurti Varia

Rishub, Kilian and Maya

CONTENTS

NOMENCLATURE

A	*Pre-exponential factor*	
A	*Area of electrode*	cm^2
A	*First order nucleation rate per active site*	s^{-1}
b	*Langmuir equilibrium constant*	
C	*Concentration*	$mol\ L^{-1}$ *or PPM*
D	*Diffusion coefficient*	$cm^2\ s^{-1}$
D_f	*Diffusion coefficient*	$cm^2\ s^{-1}$
D_P	*Diffusion coefficient*	$cm^2\ s^{-1}$
E	*Potential*	V
E_a	*Activation energy*	J
E_{cell}	*Cell potentials*	V
F	*Faraday constant*	$col\ mol^{-1}$
G	*Gibbs energy*	J
h	*The Planck constant*	$J\ s$
H	*Enthalpy*	J
H_c	*Henry constant*	$N\ m\ mol^{-1}$
K	*Equilibrium constant*	-
k_1	*Lagergren first order rate constant*	
k_2	*Pseudo second order rate constant*	$g\ mg^{-1}\ min^{-1}$
k	*Potential dependent rate constant*	$cm\ s^{-1}$
k_B	*The Boltzmann constant*	
k_{id}	*Weber Morris rate constant*	
k_H	*Henry's constant*	
K_F	*Freundlich constant*	$mmol^{(1-1/n)}\ L^{(1/n)}$ *or* $mg^{(1-1/n)}\ L^{(1/n)} g^{-1}$
m	*Mols*	mol
M	*Molar Mass*	$g\ mol^{-1}$
M_r	*Mass of single bacterial cell*	g
M_c	*Mass of sorbent*	g
N	*Flux*	$mol\ m^{-2}\ s^{-1}$
n	*number if electrons transfer in reactions*	-

P	*Pressure*	$N\ m^{-2}$
p	*Momentum of a electron*	$N\ m^{-1}\ s^{-2}$
q	*Amount of metal adsorbed by cells*	$mmol\ g^{-1}$ *or* $mg\ g^{-1}$
q	*Heat*	J
q_{max}	*Maximum sorption capacity*	$mmol\ g^{-1}$ *or* $mg\ g^{-1}$
r	*Reaction order*	
r_d	*Radius of disc*	
r_0	*Radius of a spherical adsorbent*	
R	*Gas constant*	$J\ K^{-1}\ mol^{-1}$
R_u	*Resistance*	*ohm*
U	*Internal energy*	J
t	*Time*	*min or s*
S	*Entropy*	J
T	*Temperature*	K
V_b	*Volume of bacterial solution*	cm^3
V	*Volume of solution*	L
W	*Work*	J
z	*Distance between working electrode and reference electrode*	*cm*

Sub-scripts

°	*Standard conditions*
e	*Equilibrium*
$x = o$	*Electrode surface*
$x = \omega$	*Bulk conditions*

Greek

α	*Activity coefficient*		
η	*Over potential*		*V*
γ_i	*Activity coefficient*	-	
μ	*Chemical potential*		$J\ mol^{-1}$
ρ	*Density*		$g\ cm^{-3}$
κ	*Electrolyte conductivity*		$mS\ cm^{-1}$
$\Delta\Psi$	*Outer potential*		*V*
Φ	*Galvani potential*		*V*
λ	*Tafel slope*		*V*
β	*Symmetry factor*		

α	*Transfer coefficient*	
ω	*frequency*	s^{-1}
$\Delta\chi$	*Surface potential*	*V*

ABBREVIATIONS

ATP : Adenosine Triphosphate

DMR : Dissimilatory Metal Reduction

ETS : Electron Transport System

EMF : Electromotive Force

IHL : Inner Helmholtz Layer

LDS : Lipopolysaccharide Layer

KDO : Ketodeoxyoctonoate

OHL : Outer Helmholtz Layer

MRRT : Microbial Redox Resistance Transformation

PEM : Proton Motive Force

QET : Quantum Electron Tunnelling

RDS : Rate Determining Step

TEM : Transmission Electron Microscopy

TSA : Trypcase Soy Agar

TSB : Trypcase Soy Broth

SCE : Saturated Calomel Electrode

RDE : Rotating Disc Electrode

RDS : Rate Determining Step

WEEE : Waste Electrical and Electronic Equipment

LIST OF FIGURES

LIST OF TABLES

Chapter 1: Introduction to thesis

Chapter 1: Introduction to thesis

1.1 Aims and background of this investigation

Clean water is essential to humans and other life forms. Global problems with the significant increase in supply and demand of clean water would be anticipated in years to come from global warming (Nigel W 1999) and rising populations (Falkenmark 1997). At least 1 billion people do not have access to safe drinking water, according to the World Health Organisation (WHO 2004).

Global warming due to enhanced greenhouse effects from anthropological activity is likely to have significant effects on the hydrological cycle, with predicted higher evaporation and uneven global distribution of precipitation leading to major alterations in wet and dry seasons of semi-arid regions of Africa and Asia. These regions are characterised by dry climates and are regions of rapid economic and population growth. Predictions state that over the next 30 years these areas will account for nearly 80% of the world's population (Kelley 1988).

Metals have requirements for remediation from ground water, their presence in toxic concentrations in the environment due largely to the discharge of unregulated aqueous effluents characterised with low acidic pH (> 3 pH) (Banks, Younger et al. 1997) and metal ion concentrations less than 500 ppm from manufacturing waste streams (Johnson and Hallberg 2003) and mining activity (Brown, Barley et al. 2002).

The aims of this research are to develop strategies and further develop scientific theory for cleaning of such aqueous systems using microbiological and electrochemical processes to acceptable levels for regulatory standards discharge into the environment and recovery of contaminate, which in this study is the metallic content in the effluent in a form acceptable for sale and reuse.

This research project has routes in the practical application of the electrochemical (Bockris and Reddy 1970) and microbiological sciences (Madigan and Brock 2009). The aim and objectives being to reduce metal ion concentrations in polluted local

hydrological water sources with the recovery of the high value metallic product. Focused on the reduction in concentration of metal ions such as Au^{3+}, Fe^{3+}, Co^{2+} to less than 1 ppm, as basis for further optimization and possible application with highly toxic heavy metal ions of lead (Pb), cadmium (Cd), zinc (Zn), mercury (Hg), arsenic (As), silver (Ag), chromium (Cr) and copper (Cu) (Klaus-Joerger, Joerger et al. 2001) and develop and reason the feasibility of novel and creative methodologies, regarding the application of electrochemical and/or microbiological process for the remediation of metal contaminated waste effluents.

Reflection is also given to innovative green synthesis of biogenic nanoparticles as part of the process (Klaus-Joerger, Joerger et al. 2001). Secondly, where applicable we aimed to further the state of art regarding the processes and interactions of Au^{3+}, Co^{2+} and Fe^{3+} aqueous metal ions (see Figure 1.1) with electroactive microbiological organisms and/or electrified substrates within bioelectrochemical system (BES).

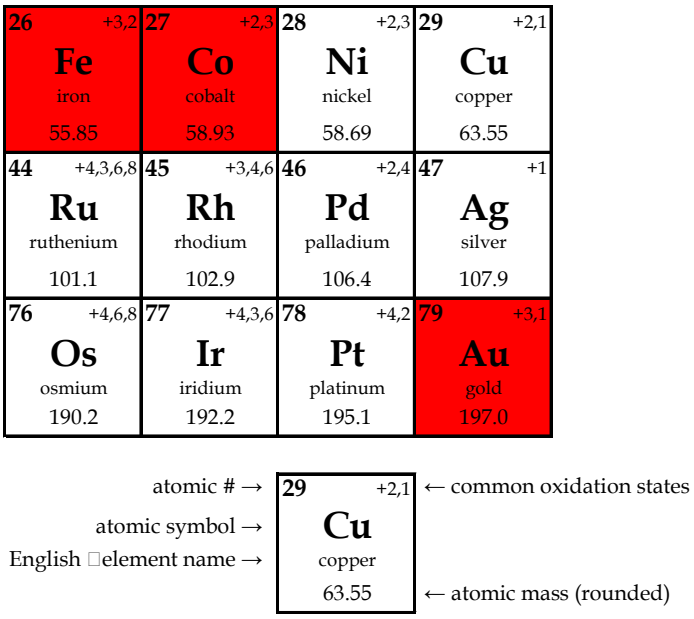

Figure 1.1 : Metals for remediation and recovery of key focus in this thesis highlighted in red.

1.2 Mine and industrial inorganic effluents containing metal ions with low concentration and low pH – gold, cobalt and iron

The introduction of oxygen by mining activity to deep geological environments leads to the oxidation of minerals to a dissolved ionic state leading to the formation of

contaminated mine water from minerals. Mechanisms of mineral dissolution can be chemical or microbiological in nature (Brown, Barley et al. 2002). Contaminated mine water is generated when rock containing metal minerals is exposed to water and oxygen, resulting in elevated concentrations of protons [H^+] and metal ions [M^{n+}] and anions such as sulphate [SO_4^{2-}] in the surrounding hydrology. The most common of these minerals are the sulphites (Banks, Younger et al. 1997). Pyrite for example (FeS_2) is ubiquitous in most metal sulphate and coal deposits and exists in potential association with other chalcophile elements such as cobalt (Banks, Younger et al. 1997).

Weathering of minerals will continue as long as the exposed area is present, which is likely to occur for many hundreds of years after mining operations have ceased (Brown, Barley et al. 2002). Metal ions are ubiquitous in nature, their presence caused by mineral oxidation occurring at slow rates due to minimal exposure to oxygen. This process is accelerated when mining activity increases exposure to atmospheric oxygen, causing the elevated release of these metals ions into the environment.

The formation of contaminated mine water from the sulphite mineral pyrite (FeS_2) is a chemical and microbiological reaction. The reaction can involve a multitude of steps (Rimstidt and Vaughan 2003) but in general the mechanism can be described by an initiation reaction eq^n 1.1, where pyrite can break down in the presence of oxygen and water releasing ferrous ions and protons. Followed by further oxidation of ferrous Fe^{2+} to ferric Fe^{3+} ion described by eq^{n}1, where bacteria such as *T. ferrooxidans* have been known to accelerate these reactions (Sand, Gehrke et al. 2001).

$$FeS_2 + 1/2O_2 + H_2O \rightarrow FeSO_4 + H^+ \qquad (1.1)$$

$$Fe^{2+} + 1/4O_2 + H^+ \rightarrow Fe^{3+}\ 1/2H_2O \qquad (1.2)$$

Microorganisms are the "villains" of this process here where an array of chemolithotrophic[1] bacteria and archaea oxidise metal ions as electron donors for respiration. This process can be reversed by the application of dissimilatory metal ion reducing bacteria such as *Shewanella putrefaciens* which reduce Fe^{3+} to Fe^{2+} as part of

[1] Chemo → Chemicals, Litho → stone, Tropic → of a turn. Bacteria able to utilize inorganic electron donors as an energy source, see section 1.7.3.

dissimilative respiration by passage of electrons through a biological electron transport system (ETS) (Madigan and Brock 2009).

Acid mine waters are characterized by high conductivities of various dissolved ionic species, cations such as metal ions (M^{n+}), protons (H^+), sodium (Na^+) and elevated concentrations of anions such as sulphate (SO_4^{2-}), nitrate (NO_3^-) and chloride (Cl^-). These ionic species not only act as transporters of electronic charge but may affect reaction mechanisms of electronation reactions occurring at the surface of the electrified interface. High conductivities are an advantage in an electrochemical system with a reduction in ohmic losses and hence savings in energy (Rabaey, Clauwaert et al. 2005).

To summarise, the products of acid mine drainage lead to a reduction in pH of aqueous effluents and the destruction of the natural carbonate buffering systems. This leads to the elevated concentrations of soluble Fe^{3+} imparting the characteristic red colour in extremely acid mine waters and other associated toxic metal ions such as Co^{2+} and Au^{3+} investigated here in effluents characterised by low pH (< 3) and relatively high conductivity κ, ranging from 0.8 mS/cm for two streams polluted by AMD in Durham, Coldfield (Jarvis and Younger 1997) to as high as 3.5 mS/cm from abandoned Pb-Zn sulfide mine, NW Anatolia, Turkey (Aykol, Budakoglu et al. 2003).

Electronic waste or e-waste is also an emerging problem as well a business opportunity of increasing significance (Widmer, Oswald-Krapf et al. 2005). As are spent effluents from the chemical industry (Pletcher and Walsh 1990) for the recycling of both valuable and toxic materials in them (Robert U 1997; Jeremy 2006) especially in the growing industrial third world countries of India and China. In the European community the European commission has adopted regulation in force from 2003 promoting the recovery and recycling of Waste Electrical and Electronic Equipment (WEEE) (Widmer, Oswald-Krapf et al. 2005).

Elevated concentration of metal ions in the hydrology of local communities is due to the unregulated discharge of metal contamination effluents and mining operations. Metal pollutants can have severe toxic effects on the natural ecosystem, as well as to humans by contamination of local drinking water and biomagnification and bioaccumulation of these metal ions through the food chain (Streit 1992).

Cobalt is a strategic and critical metal. Its application has significantly increased these last two decades with application in the aeronautical industry to produce corrosion-resistant, high temperature super alloys for gas turbine engines (Jeffrey, Choo et al. 2000). To a lesser extent it also has been applied in the chemical industry as a catalyst for various reactions, carbide and diamond tools, magnets, medical implants, oil desulphurization, ceramics and the computer industry. Due to its association with heavy metals such as nickel, zinc and copper it is usually extracted in small quantities from non-ferrous metal production and mining operations (Brown, Barley et al. 2002). Cobalt toxicity to humans includes cardiomyopathy[2], adverse pulmonary effects and carcinogenicity, as reported by Karovic et al (Karovic, Tonazzini et al. 2007).

The extraction and recovery of gold is one of the World's most important metallurgical processes. Current methods have changed little over the last 50 years, which used cyanide, a highly dangerous environmental pollutant, as an extraction agent (Adamson and Ayres 1972; Kongolo and Mwema 1998). Gold has vast application in the field of electronics for example in cellular phones, personal computers and a variety of portable electronic devices.

1.2.1 Microbiological redox transformations of metal ions and application to bio-electrochemistry. "Metals ions…friend or foe?"

Metal ions are involved in all aspects of microbial life. In general terms their roles involve the stabilization of a range of biological structures such as cell wall proteins and play a part in cell growth and maintenance of metabolic activity (Bockris, Bonciocat et al. 1974). They also have effective catalytic properties for a range of biochemical processes. For example transition metals such as iron and copper are important catalysts of biological redox processes. Their effectiveness based on their ability to adopt alternative coordination numbers, geometries and oxidation states as described by Vallee and Williams as the entatic state hypothesis (Vallee and Williams 1968), allowing the ready transfer of electrons as part of metabolic activity (Hughes and Poole 1989).

[2] Cardiomypathy is a disease of the heart muscle.

However, when a metal with no biological function competes or replaces a functional metal, toxicity can result. Thus, metal resistance by living cells is a specific case of biological metal homoeostasis. Transition elements with varied configurations of electrons in the atomic d-subshell, such as cadmium, mercury and silver, and the post-transitional metals with varied configurations of electrons in the atomic p-subshell, such as thallium, tin, lead and arsenic, are examples of toxic elements to living cells.

Their toxicity derived from displacing native metals from their binding sites in bio-molecules or binding to proteins or nucleic acids, alternating their geometry and function. There are also reports of their effects on oxidative phosphorylation and membrane permeability (Hughes and Poole 1989). This means that many metal ions that are essential to microorganism at low concentrations become toxic at elevated concentrations within the ecosystem. Microorganisms have evolved redox resistance mechanisms as a strategy in dealing with elevated metal ion concentrations, which may also be applied for metal ion remediation.

A wide diversity of bacteria, archaea and fungi have the ability to transfer electrons to metal ions in solution (Madigan and Brock 2009) and transfer and receive electrons from electrified interfaces by direct electrical transfer (DET) and mediated electron transfer (MET) as part of respiration. The reduction of metal ions to less toxic states by a microbiological organism has also been reported as part of defensive resistance mechanisms (Nies 1999). This research describes the conclusions of our research aims, here being to conceptualize and analyse the bioremediation via bio-sorption, bio-reduction and bioelectrochemical remediation processes of Au^{3+}, Co^{2+} and Fe^{3+} ions with particular consideration paid to microbial metal ion bio-reduction and bio-nucleation integrated within the overall biosorption process.

These various processes can be coupled within electroreduction processes, i.e. with their application in bioelectrochemical systems (BES) (Rabaey 2010) which incorporate microbiological processes of electro-active bacteria at electrified electrode substrates. The concept being a symbiotic alliance in a bioelectrochemical system of microbiological organisms (*Shewanella putrefaciens* applied as an archetypal electroactive Gram-negative bacterium) and physical-chemical electrochemical environmental remediation strategies, where:

a. Electro-remediation of metal ions by phase change and reduction in mobility of metal ions by electrodeposition, carried out with the simultaneous production of hydrogen, which chemolithotrophic bacteria utilize as an electron donor as part of respiration. This coupled with the simultaneous biosorption of metal ions by ionized groups located on the outer lipopolysaccharide leaf of the outer cell membrane of Gram-negative bacteria and the bioreduction of metal ions as electron acceptors by outer membrane protein enzymes or as part of redox resistance mechanisms.

b. Bacteria and bacterial artefacts enhance electrochemical charge transfer electronation reactions qualified and quantified within a paradigm of reaction mechanisms (which describe individual steps of charge transfer of various ionic species located or specifically adsorbed to the electrode substrate (in the Helmholtz layer of the electrified interface), thermodynamics (and associated changes in the Gibbs free energy of various reactions) and kinetics (changes in rates of reactions upon departure or on route to equilibrium).

1.3 Green Chemistry and bioelectrochemical remediation

This project aims to work within a green chemistry philosophy where feasible. Green Chemistry's roots start in the early 1990's and it has grown into a significant internationally engaged focus area within chemistry (Anastas and Kirchhoff 2002). The origins and basis of green chemistry chart a course for achieving environmental and economic prosperity in a sustainable developing world (Anastas and Kirchhoff 2002). Electrochemistry can be seen as a branch of green chemistry, fittingly summarised by Keith Scott (Clark and Macquarrie 2002) as :

> *"concerned with the utilization of a set principles that can reduce or eliminate the use of hazardous substances in the design, manufacture and application of chemical process…"*

and

"…solutions included bioelectrochemistry and improved process engineering."

The cost of the electricity (£0.08 kWh-1, 3.5V, 8-10 £kmol-1) compares favourably to other commonly used chemical reducing agents such as sodium peroxide (50 £/kmol-1) (Clark and Macquarrie 2002). The application of bio-catalysts as an alternative to its chemical equivalent usually results in a more sustainable process, though their use is held back by cost constraints regarding the need for specialised equipment and short lifetimes. When one takes into account that only a small fraction of the potential microorganisms have been investigated, there is still huge scope in the future to exploit these microorganisms for environmental application.

We here investigate only one example, that being the application and interactions of bio-electro-active bacteria and electrochemical processes of metal ion transformations for remediation and recovery of metal ions from industrial and mine water effluents with an outlook for the recovery of bio-genic nanoparticles which can be recycled or reused in various industrial applications (Hennebel, De Gusseme et al. 2009). Figure 1.2 gives a review of green chemistry targets and possible application in this investigation.

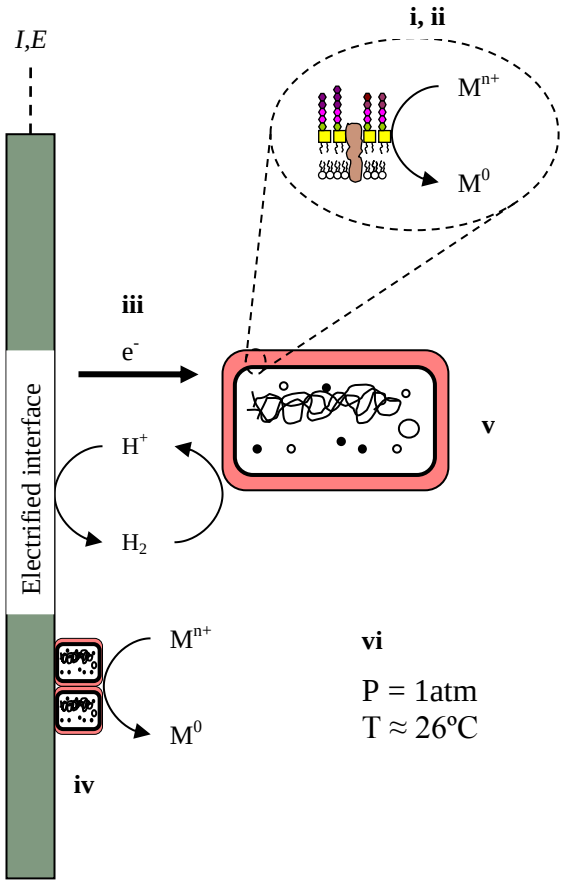

Targets within a green chemistry philosophy

(i) Clean Synthesis
Bacteria as eco-friend "bio-nano-factories".

(ii) Alternative feedstock's
Application of industrial and mining wastewater for novel production of metallic biogenic nanoparticles.

(iii) Enhanced atom utilisation

(iv) Novel separation technologies
Application of biological electro-active bacteria and electrochemical process for enhanced bio-adsorption and electrodeposition and of metal ions in aqueous waste streams.

(v) New, safer chemicals and materials
In situ on on-demand electrochemical production of $H_2(g)$ as the electron donor or electrode as the direct electron donor for chemo-lithotrophic bacteria such as Shewanella putrefaciens which utilize $H_2(g)$ as the electron donor in respiration process.

(vi) Mild conditions of operation
Processes occurring at atmospheric pressure and room temperature.

Figure 1.2: Green Chemistry overview.

1.4 Atypical electroactive bacterial cells applied in this research: Shewanella putrefaciens

The Shewanella genus named after James Shewan in honour of his work in marine microbiology (Venkateswaran, Moser et al. 1999) shows great promise for metal ion remediation. Members of this genus have been associated with food spoilage and implicated as an opportunistic pathogen to aquatic animals (Holt, Gahrn-Hansen et al. 2005). With reports of the ability of the *Shewanella* genus to thrive chemically and redox diverse environments, the genome sequence of *S. oneidensis* predicts a highly diverse electron-transport system that includes up to 42 c-type cytochromes[3] (Fredrickson, Romine et al. 2008). Previous reports regarding the *Shewanella* genus

[3] Cytrochromes are proteins that contain a heme prosthetic group and involved (biological quantum electron tunnelling, see D. Devault (1981), The Quantum Mechanical Tunnelling in Biological Systems. Cambridge University Press. London).

concerning the bio-reduction of Au^{3+} (Konishi, Tsukiyama et al. 2006; Konishi, Tsukiyama et al. 2007) and Fe^{3+} (Liu, Gorby et al. 2002) and biosorption of Co^{2+} by *Shewanella putrefaciens* (Mamba, Dlamini et al. 2009).

Reports of the integration of *S. putrefaciens* (see Figure 1.3) in bioelectrochemical systems have also shown promise (Kim, Park et al. 2002). We here selected *S. putrefaciens* as the model organism representing Gram-negative, fluctuate and rod-shaped dissimilatory metal-reducing bacterium proven to produce its own electron mediators which catalyse the enzymatic transformation and precipitation of metal ions and radio-nucleotides (Gorby, McLean et al. 2008).

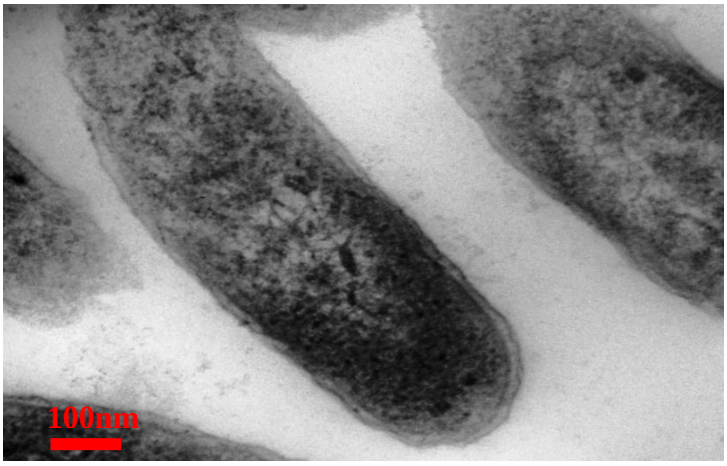

Figure 1.3 : TEM image of *S. putrefaciens,* taken from control biosorption experiments described in chapter 3.

1.5 Graphite electrodes as solid conducting electrode applied in bioelectrochemical experimentation

Nobel metals such as platinum can be utilised as electrocatalysis of various electron transfer reactions such as O_2 reduction and H_2 evolution are of particular interest to fuel cells (Clark and Macquarrie 2002), although their application as conducting substrates with electrochemical cells for metal ion reduction is limited by high economic cost. The majority of research regarding electrochemical systems focused mainly upon carbon (Thrash and Coates 2008) primarily due to its low cost, high electrical conductivities, extremely low coefficient of thermal expansion, light weight and a good resistance to chemical attack and corrosion (Guenbour, Iken et al. 2006). Also its irregular interfacial surface is good for bacterial adhesion (Thrash and Coates 2008). With the proven

concept of direct electron transfer (DET), where bacterial exchange electrons directly from the electrified interface and mediated electron transfer (MET). MET involves a consortia of redox electron carriers such as NAD (nicotinamide adenine dinucleotide). Here electrodes behave as electron donors or electron acceptors as part of dissimilatory bacterial respiration (Gregory, Bond et al. 2004; Thrash and Coates 2008).

Graphite G10 electrodes (Figure 1.4) were supplied for bio electrochemical metal ion remediation reactions to take place. The material grade of graphite was chosen based upon previous investigation of bioelectrochemical water remediation studies using dissimilatory bacterial cells (Gregory, Bond et al. 2004; Gregory and Lovley 2005; Rhoads, Beyenal et al. 2005).

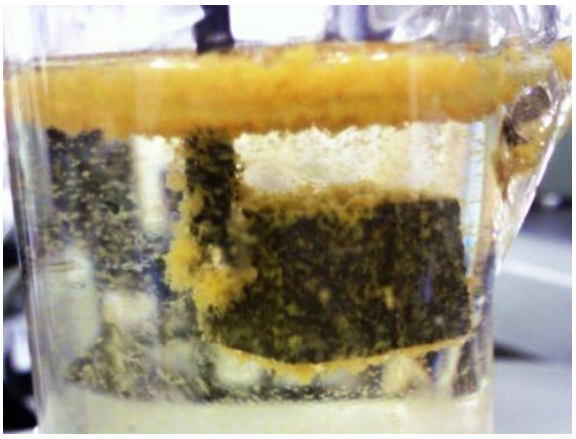

Figure 1.4 : Graphite electrodes utilized as solid conducting substrates for bioelectrochemical remediation of metal ions.

1.6 Current metal ion physic-chemical, biosorption and electrodeposition technology

1.6.1 Alternatives to electrochemical and microbiological metal ion remediation

The standard method of removing these metals involves precipitation as oxides and hydroxides as for treatment of acid mine drainage, with the result of a sludge containing a mixture of metal ions requiring further chemical treatment.

Traditionally, chemical neutralisation of acidic mine water and industrial effluents with limestone, calcium carbonate or sulphate (Banks, Younger et al. 1997; Brown, Barley et al. 2002), results in ampoteric co-contaminate precipitation of metal hydroxides. The

processes are efficient and relatively cheap reducing the concentrations of metal ions to acceptable limits. The recovery and disposal of the resultant sludge can be expensive and the recovery of the metals impossible. For example precipitation of 100 ppm of Cu^{2+}, Cd^{2+} and Hg^{2+} heavy metals by lime produce as much as 1000, 900 and 500 ppm of sludge (Gadd and White 1993).

Passive treatments like constructed wet lands have some promise but the control of such processes is poor and furthermore large areas of land are required for the treatment (Banks, Younger et al. 1997) which in developing and developed countries is an expensive solution.

Ion exchange and reverse osmosis are applied on a commercial scale (Harry 1999), but have their economic drawbacks; i.e. high cost resins required in ion exchange and high cost of membranes and high pressures required in reverse osmosis (Harry 1999). As reported by Eccles (Harry 1999), for a plant with a process capacity of 1000 m^3/d a precipitation, membrane and iron exchange process would require 12.5, 12.5 and 100 US$/$m^3$ capital and up to 0.013, 0.050 and 0.250 US$/$m^3$ operating costs respectively.

Industrial electrowinning of metals from metal baths of high concentration is the oldest industrial electrolytic process; Sir Humphry Davy was the first to apply the principles for recovery of sodium metal in elemental in 1807 by the electrolysis of molten sodium hydroxide. The electrodeposition and recovery of metals are from relatively dilute metal ion concentrations of (< 500 ppm) in comparison. They have shown little economic viability and are energy inefficient due to high mixing requirements, large electrode surface areas to improve mass transfer of metal ions to electrode surfaces and side reactions such as hydrogen evolution or reaction of other ions present, which may interfere with electrodeposition kinetics.

The strategic aim here is to develop symbiotic biosorption and electrochemical deposition metal ion remediation strategies by their co-operative enhancement.

1.6.2 Current biosorption technology for metal ion remediation

Biosorption processes are an ideal solution for applicability for metal contaminated effluents of concentrations as low as 20 ppm (Brierley 1990) but have only achieved small-scale operation. The majority of academic literature focuses on deactivated/pre-treated biomass with extensive investigation of biosorption thermodynamics and kinetics (Febrianto, Kosasih et al. 2009).

Biosorption processes for metal recovery involve solid (biosorbent) and liquid (solvent containing the metal ions) contact in batch or continuous process with a metal uptake cycle and solid liquid separation (Volesky 1990). Batch operation would involve mixing of the biosorbent and metal contaminated effluent. The suspension is stirred to a high enough degree to achieve homogeneity and mass transfer. Once equilibrium or the required concentration of metal ions in the solution is achieved, a solid separation such as settling, floating, filtration and centrifugation (B 2001) is carried out, resulting in clear purified water. Continuous operation would involve continuous supply of metal bearing effluent with fresh biosorbent unremittingly fed and harvested by solid sequencing or a certain amount of adsorbent retained in the reactor, with sequential batch feeding of new bacteria. Fixed packed-bed, pulsating-bed, fluidized-bed and rotating-disc reactors have also shown some promise (Volesky 1990; Gadd and White 1993; Butter, EvisOn et al. 1998; Yin, Yu et al. 1999) for mediation of a range of heavy metal ions. On a commercial scale biosorption processes have been developed by companies such B. V. Sorbex[4] operating in Canada specializing in heavy metal and arsenic removal using high metal-sorbing materials produced from industrial fermentation products.

The biosorption through growing cells has been reviewed by Malik (Malik 2004) regarding the bacterial “active” uptake as part of metabolic respiration and “passive” biosorption of metal ions by interfacial membrane ion exchange processes. Biosorption by deactivated cells has progressed more than investigation using active cells. The later having drawbacks and difficulties in the recovery of metal from the resultant biomass sludge in resalable form and cost in regeneration and replacement of biosorbent (Malik 2004). The practical application of living cells has many challenges, in light of practical

[4] For further information see : http://www.bvsorbex.net

limitations of system sensitivities to pH, high metal/salt concentrations and requirements of external sources of metabolic energy donors (Malik 2004). The selection of strain and isolation of metal-resistant bacteria with employment of single or mixed strains of bacterial communities would be a key bottleneck in the design of robust systems. Reports of a consortium of acidophilic bacteria able to respire in extremely acid environments (pH < 3) have been reviewed by Johnson et al. (Johnson and Hallberg 2003). An efficient process, requiring bacteria able to maintain high removal efficiency, with possible economic recovery of high value biogenic particles, formed by bio-redox reactions, would be the ideal.

The integration of chemical precipitation and biological sulphate removal by sulphate reducing bacteria (SRB) have also been reported to show some success (Glombitza 2001; Tabak, Scharp et al. 2003) where multiple stages can be integrated for metal and sulphate ion removal and an increase in pH of acid mine drainage.

1.6.3 Current electrodeposition technology for metal ion remediation

The application of electrochemistry from a green chemistry point of view for the production of metals and for the water purification of metal ion contaminated effluents appears to be a reasonable process for metal recovery from waste solution (Pletcher and Walsh 1990) because no other chemicals are introduced which means that the carbon footprint of this process is low. In addition, the electrical energy can be supplied from renewable sources (Junginger, Faaij et al. 2004).

The selective electrodeposition is therefore attractive with several established cell designs helping to provide an established technology for a cleaner environment (Walsh and Reade 1994; Walsh and F 2001). These include plate-in-tank-cells, plate-and-frame cells, turbulence-promoted electrolytes, moving-cathode cells, fluidized-bed electrodes and concentric cathode cells (Pletcher and Walsh 1990).

Metal ion recovery by electrodeposition by batch and continuous operation in solutions containing single and multi-component mixtures of metal ions has been investigated extensively with the predominance of small scale laboratory cell designs for investigation of synthetic liquors. Development of pilot plant and full scale commercial

operations is still relatively in its infancy with much need of engineering development (Walsh and Reade 1994).

The modelling of metal recovery in single and mixed metal ion solution by electrodeposition described by Scott and Paton (Scott and Paton 1993) gives a good fit for cadmium removal from process solutions containing ferric ions (Scott and Paton 1993). The selective electrodeposition of metal from simulated waste binary Cd/Co and Cd/Ni solutions has also been proven by Armstrong et al. (Armstrong, Todd et al. 1996), together with the feasibility of the recovery of cadmium, cobalt and nickel as a pure metal (≈99%) and reduction of metal ion concentrations to less than 20 ppm. The application of carbon-based electrodes such as porous carbon felt (Roberts and Yu 2002) and carbon aerogel (Walsh and F 2001; Rana, Mohan et al. 2004), electrodes for chromium removal from waste water and cadmium removal using reticulated vitreous carbon (RVC) (Walsh and F 2001; Tzanetakis and Scott 2004) has also shown some promise.

The recycling of metals from batteries by a combination of hydrometallurgical and electrochemical methods has been demonstrated for nickel-cobalt recovery by Tzanetakis and Scott (Tzanetakis and Scott 2004) and Dew and Phillips with application of the Chemelc Cell[5] (Dew and Phillips 1985) for copper electrowinning from dilute solutions (< 2000 ppm). The feasibility of recovery of copper, lead and tin from scarp printed circuits boards has also shown promise, investigated by Mecucci and Scott (Mecucci and Scott 2002).

The key bottleneck for such a process is usually mass transfer factors where the mass transfer limiting current for dilute effluents are low (Simonsson 1997) and would require large electrode surface areas. Several designs have overcome these limitations such as a rotating cylinder, fluidized bed and packed bed electrochemical reactors, (Pletcher and Walsh 1990) with two and three dimensional cathodic electrodes made of materials such as graphite particles, metals, graphite felt, metal wool, graphite fibres and vitreous carbon (Robert U 1997; Chatelut, Gobert et al. 2000). However, a remaining

[5] Manufactured by B.E.W.T Limed of Alcester and applied commercially for Silver, Gold, Nickel, Cadmium and Zinc recovery from spent electroplating solution.

obstacle encountered with less noble metals such as Fe^{2+} and Co^{2+}, is the simultaneous hydrogen evolution reaction, with a decrease in current efficiency and a simultaneous rise in pH. A rise in pH could cause the metal ions to precipitate out as a salt. Conversely, if the evolved hydrogen is used for bacterial respiration, proton reduction may be of advantage in bioelectrochemical systems. Here, chemolithotrophic bacteria such as *S. putrefaciens* utilize hydrogen as an electron donor as part of dissimilative respiration with simultaneous biosorption of metal ions.

The possibility of a symbiotic bioelectrochemical coupling of the two processes in a bioelectrochemical reactor could provide a more energy efficient method for metal ion recovery from dilute effluents.

1.7 Microbiological redox transformations of metal ions

The processes of natural selection have produced extraordinary consortia of microorganisms able to conserve energy and reproduce using a range of electron donors and acceptors. Anaerobic respiration using different electron acceptors allows microorganism to reside in environments were oxygen is absent. Some of the electron accepters used in anaerobic respiration includes nitrate NO^{3-}, ferric ion Fe^{3+} and sulphate SO_4^{2-}. Some organisms are also able to use inorganic chemicals as electron donors, categorised as chemolithotrophs (Madigan and Brock 2009). Chemolithotrophs in contrast to chemoorganotrophs are able to utilise inorganic compounds such as hydrogen (H_2), ferrous iron (Fe^{2+}) and ammonia (NH_3^+). This project will aim to utilise the anaerobic respiration of chemolithotrophs such as Gram-negative bacteria of the Shewanella genus. Microbial reduction of metal ions can be categorised as part of dissimilatory or resistance mechanisms as summarised by Figure 1.5 and elaborated upon in the following.

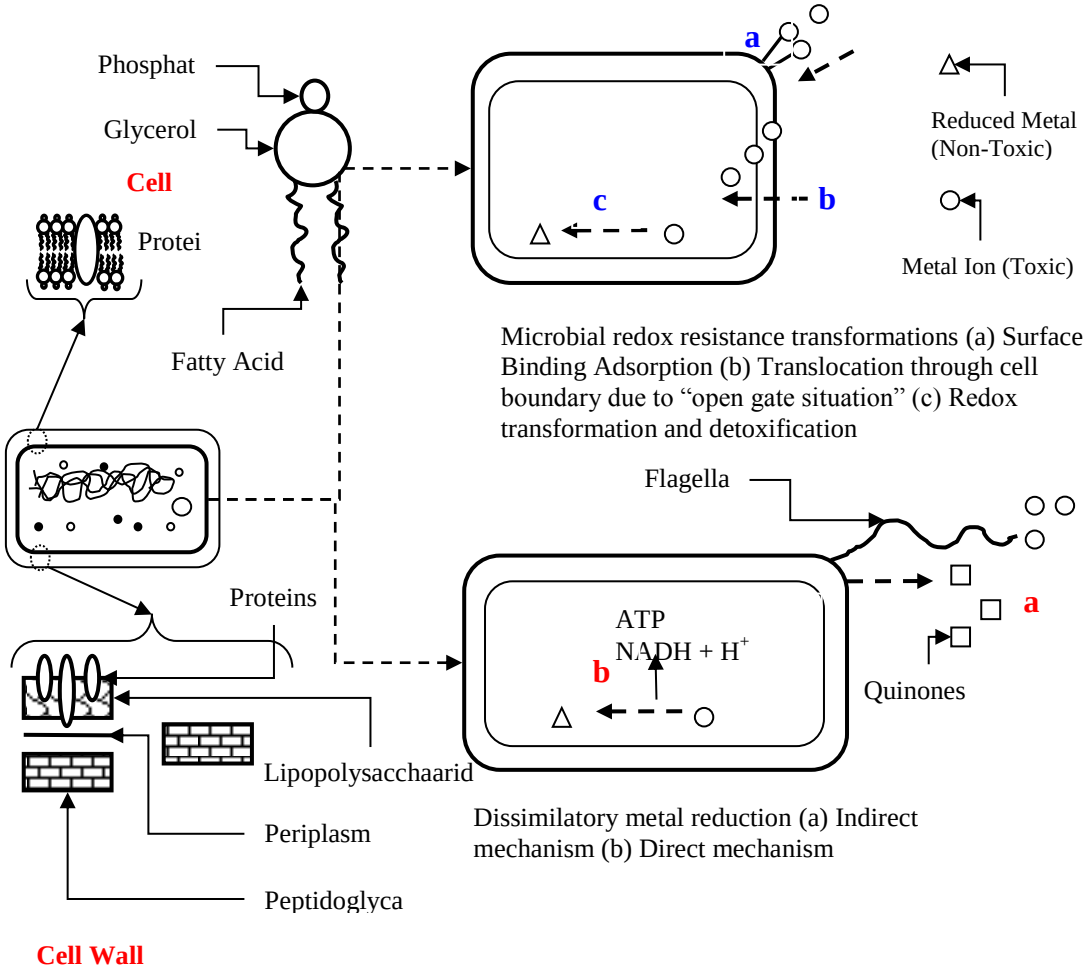

Figure 1.5 : Summary of microbiological metal redox transformations.

1.7.1 Microbiological reduction of Au^{3+}, Co^{2+} and Fe^{3+} metal ions in aqueous environments

Several microorganisms have been used to deposit gold from aqueous systems. For example prokaryotes such as bacteria (Hughes and Poole 1989; Nies 1999; Kashefi, Tor et al. 2001; Ahmad, Senapati et al. 2003; He, Guo et al. 2007) and eukaryotic organisms such as fungi (Mukherjee, Senapati et al. 2002). Konishi et al (Konishi, Tsukiyama et al. 2007) described the microbial reduction and deposition of gold nanoparticles achieved at 25°C over a pH range of 2.0 – 7.0 using the mesophilic bacteria *Shewanella algae*. Hydrogen was used as the electron donor. Their results showed that the reductive deposition of gold by the resting cells of *Shewanella algae* to be a fast process, where 1 x 10^{-3} M of Au^{3+} ions are reduced to elemental gold within 30 min. The overall reactions when using H_2 as the electron donor can be described by eq^n 1.3.

$$3H_2 + 2AuCl_4^- \rightarrow Au + 8Cl^- + 6H^+ \quad (1.3)$$

Wang et al. (Wang, Qian et al. 2009) report the influence of pH on the synthesis of gold colloids. As the system pH is increased by reducing agents, the product gold colloidal nanostructures vary. Their investigation reported that low pH (2.91 - 6.61) leads to the synthesis of well-dispersed, uniform fine Au colloids and a higher pH (> 6.61) leads to the formation of larger gold colloids. Similar relationships are also reported by Konishi et al. (Konishi, Tsukiyama et al. 2007) in regards to the bio-deposition gold nanoparticles using *S. algae* as described by eq^n 1.3. They report that the solution pH is an important factor in controlling the morphology and biogenic gold nanoparticles and the location of gold deposition.

Microorganisms utilize ferric ion Fe^{3+} for a variety of purposes, components of the prosthetic group enzymes such as cytrochrome can greatly influence the biogeochemical cycling of iron (Weber, Achenbach et al. 2006). Geochemical and microbiological evidence suggests that the reduction of Fe^{3+} may have been an early form of respiration on the earth and a candidate for the basis of life on other planets (Weber, Achenbach et al. 2006). The reduction of Fe^{3+} to Fe^{2+} by dissimilatory metal reducing bacteria is well documented (Myers and Nealson 1990; Volesky 2001).

Lui et al. (Liu, Gorby et al. 2002) describe the reduction kinetics of Fe^{3+} reduction to Fe^{2+} (species in this system were Fe(III)citrate and Fe(III)NTA in concentrations of 5 x 10^{-4} M) in the presence of H_2, lactate and acetate. The overall reactions, when using H_2 as the electron donor, can be described by eq^n 1.4. Lui et al. report the metal reduction rate to be electron donor dependent, with faster rates observed with H_2 in comparison to lactate and acetate. The kinetics were effectively modelled by a first-order rate equation.

$$2Fe^{3+} + H_2 \rightleftharpoons 2Fe^{2+} + 2H^+ \quad (1.4)$$

There is relatively little research concerning the bio-transformations of Co^{2+}, the majority of which regards Co^{2+} biosorption (Volesky 2001) by a range of living and dead biomass. Mamba et al. (Mamba, Dlamini et al. 2009) recently report the biosorption capability of *S. putrefaciens* of Co^{2+}. Their investigations, describe the

biosorptive capabilities with ion concentrations ranging from 2 mM to 0.2 M, biomass dosages of 50, 100 and 150 $1x10^4$ CFU/ml (where CFU is the colony forming units and is a measure of viable cells in solution) and solution pH 2 - 8. Optimum uptake rates for cobalt of 27% were demonstrated at pH 6.5, 2 mM Co^{2+} and cell concentration of 150 x 10^4 CFU/ml, with an efficient fit of data to the Langmuir sorption model. Absorption was significantly reduced at a lower pH. Evidence of cobalt bio-genic nanoparticles was ambiguous.

1.8 Bioelectrochemical systems (BES) for wastewater treatment

Bioelectrochemical systems (BES) are an exciting new technology (Rabaey 2010). The application of a microbial redox process for energy production and organic water purification in microbial fuel cells (Logan, Hamelers et al. 2006) in batch (Rhoads, Beyenal et al. 2005) and continuous operation (He, Minteer et al. 2005; Rabaey, Clauwaert et al. 2005; Cheng, Liu et al. 2006) has become a mature subject over the last 20 years. Water purification of nitrate (Feleke, Araki et al. 1998; Prosnansky, Sakakibara et al. 2002; Park, Kim et al. 2005; Clauwaert, Rabaey et al. 2007; Ghafari, Hasan et al. 2008), uranium (Gregory and Lovley 2005) and perchlorate (Thrash and Coates 2008) has also gained much interest in academia at present.

The development of microbial fuel cells (MFC) is of particular interest as a technology for the conversion of carbohydrates to electricity. Bacteria transfer electrons, gained from the organic electron source such as organic waste water, at the anode through an external resistance to the cathode where usually oxygen is used as the electron acceptor.

There are reports of other electron acceptors such as ferricyanide (Du, Li et al. 2007) and bio-mineralized manganese (Rhoads, Beyenal et al. 2005) applied in the cathode chamber. Hydrogen production (Ghafari, Hasan et al. 2008) at the electrode as a bacterial electron donor or the direct electron transfer to bacteria cells by nano-wires and electron mediators has been highlighted (Gregory, Bond et al. 2004). The application of biofilms and immobilized cells also show some promise (Feleke, Araki et al. 1998; Park, Kim et al. 2005; Erable, Duţeanu et al. 2009).

1.9 Enhanced Bioelectrochemical transformation of metal ions

The association of microbiological, biosorption and electrochemical electrodeposition processes for the enhanced remediation of metal ions is an exciting prospect. Three key strategies are described below. Our investigation were only able to evaluate changes in charge transfer thermodynamics of metal ion electronation upon graphite electrodes with the expectation of further investigation of bacterial biocatalysts of metal reduction and application of electrodes as electron donors to initially active bacterial metal ion biosorbents.

1.9.1 Enhancement of charge transfer thermodynamics of metal ion electronation

Bacterial cells added to the electrodeposition bath may reduce the overall energy requirements of metal ion deposition described by the Gibbs free energy of reaction (ΔG) evaluated upon changes in reversible potentials of metal ions in electrolyte. Natural humic and electron shuttling molecules produced in-situ by electro-active bacterial cells such as *Shewanella putrefaciens* as reported by Gorby et al (Gorby, McLean et al. 2008) could further reduce energy barriers of electrochemical and bioelectrochemical phase transformation of metal ions in our system.

1.9.2 Enhancement of charge transfer kinetics of metal ion electronation

The reduction of metal ions by charge transfer processes at an electrode surface may be enhanced by the application of live electroactive cells. Reactions in electrochemical systems may occur if only at high overpotentials because of slow kinetics, i.e. such reactions have a low exchange current density i_o (Bockris and Reddy 1970). The objective of electro-catalysis is therefore to seek to provide alternative, lower energy of activation pathways of the processes and speed up the reaction kinetics with reductions in reaction time. The possibility of biocatalysis by live cells and electroactive cellular redox enzyme proteins offer many attractive possibilities as discussed by Hill and Higgins (Hill and Higgins 1981). The biocatalysts of cathodic reductions such as of oxygen reduction has been demonstrated on carbon electrodes using a variety of Gram-positive and Gram-negative bacteria (Rabaey, Read et al. 2008; Cournet, Délia et al. 2010).

1.9.3 Electrode as an electron donor to bacterial cells with simultaneous bio-sorption and bioreduction of metal ions by living bacterial cells

The coupling of biological remediation of inorganic contaminated water with proton reduction at electrified interfaces shows some promise. Where the electrochemical reduction of protons in solution to $H_2(g)$, acting as an in-situ electron donor for respiring bacterial cells, or the direct electron transfer to bacterial cells in solution or bacterial biofilm communities grown upon the electrode surface is a proven concept. With reports regarding effluents containing nitrate reviewed by Ghafari et al. (Ghafari, Hasan et al. 2008), uranium reported by Gregory and Lovely (Gregory and Lovley 2005) and perchlorate by Thrash et al. (Thrash, Van Trump et al. 2007). We further hope to develop the application of polarised electron substrates as electron donors to electroactive chemolithotrophic bacteria who simultaneously biosorb metal ions such as Au^{3+}, Co^{2+} and Fe^{3+}. Two key dichotomies of electron transfer mechanisms with electroactive dissimilative bacteria of direct electron transfer (DET) and mediated electron transfer (MET) (Gregory, Bond et al. 2004; Thrash and Coates 2008).

DET can be carried out directly by protein enzymes such as periplasmic c-type cytochromes and NADH dehydrogenise (Madigan and Brock 2009) embedded in the cell membrane and indirectly extracellular via microbial nanowires (Reguera, McCarthy et al. 2005; Gorby, Yanina et al. 2006). Alternatively MET has been reported to involve a number of soluble redox molecules capable of undergoing redox cycling classified as "election shuttlers", such as extra cellular cytochromes (Armstrong, Hill et al. 1988), humic substance (Lovley, Coates et al. 1996) and other bio molecules (Gorby, McLean et al. 2008).

1.10 Summary and Hypothesis

This thesis describes the advancement and intellectual proposition pertaining to the interactions of metal ions and electro-active bacteria, metal ions and electrified electrode substrates and their alliance for application in water remediation of metal contaminated effluents. This can be summarised by two comprehensive hypotheses.

Hypothesis 1*: Electroactive microorganisms have novel application in the remediation and recycling of toxic and precious metals ions from aqueous effluent streams.*

As discussed in this introductory chapter the application of electrochemical processes for the remediation and recovery of metal ions from aqueous effluents is a proven technology. Furthermore, as elaborated here, there is a huge array of microorganisms which bio-sorb and bio-reduce metals as part of dissimilatory and resistance mechanisms.

The *Shewanella* genus shows great promise for biosorption and dissimilatory reduction of metal ions. This research aims to further evaluate their application in regards to metal ion biosorption and bioreduction phenomena evaluated in chapter 3.

Fundamental to this project is the cleaning of harmful and toxic metals from aqueous effluents. However if the product waste can be recycled with economic payback this has advantage for viable application in the future and follows a more benign green chemistry outlook. This will be further explored in the possible application of the biogenic metallic products in nanotechnology.

Hypothesis 2*: An enhancement of contaminated remediation processes can be achieved by the alliance of electrochemical and microbiological phenomena*

This research also aims to lay some foundations for the future exploration of bioelectrochemical systems for the remediation of aqueous metal contaminated wastewater effluents, further elaborated upon in chapter 4, where bacteria and bacterial components may further enhance the electrochemical phase transformation of metal ions.

References

Adamson, R. J. and D. E. R. Ayres (1972). Gold metallurgy in South Africa. Johannesburg, Chamber of Mines of South Africa.

*Ahmad, A., S. Senapati, et al. (2003). "Extracellular Biosynthesis of Monodisperse Gold Nanoparticles by a Novel Extremophilic Actinomycete, Thermomonospora sp." Langmuir **19**(8): 3550-3553.*

*Anastas, P. T. and M. M. Kirchhoff (2002). "Origins, Current Status, and Future Challenges of Green Chemistry†." Accounts of Chemical Research **35**(9): 686-694.*

*Armstrong, F. A., H. A. O. Hill, et al. (1988). "Direct electrochemistry of redox proteins." Accounts of Chemical Research **21**(11): 407-413.*

*Armstrong, R. D., M. Todd, et al. (1996). "Selective electrodeposition of metals from simulated waste solutions." Journal of Applied Electrochemistry **26**(4): 379-384.*

*Aykol, A., M. Budakoglu, et al. (2003). "Heavy metal pollution and acid drainage from the abandoned Balya Pb-Zn sulfide Mine, NW Anatolia,Turkey." Environmental Geology **45**(2): 198-208.*

*B, V. (2001). "Detoxification of metal-bearing effluents: biosorption for the next century." Hydrometallurgy **59**(2-3): 203-216.*

*Banks, D., P. L. Younger, et al. (1997). "Mine-water chemistry: the good, the bad and the ugly." Environmental Geology **32**(3): 157-174.*

Bockris, J. O. M., N. Bonciocat, et al. (1974). An introduction to electrochemical science. London, Wykeham Publications.

Bockris, J. O. M. and A. K. N. Reddy (1970). Modern electrochemistry : an introduction to an interdisciplinary research. New York, Plenum Press.

*Brierley, C. L. (1990). "Bioremediation of metal-contaminated surface and groundwaters." Geomicrobiology Journal **8**(3-4): 201-223.*

Brown, M., B. Barley, et al. (2002). Minewater treatment : technology, application and policy. London, IWA.

*Butter, T. J., L. M. EvisOn, et al. (1998). "The kinetics of metal uptake by microbial biomass: Implications for the design of a biosorption reactor." Water Science and Technology **38**(6): 279-286.*

*Chatelut, M., E. Gobert, et al. (2000). "Silver electrowinning from photographic fixing solutions using zirconium cathode." Hydrometallurgy **54**(2–3): 79-90.*

*Cheng, S., H. Liu, et al. (2006). "Increased Power Generation in a Continuous Flow MFC with Advective Flow through the Porous Anode and Reduced Electrode Spacing." Environmental Science & Technology **40**(7): 2426-2432.*

Clark, J. H. and D. J. Macquarrie (2002). Handbook of green chemistry and technology. Oxford England ; Malden, MA, Blackwell Science.

*Clauwaert, P., K. Rabaey, et al. (2007). "Biological Denitrification in Microbial Fuel Cells." Environmental Science & Technology **41**(9): 3354-3360.*

*Cournet, A., M.-L. Délia, et al. (2010). "Electrochemical reduction of oxygen catalyzed by a wide range of bacteria including Gram-positive." Electrochemistry Communications **12**(4): 505-508.*

*Dew, D. W. and C. V. Phillips (1985). "The effect of Fe(II) and Fe(III) on the efficiency of copper electrowinning from dilute acid Cu(II) sulphate solutions with the chemelec cell: Part I. Cathodic and anodic polarisation studies." Hydrometallurgy **14**(3): 331-349.*

*Du, Z., H. Li, et al. (2007). "A state of the art review on microbial fuel cells: A promising technology for wastewater treatment and bioenergy." Biotechnology Advances **25**(5): 464-482.*

*Erable, B., N. M. Duţeanu, et al. (2009). "Application of electro-active biofilms." Biofouling **26**(1): 57-71.*

*Falkenmark, M. (1997). "Meeting water requirements of an expanding world population." Philosophical Transactions of the Royal Society of London. Series B: Biological Sciences **352**(1356): 929-936.*

*Febrianto, J., A. N. Kosasih, et al. (2009). "Equilibrium and kinetic studies in adsorption of heavy metals using biosorbent: A summary of recent studies." Journal of Hazardous Materials **162**(2-3): 616-645.*

*Feleke, Z., K. Araki, et al. (1998). "Selective reduction of nitrate to nitrogen gas in a biofilm-electrode reactor." Water Research **32**(9): 2728-2734.*

*Fredrickson, J. K., M. F. Romine, et al. (2008). "Towards environmental systems biology of Shewanella." Nat Rev Micro **6**(8): 592-603.*

*Gadd, G. M. and C. White (1993). "Microbial treatment of metal pollution — a working biotechnology?" Trends in Biotechnology **11**(8): 353-359.*

*Ghafari, S., M. Hasan, et al. (2008). "Bio-electrochemical removal of nitrate from water and wastewater—A review." Bioresource Technology **99**(10): 3965-3974.*

*Glombitza, F. (2001). "Treatment of acid lignite mine flooding water by means of microbial sulfate reduction." Waste Manag **21**(2): 197-203.*

*Gorby, Y., J. McLean, et al. (2008). "Redox-reactive membrane vesicles produced by Shewanella." Geobiology **6**(3): 232-241.*

*Gorby, Y. A., S. Yanina, et al. (2006). "Electrically conductive bacterial nanowires produced by Shewanella oneidensis strain MR-1 and other microorganisms." Proceedings of the National Academy of Sciences **103**(30): 11358-11363.*

*Gregory, K. B., D. R. Bond, et al. (2004). "Graphite electrodes as electron donors for anaerobic respiration." Environmental Microbiology **6**(6): 596-604.*

*Gregory, K. B. and D. R. Lovley (2005). "Remediation and Recovery of Uranium from Contaminated Subsurface Environments with Electrodes." Environmental Science & Technology **39**(22): 8943-8947.*

*Guenbour, A., H. Iken, et al. (2006). "Corrosion of graphite in industrial phosphoric acid." Applied Surface Science **252**(24): 8710-8715.*

*Harry, E. (1999). "Treatment of metal-contaminated wastes: why select a biological process?" Trends in Biotechnology **17**(12): 462-465.*

*He, S., Z. Guo, et al. (2007). "Biosynthesis of gold nanoparticles using the bacteria Rhodopseudomonas capsulata." Materials Letters **61**(18): 3984-3987.*

*He, Z., S. D. Minteer, et al. (2005). "Electricity Generation from Artificial Wastewater Using an Upflow Microbial Fuel Cell." Environmental Science & Technology **39**(14): 5262-5267.*

*Hennebel, T., B. De Gusseme, et al. (2009). "Biogenic metals in advanced water treatment." Trends in Biotechnology **27**(2): 90-98.*

*Hill, H. A. O. and I. J. Higgins (1981). "Bioelectrocatalysis." Philosophical Transactions of the Royal Society of London. Series A, Mathematical and Physical Sciences **302**(1468): 267-273.*

*Holt, H. M., B. Gahrn-Hansen, et al. (2005). "Shewanella algae and Shewanella putrefaciens: clinical and microbiological characteristics." Clinical Microbiology and Infection **11**(5): 347-352.*

Hughes, M. N. and R. K. Poole (1989). Metals and micro-organisms. London ; New York, Chapman and Hall.

*Jarvis, A. P. and P. L. Younger (1997). "Dominating Chemical Factors in Mine Water Induced Impoverishment of the Invertebrate Fauna of Two Streams in the Durham Coalfield, Uk." Chemistry and Ecology **13**(4): 249-270.*

*Jeffrey, M. I., W. L. Choo, et al. (2000). "The effect of additives and impurities on the cobalt electrowinning process." Minerals Engineering **13**(12): 1231-1241.*

*Jeremy, R. (2006). "'"Precious" metals: The case for treating metals as irreplaceable." Journal of Cleaner Production **14**(3-4): 324-333.*

*Johnson, D. B. and K. B. Hallberg (2003). "The microbiology of acidic mine waters." Research in Microbiology **154**(7): 466-473.*

*Junginger, M., A. Faaij, et al. (2004). "Cost Reduction Prospects for Offshore Wind Farms." Wind Engineering **28**(1): 97-118.*

*Karovic, O., I. Tonazzini, et al. (2007). "Toxic effects of cobalt in primary cultures of mouse astrocytes: Similarities with hypoxia and role of HIF-1α." Biochemical Pharmacology **73**(5): 694-708.*

*Kashefi, K., J. M. Tor, et al. (2001). "Reductive Precipitation of Gold by Dissimilatory Fe(III)-Reducing Bacteria andArchaea." Applied and Environmental Microbiology **67**(7): 3275-3279.*

*Kelley, A. C. (1988). "Economic Consequences of Population Change in the Third World." Journal of Economic Literature **26**(4): 1685.*

*Kim, H. J., H. S. Park, et al. (2002). "A mediator-less microbial fuel cell using a metal reducing bacterium, Shewanella putrefaciens." Enzyme and Microbial Technology **30**(2): 145-152.*

*Klaus-Joerger, T., R. Joerger, et al. (2001). "Bacteria as workers in the living factory: metal-accumulating bacteria and their potential for materials science." Trends in Biotechnology **19**(1): 15-20.*

*Kongolo, K. and M. D. Mwema (1998). "The extractive metallurgy of gold." Hyperfine Interactions **111**(1): 281-289.*

*Konishi, Y., T. Tsukiyama, et al. (2006). "Intracellular recovery of gold by microbial reduction of AuCl4− ions using the anaerobic bacterium Shewanella algae." Hydrometallurgy **81**(1): 24-29.*

*Konishi, Y., T. Tsukiyama, et al. (2007). "Microbial deposition of gold nanoparticles by the metal-reducing bacterium Shewanella algae." Electrochimica Acta **53**(1): 186-192.*

*Liu, C., Y. A. Gorby, et al. (2002). "Reduction kinetics of Fe(III), Co(III), U(VI), Cr(VI), and Tc(VII) in cultures of dissimilatory metal-reducing bacteria." Biotechnology and Bioengineering **80**(6): 637-649.*

*Logan, B. E., B. Hamelers, et al. (2006). "Microbial Fuel Cells: Methodology and Technology†." Environmental Science & Technology **40**(17): 5181-5192.*

*Lovley, D. R., J. D. Coates, et al. (1996). "Humic Substances as Electron-Acceptors for Microbial Respiration." Nature **382**(6590): 445-448.*

Madigan, M. T. and T. D. Brock (2009). Brock biology of microorganisms. San Francisco, CA, Pearson/Benjamin Cummings.

*Malik, A. (2004). "Metal bioremediation through growing cells." Environment International **30**(2): 261-278.*

*Mamba, B. B., N. P. Dlamini, et al. (2009). "Biosorptive removal of copper and cobalt from aqueous solutions: Shewanella spp. put to the test." Physics and Chemistry of the Earth, Parts A/B/C **34**(13-16): 841-849.*

*Mecucci, A. and K. Scott (2002). "Leaching and electrochemical recovery of copper, lead and tin from scrap printed circuit boards." Journal of Chemical Technology & Biotechnology **77**(4): 449-457.*

*Mukherjee, P., S. Senapati, et al. (2002). "Extracellular Synthesis of Gold Nanoparticles by the Fungus Fusarium oxysporum." ChemBioChem **3**(5): 461-463.*

*Myers, C. R. and K. H. Nealson (1990). "Respiration-linked proton translocation coupled to anaerobic reduction of manganese(IV) and iron(III) in Shewanella putrefaciens MR-1." J Bacteriol **172**(11): 6232-6238.*

*Nies, D. H. (1999). "Microbial heavy-metal resistance." Applied Microbiology and Biotechnology **51**(6): 730-750.*

*Nigel W, A. (1999). "Climate change and global water resources." Global Environmental Change **9, Supplement 1**(0): S31-S49.*

*Park, H. I., D. k. Kim, et al. (2005). "Nitrate reduction using an electrode as direct electron donor in a biofilm-electrode reactor." Process Biochemistry **40**(10): 3383-3388.*

Pletcher, D. and F. Walsh (1990). Industrial electrochemistry. London ; New York, Chapman and Hall.

*Prosnansky, M., Y. Sakakibara, et al. (2002). "High-rate denitrification and SS rejection by biofilm-electrode reactor (BER) combined with microfiltration." Water Res **36**(19): 4801-4810.*

Rabaey, K. (2010). Bioelectrochemical systems : from extracellular electron transfer to biotechnological application. London ; New York, IWA Publishing.

*Rabaey, K., P. Clauwaert, et al. (2005). "Tubular Microbial Fuel Cells for Efficient Electricity Generation." Environmental Science & Technology **39**(20): 8077-8082.*

*Rabaey, K., S. T. Read, et al. (2008). "Cathodic oxygen reduction catalyzed by bacteria in microbial fuel cells." ISME J **2**(5): 519-527.*

*Rana, P., N. Mohan, et al. (2004). "Electrochemical removal of chromium from wastewater by using carbon aerogel electrodes." Water Research **38**(12): 2811-2820.*

*Reguera, G., K. D. McCarthy, et al. (2005). "Extracellular electron transfer via microbial nanowires." Nature **435**(7045): 1098-1101.*

*Rhoads, A., H. Beyenal, et al. (2005). "Microbial Fuel Cell using Anaerobic Respiration as an Anodic Reaction and Biomineralized Manganese as a Cathodic Reactant." Environmental Science & Technology **39**(12): 4666-4671.*

*Rimstidt, J. D. and D. J. Vaughan (2003). "Pyrite oxidation: a state-of-the-art assessment of the reaction mechanism." Geochimica et Cosmochimica Acta **67**(5): 873-880.*

*Robert U, A. (1997). "Metals recycling: economic and environmental implications." Resources, Conservation and Recycling **21**(3): 145-173.*

*Roberts, E. P. L. and H. Yu (2002). "Chromium removal using a porous carbon felt cathode." Journal of Applied Electrochemistry **32**(10): 1091-1099.*

*Sand, W., T. Gehrke, et al. (2001). "(Bio)chemistry of bacterial leaching—direct vs. indirect bioleaching." Hydrometallurgy **59**(2–3): 159-175.*

*Scott, K. and E. M. Paton (1993). "An analysis of metal recovery by electrodeposition from mixed metal ion solutions—part I. Theoretical behaviour of batch recycle operation." Electrochimica Acta **38**(15): 2181-2189.*

*Scott, K. and E. M. Paton (1993). "An analysis of metal recovery by electrodeposition from mixed metal ion solutions—part II. Electrodeposition of cadmium from process solutions." Electrochimica Acta **38**(15): 2191-2197.*

*Simonsson, D. (1997). "Electrochemistry for a cleaner environment." Chemical Society Reviews **26**(3): 181-189.*

*Streit, B. (1992). "Bioaccumulation processes in ecosystems." Cellular and Molecular Life Sciences **48**(10): 955-970.*

*Tabak, H. H., R. Scharp, et al. (2003). "Advances in biotreatment of acid mine drainage and biorecovery of metals: 1. Metal precipitation for recovery and recycle." Biodegradation **14**(6): 423-436.*

*Thrash, J. C. and J. D. Coates (2008). "Review: Direct and Indirect Electrical Stimulation of Microbial Metabolism." Environmental Science & Technology **42**(11): 3921-3931.*

*Thrash, J. C., J. I. Van Trump, et al. (2007). "Electrochemical Stimulation of Microbial Perchlorate Reduction." Environmental Science & Technology **41**(5): 1740-1746.*

*Tzanetakis, N. and K. Scott (2004). "Recycling of nickel–metal hydride batteries. II: Electrochemical deposition of cobalt and nickel." Journal of Chemical Technology & Biotechnology **79**(9): 927-934.*

*Vallee, B. L. and R. J. Williams (1968). "Metalloenzymes: the entatic nature of their active sites." Proceedings of the National Academy of Sciences **59**(2): 498-505.*

*Venkateswaran, K., D. P. Moser, et al. (1999). "Polyphasic taxonomy of the genus Shewanella and description of Shewanella oneidensis sp. nov." International Journal of Systematic Bacteriology **49**(2): 705-724.*

Volesky, B. (1990). Biosorption of heavy metals. Boca Raton, Fla., CRC Press.

*Volesky, B. (2001). "Detoxification of metal-bearing effluents: biosorption for the next century." Hydrometallurgy **59**(2-3): 203-216.*

Walsh and C. F (2001). Electrochemical technology for environmental treatment and clean energy conversion. Research Triangle Park, NC, ETATS-UNIS, Pure and applied chemistry.

*Walsh, F. C. and G. W. Reade (1994). Electrochemical Techniques for the Treatment of Dilute Metal-Ion Solutions. Studies in Environmental Science. C. A. C. Sequeira, Elsevier. **Volume 59:** 3-44.*

*Wang, S., K. Qian, et al. (2009). "Influence of Speciation of Aqueous HAuCl4 on the Synthesis, Structure, and Property of Au Colloids." The Journal of Physical Chemistry C **113**(16): 6505-6510.*

*Weber, K. A., L. A. Achenbach, et al. (2006). "Microorganisms pumping iron: anaerobic microbial iron oxidation and reduction." Nat Rev Micro **4**(10): 752-764.*

WHO. (2004). "Water, sanitation and hygiene links to health: facts and figures." Retrieved March 31st 2011, from http://www.who.int/water_sanitation_health/en/factsfigures04.pdf.

*Widmer, R., H. Oswald-Krapf, et al. (2005). "Global perspectives on e-waste." Environmental Impact Assessment Review **25**(5): 436-458.*

*Yin, P., Q. Yu, et al. (1999). "Biosorption removal of cadmium from aqueous solution by using pretreated fungal biomass cultured from starch wastewater." Water Research **33**(8): 1960-1963.*

Chapter 2: Theory in relation to electrochemical, microbiological and bioelectrochemical metal ion remediation

Chapter 2: Theory in relation to electrochemical, microbiological and bio-electrochemical metal ion remediation

2.1 *Introduction*

This research comes under the umbrella of the scientific subfields of (electro)chemistry and (micro)biology which even though having evolved from similar routes, have considerably different outlooks and often can fail to agree because one is often looking at data at hand through the prism of different sub-paradigms, perceptions and values.

To overcome any vagueness in communication an overall paradigm will be applied to this thesis based on a qualitative description of chemical, electrochemical and bio-electrochemical reaction mechanisms, a thermodynamic analysis of energy transformations of the system with its surroundings and a quantitative analysis of microbial biosorption kinetics. This forming the foundation for a comparison and analysis of changes in reaction mechanisms and fundamental qualitative comparison of the associated (Gibbs) free energy of microbiological, electrochemical and bio-electrochemical reactions described by a state of equilibrium and the modelling of kinetics in journey there or in departure there upon.

2.2 *Electrochemical phenomena in relation to metal remediation*

The study of electrochemistry can be divided into two branches of ionics and electrodics (Conway and Salomon 1967). Our investigations here focuses on the electrodics of metal ion electronation as remediation strategies by phase change electrochemical reactions at an electrified interface (Figure 2.1) in excess or deficiency of charge. Electrochemical systems usually consist of charge carriers which can be utilised to do some purpose. Where the solid conducting substrate (electrode) is charged with electrons and a negative charge is built up and opposed by positive charge in the liquid conducting medium (electrolyte) containing ionic charge carriers.

A structural depiction of the particles in solution at an electrified interface is of great importance when finding possible explanations for changes in reaction mechanisms,

changes in reaction free energies and/or reaction dynamics by the addition of live electroactive bacterial cells to the electrolyte.

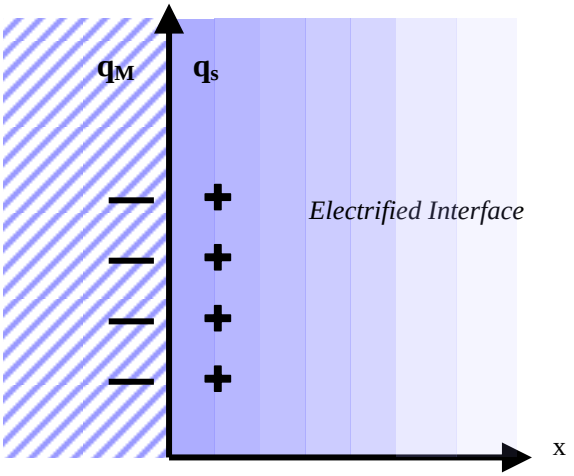

Figure 2.1 : The electrified interface.

Our reacting ionic species make a long intricate journey from the homogenous bulk phase through a Nernst diffusion film layer to the area closest to electrode surface described as the Helmholtz layer (thickness ≈ 10 Å). Here electron tunnelling from the surface of the charge carrier to (electronation) ionic species, or from (de-electronation) ionic species, located in the inner Helmholtz layer, can be controlled by application of potential (or current) in an electrochemical cell. These electrons then pass through an external circuit from the anode (the electron source) to the cathode (the electron sink).

A further dichotomy can be illustrated if the electrochemical transformation occurring at our electrified interfaces(s) leads to the spontaneous production of current (e.g. a battery) the electrochemical cell is deemed a galvanic cell. If a current (or energy) input is required for specified transformations (such as metal ion deposition) the electrochemical cells is deemed an electrolytic cell, the later of most relevance to our investigation.

2.2.1 The electrode electrolyte interface of aqueous effluents containing metal ions

Figure 2.2 gives a systematic elementary qualitative representation of a boundary interface between the solid electrode and liquid electrolyte phases, including an inner layer which describes the area closest to the electrode surface (Bockris and Reddy 1970).

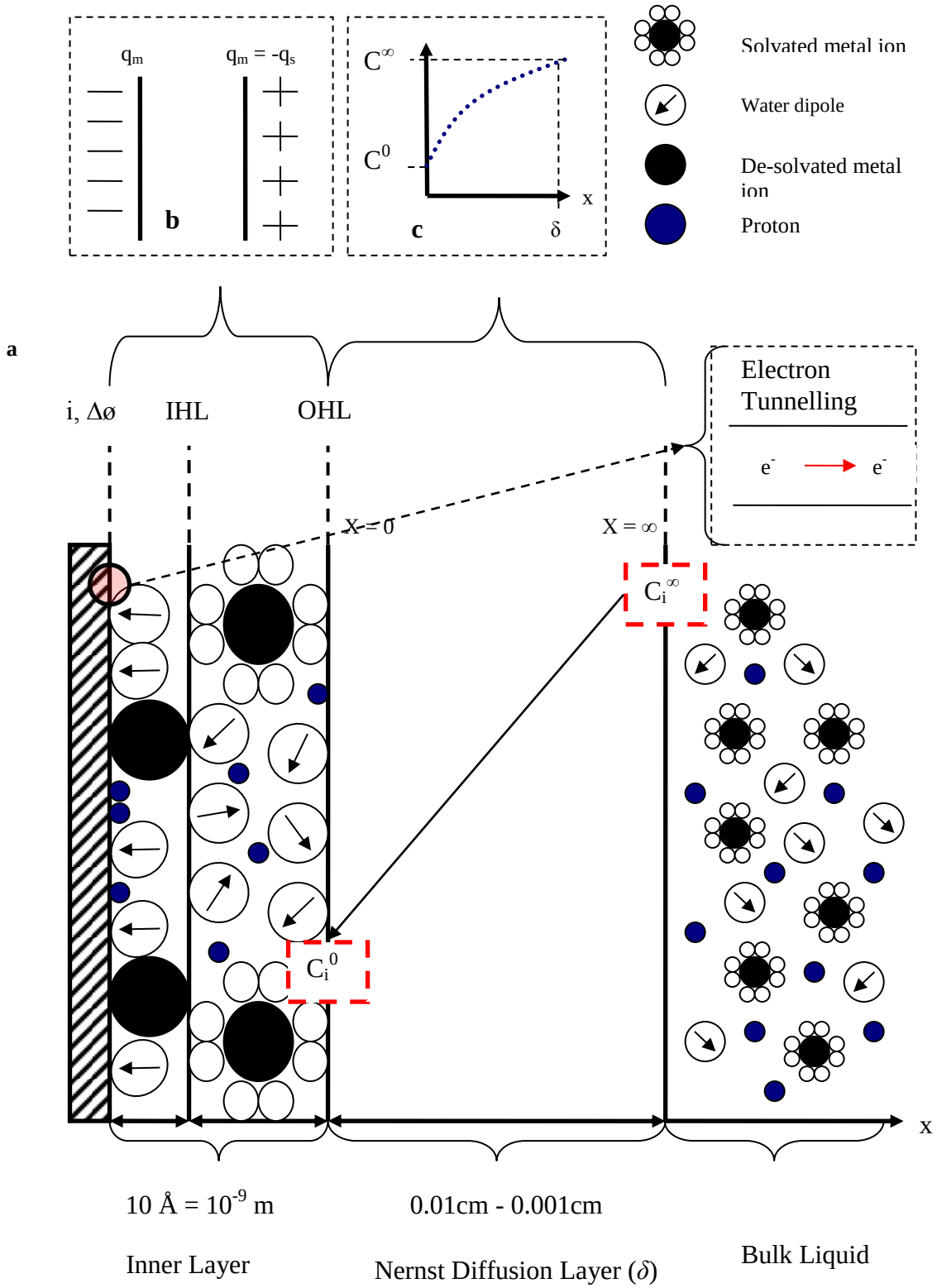

Figure 2.2 : (a) The electrochemical double layer. (b/c) Concentration profile for electroactive species through the Nernst diffusion layer to the outer Helmholtz layer where δ is the diameter of the Nernst diffusion layer the thickness of which depends on forced convective mixing and electrolyte properties.

For an electrode surface charged in excess of free electrons the IHP consists of a hydration sheath of water molecules and de-solvated ions specifically adsorbed to the electrode surface while OHP consists of solvated ions and a second hydration sheath of water molecules loosely bound to the electrode surface. In the simplest case the excess charge density at the OHP is due to the locus of solvated ions equal and opposite to the excess charge on the electrode surface, the electrical equivalent being a capacitor (Bockris and Reddy 1970). Reactions in the electrified interphase may also involve adsorption phenomena, with the accumulation of particles in the interphase region (Conway 1965).

The inner layer can be further described to consist of an inner Helmholtz (IHL) and outer Helmholtz layer (OHL). This double layer describes the basic anisotropic phenomena at an electrified interface in contrast to the isotropic nature of the bulk solution outside of this interface.

2.2.2 Liquid conducting phase: the Nernst diffusion layer and bulk solution.

The Nernst diffusion layer describes the stagnant volume which extends out from the OHP where transport is chemical diffusion controlled; the thickness of this layer depends largely on bulk conditions governed by electrode geometry, kinematic viscosity, diffusion coefficient of ions or anions in solution and the velocity of stirring of the electrode or electrolyte. Diffusion described by a “random walk” of atomic or molecular species from a location of high concentration to low concentration (Crank 1975). From the Nernst diffusion layer one is lead to the bulk solution which describes the area outside of the charge transfer interface. Properties of the ions in solution can be described as isotropic and unaffected by the electrical interface. In dilute aqueous solutions, ions enter into interactions with solvent molecules and become wrapped in solvent sheaths, the properties of which are described by solutions ionics (Bockris and Reddy 1970).

2.2.3 Solid conducting phase: Pt, Au and graphite electrode surface chemistry

Experiments for bioelectrochemical remediation of metal ions will focus upon graphite electrodes upon previous investigation (Gregory, Bond et al. 2004). Nobel electrodes

were first used to investigate respective metal ion reactions for comparison to experiments with graphite electrodes shown to be suitable materials for both metal plating and electron transfer with electroactive bacterial cells. The surface chemistry of noble and carbon based electrodes charge carries would differ. Nobel metals forming an passive oxide films approximately 1-10 nm thick and graphite surfaces have a layered, planar structure wherein each layer, the carbon atoms are arranged in a hexagonal lattice.

Both platinum and gold form passive oxide layers upon exposure to oxygen where break down of these layers occurs only for high anodic potentials via formation of an oxide film. Break down of this oxide layer occurs for potentials greater than 1.260 V vs. Ag/AgCl for gold (Burke, Buckley et al. 1994) and between 0.6 and 1.3 V vs. Ag/AgCl for platinum (Burke, Casey et al. 1993). Rand and Woods report high degree of oxygen adsorption upon platinum and gold electrodes while negligible adsorption of hydrogen for gold for potentials where hydrogen gas is evolved (Rand and Woods 1972).

Nearly all carbon materials are prone to reactions with oxygen and water forming surface oxides with considerable electrochemical effects on adsorption and electrochemical kinetics (McCreery 2008). Graphite forms two types of oxides in acid media a protective oxide (graphite oxide) and a surface oxide which forms upon the former surface (Guenbour, Iken et al. 2006). Cyclic voltammetry study by Guenbour et al. confirmed high chemisorption of molecular oxygen upon graphite surfaces (Guenbour, Iken et al. 2006).

2.2.4 Electrochemical ion reduction (electronation) and electrodeposition

Electroreduction (or electronation) of a metal ion occurs in the inner Helmholtz layer where electrons tunnel from the electrode surface to the ions adsorbed or located at electrode surface. The overall process may involve a number of steps (Conway 1965):

1. Mass transfer of the metal ions through a "stagnant" liquid film (Nernst diffusion layer) to the Helmholtz layer.
2. De-solvation of the hydration sheath around the metal ions and localization of metal ions to the inner and outer Helmholtz layer.

3. Chemical reactions pre or proceeding electron transfer leading to electronucleation or alteration of the ionic charge of the metal ion by the gain or loss of electrons.
4. Incorporation of the product of electro-reduction into the lattice of the electrode or elimination of the product from the electrode surface which usually occurs by surface diffusion processes.

A simplified view of the rate of electroreduction of metal ions could be limited to electronation of metal ions located in the inner layer of the electrified interface or the transported of metal ions through the Nernst diffusion layer to the Helmholtz inner layer. A basic dichotomy can be used to describe the overall rate of reactions of importance to water remediation strategies, where the rate limiting (slowest) step would be charge transfer (electronation or de-electronation) to ionic species by electron tunnelling occurring in the IHL where low interfacial potentials are applied. Or where significantly higher potentials are applied to the electrode interface, the charge transfer at the IHL will be significantly faster and the overall rate of reaction would be limited by the (slower) diffusion of metal ions through the Nernst film diffusion layer from the bulk electrolyte solution. The thickness of this diffusion layer being the key parameter in increasing the rate of reaction further and could be reduced by efficient mixing of the solution by rotation of the electrode or agitation of the electrolyte.

2.2.5 Metal ion electronation reaction mechanism

A summary of bulk ionic reactions and Helmholtz layer inner and outer layer electrodics charge transfer reactions are given here and illustrated in Figure 2.3. Although investigation regarding changes in reaction mechanisms and limiting "bottlenecked" change transfer reaction with electroactive bacteria added to the solution is beyond the scope of this project. They are given here as the basis for future theoretical impending investigation discussed in chapter 5.

Bulk Solution hydration of metal cations and proton molecules by water dipoles (Bockris and Reddy 1970) :

$$M^{3+} + 6H_2O \rightarrow M(H_2O)_6{}^{3+} \qquad (2.1)$$

$$M^{2+} + 6H_2O \rightarrow M(H_2O)_6{}^{2+} \qquad (2.2)$$

$$M^{3+} + SO_4^{2-} \rightarrow MSO_4^{+} \quad (2.3a)$$

$$M^{3+} + 2SO_4^{2-} \rightarrow M(SO_4)_2^{-} \quad (2.3b)$$

$$M^{3+} + 3SO_4^{2-} \rightarrow M(SO_4)_3^{3-} \quad (2.3c)$$

Outer Helmholtz layer de-solvation of metal cation (Bockris and Reddy 1970) :

$$M(H_2O)_6^{n+} \rightarrow M^{n+} + 6H_2O \quad (2.4)$$

Inner Helmholtz layer proton reduction (Bockris and Reddy 1970) :

$$2(H_3O^{+} + e^{-} \rightarrow H_{(ads)} + OH^{-}) \quad (2.5)$$

$$H_{(ads)} + H_{(ads)} \rightarrow H_2 \quad (2.6)$$

Trivalent iron Fe^{3+} electroreduction (in sulphate base electrolyte) (Samec and Weber 1977; Gil, Salgado et al. 1995) :

$$M(H_2O)_6^{3+} + e^{-} \rightarrow M(H_2O)_6^{2+} \quad (2.7)$$

$$M(SO_4)^{+} e^{-} \rightarrow MSO_4 \quad (2.8)$$

$$M(SO_4)_2^{-} + e^{-} \rightarrow M(SO_4)_2^{2-} \quad (2.9)$$

$$M(SO_4)_3^{3-} + e^{-} \rightarrow M(SO_4)_3^{4-} \quad (2.10)$$

Trivalent electrodeposition of $AuCl_3^{-}$ (Harrison and Thompson 1973) :

$$MCl_3^{-} \rightarrow MCl_{3(ads)} \quad (2.11)$$

$$MCl_{3(ads)} + 2e^{-} \rightarrow MCl_{(ads)} + 2Cl^{-} \quad (2.12)$$

$$MCl_{(ads)} + e^{-} \rightarrow M + Cl^{-} \quad (2.13)$$

Divalent cobalt Co^{2+} and ferrous iron Fe^{2+} electrodeposition leading to electronucleation and electrocrystallization (Bockris, Drazic et al. 1961; Soto, Arce et al. 1996; Jeffrey, Choo et al. 2000) :

$$M^{2+} + H_2O \rightarrow MOH^{+}_{(ads)} + H^{+} \quad (2.14)$$

$$MOH^{+}_{(ads)} + e^{-} \rightarrow MOH_{(ads)} \quad (2.15)$$

$$MOH_{(ads)} + H^{+} + e^{-} \rightarrow M + H_2O \quad (2.16)$$

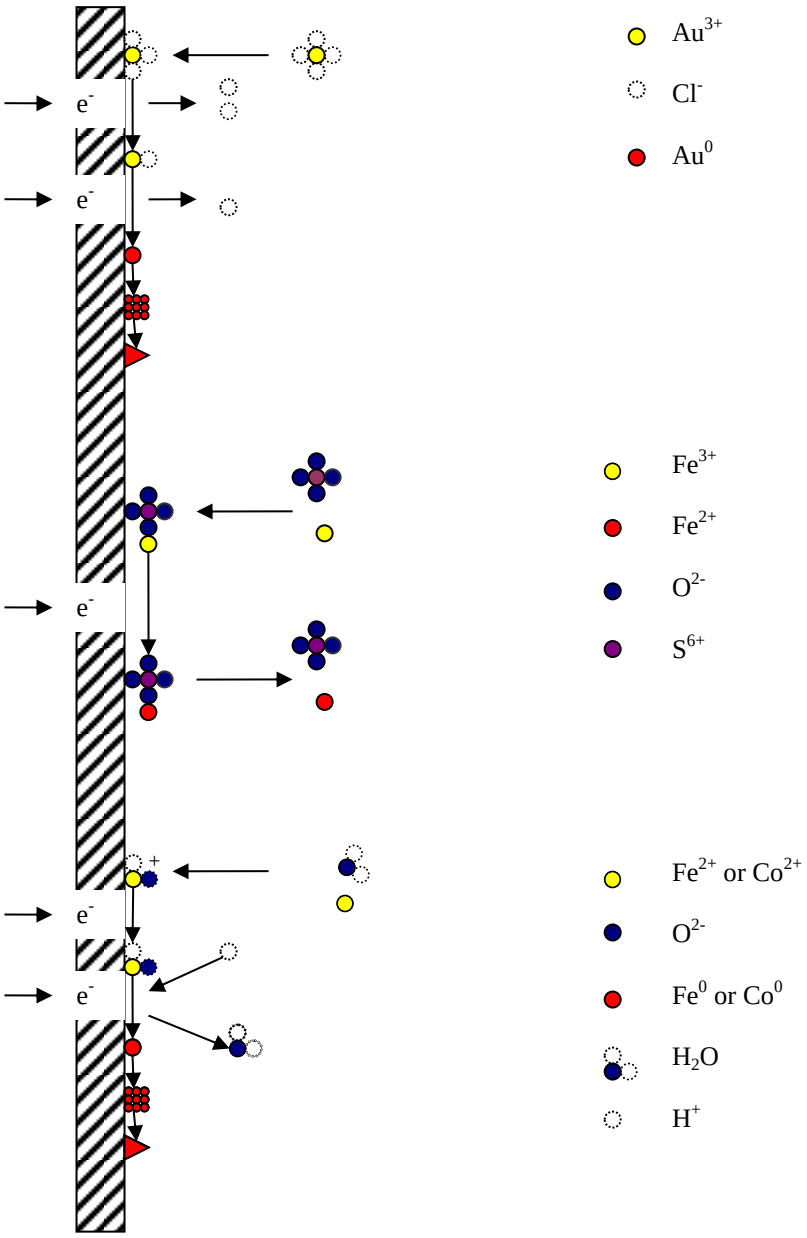

Figure 2.3 : Summary of reaction mechanisms of metal-ion located in the electrified interface.

2.3 *Microbiological phenomena in relation to metal ion remediation*

2.3.1 Metal ions biosorption and bio-reduction interface

While virtually all biological material have some affinity for toxic metals and radionuclides (White, Wilkinson et al. 1995), some bio-molecules intra and extracellular media function specifically to bind metals and are induced in their presence. The cell envelope (microbial charge transfer and adsorption interface) of Gram-negative

bacteria, applied in this research is illustrated by Figure 2.4 and 2.5, consists of a cytoplasmic inner phospholipid bilayer surrounded by a murin pepitidoglycan (PG) cell wall. The PG is anchored via Braun lipoprotein to an inner phospholipid outer membrane leaf and outer lipopolysaccharide (LDS) layer. The outer membrane constituting of proteins and porin channels, that allow exchange of low molecular weight chemical species (Madigan and Brock 2009). The LDS is also thought to play an important role in the binding of metal ions to the cell exterior (Haas, Dichristina et al. 2001).

The LDS consists of an O-Polysaccharide complex which projects a R-Core polysaccharide linked via ketodeoxyoctonoate (KDO) to lipid A. The O-Polysaccharide consists of a branched repeating sequence of sugars such as galactose, rhamnose, mannose, N-acetylabequose etc. The composition of the outer membrane LDS leaf of *S. putrefaciens* characterised by Moule and Wilkinson (Moule and Wilkinson 1989) who reported it to composed of a number of ionized groups such as carboxyl ($R\text{-}COO^-$), amine ($R\text{-}NH_2$) and phosphoryl ($R\text{-}POO^-$) which collectively contribute to the binding of metal ions by an electronegative charge on the cell membrane.

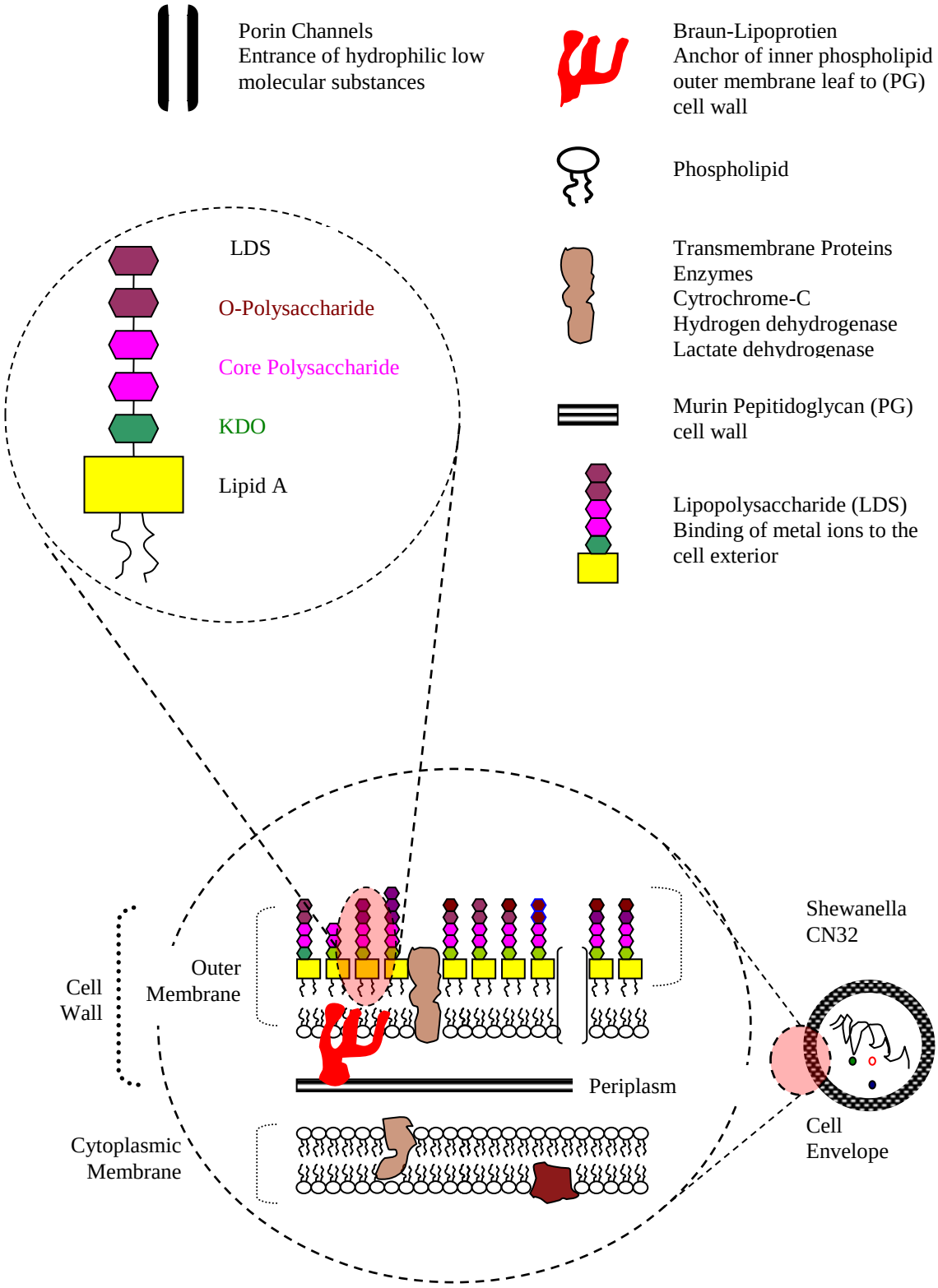

Figure 2.4 : Microbiological biosorption of metal ions.

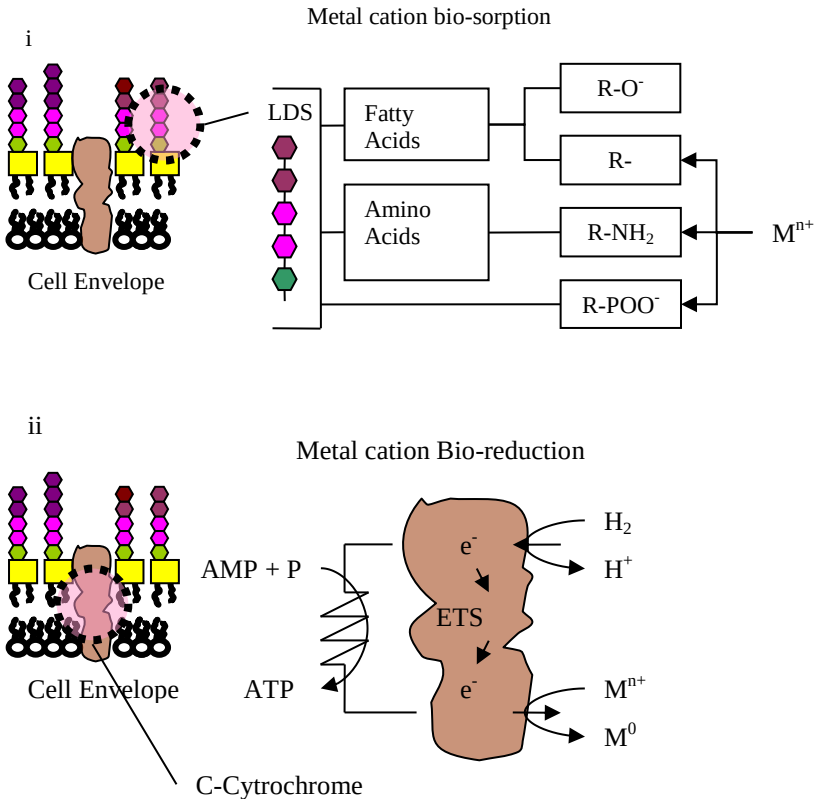

Figure 2.5 : Microbiological biosorption of metal ions (i) metal ion bio-complex (ii) metal ion bio-reduction.

Haas et al. (Haas, Dichristina et al. 2001) conducted acid-base potentiometric titrations and U^{6+} sorption experiments and reported that *S. putrefaciens* exhibited positive charged surfaces in low pH environments. Their study also reported strong U^{6+} sorption at pHs as low as 2 which goes against surface complexation theory (Daughney and Fein 1998), which predicts that a net positive charged surface would repel cations such as Au^{3+}, Co^{2+} and Fe^{3+} electro-statically. A potential explanation they gave was that positive charges on the bacterial surface tend to be localized. A separation of greater than ~1 nm would be greater than the thickness of the electrical double layer, allowing each point charge to interact quasi-independently with ions in the surrounding solution.

2.3.2 Dissimilatory transformations of metal ions in relation to metal ion remediation

For a bacterial cell to replicate and so pass on its genetic heritage (DNA) it must coordinate a number of chemical reactions and organise molecules into specific

structures, collectively referred to as cell metabolism. Thereby allowing the cell to conserve energy and grow. There are two forms of energy conservation in chemoorganotrophs, fermentation and respiration. In fermentation the redox process occurs in the absence of exogenous electron acceptors whereas in respiration molecular oxygen or some other electron acceptor is present.

The basic energy unit of biological cells is adenosine triphosphate (ATP) which consists of ribonucleoside adenosine to which three phosphate molecules are bonded in series. ATP is an energy rich phosphorylated compound. The hydrolysis of ATP to adenosine monophosphate (AMP) and AMP to adenosine diphosphate (ADP) releases approximately 32 kJ/mol (Madigan and Brock 2009).

This method of respiration can be utilized for various cellular functions. The mechanisms of ATP synthesis by respiration and fermentation differ significantly. In fermentation ATP is produced by substrate-level phosphorylation by the catabolism of an organic compound. In contrast respiration occurs by oxidative phosphorylation where ATP syntheses occurs by the generation of a proton motive force (PMF). The PMF is a form of potential energy which the cell can use for functions such as ATP biosynthesis and microbial locomotion by means of rotating flagella.

Aerobic respiration utilizes $O_2(g)$ as the terminal electron acceptor. A number of microorganisms have been shown to be able grow in anaerobic conditions by coupling the oxidation of inorganic electron donors such as H_2 and utilizing a range of electron acceptors such as ionic transitional metals such as Fe^{3+}, Mn^{4+}, radionuclide's such as U^{6+} and Tc^{7+} and heavy metals such as Cr^{3+} (Liu, Gorby et al. 2002; Lloyd 2003), precious metals such as Au^{3+} (Konishi, Tsukiyama et al. 2006; Konishi, Tsukiyama et al. 2007), $PtCl_6^{2-}$ (Konishi, Ohno et al. 2007) and Pd^{2+} (Windt, Aelterman et al. 2005) and other compounds such as nitrate and sulphate (Madigan and Brock 2009).

Oxidation-reduction reactions for electron transfer from the primary donor to the terminal acceptor are carried out by several protein enzymes. Such as NADH dehydrogenases, flavoproteins, iron-sulphur proteins and cytochromes which contain an iron atom in its heme and non-protein quinones containing hydrophilic molecules (Madigan and Brock 2009). The mechanisms of dissimilatory process have been studied

in great detail (Myers and Nealson 1990) and two mechanisms can be put forward here, direct and indirect electron transfer.

The b and c-type cytochrome in the electron transport chain (oxidative phosporolation) has been implicated in the "direct" electron transport to metal ions (Madigan and Brock 2009). A number of soluble "election shuttles" such as quinones-containing humic acids are utilized as electron acceptors by certain prokaryotes in the "indirect" electron transport to soluble metal ions and metal precipitates. The oxidized electron shuttles are then able to transfer electrons to Fe^{3+} minerals. Certain bacteria have also been reported to synthesize pili and flagella (Gorby, Yanina et al. 2006) when grown in anoxic conditions on insoluble Fe^{3+} minerals thus allowing movement, attachment and dissimilatory metabolic activity with Fe^{3+} minerals.

2.3.3 Microbiological redox-resistance transformations of metal ions

The microbial resistance transformations of metals and metal compounds by microorganisms can fall into two broad categories; oxidation or reduction of the inorganic forms (MRRT) and conversions from inorganic to less toxic organic forms (Nies 1999). This project will focus on MRRT of Co^{2+} and Fe^{2+} in aqueous effluents. Metal transformation by microbiology may involve the following pathway (Nies 1999).

1. Surface binding of metal cation to cell membrane or cell wall
2. Translocation of the metal cation into the cell (intraparticular diffusion)
3. (a) Redox-transformation by microbial enzymes (b) bio-precipitation of metal by the formation of metal-containing precipitates (c) active efflux
4. Detoxification of the metal ion by bio-transformation

Most metal ions are transported in and out of the cell against huge concentrate gradients. Translocation across the boundary layer (cell wall or cell membrane) of the cation is usually slower and requires some form of energy such as ATP or proton motive force (Madigan and Brock 2009). There are three common systems for transporting substances across cell boundaries (Madigan and Brock 2009).

(a) Simple transport, driven by energy in the proton motive force

(b) Group translocation, involving chemical modification of the transported substance
(c) The "ABC" system, consuming ATP as an energy source and utilizing periplasmic proteins

The cell boundary is the primary barrier to elevated metal ions in solution, but in some cases toxic metals are surface binded and translocated by systems normally employed for other essential metals (Dietrich H 1992). Also "the open gate situation" (Nies 1999), involving the fast uptake of heavy metals by unspecific protein transporters such the membrane-integral protein CorA is also possible. These are driven by chemiosmotic gradients in the cytoplasmic membrane and are continuously expressed and require less energy, as opposed to specific, slow systems requiring costly ATP hydrolysis (Nies 1999).

Once inside the cell, the metal-cation may inhibit the functioning of sensitive enzymes or interact with other physiological ions thereby inhibiting their function. Due to the transport of toxic metal cations mistaken as essential metal cations and the "open gate situation" microorganisms have developed during their evolution metal-ion homeostasis factors and metal-resistance determinates. Detoxification of the metal cation, generally involve a combination of three mechanisms (Silver 1996). (a) Active extrusion of the metal cation by efflux. (b) Segregation of the cation into complex compounds. (c) Reduction of the metal ion to a less toxic oxidation state (of particular interest in this study).

We here aim to further investigate the biosorption and bioreduction reaction mechanisms, thermodynamics and dynamics of the process with the aim to quantitatively compare and integrate microbiological and electrochemical metal ion reduction processes for social remediation strategies. Eq^{n} 2.17 – 2.23 describes reaction in the overall biosorption of metal summarised in Figure 2.6 of bio-oxidation (hydrogen used as electron donor), bio-reduction, bio-precipitation and bio-nucleation (metal ions used as an electron accepter or reduced as part of redox resistance mechanisms at our microbiological charged transfer interface.

$a : C_0''' \rightarrow C_0'' :$ *External diffusion* *(2.17)*

$b : C_0'' \rightarrow C_0' :$	*Film diffusion*	*(2.18)*
$c : C_0' \rightarrow C_0 :$	*Intra-particular diffusion*	*(2.19)*
$d : C_0 + [A]_{(surface)} \rightarrow [A]\text{-}C_0 :$	*Bio-complexion*	*(2.20)*
$e : (i)\ M^{n+} + e^- \rightarrow M^{m+}$	*Bio-reduction*	*(2.21)*
$e : (ii)\ M^{n+} + ne^- \rightarrow M$	*Bio-nucleation*	*(2.22)*
$e : (iii)\ H_2 \rightarrow H^+ + 2e^-$	*Bio-oxidation*	*(2.23)*

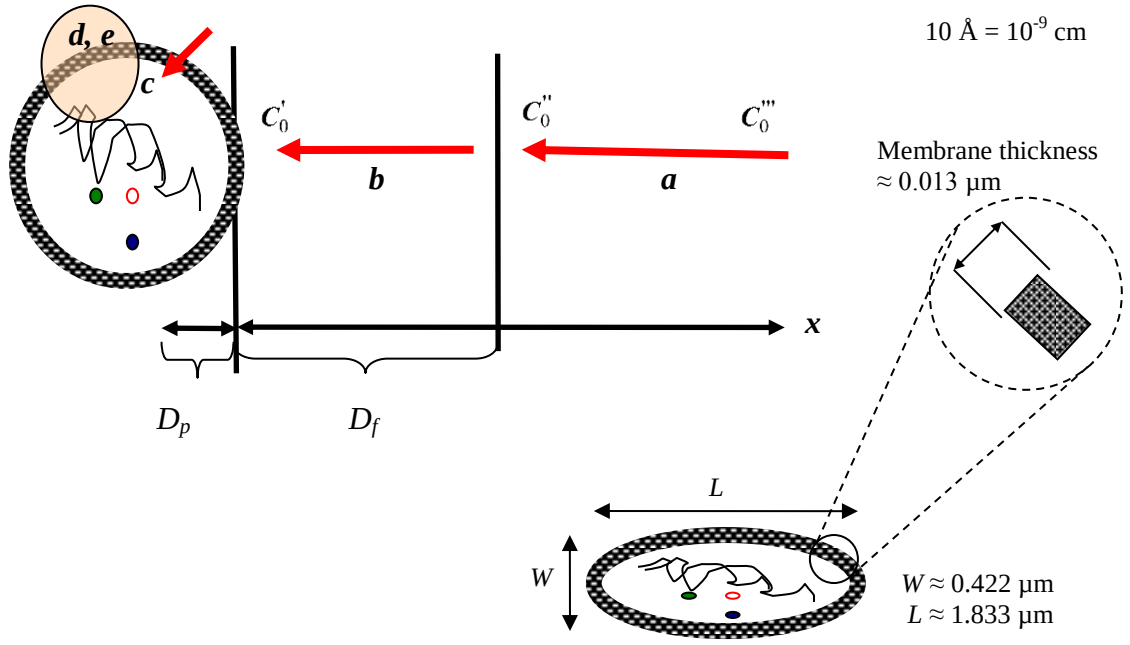

Figure 2.6 : Summary of intermediate bio-adsorption reaction mechanisms of metal ion biosorption at the microbiological interface [1].

2.4 *Bio-electrochemical phenomena : the interaction of electroactive bacterial and the electrified interface*

Bacteria may enhance electrochemical electronation phenomena, leading to remediation of metal ions. Two key variables in the determination of the process will be the free energy required for heterogeneous electroreduction processes evaluated from cyclic voltammetry and determination of reverse potentials (E_r) and the time required in carrying out the conversion. Reactions in our system may occur, if at all, only at high overpotential because of slow kinetics, i.e. such reactions have a low exchange current density i_o. Although we unable to carry out experimentation upon possible bio-catalysis

[1] Size of bacteria based on TEM imagery of control bacteria cultures elaborated more in chapters 3.

of electronation reaction by bacterial cells we were able to evaluate changes in reaction thermodynamics described in chapter 4.

Figure 2.7 summaries symbiotic reaction mechanisms which could also be employed for metal remediation strategies. The key initiative as discussed in chapter 1 being the simultaneous biosorption by bacterial cells and electrodeposition of metal ions at the electrified interface. Where bacteria also respire directly upon the electrode surface or via hydrogen evolution as the electron donor and reduce metal ions in as the terminal electron acceptors in dissimilative respiration or resistance mechanisms.

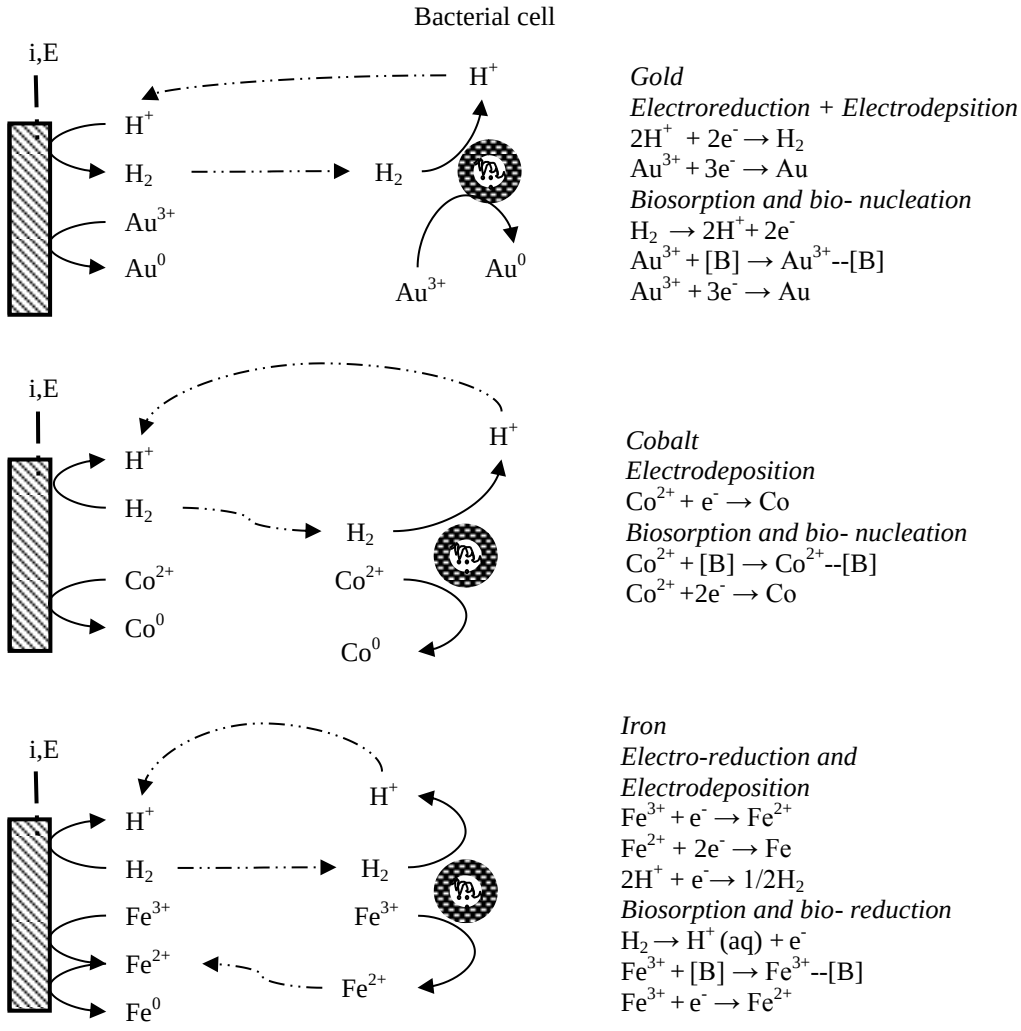

Figure 2.7 : Bioelectrochemical process regarding (a) gold, (b) cobalt and (c) iron in bioelectrochemical systems.

2.5 *Thermodynamics of electroreduction and biosorption of metal ions*

Thermodynamics is principally a study of the transformations of energy into heat and work and vice versa (Atkins 2001) as described by Figure 2.8. Fundamental to chemistry it describes key concepts as to why reactions reach equilibrium, their composition at equilibrium and also of key relevance to this research, how these reactions can be used in bioelectrochemical systems to carry out specific processes.

Gibbs free energy ΔG is the fundamental parameter for evaluation of energy costs of electrochemical, microbiological and bioelectrochemical reduction of metal ions and will be applied in this investigation forth with.

A fundamental definition of Gibbs free energy (ΔG) incorporates the state functions of internal energy (U), enthalpy (H) and entropy (S). Which leads to eq^{n} 2.25 which describes change in Gibbs free energy (G) in terms of change of system enthalpy and entropy at constant temperature and pressure, see Appendix A2.1. The apparent driving force of spontaneous change is the tendency of energy and matter to become disordered quantitatively described by a change of entropy of the system and surroundings.

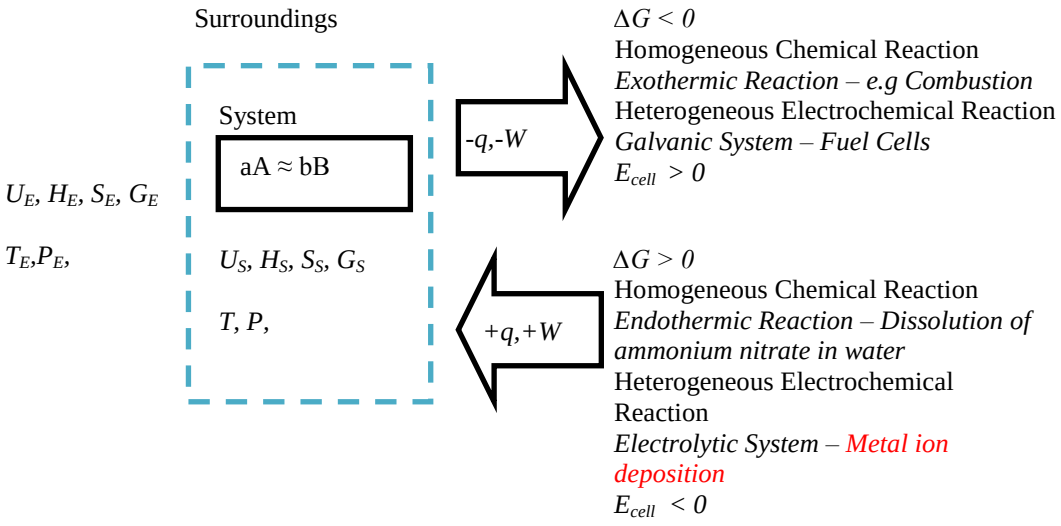

Figure 2.8 : Thermodynamic system.

Gibbs free energy is therefore a thermodynamic parameter describing the total entropy change in terms of system (or reactions occurring under study to carry out a process) properties alone. From the 2nd law of thermodynamics, the entropy of the universe tends to increase and thus from eq^{n} 2.24 and 2.25 we can reason that a reaction that

occurs spontaneously would lead to an increase in the total entropy ($TdS_{total} > 0$) of the system and surroundings and therefore a negative Gibbs free energy ($dG < 0$) at constant temperature. The reverse also holds where a positive Gibbs free energy ($dG > 0$) would be indicative of a decrease ($TdS_{total} < 0$) in the total entropy of the system at constant temperature and can be deemed a non-spontaneous reaction. Thus the input of energy required to drive a chemical, electrochemical or (micro)biological reaction, can be thought as entropic barriers to reaction mechanisms.

$$dS_{total} = dS + dS_{surr} \quad (2.24)$$

$$dG = -TdS_{total} = dH - TdS \quad (2.25)$$

2.5.1 Chemical and electrochemical thermodynamics of electronation and electrodeposition reactions

An electrochemical reaction is a heterogeneous chemical process involving the transfer of charge to or from an electrode such as metal, carbon or semi-conductor. Starting from fundamentals, the reaction Gibbs energy ΔG_r (J/mol) for the chemical reaction below (eq^n 2.26) is described by eq^n 2.27 and eq^n 2.28 where μ_i is the chemical potential of species i (J/mol). The equilibrium constant K is defined by eq^n 2.29 and species activity by eq^n 2.30. Where the activity coefficient γ_i is an empirical parameter, the activity a_i of the species i can be approximated in dilute systems as molar concentration C_i (mol/ cm^3) (Atkins 2001).

$$aA + bB \rightleftharpoons cC + dD \quad (2.26)$$

$$\Delta_r G = \Delta_r^0 G + RT \ln[K] \quad (2.27)$$

$$G = n_A \mu_A + n_B \mu_B \quad (2.28)$$

$$K = \frac{[C]^c[D]^d}{[A]^a[B]^b} \quad (2.29)$$

$$a_i = \lambda_i C_i \quad (2.30)$$

Industrial process are generally not allowed to reach equilibrium but knowing where equilibrium lies in favour of reactants and products under certain condition is an indication of the feasibility of a process. The link for redox systems and classical

thermodynamics described above being that an electrolytic cell is a device for using energy for non-spontaneous reactions as non-expansive work, described by eq^{n} 2.31, where W_e is electrical work (J/mol) carried out by the system. In an electrolytic cell, the work that a given transfer of electrons can do depends on the potential difference E_{cell} (V) between the two electrodes described by eq^{n} 2.32, where E^{e}_{cell} (eq^{n} 2.33) describes the equilibrium standard cell potential and E^{c}_{e} and E^{a}_{e} are cathodic and anodic equilibrium potentials and F is Faraday's constant (col/mol).

$$\Delta_r G = -W_e(\max) \qquad (2.31)$$

$$\Delta_r G = -nFE^{e}{}_{CELL} \qquad (2.32)$$

$$E^{e}{}_{CELL} = E^{e}_{c} - E^{e}_{a} \qquad (2.33)$$

A thermodynamic (Nernstian) discussion would conclude that for system negative free energy (and positive cell potential) the overall cell reaction in an electrolytic cell would occur spontaneously with the flow of current through the external circuit, defined as a galvanic cell. Examples of some relevance to this research being microbial fuel cells where electroactive bacteria are generally applied in the anodic chamber of cell and are able to biocatalyse organic wastewater degradation and respire upon the electrode surface (Logan, Hamelers et al. 2006). In a system with a positive free energy (and negative cell potential), the reactions are non-spontaneous and require an input of energy to drive the chemical change, as are the cathodic metal ion electronation reactions of relevance to environmental remediation processes.

The absolute potential difference or Galvani potential ($\Delta\Phi$) between the electrode under study (working electrode) (Φ_E) and electrolyte (Φ_S) can be conceptualised as charge (outer) and dipole (surface) contributions (Bockris and Reddy 1970). The outer potential, $\Delta\Psi$ can be perceived as the work done in bringing a "test" charge in the interfacial region to the surface of the charged interface. The dipole-dependent surface potential, $\Delta\chi$ potential described the work done in taking this test charge across the charged surface interphase with a dipole layer. Thus the work done for the transportation of a charge in the interphase region to a point into the charged surface phase wrapped in a dipole layer can be described by eq^{n} 2.34, further elaborated by Figure 2.9. This can be conceptualised with two "thought experiments" involving the

transfer of a test positive charge in a vacuum. Where the outer potential (Figure 2.9a) represents the electrical energy necessary in bringing a "test charge" in electrical interfacial region from "∞" to the surface of the electrified interface which has had its dipole layer removed and the surface potential (Figure 2.9b) represents the electrical energy necessary in taking a "test charge" across an uncharged surface inter-phase surrounded by a dipole layer.

$$\Delta\phi = \Delta\Psi + \Delta\chi \qquad (2.34)$$

The chemical and electrochemical potential can be described by eq^{n} 2.35 and eq^{n} 2.36 of a particular species *i*. The change in electrochemical potential (eq^{n} 2.37) of a species at an electrified interface describes the total work required to bring species *i* from the bulk of phase to the surface of the electrode and can conceptually separate into chemical (diffusive) forces and conductive (electrical) driving forces.

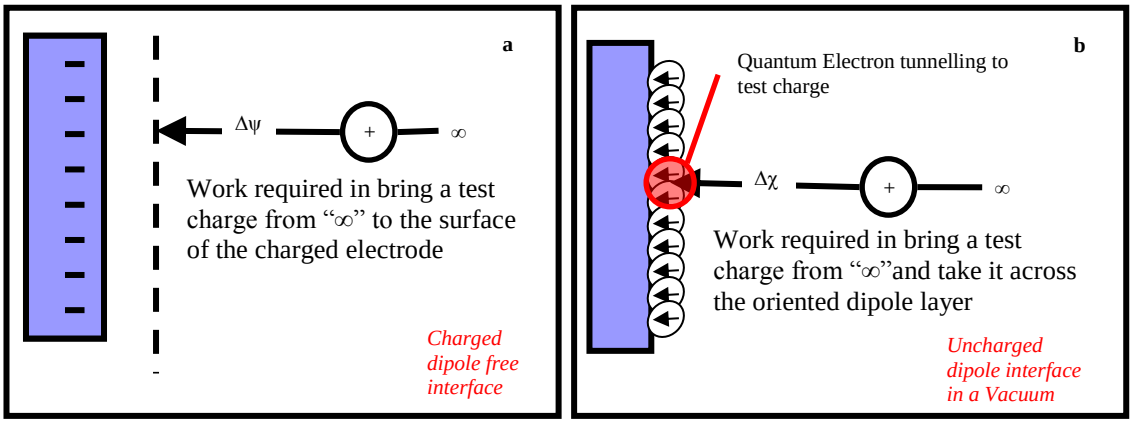

Figure 2.9 : (a) The transfer of a test charge to the surface of a charged interface free of the surrounding dipole layer in a vacuum, (b) the transfer of a test charge to the surface of an un-charged interface surrounded by a dipole layer in a vacuum.

$$\mu_i = \mu_i^0 + RT\,Ln[a_i] \qquad (2.35)$$

$$\overline{\mu}_i = \mu_i^0 + RT\,Ln[a_i] + n_i F\Phi \qquad (2.36)$$

$$\frac{\overline{\partial\mu_i}}{\partial x} = \frac{\partial\mu_i}{\partial x} + n_i F\frac{\partial\Phi}{\partial x} \qquad (2.37)$$

The absolute potential cannot be measured as the use of measuring instrument generates at least one other electrified interface (Bockris and Reddy 1970). But the introduction of a non-polarisable (reference) electrode allows the measurement of the relative potential values of the electrified interface E (Volta). The reversible potential (E_r) for an electrochemical reaction described by eq^n 2.38 can be predicted using the Nernst equation (eq^n 2.39) where K the equilibrium constant is defined by eq^n 2.40. E_r describes equilibrium potentials of electron transfer reactions where no net current is produced and the forward electronation and de-electronation reactions are in dynamic equilibrium. A shift in reversible potentials is a key indicator for changes in reaction thermodynamics with the addition of bacterial cells to the electrolyte and would be a key parameter for the evaluation of bacterial effects on the Gibbs free energy of electrochemical reactions occurring at a charged interface.

$$O + ne^- \rightleftharpoons R \tag{2.38}$$

$$E_e = E_e^\theta + \frac{RT}{nF}\ln\left[\frac{1}{K}\right] \equiv E_r \tag{2.39}$$

$$K = \frac{a_R}{a_O} \tag{2.40}$$

The absolute potential cannot be measured as the use of measuring instrument necessarily generates at least one other electrified interface. But the introduction of a non-polarisable (reference) electrode allows the measurement of the relative potential values of the electrified interface E (Volta). The reversible potential (E_r) for an electrochemical reaction calculated using the Nernst equation can compared to analysis of linear sweep voltammetry (using slow scan rates of 0.010 V/s) of the working electrode.

Though thermodynamics gives an indication of which reactions will occur in our system and the energy transformation that accompanies them it does not account for the rate of chemical change, which prior to the 1950's was deemed sufficient to describe electrochemical systems. Some electrode reactions are inherently fast and hence reactions can occur close to equilibrium potentials. Others are slow and hence will require a large deviation from equilibrium potentials quantified by an overpotential η (eq^n 2.41).

$$\eta = E - E_e \tag{2.41}$$

For a specific process one desires to carry out, reactions close to equilibrium potentials, as an increase in overpotential would lead to an increase in energy requirements and hence cost. Most processes on an industrial scale are carried out with large overpotentials where the overall charge transfer reactions are limited by mass transfer of reacting and reacted species through the Nernst diffusion layer. Taking this into account the cell voltage required to observe a current *I* (A) is given by eq^{n} 2.42 the product of OCP, overpotential and ohmic losses (Clauwaert, Aelterman et al. 2008), where open circuit potential (OCP) is a sum of reversible anodic and cathodic potentials described by eq^{n} 2.43. Overpotential losses as described by eq^{n} 2.44 are due to slow reaction kinetics with required activation potentials of electron transfer and concentration overpotentials associated with concentration gradients of reagents and products in proximity to the electrode surface. Finally, ohmic loss (eq^{n} 2.45) relates to potential losses through solid and liquid electron conducting interfaces. A reduction in required overpotentials to carry out a conversion for a specified time would be key parameter for optimization of the process.

$$E_{CELL} = OCV - \Delta E_{\eta} - \Delta E_{\Omega} \tag{2.42}$$

$$OCP = E_e^c - E_e^a \tag{2.43}$$

$$\Delta E_{\eta} = \Sigma \eta_a - \Sigma \eta_c \tag{2.44}$$

$$\Delta E_{\Omega} = I\, \Sigma R_{\Omega} \tag{2.45}$$

2.5.2 Thermodynamics of bacterial biosorption of metal ions using isothermal analysis

The semi-empirical hyperbolic Langmuir (eq^{n} 2.46) and empirical exponential Freundlich models (eq^{n} 2.48) were applied as isotherm models to describe the distribution of a metal ion between the solid and liquid phase at equilibrium, with extensive application hitherto in literature for the phenomenological modelling of the biosorption process of metal ions (Febrianto, Kosasih et al. 2009). Analysis of biosorption isotherms yield quantitative and qualitative information upon the

spontaneity of the reaction Assumptions and derivation of the models can be found in Appendix A2.2. Both models suggest a monolayer sorption mechanism. The Freundlich model assumes that the energetic distribution of sorption sites is heterogeneous, with lateral interaction between the sorbed molecules, while the Langmuir model hypothesises homogeneous distribution of sorption sites and sorption energies with no interaction between sorbed molecules.

$$q_e = \frac{q_{\max} K[C_e]}{1 + K[C_e]} \qquad (2.46)$$

$$\frac{1}{q_e} = \frac{1}{q_{\max}} + \frac{1}{(q_{\max} K) C_e} \qquad (2.47)$$

$$q_e = K_F (C_e)^{(1/n)} \qquad (2.48)$$

$$Ln(q_e) = Ln(K_F) + \frac{1}{n} Ln(C_e) \qquad (2.49)$$

$$\Delta G = -RT\ Ln[K] \qquad (2.50)$$

Linear forms of the sorption isotherms and were used as described by eq^n 2.47 and 2.49 where q_e (mmol/g or mg/g) is the equilibrium sorption capacity; q_{max} (mmol/g or mg/g) corresponding to complete monolayer coverage; K (L/mmol or L/mg) is the equilibrium constant; C_e is the metal ion concentration at equilibrium assumed as metal ion concentration at t = 24 h and K_F and n are Freundlich constants related to adsorption capacity and intensity of the sorbent respectively. Eq^n 2.50 can used to calculate the Gibbs free energy change for the bio-sorption process. Where ΔG (J/mol) is the Gibbs free energy change; R (J/K mol) is the gas constant; T (K) is the absolute temperature.

2.6 *Kinetics of metal ion electroreduction at an electrified interface and biosorption by bacterial cells*

2.6.1 Electrochemical kinetics of electroreduction and electrodeposition

Application of the electrochemical sciences were in many ways held back before the 1950's from the influence of Nernst (Bockris and Reddy 1970). Electrochemical sciences were based only on the thermodynamics, not taking into account the kinetics of reactions occurring in the system. Thus though the thermodynamic calculation for the

feasibility of a reaction to take place was never wrong, the full story was not given. Kinetics here is concerned with the rate of microbiological, electrochemical and bioelectrochemical reactions, i.e. how fast reactants are consumed and products formed and the possible increase in the rate of specified reaction in the presence of a perspective catalyst (Atkins 2001). Following classical chemical reaction kinetics, we can write an empirical expression in the form where the reaction order *r* can usually be assumed to equal 1, described as eq^{n} 2.51.

$$v_1 = \frac{dm(t)}{dt} = k_1 c^r \qquad (2.51)$$

For cathodic process described by eq^{n} 2.52, the charge required to convert *m* (mols) of starting material to product in a ne^{-} electron reaction is readily calculated using Faradays laws of electrolysis described by eq^{n} 2.53 where *F* is the Faraday constant (96 485 C/mol). Differentiation of eq^{n} 2.53 with respect to time gives the rate of reaction expressed for v_1 eq^{n} 2.54, v_2 eq^{n} 2.55 and v_3 eq^{n} 2.56, where *dm/dt* is the molar reaction rate (mol/s) , *N* is flux (mol cm^{-2} s^{-1}) and *dc(t)/dt* is the reaction rate (mol cm^{-3} s^{-1}), *k* the reaction rate constant and has units of cm^3/s, (eq^{n} 2.54) cm/s, (eq^{n} 2.55) or 1/s, (eq^{n} 2.56) and *C* the bulk concentration (mol/cm^3) of reactant metal ion.

$$O + ne^- \rightarrow R \qquad (2.52)$$

$$q = nmF = \int_0^t i dt \qquad (2.53)$$

$$v_1 = \frac{dm(t)}{dt} = \frac{I}{nF} = k_1 C_0 \qquad (2.54)$$

$$v_2 = \frac{1}{A}\frac{dm(t)}{dt} = \frac{I}{nAF} = k_2 C_O \qquad (2.55)$$

$$v_3 = \frac{dc(t)}{dt} = \frac{I}{nV_R F} = k_3 C_O \qquad (2.56)$$

2.6.2 Electronation kinetics: electron transfer limited reaction

The rate of a heterogeneous electron transfer process is dependent on the potential field close to the electrode surface ($x = 0$). Where electron transfer in the simplest case of one

electron transfer can be described by a hyperbolic sine type function, the Butler-Volmer equation (Bockris and Reddy 1970) (eq^{n} 2.57). Here β is the symmetry factor, describing the change in the activation energy barrier for the electron transfer reaction by the application of a moderate overpotential where the slowest (rate limiting) step of the overall reaction is the charge transfer step and can normally be approximated as 1/2 (Bockris and Reddy 1970). Eq^{n} 2.58 describes the more general description of the Butler-Volmer equation which is valid for a multistep overall electrodiotic reaction in which there may be more electron transfers other then the rate determining step (Bockris and Nagy 1973). Eq^{n} 2.59 and 2.60 described the relation between the symmetry factor and transfer coefficient where the rate determining step (RDS) reaction occurs υ times as part of the overall reaction involving $\overrightarrow{\gamma}$ reaction steps preceding and $\overleftarrow{\gamma}$ steps proceeding the RDS. With "*N*" reaction steps in the overall reaction mechanism and "*r*" electrons transferred in the rate determining step. Therefore the evaluation of the Tafel slope can give some indication of any changes in reaction mechanisms of electronation reactions when bacterial cells are added to the electronic bath.

$$i = i_0\left[\exp\left[\frac{(1-\beta)F\eta}{RT}\right] - \exp\left[\frac{-\beta F\eta}{RT}\right]\right] \qquad (2.57)$$

$$i = i_o\left[\exp\left[\frac{\alpha_a F\eta}{RT}\right] - \exp\left[\frac{-\alpha_c F\eta}{RT}\right]\right] \qquad (2.58)$$

$$a_c = \frac{\overleftarrow{\gamma}}{\nu} + r\beta \qquad (2.59)$$

$$a_a = \frac{N-\overrightarrow{\gamma}}{\nu} + r\beta \qquad (2.60)$$

For a cathodic process the currents from anodic reactions become insignificant to cathodic reactions and Butler-Volmer equation reduces to eq^{n} 2.61, taking the logarithm of which leads to the Tafel eq^{n} 2.62 .

$$i = -i_0\exp\left(\frac{-\alpha_c F\eta}{RT}\right) = -i_0\exp\left(-\frac{2.3\eta}{\lambda}\right) \qquad (2.61)$$

$$Log(|-i|) = Log(i_0) - \frac{\eta}{\lambda} \qquad (2.62)$$

A kinetic analysis of bio-catalysis of electronation reactions using Tafel Analysis is outside the scope of this investigation, but future experimentation is elaborated upon in chapter 5.

2.6.3 Biosorption kinetics: modelling using the pseudo-first/second and intra-particular diffusion model.

In order to investigate the mechanism of biosorption sorption assays were modelled (with deviations provided in Appendix A2.3) using:

- a pseudo-first order model of Lagergren (Yuh-Shan 2004)
- a pseudo-second order model (Ho and McKay 1999)
- an intra-particular diffusion model of Weber and Morris (Poots, McKay et al. 1978)

The amount of metal ions adsorbed for a given volume of solvent and mass of bacterial cells can be described by eq^n 2.63. Where q_t (mg/g) is the amount of metal ions sorbed at time *t*, C_o and C_t is the initial and concentration at time *t* of metal ions in solution, *V* is the volume of the solution and M_c is the mass of adsorbent added to solution [2].

$$q_t = (C_o - C_t)\frac{V}{M_c} \qquad (2.63)$$

The pseudo first order model or Lagergren model can be described by eq^n 2.64, where q_e (mg/g) is the amount of metal ions sorbed at equilibrium and k_1 is the first order rate constant. Integrating this using the boundary conditions $t = 0$ to $t = t$ and $q_t = 0$ to $q_t = q_t$ yields eq^n 2.65. If the metal ion removal follows a Lagergren first order model a plot of $Log(q_e-q_t)$ vs. $1/t$ will give a straight line where k_1 and q_e can be calculated from the gradient and y-intercept respectively.

[2] Allometry analysis of TEM imagery was applied to determine M_c, see chapter 3.

$$\frac{dq_t}{dt} = k_1(q_e - q_t) \qquad (2.64)$$

$$Log(q_e - q_t) = Log(q_e) - \frac{k_1}{2.303\ t} \qquad (2.65)$$

The pseudo second order model can be described by eq^n 2.66 Integrating this using the boundary conditions $t = 0$ to $t = t$ and $q_t = 0$ to $q_t = q_t$ gives eq^n 2.67. Where k_2 (g mg^{-1} min^{-1}) is the second order rate constant and the initial sorption rate is described by eq^n 2.68). A plot of $1/q_t$ vs. t for application of this model would be straight line where q_e and k_2 can be calculated from the gradient and y-intercept of the plot.

$$\frac{dq_t}{dt} = k_2(q_e - q_t)^2 \qquad (2.66)$$

$$\frac{t}{q_t} = \frac{1}{q_e} + \frac{1}{q_e^2 k_2 t} \qquad (2.67)$$

$$v_o = kq_e^2 \qquad (2.68)$$

The intra-particular diffusion model assumes that film diffusion is negligible and intra-particular diffusion is the only rate limiting step in accord with the model postulated by Weber and Morris (Poots, McKay et al. 1978). If the final chemo-physical biosorption reaction is instantaneous than intraparticular diffusion of the metal ions can be deemed rate limiting. Alternative models have also been reported by Urano and Tachikawa (Urano, Tachikawa et al. 1992).

The Weber Morris intraparticular model states that the amount adsorbed q_t at any time t will thus be proportional to the square root of contact time. As described by eq^n 2.69 where k_{id} is the intra-particular rate constant (mg g^{-1} min$^{-0.5}$). The logarithmic form of eq^n 2.69 can be defined as eq^n 2.70. A plot of Log(q_e) vs. 0.5 Log(t) should give a straight line with a positive intercept if the intraparticular model applies from which the intra-particular rate constant k_{id} can also be determined. The diffusion coefficient $D_{(WM)}$ can then be calculated from the Weber Morris plot using eq^n 2.71 as described by Cranks (Crank 1979) for diffusion in a spear and as applied by Selatnia et al. (Selatnia, Bakhti et al. 2004) (see Appendix A2.4).

$$q_t = k_{id} t^{0.5} \quad (2.69)$$

$$Log(q_t) = Log(k_{id}) + 0.5Log(t) \quad (2.70)$$

$$D_{(WM)} = \pi \left[\frac{d_p k_{id}}{12 q_e} \right]^2 \quad (2.71)$$

Bio-sorption diffusion processes

In a well agitated batch system concentration differences are constantly levelled out. Agitation effects neither the film diffusion through the liquid surface that surrounds the adsorbent nor the intra-particular diffusion through the adsorbent. Thus we are faced with two potentially rate determining steps either of which may be rate controlling. To assess the nature of the diffusion process responsible for remediation of the metal ions attempts were made to calculate the diffusion coefficients of the process. The diffusion process is typically described by Flicks first law of diffusion (Crank 1979).

Flux would thus be proportional to the concentration gradient and thus diffusion coefficients for film and inter-particular diffusion process remain constant. Determination of film D_f and intra-particular diffusion D_p coefficients would be an useful indicator in determining the nature of the rate determining step on the assumption that sorption reaction subsequent to inter-particular diffusion is instantaneous and diffusion process are rate controlling for the overall reaction.

Film (D_f) and intra-particular (D_p) diffusion parameters for our system where derived from ion exchange theory and described in detail by Helfferich (Helfferich 1995) with eq^n 2.72 and eq^n 2.73, with application reported for the biosorption of Cadmium (Bhatnagar, Minocha et al. 2010), azo dyes (Mohan and Singh 2002) and chrome dyes (Gupta, Prasad et al. 1990) with a variety of adsorbents. A basic derivation of equations is provided in Appendix A2.4. Here d_p^2 is the diameter of the sorbent (bacterial cell) taken as an average of 2.11×10^{-5} cm from TEM imagery, ζ is the film thickness taken as 10^{-3} cm (Helfferich 1995) upon a crude approximation of near spherical geometry of the bacterial cells and $t_{1/2}$ as the half time of biosorption, extracted from sorption modelling

of biosorption dynamics described in chapter 3.

If film diffusion is the rate controlling step than D_f values will be of the range 10^{-6} to 10^{-8} cm^2/s while if intra-particular diffusion is the rate controlling step D_p will be in the range 10^{-11} to 10^{-13} cm^2/s as described in previous biosorption investigations (Gupta, Prasad et al. 1990; Mohan and Singh 2002; Bhatnagar, Minocha et al. 2010).

$$D_p = 0.03\left[\frac{R_p^2}{t^{1/2}}\right] \qquad (2.72)$$

$$D_f = 0.23\left[\frac{R_p \zeta}{t^{1/2}}\frac{C_e}{C_0}\right] \qquad (2.73)$$

2.7 *Experiential and analytical methods*

For effective and successful realization of metal recovery from aqueous solutions effective analytical methods are essential to manage and improve the process. A brief description of analytical methods of relevance to this project are given here, the use of which determined upon evaluation of time and cost constraints.

Analytical chemistry can be divided into two areas of qualitative and quantitative analysis. Selection of the appropriate method of analysis is based on criteria such as accuracy, precision, sensitivity, urgency for results, cost, number of samples etc (Fifield and Kealey 2000). Electrochemical linear sweep voltammetry was applied for the analysis of reaction mechanism, thermodynamics and kinetics of metal ion reduction and nucleation.

2.7.1 Electrochemical and bio-electrochemical analytical methods

The analysis of an electrochemical process requires the quantification and qualification of reacting species in the system under investigation. A potentiostat in a three electrode system (Figure 2.10) is now widely used in academic electrochemical analysis and was first introduced by Hickling (Hickling 1942) in 1942, with the application of an electronic feedback technique to maintain a chosen electrode potential.

The potentiostat controls the voltage between the working and counter electrode and adjusts the potential difference between the working and reference electrode via a high-impedance feedback circuit. To reduce ohmic losses between the working and reference electrode, the reference electrode is placed in a Luggin probe the tip which is placed very close (< 5 mm) from the working electrode using a saturated calomel electrode. Or placed as close as possible (< 5 mm) to the working electrode where bioelectrochemical phenomena were investigated using a silver/silver chloride reference electrode.

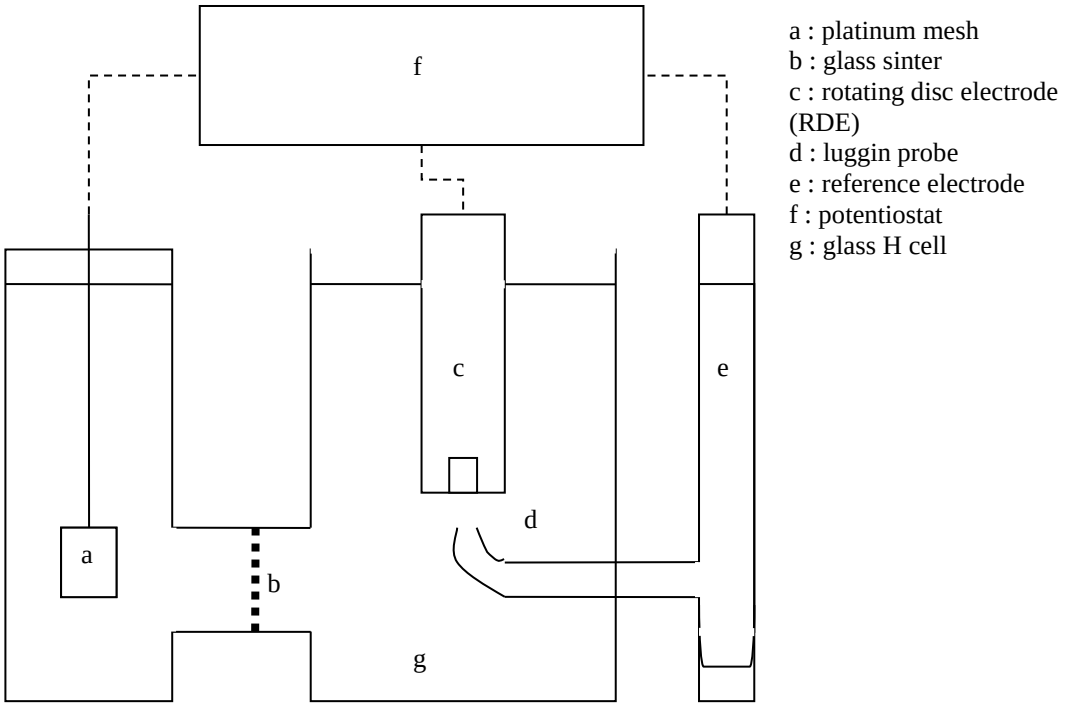

Figure 2.10 : Basic cell schema for electrochemical experimentation.

Linear sweep and cyclic voltammetry using slow scan rates of 0.010 V/s and poteniodynamic voltammetry using fast scan rates of (> 0.050 V/s) (Figure 2.11) were used in this study for qualitative elucidation of reactions occurring and evaluation of reaction thermodynamics. Potential is the main controlling variable of current. Steady state polarisation applies a series of step potentials allowing the system to reach steady state and measuring the current. Linear sweep voltammetry using slow potential scan rates of 1 - 0.010 V/s allow near steady state conditions in the region near to the electrode surface (Southampton Electrochemistry 1985) and have been applied for the determination of electronation reversible potentials and evaluation of electronation thermodynamics. Chronoamperometeric method involves perturbations of the working

electrode by step-functional changes in potential. As current and potential are related functionally, the current response would be our experimental observable.

Chronoamperometeric methods involve potentials stepped from rest potentials to potentials where reactions of investigation occur with the observation of the resultant current transient from the time of step potential.

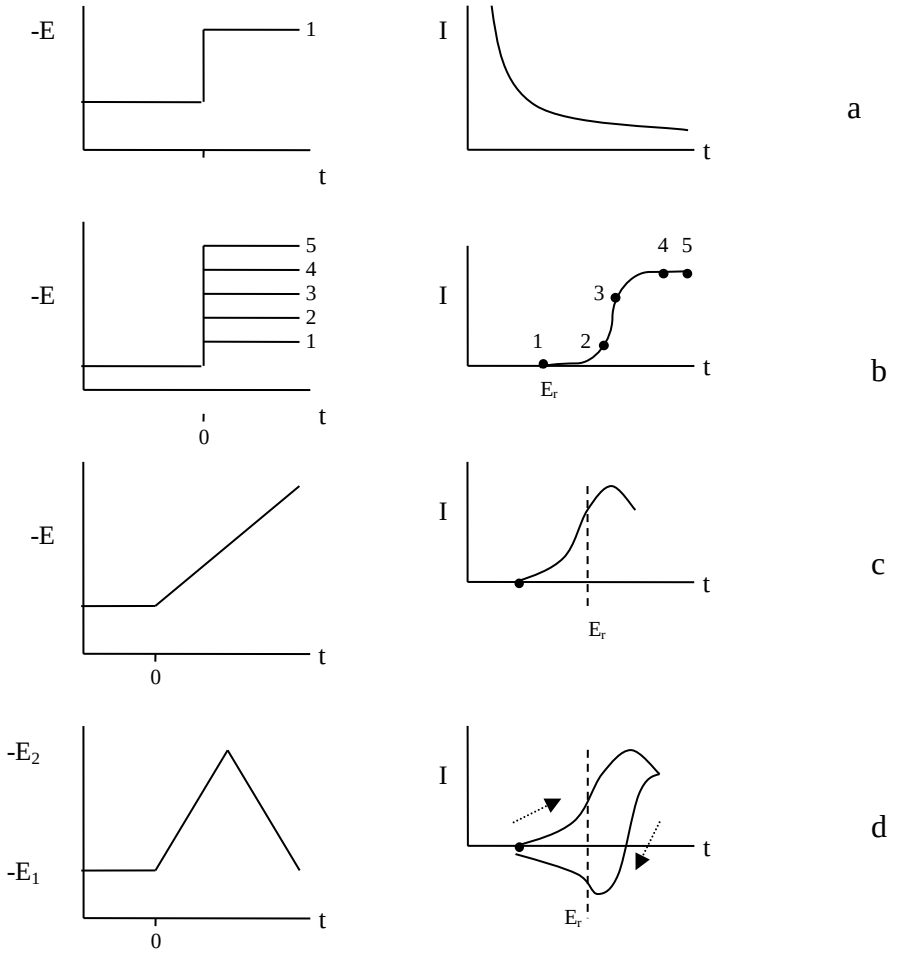

Figure 2.11 : Representation of electrochemical techniques and voltammograms by changes in experimentation variable potential and resultant *i*,*E* or *i*,*t* curves. (a) Chronoamperometeric potential step method. (b) Sampled-current steady state scans. (c) Linear sweep voltammetry. (d) Cyclic voltammetry.

Poteniodynamic voltammetry involving faster scan rates using potential scans greater than 0.050 V/s displayed and logged by a recorder. As the scan rate is increased the diffusion layer is not allowed to reach its equilibrium state and the concentration gradients at the surface of the electrode significant, with an increase in current response.

Once $(Co)_{x=0}$ reaches zero and the potential is swept further, the concentration gradient starts to decrease and a decrease in current is therefore observed. Overall, a peak-shaped current potential response is produced.

The complexity of various reaction mechanisms for the interactions of live electroactive bacterial cells, microbiologically "in-situ" generated redox mediating species, dissolved ionic species (such as metal ions) and electrified electrode substrates is a controversial subject as much of the proposed transfer mechanisms is based on a putative disclosure.

Linear sweep and cyclic voltammetry techniques applied in this research have been demonstrated as a qualitative and quantitative macro-analytical tool. From which much valuable information for electron transfer interactions of microorganisms, dissolved redox species and electrified electrode substrates as a basis for further strategic creation of socially and environmentally benign engineering applications and scientific exploration on the present state of art (Fricke, Harnisch et al. 2008).

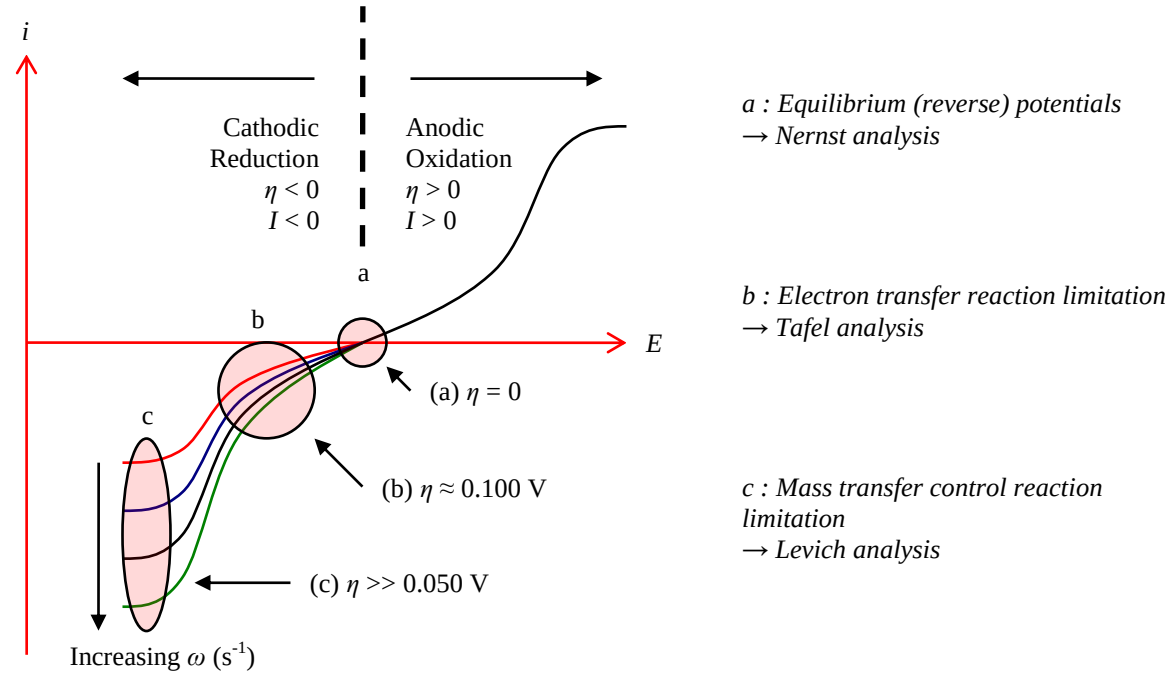

Figure 2.12 : Characteristic voltammograms from linear sweep voltammetry using slow scan rates.

Figure 2.12 illustrates a characteristic *i/E* voltammogram using slow scan rates and summarises appropriate analysis regarding thermodynamics and kinetics of electron transfer limited reactions and mass transfer limited reactions.

2.7.2 Biosorption assays

Microbiological assays of bacterial and metal ion solutions were conducted in batch mode where we aimed to identify the possible products of biosorption processes and the location of any biogenic particles within the bacterial cell wall or cytoplasm and quantify the overall thermodynamics of the reaction as described by a state of equilibrium, with modelling of the dynamics on reaching this quiescent state taken after 24 hours of bacterial contact in batch systems.

2.7.3 Microbiological analytical methods

Presently there are a range of physical-chemical methods employed in hydrometallurgy such as photometric methods fundamentally categorised as absorption spectrometry and emission spectroscopy.

Adsorption spectroscopy is based on the passage of radiation through solution and the measurement of its adsorption in a particular waveband. The amount of radiation absorbed is correlated to properties of the chemical species under study. Examples include ultraviolet and visible spectrometry, atomic absorption spectroscopy (AAS) and flame absorption spectrophotometry (Day and Underwood 1986). For colorimetric methods, the metal ion is often complexed with organic reagent (Burger 1973; Vogel and Svehla 1987) such a ferrozine for iron (Stookey 1970; Dawson and Lyle 1990; Riemer, Hoepken et al. 2004).

In contrast, emission spectroscopy involves the measurement of the emission of electromagnetic radiation from a substance energised from a ground state to an excited state. On return to its ground state radiation is emitted which is measured and correlated to properties of the substance. Examples include atomic emission spectroscopy (AES), flame emission spectroscopy (FES), inductively coupled plasma (ICP) and atomic fluorescence spectroscopy (AFS) (Day and Underwood 1986). The application of ion (Steinmann and Shotyk 1995) has also been noted. Titration methods such redox titrimetry (Day and Underwood 1986) also have potential due to the ease and speed of application for quantitative analysis. Redox titrimetry is based on redox reactions between the analyte and titrant using various oxidizing agents and redox indicators.

A range of methods are available for viable cell count in our system as a measure of bacterial growth on the electron acceptor in question using standard serial dilution and pour-plate methods (Collins and Lyne 1984). UV-spec is also a good candidate for the identification of any bio-nanoparticles produced (Mukherjee, Senapati et al. 2002; Ahmad, Senapati et al. 2003; Deplanche and Macaskie 2008; Deplanche, Woods et al. 2008). The location of reduced metal with the bacterial cells has been studied extensively in the microbiological community using transmission electron microscopy (TEM) (Watt 1997).

In our work particular application to adsorption dynamics of metal ion adsorption, metal ion concentrations of $Au^{3+}$and Co^{2+} were determined using ICP. Total ionic iron (Fe^{3+} + Fe^{2+}) in solution were determined with the ferrozine assay as described in Appendix A2.5, the assay chosen for its simplicity, ease of use and relative low expense (Lovley and Phillips 1987).

2.8 *Metal-ion Speciation*

The distribution, mobility, biological availability and toxicity of chemical elements depend not simply on their concentrations but critically on their forms. Changes in environmental conditions, whether natural or androgenic can strongly influence the behaviour of both essential and toxic elements by altering the forms in which they occur (Ure and Davidson 2002). A key controlling factor in our system would be pH. An increase in pH could cause metal ions to precipitate out as oxides or hydroxides. Metabolic by-products of bacterial cells for microbial reduction assays may cause changes in system pH and therefore before any statement regarding remediation of metal ions by microbial adsorption and bioreduction is made, pH changes in solution must be taken into account.

Pourbaix diagrams associated with work by Marcel Pourbaix, describe thermodynamic equilibrium diagrams (Pourbaix 1966) of potential vs. pH from which the speciation of metal ions in solution can be related to pH and valuable inferences can be made regarding heterogeneous cathodic and anodic reactions which occur by the application of a potential field.

Figure 2.13 reproduces the thermodynamics gold-halide-water systems in terms of Pourbaix potential-pH as investigated by Kelsall et al. (Kelsall, Welham et al. 1993) at 298 K and a_{Au} = 1 mM. Tetrachloaurate(III) is the predominant species in solution at pH < 8. The possibility of dichloroaurate(I) formation could also occur in a narrow Nernst potential range as illustrated by Figure 2.13. Previous investigation by Wang et al. (Wang, Qian et al. 2009) demonstrate that the specification of $HAuCl_4(aq)$ varies with pH. They report that $[AuCl_4]^-$ undergoes pH dependent stepwise hydrolysis described by eq^n 2.74.

$$[AuCl_4]^- + xOH^- \rightarrow [AuCl_{(3-x)}(OH)_x]^- \qquad (2.74)$$

Figure 2.14 reproduces the Pourbaix cobalt-water systems solutions in this study. For low pH 1 - 3 region cobalt ions exist as hydrated ions as $Co(H_2O)_6^{2+}$ (Chivot, J et al. 2008). Figure 2.15 reproduces iron-water Pourbaix relationship describe by Pourbaix (Pourbaix 1966) and Figure 2.16 reproduces iron-sulphate Pourbaix relationship described by Gil et al. (Gil, Salgado et al. 1995) for Fe^{3+} and Fe^{2+} in sulphate solvents. For solution of pH < 4, Fe^{3+} stays dissolved in solution as ionic species.

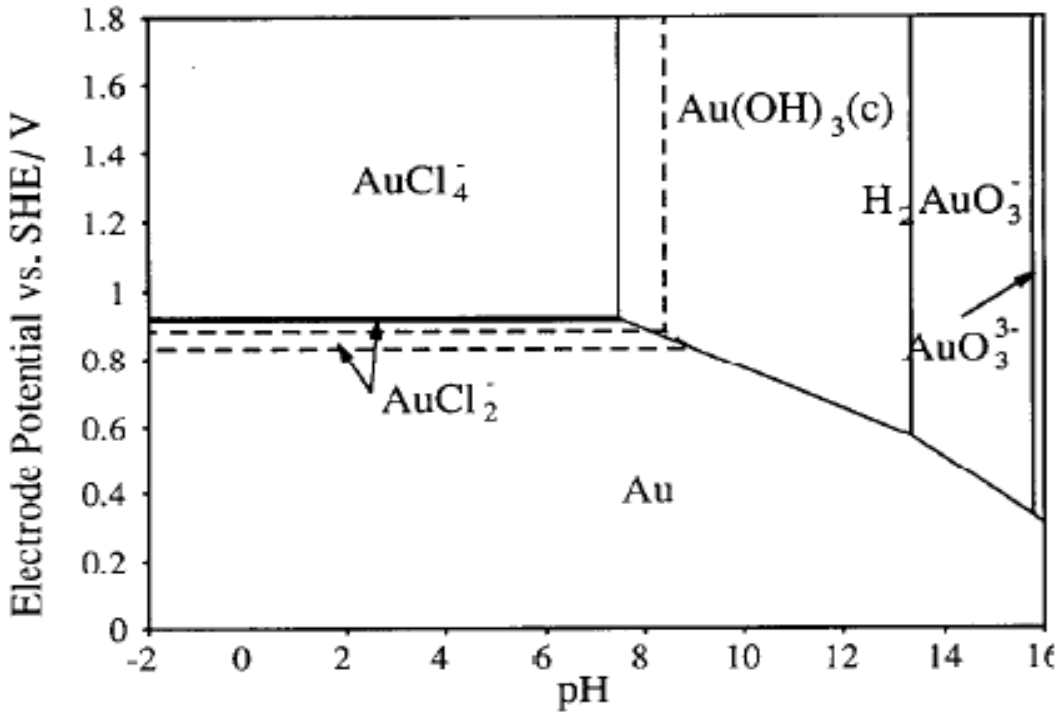

Figure 2.13 : Potential-pH diagram for a gold-chloride-water system at 298.15 K for Au = 10^{-3} M as described by Kelsall et al. (Kelsall, Welham et al. 1993).

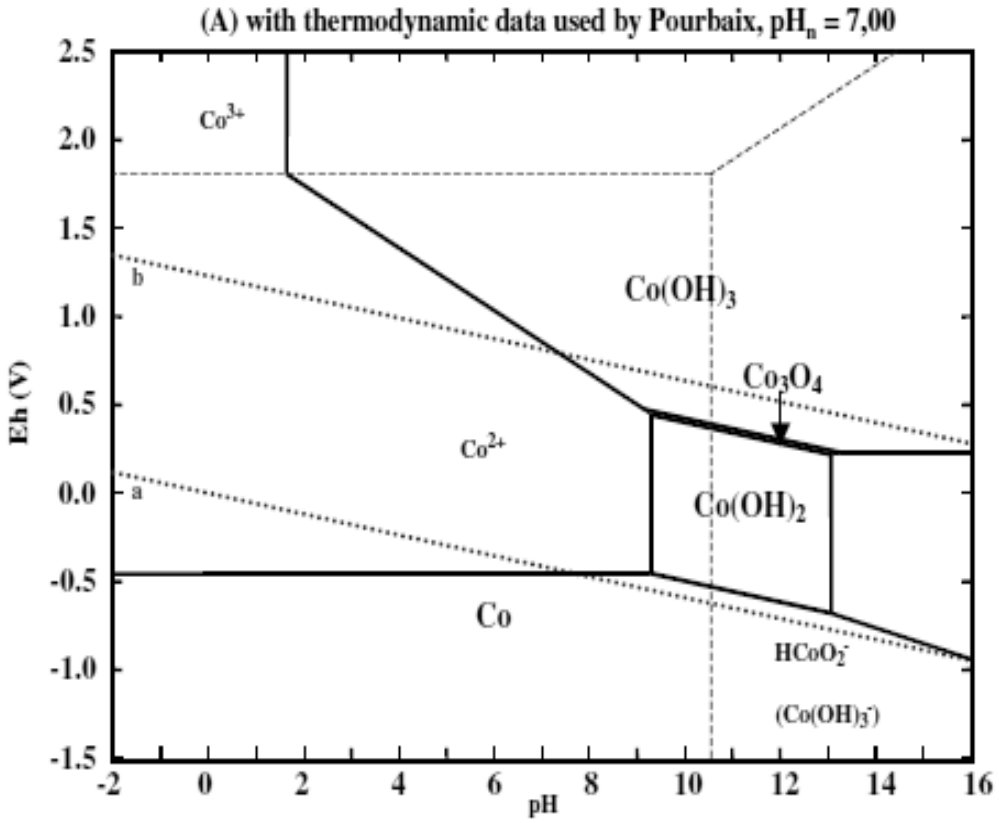

Figure 2.14 : Potential-pH diagram for a cobalt-sulphate-water system at 298.15 K for Co = 10^{-3} as described by Chivot et al. (Chivot, J et al. 2008).

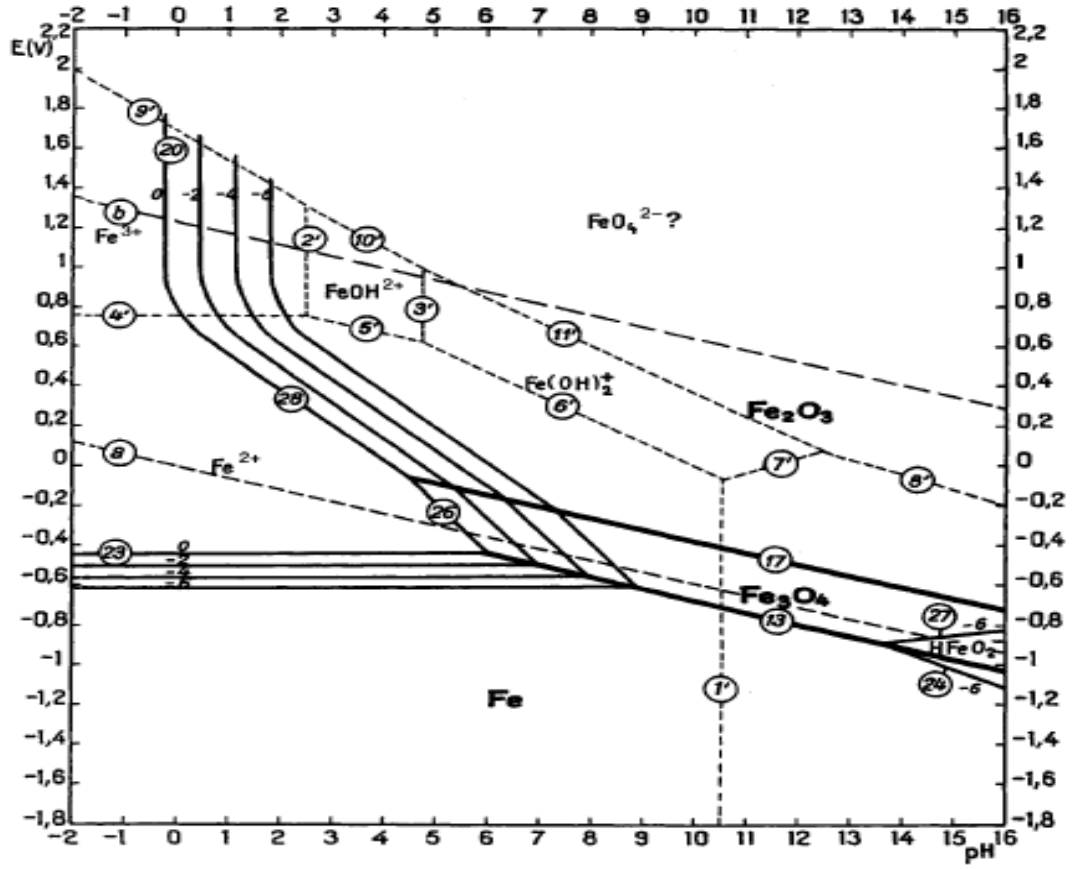

Figure 2.15 : Potential-pH equilibrium diagram for iron-water system at 298K, $a_{Fe} = 1$ considering solid substances only Fe, Fe_3O_4, and Fe_2O_3 as reproduced from Pourbaix (Pourbaix 1966).

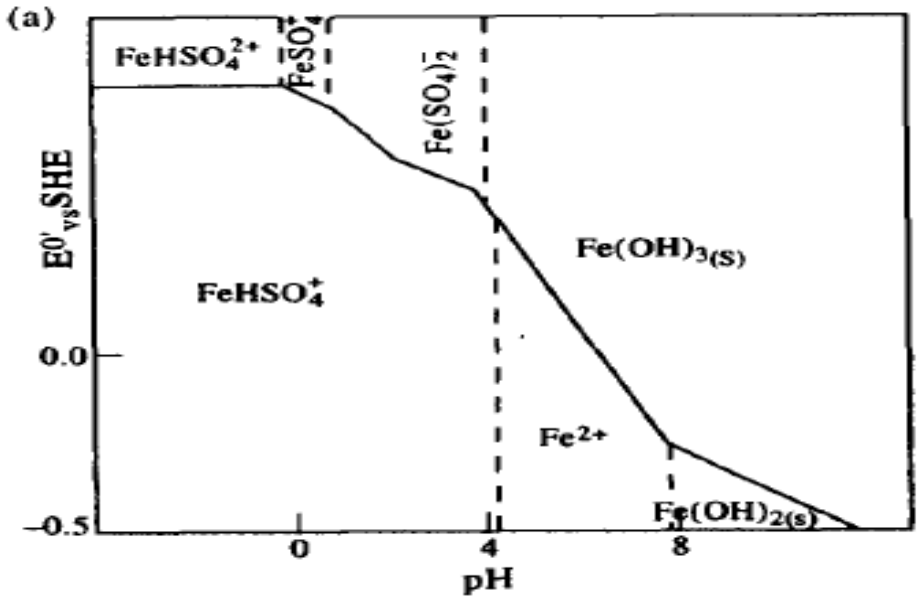

Figure 2.16 : Potential-pH equilibrium diagram for Fe(III), Fe(II)/$SO_4^{'}$/H2O at 298K, $C_{Fe(III)} = C_{Fe(II)} = 2 \times 10^{-3}$ M described by Gil et al. (Gil, Salgado et al. 1995).

2.9 *Electrolyte properties*

The composition of mine waters and spent industrial effluents from electrochemical industry would contain a consortium of inorganic anions and cations which would be advantageous, where these "supporting" species raise the electrolyte conductivity and charge transfer by reducing ohmic resistances and energy loses. Such effluents would therefore be ideal candidates for electrochemical systems. Low pH of these systems would also be advantageous where metal electrodeposition of Co^{2+}/Co and Fe^{3+}/Fe ions occur simultaneously with hydrogen evolution H^{+}/H_2, H_2O/H_2 which may be applied as electron donors to lithotropic, electroactive inorganic biosorbing microbiological bacterial cells. Any future engineering development would need to take into account solution conductivities, for now experimentation will focus only upon changes in remediation reactions with and without bacterial cells in identical aqueous electrolytes which were un-buffered and not degassed to represent "real" metal contaminated effluents. Electrolyte bath compositions are summarised in Table 2.1.

2.10 *Experimental Overview*

Electrochemical, microbiological and bioelectrochemical experimentation has been summarised by Tables 2.1. Experimentation can be divided into three categories.

- Chapter 3 : Microbiological experimentation

Experimentation carried out with batch metal assays of various pH and metal ion species and concentrations with the addition of various concentrations of 1 x 10^{10} CFU/ml *S. putrefaciens* cells, with modelling of biosorption dynamics and thermodynamics and further analysis of biosorption mechanisms using transmission electron microscopy.

- Chapter 4 : Qualitative analysis of bio-electrochemical reaction mechanisms and thermodynamics

Linear and cyclic voltammetry were used to study reaction mechanisms and kinetics of metal ion electroreduction in the absence of bacterial cells in various media as a foundation for later experimentation upon bioelectrochemical metal ion electron transfer phenomena. Following on, a qualitative analysis of electroreduction and electrodeposition of metal ions using G10 graphite electrode with and without 10 ml of

1 x 10^{10} CFU/ml *S. putrefactions* cells. Experiential focuses upon changes in thermodynamics of respective electronation reactions.

	Species	Electrolyte	Metal ion $[C_o]$ ppm	pH	κ mS/cm	Notes
Microbiological : Chapter 3	Au^{3+}	0.254 x 10^{-3} M – 1.523 x 10^{-3} M $HAuCl_4$(aq)	50 - 300	1 - 3	≈ 30	Batch metal assays of various pH and metal ion concentrations and volumes of 1 x 10^{10} CFU/ml *Shewanella purtrificans* bacterial cells. Modelling of biosorption dynamics and thermodynamics with further analysis of biosorption mechanisms using transmission electron microscopy.
	Co^{2+}	3.394 x 10^{-3} M Co^{2+} + 0.9% NaCl(aq)	≈ 200	3	24.7	
	Fe^{3+}	3.581 x 10^{-3} M Fe^{3+} in 0.5 M HNO_3 matrix	≈ 200	1 - 2	33.1	
Bioelectrochemical : Chapter 4	Au3+	1 x 10^{-3} M AuCl4- in 2 M HCl matrix	197	1.46	36	Linear sweep and cyclic voltammetry using Pt and Au rotating disc electrode.
	Co2+	5.080 x 10^{-3} M Co^{2+} + 0.0246 M Na_2SO_4(aq)	300	3.77	4.73	
	Fe3+	3.574 x 10^{-3} M Fe^{3+} + 0.0246 M Na_2SO_4 (aq)	200	2.72	5.77	
	Au^{3+}	1.015 x 10^{-3} M $AuCl_4^-$ in 2 M HCl matrix	≈ 200	2	35.2	Linear sweep and cyclic voltammetry using G10 graphite electrodes with and without 5 ml addition of 1 x 10^{10} CFU/ml *Shewanella purtrificans* bacterial cells.
	Co^{2+}	3.394 x 10^{-3} M Co^{2+} + 0.9% NaCl(aq)	≈ 200	2	24.7	
	Fe^{3+}	3.581 x 10^{-3} M Fe^{3+} + 0.9% NaCl(aq)	≈ 200	2	42.7	

Table 2.1 : Summary of electrolyte composition and electrochemical experimentation.

References

*Ahmad, A., S. Senapati, et al. (2003). "Extracellular Biosynthesis of Monodisperse Gold Nanoparticles by a Novel Extremophilic Actinomycete, Thermomonospora sp." Langmuir **19**(8): 3550-3553.*

Atkins, P. W. (2001). The elements of physical chemistry : with applications in biology. New York, W.H. Freeman.

*Bhatnagar, A., A. K. Minocha, et al. (2010). "Adsorptive removal of cobalt from aqueous solution by utilizing lemon peel as biosorbent." Biochemical Engineering Journal **48**(2): 181-186.*

*Bockris, J. O. M., D. Drazic, et al. (1961). "The electrode kinetics of the deposition and dissolution of iron." Electrochimica Acta **4**(2–4): 325-361.*

*Bockris, J. O. M. and Z. Nagy (1973). "Symmetry factor and transfer coefficient. A source of confusion in electrode kinetics." Journal of Chemical Education **50**(12): 839.*

Bockris, J. O. M. and A. K. N. Reddy (1970). Modern electrochemistry : an introduction to an interdisciplinary research. New York, Plenum Press.

Burger, K. (1973). Organic reagents in metal analysis. Oxford; New York, Pergamon Press.

*Burke, L. D., D. T. Buckley, et al. (1994). "Novel view of the electrochemistry of gold." Analyst **119**(5): 841-845.*

*Burke, L. D., J. K. Casey, et al. (1993). "An investigation of some of the variables involved in the generation of an unusually reactive state of platinum." Electrochimica Acta **38**(7): 897-906.*

Chivot, J, et al. (2008). New insight in the behaviour of Co-H[2]O system at 25-150 °C, based on revised Pourbaix diagrams. Kidlington, ROYAUME-UNI, Elsevier.

*Clauwaert, P., P. Aelterman, et al. (2008). "Minimizing losses in bio-electrochemical systems: the road to applications." Applied Microbiology and Biotechnology **79**(6): 901-913.*

Collins, C. H. and P. M. Lyne (1984). Microbiological methods. London ; Boston, Butterworths.

Conway, B. E. (1965). Theory and principles of electrode processes. New York, Ronald Press Co.

*Conway, B. E. and M. Salomon (1967). "Electrochemistry: Its role in teaching physical chemistry." Journal of Chemical Education **44**(10): 554.*

Crank, J. (1975). The mathematics of diffusion. Oxford, Eng, Clarendon Press.

Crank, J. (1979). The mathematics of diffusion, Clarendon Press.

*Daughney, C. J. and J. B. Fein (1998). "The Effect of Ionic Strength on the Adsorption of H+, Cd2+, Pb2+, and Cu2+byBacillus subtilisandBacillus licheniformis:A Surface Complexation Model." Journal of Colloid and Interface Science **198**(1): 53-77.*

*Dawson, M. V. and S. J. Lyle (1990). "Spectrophotometric determination of iron and cobalt with Ferrozine and dithizone." Talanta **37**(12): 1189-1191.*

Day, R. A. and A. L. Underwood (1986). Quantitative analysis. Englewood Cliffs, N.J., Prentice-Hall.

*Deplanche, K. and L. E. Macaskie (2008). "Biorecovery of gold by Escherichia coli and Desulfovibrio desulfuricans." Biotechnology and Bioengineering **99**(5): 1055-1064.*

*Deplanche, K., R. D. Woods, et al. (2008). "Manufacture of stable palladium and gold nanoparticles on native and genetically engineered flagella scaffolds." Biotechnology and Bioengineering **101**(5): 873-880.*

*Dietrich H, N. (1992). "Resistance to cadmium, cobalt, zinc, and nickel in microbes." Plasmid **27**(1): 17-28.*

*Febrianto, J., A. N. Kosasih, et al. (2009). "Equilibrium and kinetic studies in adsorption of heavy metals using biosorbent: A summary of recent studies." Journal of Hazardous Materials **162**(2–3): 616-645.*

Fifield, F. W. and D. Kealey (2000). Principles and practice of analytical chemistry. Oxford ; Malden, MA

Abingdon England, Blackwell Science ;

Distributed by Marston Book Services.

*Fricke, K., F. Harnisch, et al. (2008). "On the use of cyclic voltammetry for the study of anodic electron transfer in microbial fuel cells." Energy & Environmental Science **1**(1): 144-147.*

*Gil, A. F., L. Salgado, et al. (1995). "Predominance-zone diagrams of Fe(III) and Fe(II) sulfate complexes in acidic media. Voltammetric and spectrophotometric studies." Talanta **42**(3): 407-414.*

*Gorby, Y. A., S. Yanina, et al. (2006). "Electrically conductive bacterial nanowires produced by Shewanella oneidensis strain MR-1 and other microorganisms." Proceedings of the National Academy of Sciences **103**(30): 11358-11363.*

*Gregory, K. B., D. R. Bond, et al. (2004). "Graphite electrodes as electron donors for anaerobic respiration." Environmental Microbiology **6**(6): 596-604.*

*Guenbour, A., H. Iken, et al. (2006). "Corrosion of graphite in industrial phosphoric acid." Applied Surface Science **252**(24): 8710-8715.*

*Gupta, G. S., G. Prasad, et al. (1990). "Removal of chrome dye from aqueous solutions by mixed adsorbents: Fly ash and coal." Water Research **24**(1): 45-50.*

*Haas, J. R., T. J. Dichristina, et al. (2001). "Thermodynamics of U(VI) sorption onto Shewanella putrefaciens." Chemical Geology **180**(1-4): 33-54.*

*Harrison, J. A. and J. Thompson (1973). "The reduction of the aquachloro complexes of rhodium." Journal of Electroanalytical Chemistry and Interfacial Electrochemistry **43**(3): 405-413.*

Helfferich, F. G. (1995). Ion exchange, Dover Publications.

*Hickling, A. (1942). "Studies in electrode polarisation. Part IV.-The automatic control of the potential of a working electrode." Transactions of the Faraday Society **38**: 27-33.*

*Ho, Y. S. and G. McKay (1999). "Pseudo-second order model for sorption processes." Process Biochemistry **34**(5): 451-465.*

*Jeffrey, M. I., W. L. Choo, et al. (2000). "The effect of additives and impurities on the cobalt electrowinning process." Minerals Engineering **13**(12): 1231-1241.*

*Kelsall, G. H., N. J. Welham, et al. (1993). "Thermodynamics of Cl-H2O,Br-H2O, I-H2O, Au-Cl-H2O, Au-Br-H2O and Au-I-H2O Systems at 298 K." Journal of Electroanalytical Chemistry **361**(1-2): 13-24.*

*Konishi, Y., K. Ohno, et al. (2007). "Bioreductive deposition of platinum nanoparticles on the bacterium Shewanella algae." Journal of Biotechnology **128**(3): 648-653.*

*Konishi, Y., T. Tsukiyama, et al. (2006). "Intracellular recovery of gold by microbial reduction of AuCl4− ions using the anaerobic bacterium Shewanella algae." Hydrometallurgy **81**(1): 24-29.*

*Konishi, Y., T. Tsukiyama, et al. (2007). "Microbial deposition of gold nanoparticles by the metal-reducing bacterium Shewanella algae." Electrochimica Acta **53**(1): 186-192.*

*Liu, C., Y. A. Gorby, et al. (2002). "Reduction kinetics of Fe(III), Co(III), U(VI), Cr(VI), and Tc(VII) in cultures of dissimilatory metal-reducing bacteria." Biotechnology and Bioengineering **80**(6): 637-649.*

*Lloyd, J. R. (2003). "Microbial reduction of metals and radionuclides." Fems Microbiology Reviews **27**(2-3): 411-425.*

*Logan, B. E., B. Hamelers, et al. (2006). "Microbial Fuel Cells: Methodology and Technology†." Environmental Science & Technology **40**(17): 5181-5192.*

*Lovley, D. R. and E. J. Phillips (1987). "Rapid assay for microbially reducible ferric iron in aquatic sediments." Appl Environ Microbiol **53**(7): 1536-1540.*

Madigan, M. T. and T. D. Brock (2009). Brock biology of microorganisms. San Francisco, CA, Pearson/Benjamin Cummings.

*McCreery, R. L. (2008). "Advanced Carbon Electrode Materials for Molecular Electrochemistry." Chemical Reviews **108**(7): 2646-2687.*

*Mohan, D. and K. P. Singh (2002). "Single- and multi-component adsorption of cadmium and zinc using activated carbon derived from bagasse—an agricultural waste." Water Research **36**(9): 2304-2318.*

*Moule, A. L. and S. G. Wilkinson (1989). "Composition of Lipopolysaccharides from Alteromonas putrefaciens (Shewanella putrefaciens)." Journal of General Microbiology **135**(1): 163-173.*

*Mukherjee, P., S. Senapati, et al. (2002). "Extracellular Synthesis of Gold Nanoparticles by the Fungus Fusarium oxysporum." ChemBioChem **3**(5): 461-463.*

*Myers, C. R. and K. H. Nealson (1990). "Respiration-linked proton translocation coupled to anaerobic reduction of manganese(IV) and iron(III) in Shewanella putrefaciens MR-1." J Bacteriol **172**(11): 6232-6238.*

*Nies, D. H. (1999). "Microbial heavy-metal resistance." Applied Microbiology and Biotechnology **51**(6): 730-750.*

*Poots, V. J. P., G. McKay, et al. (1978). "Removal of Basic Dye from Effluent Using Wood as an Adsorbent." Journal (Water Pollution Control Federation) **50**(5): 926-935.*

Pourbaix, M. (1966). Atlas of electrochemical equilibria in aqueous solutions. Oxford, New York, Pergamon Press.

*Rand, D. A. J. and R. Woods (1972). "A study of the dissolution of platinum, palladium, rhodium and gold electrodes in 1 m sulphuric acid by cyclic voltammetry." Journal of Electroanalytical Chemistry and Interfacial Electrochemistry **35**(1): 209-218.*

*Riemer, J., H. H. Hoepken, et al. (2004). "Colorimetric ferrozine-based assay for the quantitation of iron in cultured cells." Analytical Biochemistry **331**(2): 370-375.*

*Samec, Z. and J. Weber (1977). "The effect of the double layer on the rate of the Fe3+/Fe2+ reaction on a platinum electrode and the contemporary electron transfer theory." Journal of Electroanalytical Chemistry and Interfacial Electrochemistry **77**(2): 163-180.*

*Selatnia, A., M. Z. Bakhti, et al. (2004). "Biosorption of Cd2+ from aqueous solution by a NaOH-treated bacterial dead Streptomyces rimosus biomass." Hydrometallurgy **75**(1–4): 11-24.*

*Silver, S. (1996). "Bacterial resistances to toxic metal ions - A review." Gene **179**(1): 9-19.*

*Soto, A. B., E. M. Arce, et al. (1996). "Electrochemical nucleation of cobalt onto glassy carbon electrode from ammonium chloride solutions." Electrochimica Acta **41**(16): 2647-2655.*

Southampton Electrochemistry, G. (1985). Instrumental methods in electrochemistry. Chichester; New York, E. Horwood ; Halsted Press.

*Steinmann, P. and W. Shotyk (1995). "Ion chromatography of organic-rich natural waters from peatlands V. Fe2+ and Fe3+." Journal of Chromatography A **706**(1–2): 293-299.*

*Stookey, L. L. (1970). "Ferrozine---a new spectrophotometric reagent for iron." Analytical Chemistry **42**(7): 779-781.*

*Urano, K., H. Tachikawa, et al. (1992). "Process development for removal and recovery of phosphorus from wastewater by a new adsorbent. 4. Recovery of phosphate and aluminum from desorbing solution." Industrial & Engineering Chemistry Research **31**(6): 1513-1515.*

Ure, A. M. and C. M. Davidson (2002). Chemical speciation in the environment. Oxford ; Malden, MA

Vogel, A. I. and G. Svehla (1987). Vogel's qualitative inorganic analysis. Harlow, Essex, England; New York, Longman Scientific & Technical ; Wiley.

*Wang, S., K. Qian, et al. (2009). "Influence of Speciation of Aqueous HAuCl(4) on the Synthesis, Structure, and Property of Au Colloids." Journal of Physical Chemistry C **113**(16): 6505-6510.*

Watt, I. M. (1997). The Principles and Practice of Electron Microscopy, Cambridge University Press.

*White, C., S. C. Wilkinson, et al. (1995). "The role of microorganisms in biosorption of toxic metals and radionuclides." International Biodeterioration & Biodegradation **35**(1-3): 17-40.*

*Windt, W. D., P. Aelterman, et al. (2005). "Bioreductive deposition of palladium (0) nanoparticles on Shewanella oneidensis with catalytic activity towards reductive dechlorination of polychlorinated biphenyls." Environmental Microbiology **7**(3): 314-325.*

*Yuh-Shan, H. (2004). "Citation review of Lagergren kinetic rate equation on adsorption reactions." Scientometrics **59**(1): 171-177.*

Chapter 3: Microbiological experimentation upon bacterial biosorption and bioreduction of metal ions for metal ion remediation and recovery

Chapter 3: Microbiological experimentation upon bacterial biosorption and bioreduction of metal ions for metal ion remediation and recovery

3.1. Introduction

The application of bio-material for the remediation of heavy and precious metal ions is well documented in literature at large as a cost effective method for metal ion removal especially for solutions of low concentration (Febrianto, Kosasih et al. 2009) in comparison to conventional methods such as precipitation, ion exchange and flotation, which can suffer drawbacks from low performance efficiencies and the addition of expensive chemicals and problems of product disposal.

We here further explore the application of dissimilatory metal-reducing bacteria *Shewanella putrefaciens* for the bioremediation via. biosorption of Au^{3+}, Co^{2+} and Fe^{3+} from un-buffered effluents of low pH (< 3) and low concentrations (< 300 ppm) with an outlook for application of live bacterial cells as "bio-factories" for a greener method of bio-genic nanoparticle formation. The form or character of the equilibrium distribution between the aqueous and solid phases which is thermodynamically driven, was modelled using Langmuir (Langmuir 1918) and Freundlich isotherm models (Freundlich 1906) with calculation of the Gibbs energy (ΔG) of biosorption from Langmuir model parameters. Reaction dynamics regarding the establishment of this equilibrium distribution of sorbate metal ions were modelled using Lagergren pseudo first order, pseudo second order (Ho and McKay 1999) and Weber Morris intra-particular mass transfer models (Poots, McKay et al. 1978).

Although various factors govern the absorption of metal ions by bacterial cells such as initial concentration, pH, temperature, bio-sorbent nature and metal ion nature, the kinetic model is only concerned with the nature of the overall rate. Therefore, to further our understanding of sorption mechanisms in our system, the Weber Morris (D_{WM}) (Selatnia, Bakhti et al. 2004), film (D_f) and intra-particular (D_d) diffusion constants were also quantified using methods described by Helfferich (Helfferich 1995). In addition, TEM analysis for further insight into the biosorption process and the verification of any metal ion reduction and nucleation of zero-valent metallic nanoparticles was carried out.

Figure 3.1 gives a summary of reaction mechanisms investigated and phenomenological models applied regarding the microbiological remediation of metal ions by live dissimilatory Gram-negative bacteria of the *Shewanella* genus.

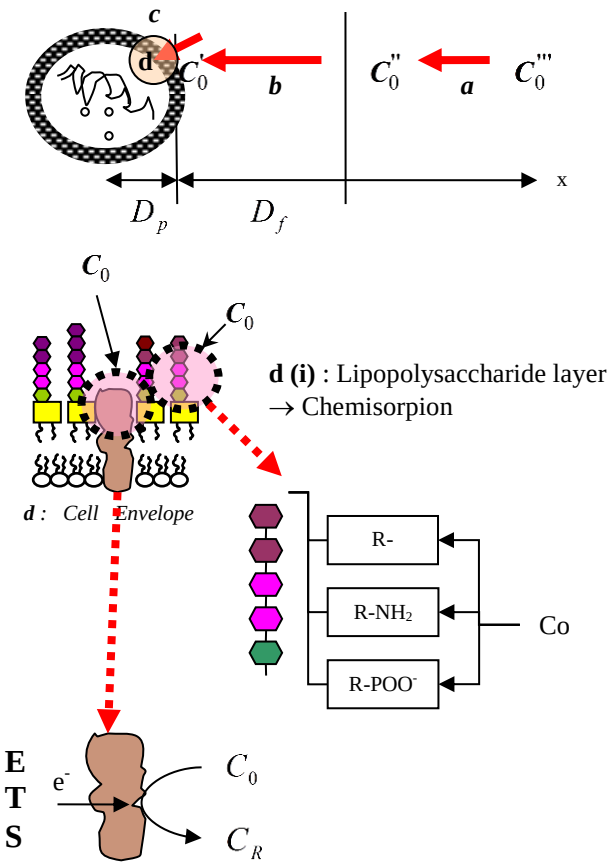

d (ii) : c-cytochrome protein enzyme
→Bioreduction

Reaction Mechanisms

- 4a : $C_O''' \longrightarrow C_O''$: External Diffusion
- 4b : $C_O'' \longrightarrow C_O'$: Film Diffusion
- 4c : $C_O' \longrightarrow C_O$: Intra-particular Diffusion
- 4d (i) : $C_O + [A] \longrightarrow [A] - C_O^*$: Bio-complexion
- 4d (ii) : Bio-reduction
  - (a) $Au^{3+}(aq) + 3e^- \longrightarrow Au^0(s)$
  - (b) $Co^{2+}(aq) + 2e^- \longrightarrow Co^0(s)$
  - (c) $Fe^{3+}(aq) + e^- \longrightarrow Fe^{2+}(aq)$
- 4d (iii) : $H_2(g) \longrightarrow 2H^+(aq) + 2e^-$: Hydrogen oxidation as electron donor for bacterial *respiration*

Thermodynamics
$t = \omega\ q = q_e$
$q_e = f(C_o, M_a)$

- *Langmuir Isotherm*
- *Freundlich Isotherm*

Kinetics
$t = t\ q = q_t$
$q_t = f(t)$

- *Lagaguern pseudo first order rate model*
- *Pseudo second order rate model*
- *Weber Morris intra-particular model*

Figure 3.1 : Overall summary of biosorption reaction mechanisms, equilibrium and kinetic models applied in this chapter in relation to the sorption of metal ions by dissimilatory bacterial cells of the *Shewanella* genus in batch systems.

3.2. Materials and methods

3.2.1. Cells and culture protocol

All containers, vials, flasks, pipettes, media were obtained pre-sterile or sterilized by autoclaving at 121°C for 15 minutes. Frozen cells of *S. putrefaciens* CN 32 (American type culture collection (ATTC) stock (frozen in 20 % glycerol at – 80°C) were revived under aerobic conditions on trypticase soy agar (TSA). Subsequently, the colonies were used to prepare a suspension with a target optical density (OD) of 0.81 ± 0.01 (OD = 600 nm). 20 mL of this suspension were inoculated in 1 L of trypcase soy broth (TSB) in order to initiate the liquid culture. Cells were grown to a stationary growth phase (24 hours UV absorbance after 24 hours $(OD)_{600} \approx 0.320$), continuously agitated at 300 rpm and at 30°C and harvested by centrifugation for 10 minutes at 10, 000 g, washed twice with sterile 0.9% NaCl and concentrated in 70 mL of the same medium. Cells were purged for 30 minutes by bubbling with N_2 (alphagaz 1, Air Liquide) sterilized by filtration through a membrane of pore size 0.2 µm (Millex FG50, Millipore). Dilutions were made from this solution for equilibrium isotherm measurements. A final concentration of $\approx 1 \times 10^{10}$ cells/ml in these cell solutions was calculated from serial plate dilutions using eq^n 3.1.

$$No.\ of\ CRU/ml = \frac{Colonies\ counted}{Volume\ plated(ml)\ \ X\ total\ dilution\ used} \qquad (3.1)$$

Some cell solutions were autoclaved at 121°C for 15 minutes for deactivation and dilutions were made from this bacterial stock solution for equilibrium biosorption isotherm measurements.

3.2.2. Metal assays preparation

Metal ion stock solutions of gold (500 ppm Au^{3+}) and cobalt (4000 ppm Co^{2+}) solutions were prepared by dissolving 1 g of gold(III) chloride hydrate (M_r = 393.83 g/mol) (Sigma-Adrich) and 19.081 g cobalt sulphate heptahydrate pellets (M_r 281.1 g/mol) (VWR) into a final water volume of 1000 ml. For iron, 1000 ppm Fe^{3+} in 0.5 M HNO_3 matrix (Spectrosol, VWR) standard solution was used. Solutions of aqueous Au^{3+}, Co^{2+} and Fe^{3+} from stock solutions of $HAuCl_4$(aq), $CoSO_4 7H_2O$(aq) or $Fe(NO_3)_3$(aq) were poured into a beaker and the pH adjusted by adding 2 M NaOH(aq) or 2 M HNO_3(aq).

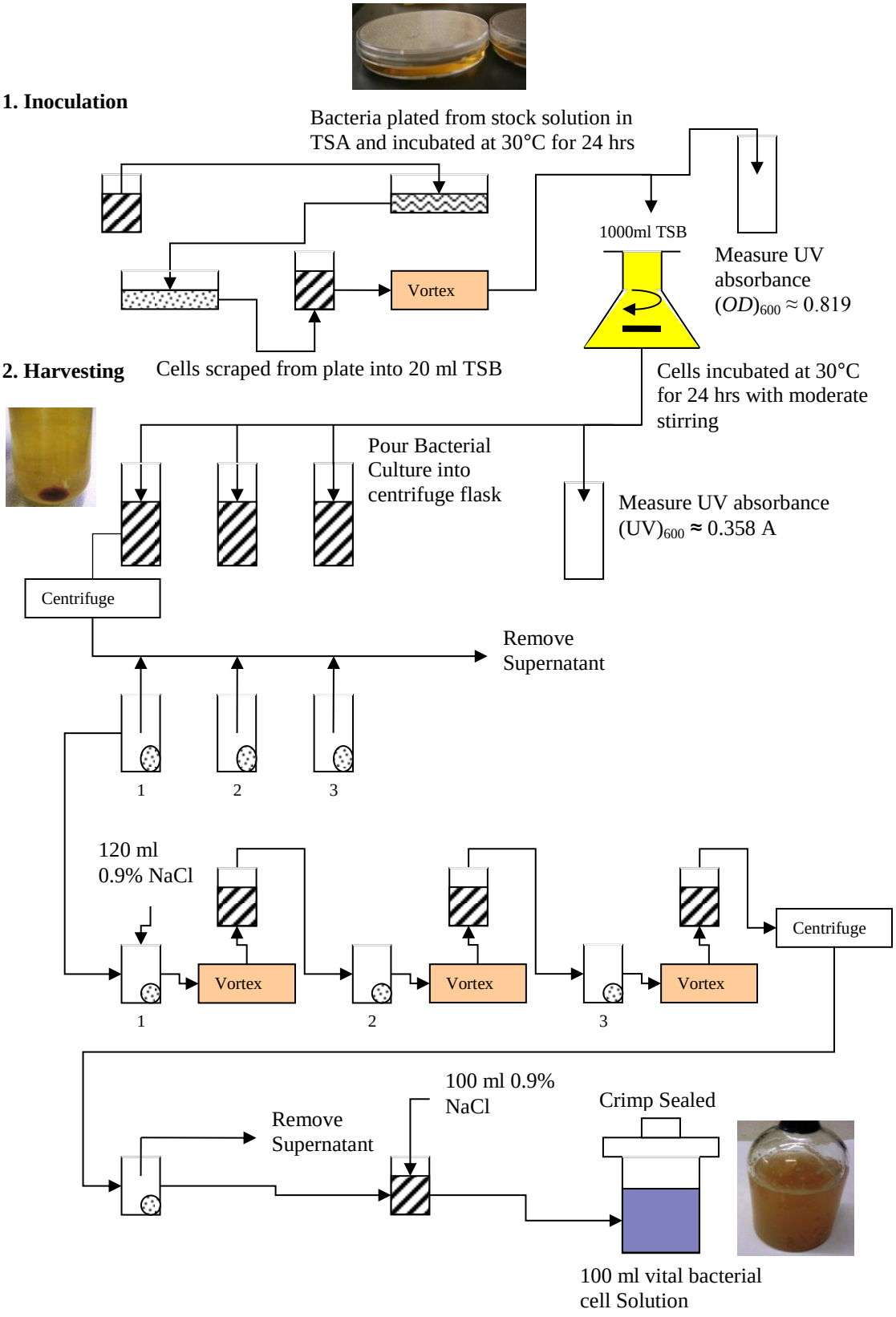

Figure 3.2 : Flow diagram of bacterial culture protocol for *Shewanella putrefaciens*.

Typically 50 ml of these solutions were poured into 100 ml vials to give final metal concentrations of 30 - 300 ppm, sealed with thick butyl rubber stoppers, aluminium crimp sealed and autoclaved at 121°C for 15 minutes. No buffer was added to the aqueous metal assays. Aqueous metal solutions and washed bacterial cells suspensions were made anoxic by bubbling for 60 minutes with N_2(g) and then purging with H_2(g) for approximately 20 seconds. The concentration of aqueous H_2(g) was calculated using Henry's constant (k_H) of 7.03 x 10^4 atm in water (Atkins 2001) to give a final concentration of 0.79 mM for 50 ml solution in 100 ml assays using eq^n 3.2 – 3.3.

$$n = \frac{PV}{RT} \qquad (3.2)$$

$$C_{H_2}(aq) = \frac{\rho_{H_2O}}{M_{H_2O}} \frac{1}{k_H} P_{H_2} \qquad (3.3)$$

Sets of experiments were carried out with solution of Au^{3+} with pH 1, 2 and 3, Co^{2+} with pH 3 and Fe^{3+} with pH 1 and 2. Assays are summarised in Tables 3.1 to 3.3. For a typical experiment, 5 ml of washed viable bacterial cells were added to the 50 ml metal assays and gently shaken in an incubator at 25ºC. Control experiments without bacteria were carried out for iron assays only as previous investigations of gold and cobalt (Anushree 2004; Konishi, Tsukiyama et al. 2006) and have shown metal removal without bacterial cells to be negligible. Some assays were also conducted with deactivated cells for further insight into the bio-remediation mechanisms. Cells were deactivated by heat treatment by autoclaving of cell vials at 121ºC for 15 minutes. Samples were taken at selected time points using sterile needles and filtered through 0.2 μm micro filters (VWR) to remove any biomass. Filtrates were diluted using distilled water and metal concentrations were measured using ICP-OES (Vista-MPX) for gold and cobalt or a ferrozine assay to determine the total iron removal (Stookey 1970), initially calibrated with a series of appropriate solution standards. The pH for the metal assays was also measured using an electrochemical analytical meter (SevenMulti, manufactured by Metter-Toledo GmbH).

A range of assays were prepared with metal concentrations ranging from 276 ppm to 50 ppm at a solution pH 3 for gold and pH 2 for cobalt and iron. Cell dilutions were made with concentrations ranging from $1x10^{10}$ to $4.25x10^8$ CFU/ml. These samples were

taken after 24 hours on the assumption that equilibrium had been reached for the biosorption process, which has been borne out in previous investigations (Veglio and Beolchini 1997).

	Au^{3+} Assay	pH	$[M^{n+}]$ ppm	Notes
set 1	Au1	3	276	Constant pH 3 vs. $[M^{n+}]$
	Au2	3	247	
	Au3	3	162	
set 2	Au4	1	265	Variation of pH vs. High $[M^{n+}]$
	Au1	3	276	
set 3	Au5	1	166	Variation of pH vs. $[M^{n+}]$
	Au6	2	166	
	Au3	3	162	

Table 3.1: Gold metal assays organisation of experiments for reaction assays sampled over initial 4 hour period.

Co^{2+} Assay	pH	$[M^{n+}]$ ppm	
Co1a	3	210	Constant pH vs. Constant $[M^{n+}]$ (≈210 ppm) in triplicate
Co1b	3	210	
Co1c	3	210	

Table 3.2 : Summary Co^{2+} metal ions of reaction assays sampled over initial 4 hour period.

Fe^{3+} Assay	pH	$[M^{n+}]$ ppm	
Fe1a	1	192	Constant pH 1 vs. $[M^{n+}]$ (≈192 ppm)
Fe1b	1	192	Duplicate
Fe2a	2	200	
Fe2b	2	217	Constant pH 2 vs. $[M^{n+}]$ (≈200 ppm)
Fe2c	2	203	
Fe3	1	184	Control Iron Experiments (No Bacteria)
Fe4	2	202	Duplicate

Table 3.3 : Summary of Fe^{3+} reaction assays sampled over initial 4 hour period.

3.2.3. Transmission electron microscopy sample preparation

S. putrefaciens cells and biogenic particles were observed by transmission electron microscopy (TEM) using a Philips CM 100 Compustage (FEI) and digital images collected using an AMT CCD camera. Samples from reaction assays were prefixed in 4% gluteraldehyde (TAAB Lab. Equip) in a Sorenson's buffer (TAAB Lab. Equip) over night. These were washed with three times with cacodylate buffer and fixed with 2% osmium tetraoxide (Agar Scientific). The cells were then dehydrated at room temperature with 25, 50, 75% acetone and twice with 100% acetone for 45 minutes at each concentration. Embedding of biological specimens was carried out using a TAAB epoxy resin kit with 25, 50, 75% resin in acetone for 45 minutes and then twice with 100% resin for 1 hour. The mixtures were polymerized at 60°C for 24 hours. Survey sections of 1 μm where cut and stained with 1% toluidine blue in 1% borax. Ultrathin sections (≈ 80 nm) where cut with a glass knife on a RMC MT-XL ultramicrotome. The sections where stretched with chloroform to eliminate compression and mounted on filmed grids. Some of the girds were stained with 2% aqueous uranyl acetate (Agar Scientific) followed by lead citrate (Leica) prior to TEM analysis. A summary of TEM sample preparation is given in Appendix A3.

3.2.4. Sonication of gold metal assays and UV analysis of solutions

Bacterial gold assay were sonicated for 2 hours using a Banson 350 sonicator as a simple physiochemical method for cell wall lysis and release of bio-nanoparticles deposited within the bacterial cell wall. The UV-spectra of the sonicated solution was then taken as a simple verification of gold bio-nanoparticles analysed using a Unicam 8700 series UV–VIS spectrophotometer.

3.2.5. Experiential Analysis

The amount of metal ions adsorbed was calculated by eq^{n} 2.63 where q (mmol/g or mg/g) is the amount of metal adsorbed by cells and hence the solid-phase concentration of the solute. C_0 (ppm or mM) is the initial concentration of the solute in the solution-phase; C_t the concentration of residual solute in the supernatant at time t (hours); V is the volume of the solution (mL). M_c is the mass (g) of bacterial cell sorbent calculated using eq^{n} 3.4. In equation 3.4, C_c (CFU/ml) is the concentration of cells, V_b is the volume (ml) of cells injected and M_r (g/cell) is taken as the dry mass of one cell. The removal efficiency η (%) was calculated using eq^{n} 3.5.

$$q = (C_o - C_t)\frac{V}{M_c} \tag{2.63}$$

$$M_c = C_c V_b M_r \tag{3. 4}$$

$$\eta\,(\%) = \frac{C_0 - C_t}{C_0} \times 100 \tag{3. 5}$$

3.2.6. Evaluation and modelling of biosorption isotherms

The semi-empirical hyperbolic Langmuir (eq^{n} 2.46) and empirical exponential Freundlich models (eq^{n} 2.47) were applied as isotherm models to describe the distribution of a metal ion between the solid and liquid phase at equilibrium, which is well known for biosorption processes of metal ions (Febrianto, Kosasih et al. 2009). Both models suggest a monolayer sorption mechanism.

$$q_e = \frac{q_{\max} K\,[C_e]}{1 + K[C_e]} \qquad (2.46)$$

$$\frac{1}{q_e} = \frac{1}{q_{\max}} + \frac{1}{(q_{\max} K) C_e} \qquad (2.47)$$

$$q_e = K_F (C_e)^{(1/n)} \qquad (2.48)$$

$$Ln(q_e) = Ln(K_F) + \frac{1}{n} Ln(C_e) \qquad (2.49)$$

Eq^n 2.50 was used to calculate the Gibbs free energy change for the bio-sorption process. ΔG where K is the equilibrium constant determined from the Langmuir equation (eq^n 2.47).

$$\Delta G = -RT \ln K \qquad (2.50)$$

3.2.7. Evaluation of biosorption diffusion processes

For further insight into diffusion processes, Weber Moris diffusion coefficients D_{WM}, D_p and D_f (Crank 1979; Helfferich 1995) were evaluated using eq^n 2.71, 2.72, 2.73, a more detailed discussion of their application is provided in Appendix A2.4.

$$D_{(WM)} = \pi \left[\frac{d_p k_{id}}{12 q_e} \right]^2 \qquad (2.71)$$

$$D_p = 0.03 \left[\frac{R_p^2}{t^{1/2}} \right] \qquad (2.72)$$

$$D_f = 0.23 \left[\frac{R_p \zeta}{t^{1/2}} \frac{C_e}{C_0} \right] \qquad (2.73)$$

3.2.8. Determination of bacterial cell dry mass

Bacterial biomass is a crucial quantity in this study for quantitative measurements of metal ion uptake by bacteria cells. Our calculation is based on the allometric relationship of biomass and volume of bacteria V_b first described by Norland et al. (Norland, Heldal et al. 1987), eq^n 3.6. Here M_r is the dry weight, c is the conversion factor between weight and volume and α is the scaling factor. Values of these constants were further optimised by M. Loferer-Krossbacher et al. (Loferer-Krossbacher, Klima et al. 1998) using transmission electron microscopy and densitometry image analysis. Their correlations are described by eq^n 3.7. The average volume of bacterial cells was calculated using eq^n 3.8 from measurements of 12 bacterial cells where w and l are the extracted widths and length of bacteria taken from transmission electron microscopy of cells unexposed to metal.

$$M_r = cV_b^{\alpha} \qquad (3.6)$$

$$M_r = 435V_b^{0.86} \qquad (3.7)$$

$$V_b = [(w^2 \times \frac{\pi}{4})(l - w) + (\pi \times \frac{w^6}{6})] \qquad (3.8)$$

As summarised by Table 3.4 a correlated average cell weight of 1.281×10^{-13} g/cell was determined. Volume calculations are based on the assumption that the bacteria collapsed such that their original projection on the supporting grid is conserved. As described Figure 3.3 for bacterial cells 1-11 a conversion factor of 1 cm : 131.58 nm and for bacterial cell 12 (taken form a different TEM image a conversion factor of 1 cm : 434.78 nm was applied as determined from the scale bar of TEM imagery.

		W			L		V_b		M_r
Control	cm	Nm	µm	cm	nm	µm	µm^3	fg	g
1	1.0	435	0.43	3.5	1522	1.522	0.204	111.004	1.110×10^{-13}
2	0.9	391	0.39	4.4	1913	1.913	0.214	115.641	1.156×10^{-13}
3	1.0	435	0.43	4.8	2087	2.087	0.288	149.212	1.492×10^{-13}
4	1.0	435	0.43	3.4	1478	1.478	0.198	107.982	1.080×10^{-13}
5	0.9	391	0.39	4.5	1957	1.957	0.219	118.062	1.181×10^{-13}
6	1.0	435	0.43	3.1	1348	1.348	0.179	98.833	9.883×10^{-14}
7	1.1	478	0.48	4.4	1913	1.913	0.315	161.022	1.610×10^{-13}
8	0.9	391	0.39	7.3	3174	3.174	0.366	183.190	1.832×10^{-13}
9	1.0	435	0.43	3.6	1565	1.565	0.211	114.012	1.140×10^{-13}
10	0.7	304	0.30	5.0	2174	2.174	0.151	85.438	8.544×10^{-14}
11	1.0	435	0.43	2.5	1087	1.087	0.140	80.094	8.009×10^{-13}
12	3.8	500	0.50	18.1	2382	2.382	0.435	212.477	2.125×10^{-13}
Average	1.192	422.101	**0.422**	5.383	1883	**1.883**	0.243	128.081	$\mathbf{1.281 \times 10^{-13}}$

Table 3.4 : Calculated average mass of bacterial cells using TEM imagery and modified Norland correlations.

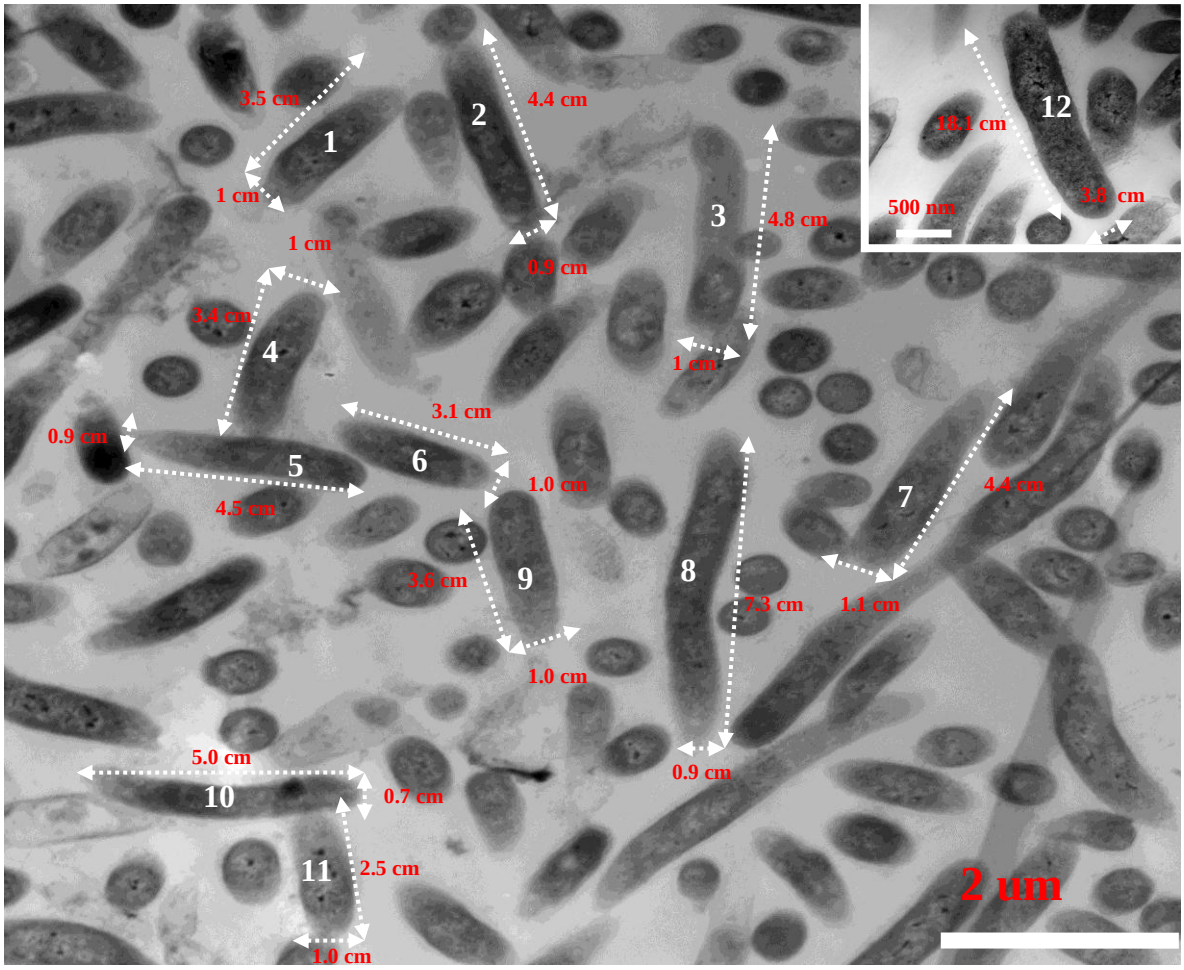

Figure 3.3 : Bacterial measurements taken from TEM imagery (not to same scale as values given in Table 3.4).

3.3. Results and discussion

3.3.1. Time Course of metal biosorption

Figure 3.4 -3.8 show the temporal evolution for the removal of aqueous Au^{3+}, Co^{2+} and Fe^{3+} metal ions by live cells of *S. putrefaciens*. The samples were collected after intervals of 3-4 hours exposure time and after 24 hours as is reported in Table 3.5. Experiments were all conducted batch-wise under anoxic conditions with a head space of H_2(g). For all experiments it was shown the biosorption was a fast process with the largest proportion of the total metal adsorbed in 1 hour followed by a slower sorption phase. Our results demonstrate higher removal efficiency of gold followed by cobalt and iron which indicates different mechanisms of removal for the metal ions.

		Assay	$[C_0]$ Initial	$[C_0]$ Final	η %	q mmol-$[M^{n+}]$/g cell	q mg-$[M^{n+}]$/g Cell	q mol-$[M^{n+}]$/cell	q mg-$[M^{n+}]$/mg Cell
Initially active cells	Au	1 pH3	275.582	119.212	57%	6.829	1342.954	8.746×10^{-13}	1.343
		2 pH3	247.104	102.330	59%	6.322	1243.368	8.098×10^{-13}	1.243
		3 pH3	162.422	101.556	37%	2.658	522.740	3.404×10^{-13}	0.523
		4 pH1	264.917	179.208	32%	3.743	736.098	4.794×10^{-13}	0.736
		5 pH1	165.694	106.950	35%	2.565	504.508	3.286×10^{-13}	0.505
		6 pH2	173.166	113.885	35%	2.589	509.124	3.31×10^{-13}	0.509
		7 pH2	165.694	106.413	35%	2.589	509.124	3.316×10^{-13}	0.509
	Co	1 pH3	208.277	169.555	19%	5.643	332.559	7.228×10^{-13}	0.333
		2 pH3	210.745	167.411	21%	6.315	372.162	8.089×10^{-13}	0.372
		3 pH3	210.964	169.516	20%	6.041	355.970	7.737×10^{-13}	0.356
	Fe	1a pH1	191.538	156.410	18%	5.402	301.693	6.919×10^{-13}	0.302
		1b pH1	172.564	158.718	7%	2.129	118.915	2.727×10^{-13}	0.119
		2a pH2	175.641	158.528	9%	2.632	146.976	3.371×10^{-13}	0.147
		2b pH2	216.907	185.773	14%	4.788	267.390	6.132×10^{-13}	0.267
		2c pH2	202.887	168.660	17%	5.263	293.951	6.741×10^{-13}	0.294
Initially deactivated cells	Au	a pH3	185.334	108.521	41%	3.354	659.690	4.296×10^{-13}	0.660
		b pH3	181.088	93.860	49%	3.809	749.143	4.879×10^{-13}	0.749

Table 3.5 : Removal efficiency η % and amount of metal removed q from solutions after 24 hours for various metal species, solution pH and initial metal ion concentrations.

3.3.2. Gold biosorption dynamics

3.3.2.1. Effects of metal ion concentrations on gold biosorption dynamics

A comparison of concentration decay in Figure 3.4 shows that for solutions with pH 3 initial metal ion concentration had relatively little effect on the removal efficiency by the bacteria with approximately 30% of ions removed within 3 hours. The total amount of metal ions biosorbed after 3 hours for metal assays with an initial concentration of

276 ppm, 247 ppm was 162 ppm of 658 mg-Au/g-cell, 663 mg-Au/g-cell and 394 mg-Au/g-cells, respectively. This would suggest that the ratio of initial metal ion concentration to fractional surface area for absorption of metal ions is relatively high; hence the percentage removal of metal is independent of initial metal concentration for solutions of low pH.

Equilibrium metal uptake of gold is shown in Table 3.5 in the first seven rows which indicate higher overall removal of metal ions for assays with higher initial metal ion concentration with up to 59% (1243 mg-Au/g-cells) and 57% (1343 mg-Au/g-cells) of gold metal ions removed for metal concentrations for 247 ppm and 276 ppm respectively compared to 37% (523 mg-Au/g-cells) for initial metal concentrations of 162 ppm. Maximum uptake values up to 6.83 mmol-Au/g-cells show an efficient reducing power of live *S. putrefaciens* cells of 8.75 x 10^{-13} mol-Au/cell for low pH systems in comparison to reports by Y. Konishi et al. (Konishi, Tsukiyama et al. 2006) as a reducing power of (2.1-3.3) X 10^{-16} mol-Au/g-cell utilizing *S. algae* cells with buffered solutions of pH 7.

Re-examination of Figure 3.4 shows that for solutions with relatively higher concentrations of metal ions with a solution pH 1 and initial Au^{3+} concentration of 265 ppm gave a much faster initial biosorption of metal ions with up to 38%, (864 mg-Au/g-cell) within the first 10 minutes. The removal remains at around 40% for 60 minutes and then reduces further to 21% i.e. 474 mg/g-cell by 3 hours. A lower initial removal for solution pH 3 with 247 ppm Au^{3+} was observed, i.e. 23%, 497 mg/g-cell within 10 minutes rising to 30%, 638 mg/g-cell after 3 hours contact time. The observed fast initial removal followed by a rise in Au^{3+} concentration after 60 minutes would suggest that solutions of low pH has significant effect on the bacteria cell surface characteristics. The rise of gold ion concentration in solution after 60 minutes was probably due to the onset of irrevocable cell damage to some bacterial cells releasing previously adsorbed metal ions back into the bulk solution. Equilibrium values taken after 24 hours (Table 3.5) show a significant overall higher rate of biosorption for assay 1 and assay 2 of 57% and 59%, compared to 32% for assay 4. Thus for metal solutions of gold concentrations above 245 ppm and lower pH there is less overall removal of metal ions over a 24 hour contact time compared with solutions of pH 3.

3.3.2.2. Effects of solution pH on gold biosorption dynamics

Examining the data from Figure 3.5 where pH variation from 1 to 3 at a constant Au^{3+} concentration is examined, it is observed that for metal assays with lower metal ion concentration (≈165 ppm), pH did not have a significant effect on the removal efficiency. Approximately 25%, (≈350 mg-Au/g-cell) of metal ions are removed within 30 minutes rising to 32% for solutions of pH 1 and 29% for solutions of pH 2. One would expect pH would have a significant effect on the initial removal efficiency but this was not observed for these metal solutions. After 24 hours a slightly higher removal for the solution of pH 3 of 37% (523 mg-Au/g-cell) was observed compared to pH 2 of 35% (504 mg-Au/g-cell) and pH 1 of 32% (736 mg-Au/g-cell).

This would suggest there to be a combined effect of metal ion toxicity and solution pH on the viability of the live bacterial cells. Initial (0 – 4 hours) remediation could be by live cells which is a biotic process, whereas further removal is carried out by deactivated dead cells or bacterial cells of reduced viability at lower pH's. To verify this TEM investigations were carried out as well as further metal removal assays using deactivated cells which is discussed shortly.

3.3.3. Cobalt and iron biosorption dynamics

Figure 3.6 show that the removal efficiency for cobalt ions was initially fast, with up to 20% (355 mg/g-cell) of the cobalt ions being removed within the first 10 minutes and remaining at this level to 24 hours. This is in agreement with previous investigations carried out by Mamba et al. (Mamba, Dlamini et al. 2009) who report 17% removal efficiency for metal assays of pH 3.

Figures 3.7 and 3.8 show that the initial removal of ferric metal ions was similar for assays conducted at pHs 1 and 2. As with all other metals there was a fast initial removal of up to 15% (280 mg-Fe/g-cell) followed by a slower absorption phase. Absorption capacities of up to 5.402 mmol-Fe^{3+}/g-cell or 302 mg-Fe^{3+}/g-cell compare well with previous reports of iron biosorption using waste biomass with *Saccharomyces cerevisiae* (Chen and Wang 2010) of 0.062 mmol-Fe^{3+}/g-cell and of 152 mg-Fe^{3+}/g-cell using sulphurised activated carbon (Krishnan and Anirudhan 2008). Metal concentrations after 24 hour contact time showed that initial pH has negligible effect on

equilibrium (24 hours) iron removal from solution. This study shows that up to 300 mg-Fe/g-cell can be removed by live *S. putrefaciens* cells from solutions of low pH which compares well with previous investigated reports of aqueous ferric ion biosorption in solutions of pH 1-3 using *Rhizopus arrhizus* fungus by Aksu and Gulen of up to 180 mg-Fe/g-cell (Aksu and Gülen 2002) and dead bacterial Streptomyces cells as investigated by Selatnia et al. (Selatnia, Boukazoula et al. 2004) with values reported of up to 122 mg-Fe/g-cell.

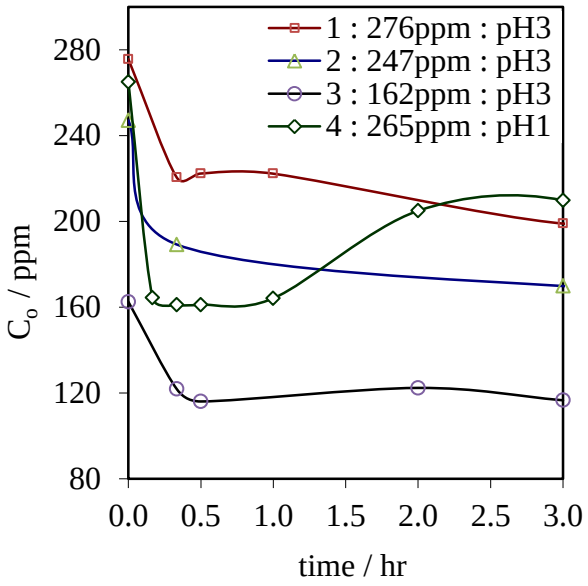

Figure 3.4 : Concentration profile of Au^{3+} biosorption for metal assays with variation with high initial Au^{3+} concentration of pH 3 for a 3 hour contact time. An additional profile at pH 1 is included to show effects of low pH.

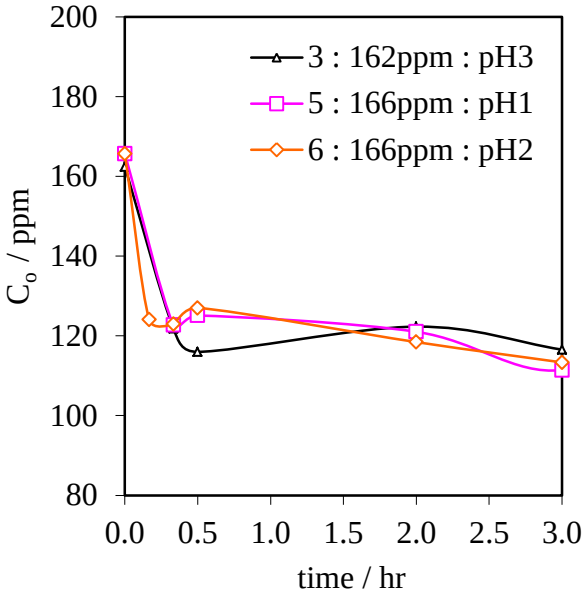

Figure 3.5 : Concentration profile of Au^{3+} biosorption for metal assays with varying in pH for a 3 hour contact time.

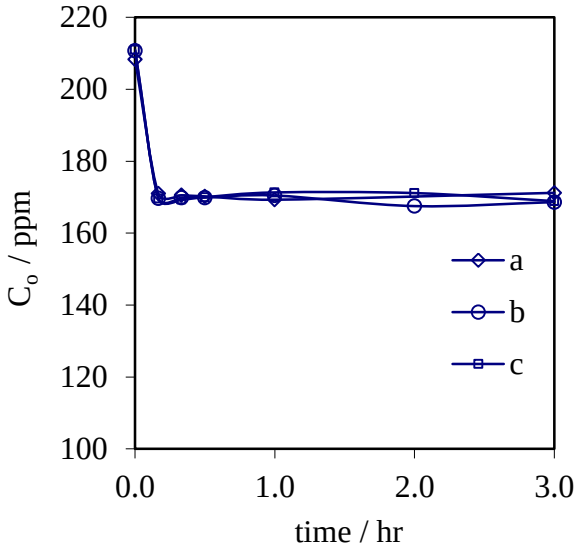

Figure 3.6 : Concentration profile of Co^{2+} biosorption for metal assays of ≈ 210 ppm initial Co^{2+} concentration and pH 3 over a 3 hour contact time.

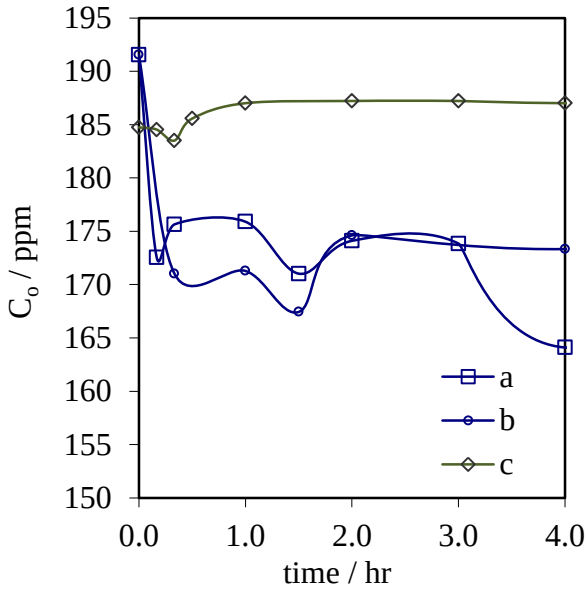

Figure 3.7 : Concentration profile for Fe^{3+} biosorption for metal assays with 192 ppm initial Fe^{3+} concentration and solution pH 1 over a 4 hour contact time, (a-b) with active cells and (c) control – no cells.

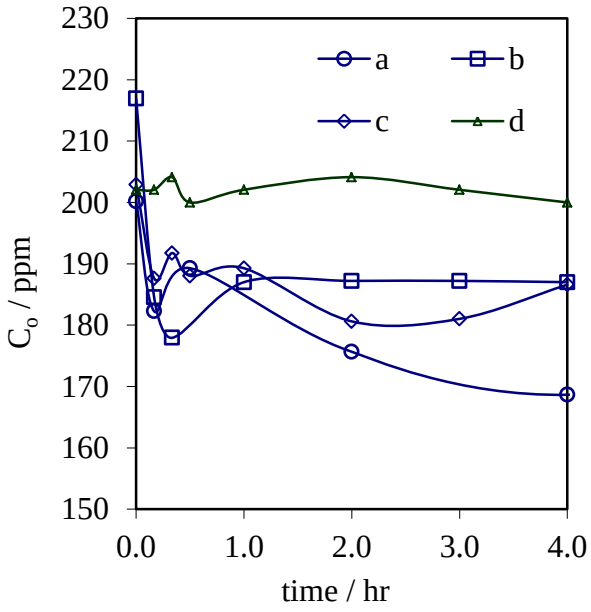

Figure 3.8 : Concentration profile for Fe^{3+} biosorption for metal assays with ≈ 220 ppm initial Fe^{3+}concentration and solution pH 2 over a 4 hour contact time, (a-c) with active cells and (d) control – no cells.

3.3.4. Kinetic model analysis of metal ion adsorption

Figures 3.9 to 3.17 illustrate modelling of metal ion biosorption for Au^{3+}, Co^{2+} and Fe^{3+} metal assays respectively and Table 3.6 summarises kinetic rate constants k_1, k_2 and k_{WM} with respective R^2 linear regression correlations. The pseudo second order rate equation generated the best model data for the metal remediation for all metal ions ($R^2 > 0.964$) which is consistent with previous investigations reported by McKay et al. (Ho and McKay 1999), Chen Can et al. for iron biosorption using *S. cerevisiae* (Chen and Wang 2010) and Bhatnagar et al. (Bhatnagar, Minocha et al. 2010) for cobalt removal using lemon peel.

The Lagergren pseudo first order ($0.82 < R^2 < 0.28$) and Weber and Morris ($0.87 < R^2 < 0.07$) did show some correlations in sorption of metal assays but of limited applicability. Values of n, the gradient of the modified Weber Morris equation show significant variation from 0.5 ($-0.432 < n < 0.491$) which indicate the diffusion process through bacterial liquid film and outer lipopolysaccharide leaf and inner polysaccharide layers of metal ions to reaction or complexation sites to be of a complex nature, with possible limiting overall reaction step, a combination of film and intra-particular diffusion.

The pseudo second order equation has been used to describe chemisorption involving vacancies through the sharing or exchange of electrons (Febrianto, Kosasih et al. 2009), this is of consistency with this study involving dissimilatory electroactive bacteria.

Iron metal assays 1b pH 1 and 2a pH 2 showed no applicability with any of the models.

			Pseudo-First-Order			Pseudo-Second-Order			Webber Morris		
			q_e	k_1		q_e	k_2		k_{id}	D_{WM}	
		$[M^{n+}]$	mg/g	(1/min)	R^2	mg/g	g /mg / min	R^2	mg/g /min$^{0.5}$	cm^2/s	R^2
Au	1 pH3	275.582	907.612	1.152×10^{-3}	0.816	1428.571	4.767×10^{-6}	0.964	192.0	7.941×10^{-13}	0.874
	2 pH3	247.104	984.238	2.303×10^{-3}	0.662	1428.571	4.217×10^{-6}	0.977	273.0	1.872×10^{-12}	0.872
	3 pH3	162.422	254.390	4.145×10^{-3}	0.282	526.316	5.286×10^{-5}	0.998	273.0	1.059×10^{-11}	0.637
	4 pH1	264.917	658.870	6.448×10^{-3}	0.797	769.231	6.842×10^{-5}	0.994	1016.7	7.408×10^{-11}	0.224
	5 pH1	165.694	286.154	6.909×10^{-3}	0.635	526.316	4.222×10^{-5}	0.990	281.6	1.210×10^{-11}	0.355
	6 pH2	173.166	169.981	6.425×10^{-2}	0.913	526.316	4.198×10^{-5}	0.994	517.8	4.017×10^{-11}	0.073
	7 pH2	165.694	238.397	8.291×10^{-3}	0.669	510.204	1.213×10^{-6}	1.000	282.0	1.192×10^{-11}	0.854
Co	1a pH3	208.277	907.612	1.152×10^{-3}	0.816	333.333	1.765×10^{-3}	1.000	320.0	3.596×10^{-11}	0.160
	1b pH3	210.745	24.055	4.145×10^{-3}	0.679	370.370	1.176×10^{-3}	1.000	337.8	3.200×10^{-11}	0.880
	1c pH3	210.964	1.169	-2.533×10^{-2}	0.631	357.143	3.015×10^{-3}	1.000	351.2	3.779×10^{-11}	0.637
Fe	1a pH1	191.538	77.535	3.040×10^{-2}	0.520	312.500	3.895×10^{-5}	0.985	91.8	3.596×10^{-12}	0.569
	1b pH1	172.564	n/a								
	2a pH2	175.641									
	2b pH2	216.907	96.472	1.175×10^{-2}	0.797	270.270	5.704×10^{-4}	1.000	249.2	3.372×10^{-11}	0.224
	2c pH2	202.887	2.504	2.303×10^{-3}	0.635	303.030	3.673×10^{-5}	0.970	66.3	1.975×10^{-12}	0.696

Table 3.6 : Values of k_1, k_2, k_{id} and D_{WM} and respective q_e using Lagergren first order kinetics, pseudo second order and Weber Morris intra-particular model.

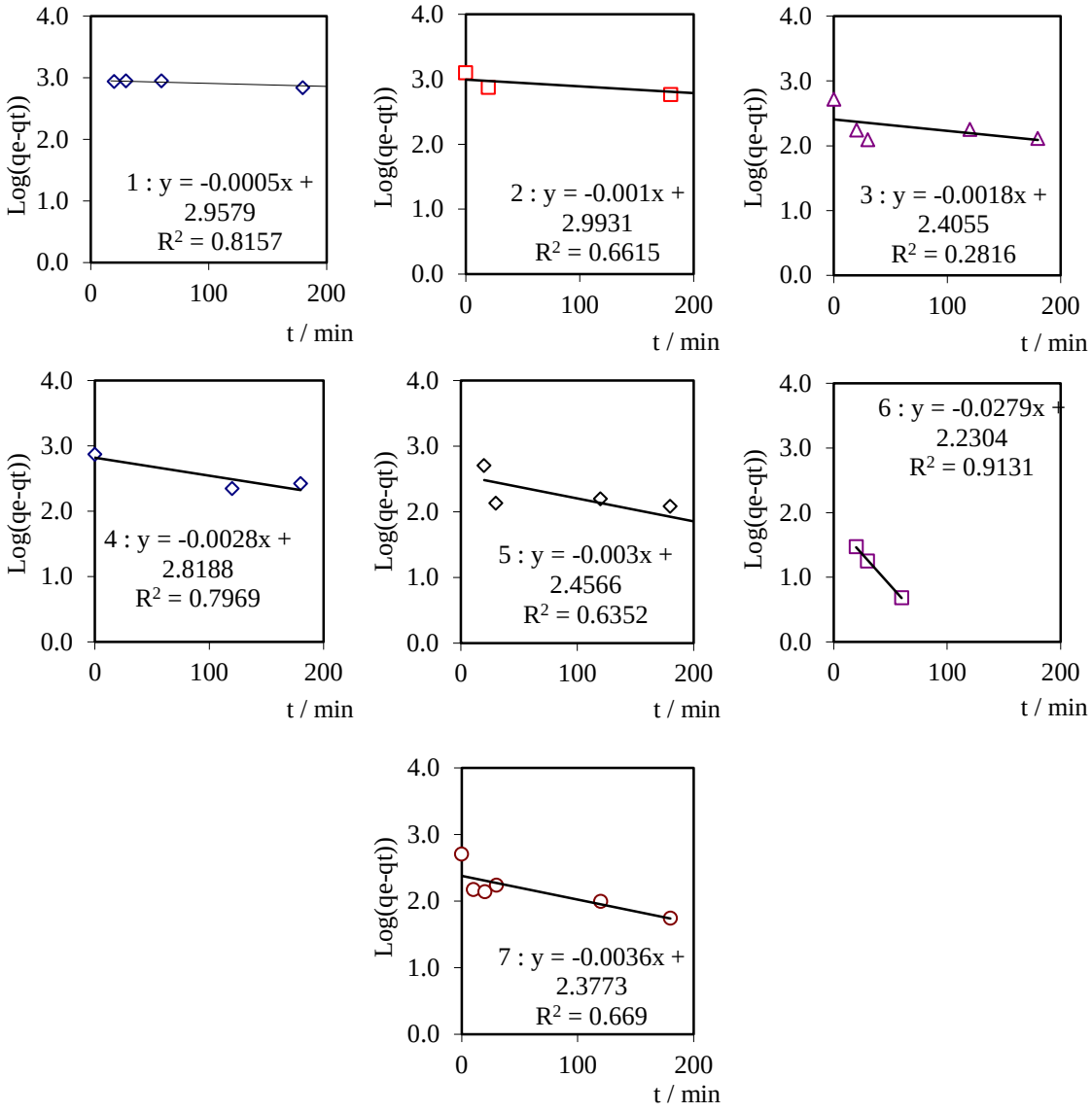

Figure 3.9 : Log(q_e-q_t) vs. *t* for first order modelling of Au^{3+} biosorption by *Shewanella putrefaciens* cells for reactions assays 1 - 7 as described by Table 3.6.

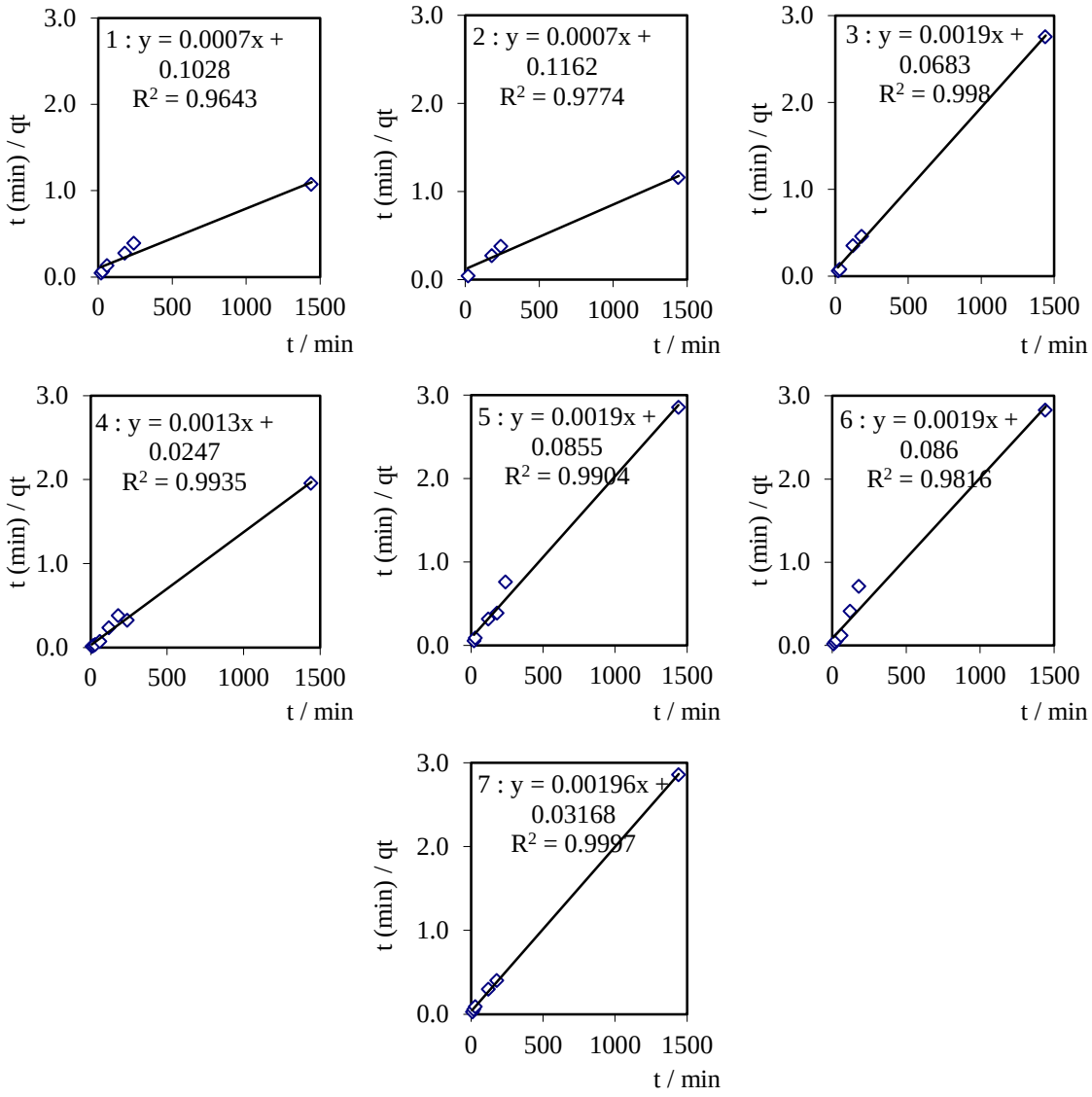

Figure 3.10 : t/q_t vs. t for second order modelling of Au^{3+} biosorption by *Shewanella putrefaciens* cells for reactions assays 1-7 as described by Table 3.6.

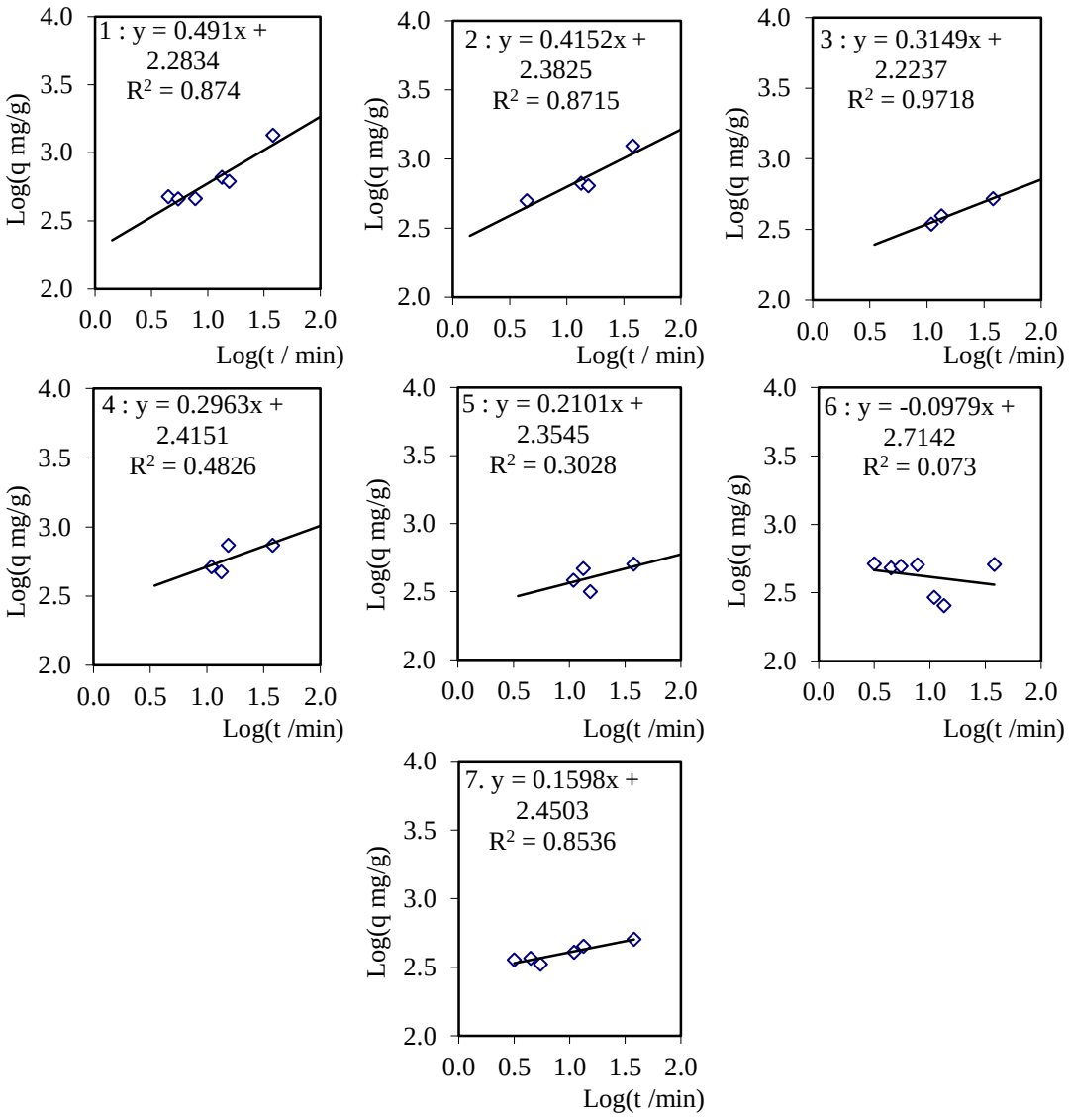

Figure 3.11 : Log(q_t) vs. Log(t) for Weber Morris modelling of Au^{3+} biosorption by *Shewanella putrefaciens* cells for reactions assays 1 - 7 as described by Table 3.6.

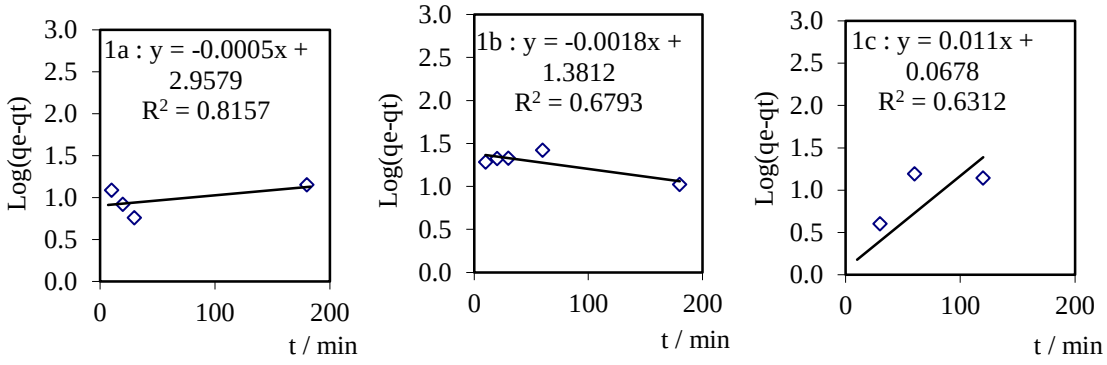

Figure 3.12 : Log(q_e-q_t) vs. t for metals cobalt assays 1a,b,c (Table 3.6) for first order modelling of Co^{2+} biosorption by *Shewanella putrefaciens* cells.

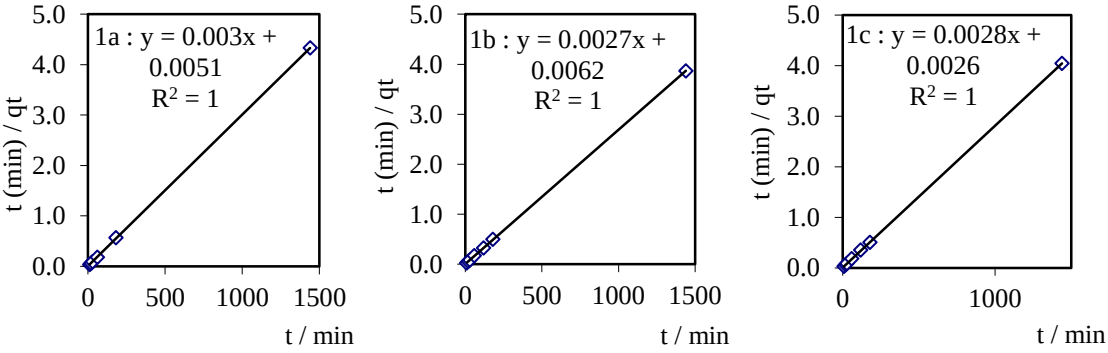

Figure 3.13 : t/q_t vs. t for second order modelling for metals cobalt assays 1a,b,c (Table 3.6) of Co^{2+} biosorption by *Shewanella putrefaciens* cells.

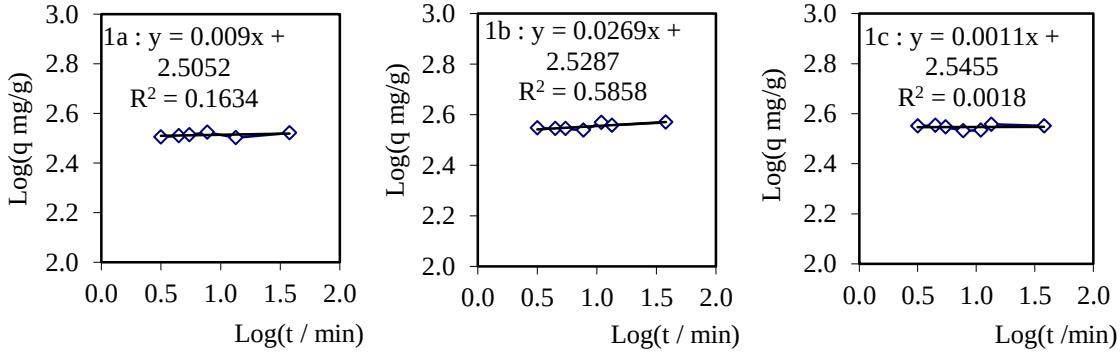

Figure 3.14 : Log(q_t) vs., Log(t) for Weber Morris modelling for metals cobalt assays 1a,b,c (Table 3.6) of Co^{2+} biosorption by *Shewanella putrefaciens* cells.

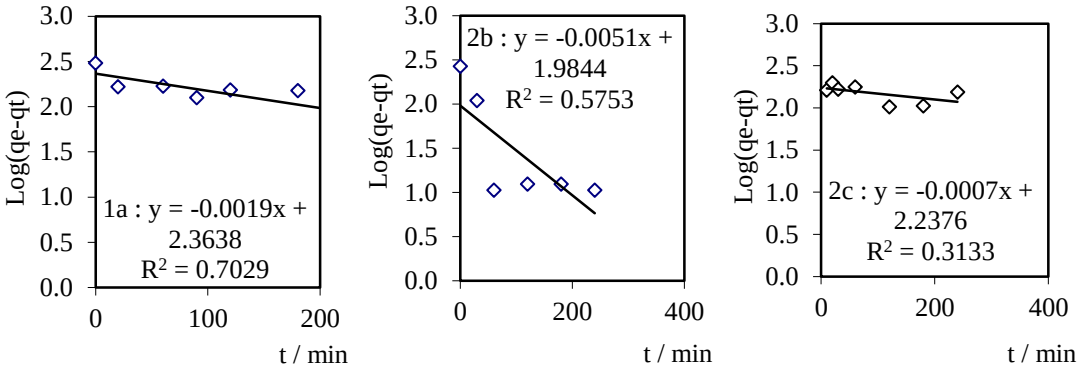

Figure 3.15 : Log(q_e-q_t) vs. *t* for metals iron assays 1a, 2b, 2c (Table 3.6) for first order modelling of Fe^{3+}biosorption by *Shewanella putrefaciens* cells.

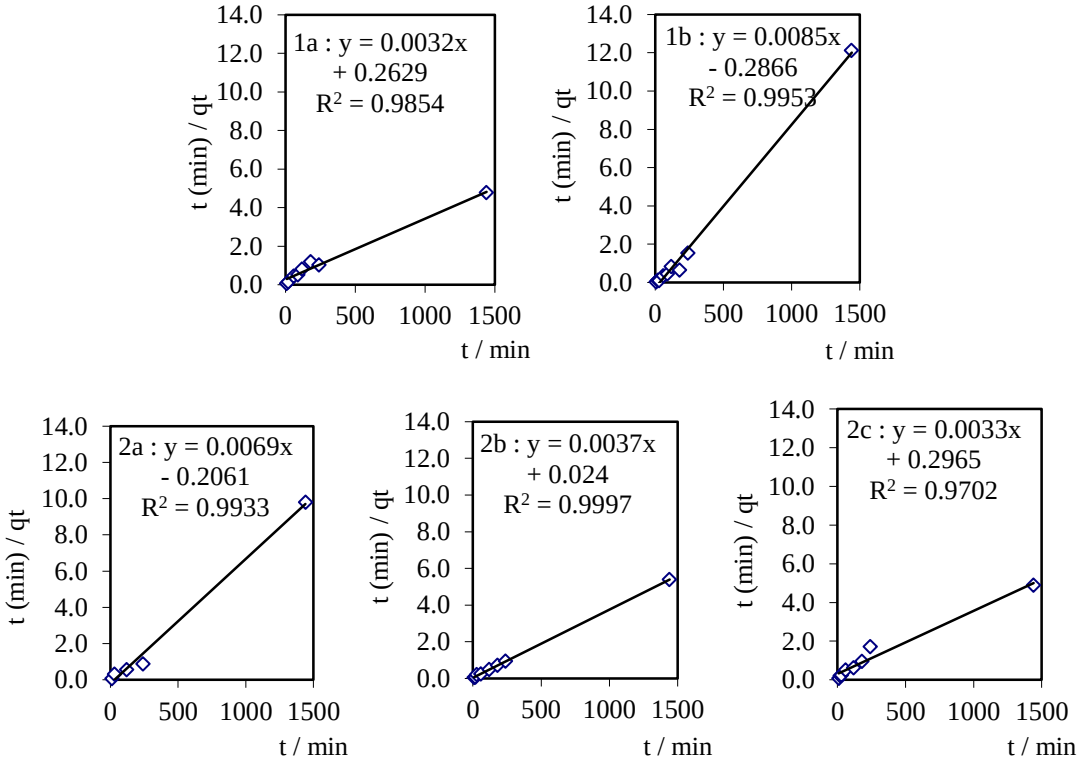

Figure 3.16 : t/q_t vs. *t* for second order modelling of Fe^{3+} iron assays 1a, 2b, 2c (Table 3.6) for first order modelling of Fe^{3+} biosorption by *Shewanella putrefaciens* cells.

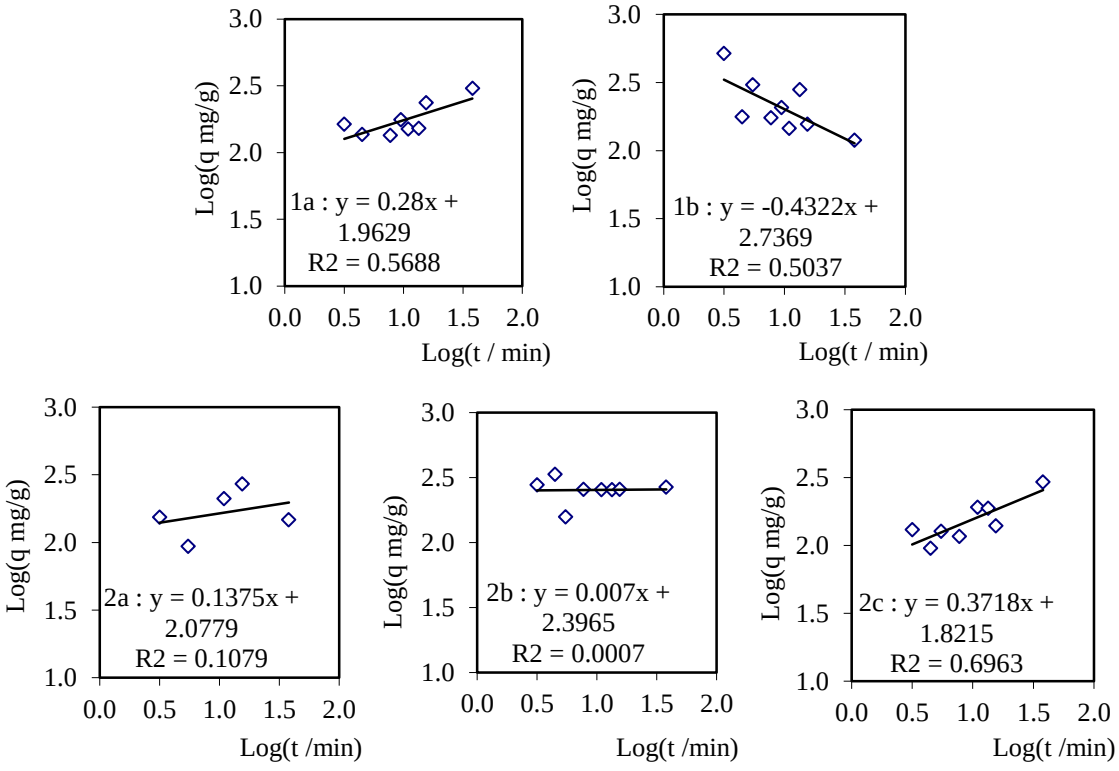

Figure 3.17 : Log(q_t) vs. Log(t) for Weber Morris modelling of Fe^{3+} iron assays 1a, 2b, 2c (Table 3.6) for first order modelling of Fe^{3+} biosorption by *Shewanella putrefaciens* cells.

3.3.5. Biosorption diffusion analysis

The diffusion coefficient could be calculated on the basis of the k_{id} calculated from fits of the Weber Morris model eq^n 2.71 and correlations described by Helfferich et al. by eq^n 2.72 and eq^n 2.73 where the pseudo second order model were used for calculation of $t_{1/2}$ for all metal assays as summarised in Table 3.7. As the Weber Morris approach gave an inadequate correlation for biosorption dynamics, further investigation of individual film and intra-particular coefficients would be desirable as to determine the rate determining step of the sorption process. The qualitative values calculated would point to the rate determining step of the biosorption process of the metal ions to be an intra-particular diffusion controlled process with reported values of D_p of all metals between 10^{-11} and 10^{-13} cm^2/s. Figures 3.18 - 3.19 illustrate calculated D_f, D_p and D_{WM} parameters as correlated to initial metal ion concentrations for solutions of pH 3 (Au Set 1). As evident in Figure 3.18, diffusion rates decrease as initial metal ion concentrations increase. This would suggest that an increase in initial concentrations has significant

effects on the cell membrane hindering film and intra-particular diffusion. Figure 3.19 shows that the effect of pH on diffusion coefficients for metal assays of initial concentration of 162 ppm. Calculated D_p and D_f values show no correlation to change in pH while that for D_{WM} does show a decrease. If the Weber Morris model is a good fit to data this would suggest that lowering of the solution pH increases the rate of intra-particular diffusion which relates well to investigations by Gaboriaud et al. (Langlet, Gaboriaud et al. 2008) discussed subsequently for TEM analysis regarding thinning and alterations of the cell wall with a decrease in pH. The R^2 of Webber Morris model application for Au (Table 4.7) assay 3 (pH 2) 0.64, assay 5 (pH 2) 0.35 and assay 7 (pH 3) 0.85 show some correlation, but are of low accuracy.

		D_f	D_p	D_{WM}
			cm^2/min	
Au^{3+}	1 pH3	2.114×10^{11}	1.025×10^{13}	7.941×10^{13}
	2 pH3	2.223×10^{11}	1.044×10^{13}	1.872×10^{12}
	3 pH3	5.128×10^{11}	3.766×10^{13}	1.059×10^{11}
	4 pH1	9.008×10^{11}	7.662×10^{13}	7.408×10^{11}
	5 pH1	4.154×10^{11}	3.225×10^{13}	1.210×10^{11}
	6 pH2	3.918×10^{11}	3.150×10^{13}	4.017×10^{11}
	7 pH2	1.079×10^{10}	8.298×10^{13}	1.192×10^{11}
Co^{2+}	1a pH3	5.332×10^{10}	7.893×10^{12}	3.596×10^{11}
	1b pH3	4.304×10^{10}	5.760×10^{12}	3.200×10^{11}
	1c pH3	1.034×10^{9}	1.448×10^{11}	3.779×10^{11}
$Fe3^{+}$	1a pH1	1.161×10^{11}	1.742×10^{13}	3.596×10^{12}
	1b pH1	n/a		
	2a pH2			
	2b pH2	1.097×10^{10}	2.103×10^{12}	3.372×10^{11}
	2c pH2	9.675×10^{12}	1.578×10^{13}	1.975×10^{12}

Table 3.7 : Diffusion coefficients for film and intra-particular diffusion and Weber Morris intra-particular diffusion coefficients calculated.

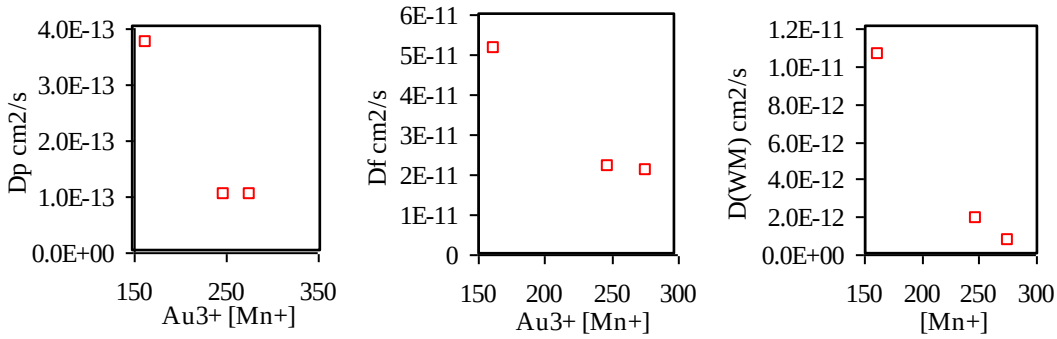

Figure 3.18: D_p, D_f and D_{WM} diffusion coefficients as a function of initial concentrations for metals of pH 3 (Au assays set1).

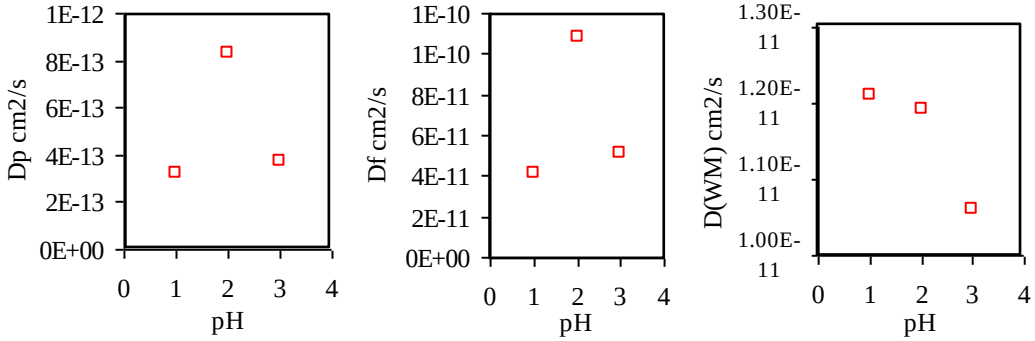

Figure 3.19 : D_p, D_f and D_{WM} diffusion coefficients as a function of pH for metal assays with initial concentrations of ≈ 162 ppm (Au assays set 3).

3.3.6. Metal Biosorption isotherms analysis in relation to biosorption thermodynamics

Langmuir and Freundlich models can be applied to obtain sorption equilibrium parameters. The equilibrium concentrations were taken after 24 hours for a range metal concentration from 300 ppm to 20 ppm and bacterial concentrations of 1.0 x10^{10} to 1.7 x 10^7 CFU/ml. From the biosorption data plotted as shown in Figure 3.20 we can deduce that the uptake rate is directly proportion to bacterial biomass for both metal ions as $1/q_e$ is proportional to $1/C_e$. The Langmuir model shows better correlation for all metal species. Table 3.8 describes all calculated model parameters.

The maximum biosorption capacity q_{max} can be interpreted as the total number of binding sites available for biosorption. Values of 3.794 mmol-Au^{3+}/g-cells show superior biosorption capabilities in comparison to reports by Khoo and Ting et al.

(Khoo and Ting 2001) of gold biosorption with immobilized fungal biomass with q_{max} values of 94 mg-Au^{3+}/g-cells (0.477mmol-Au^{3+}/g-cell). Values of q_{max} for Co^{2+} ions of 417 mmol-Co^{2+}/g-cells are three orders of magnitude higher to that of previous investigations for cobalt biosorption. Chen Can et al. gave reports of q_{max} for Co^{2+} using waste biomass of *S. cerevisiae* as 0.128 mmol-Co^{2+}/g-biomass (Chen and Wang 2010).

This would suggest a considerably higher affinity of live cells to Co^{2+} ions compared to dead cells as reported in the literature. Langmuir parameters of q_{max} for $Fe^{3+}$of 25.126 mmol-Fe^{3+}/g-cells (1403 mg-Fe^{3+}/g-cells) compare favourably with previous investigations with solutions of low pH. With reported values for q_{max} 125 mg-Fe^{3+}/g-cells using dead *Streptomyces rimosus* cells by Selatnia et al. (Selatnia, Boukazoula et al. 2004) and up to 46 mg-Fe^{3+}/g-sorbent by activated carbon as reported by Mohan and Chander (Mohan and Singh 2002).

Standard Gibbs free energy values where calculated using eq^{n} 2.50 as a measure of the thermodynamic spontaneity of the reaction. The negative values of ΔG for all metal ions indeed do indicate that the reaction is spontaneous and with preference of Au^{3+} > Fe^{3+} > Co^{2+}.

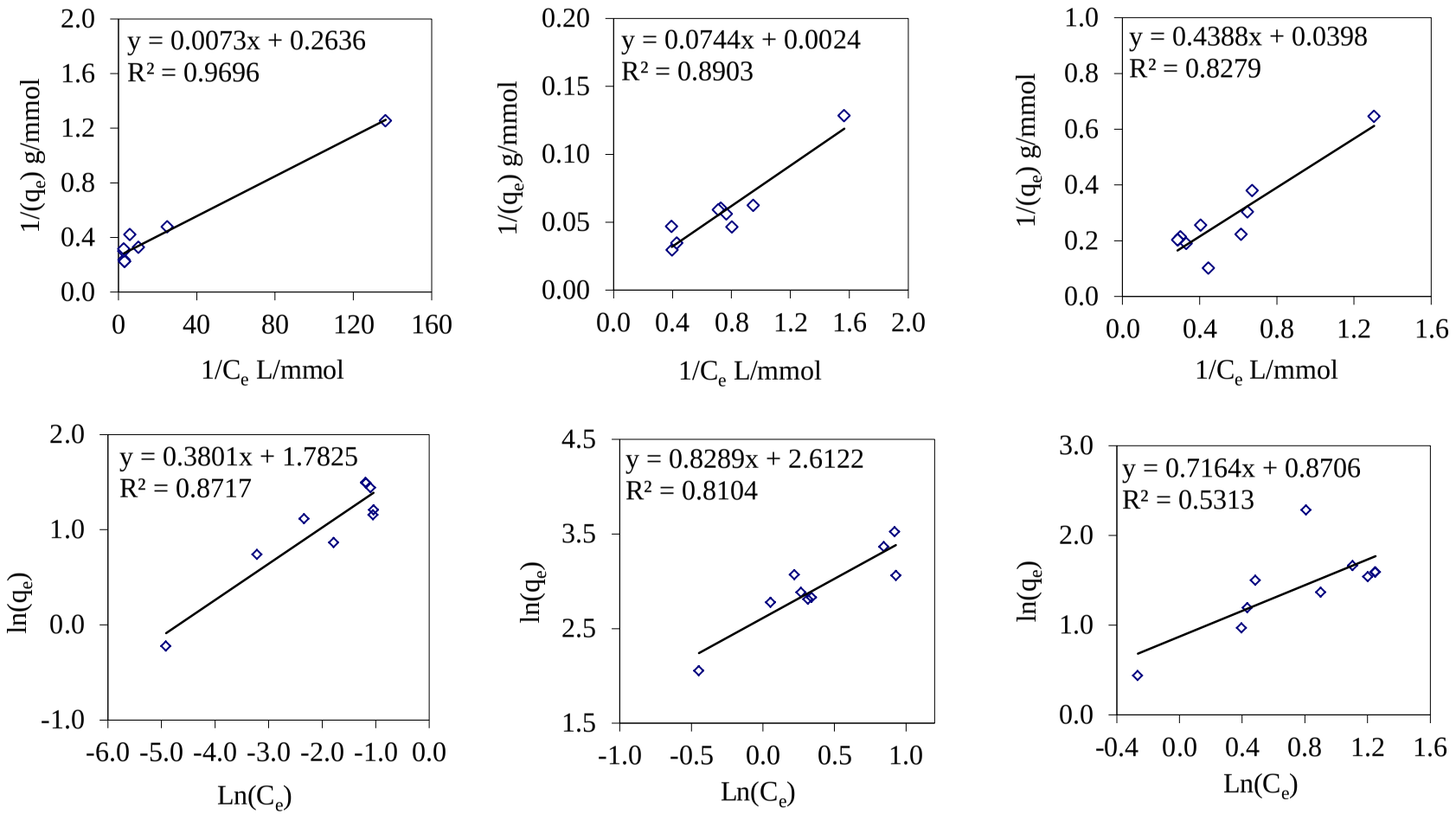

Figure 3.20 : Sorption metal isotherms of gold, cobalt and iron metal ions (a) Au^{3+}, (b) Co^{2+} and (c) Fe^{3+} Langmuir sorption isotherms and (d) Au^{3+}, (e) Co^{2+} and (f) Fe^{3+} Freundlich sorption isotherms.

Langmuir Adsorption Isotherm

$1/(q_e) = 1/(C_e\ q_{max}\ b) + 1/q_{max}$

	Equation	c	q_{maz}		ΔG		m	b		R^2
Au^{3+}	y = 0.0073x + 0.2636	0.26	3.794	mmol/g	-26.014	kJ/mol	0.01	36.1	L/mmol	0.97
Co^{2+}	y = 0.0744x + 0.0024	0	416.67	mmol/g	-11.173	kJ/mol	0.07	0.03	L/mmol	0.89
Fe^{3+}	y = 0.4388x + 0.0398	0.04	25.126	mmol/g	-8.611	k/Jmol	0.44	0.09	L/mmol	0.828

Freundlich Adsorption Isotherm

$Ln(q_e) = (1/n)Ln(C_e) + Ln(K_f)$

	Equation	c	K_f		m	n	R^2
Au^{3+}	y = 0.3801x + 1.7825	1.783	5.945	mmol^(1-1/n) L^(1/n) g^-1	0.38	2.63	0.8717
Co^{2+}	y = 0.8289x + 2.6122	2.612	13.629	mmol^(1-1/n) L^(1/n) g^-1	0.83	1.21	0.8104
Fe^{3+}	y = 0.7164x + 0.8706	0.871	2.388	mmol^(1-1/n) L^(1/n) g^-1	0.72	1.4	0.5313

Table 3.8 : Parameters of the Langmuir and the Freundlich models for metal adsorption determined from fits to experimental data.

3.3.7. Change in pH of metal ion assays

Solution pH has been implicated as one of the most important factors in the bio-sorption process (Volesky 2001), affecting solution chemistry of the metals and activity of functional groups in the bacterial cell walls implicated in the biosorption of metallic ions. Samples from reaction assays were also monitored for changes in pH which if increased by the bacterial activity could cause the metals to precipitate out. Our results showed that the pH of metal assays were unaffected (Figure 3.21) and hence we can further conclude that the metal ion removal from solutions is indeed exclusively microbiological as opposed to a chemical precipitation process.

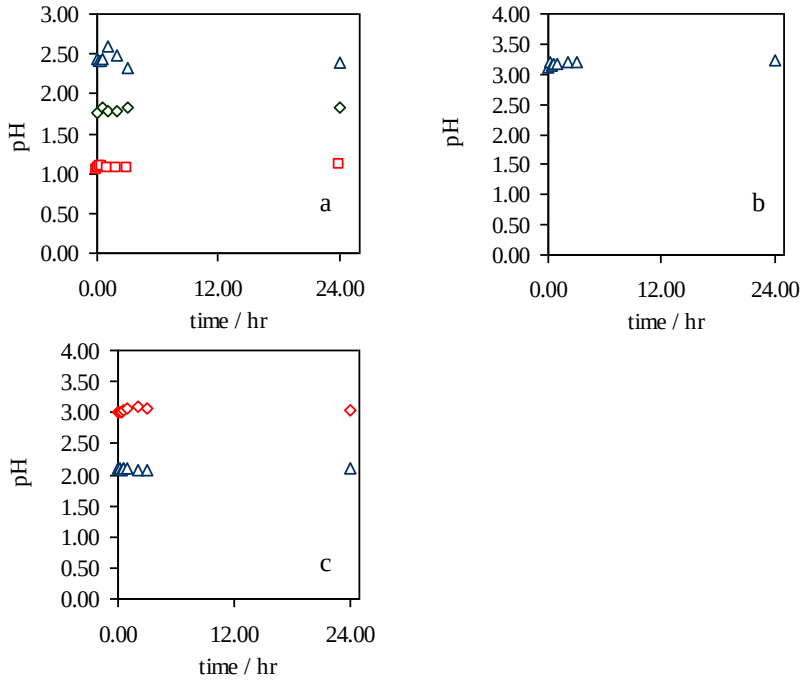

Figure 3.21 : pH changes in metal assays injected with 5 ml of 1 x 10^{10} CFU/ml *Shewanella putrefaciens* cells for (a) gold assays, (b) cobalt assays and (c) iron assays.

3.3.8. Ultra-sonication of gold metal assays and UV analysis of solutions

Figure 3.22 shows the UV spectra recorded from $HAuCl_4$(aq) solution with Au^{3+} concentrations of 200 ppm before exposure to bacterial cells (Figure 3.22) and after exposure to cells for 48 hours and subsequent sonication of the solution for 3 hours. After osmotic lyses by sonication of bio-metal assay containing 200 ppm Au^{3+}, pH 3 for 3 hours, the solution turned from an opaque yellow to a vivid purple which indicates the presence of gold nanoparticles in the solution. Gold nanoparticles adsorb radiation in

the visible region of the electromagnetic spectrum around 520 nm (Mulvaney 1996), caused by the excitation of surface plasma. UV spectra of exposed cells show a distinct absorption around 550 nm which is consistent with previous reports (Mukherjee, Senapati et al. 2002; Ahmad, Senapati et al. 2003; Deplanche and Macaskie 2008; Deplanche, Woods et al. 2008) as a conclusive indicator of the presence of gold nanoparticles.

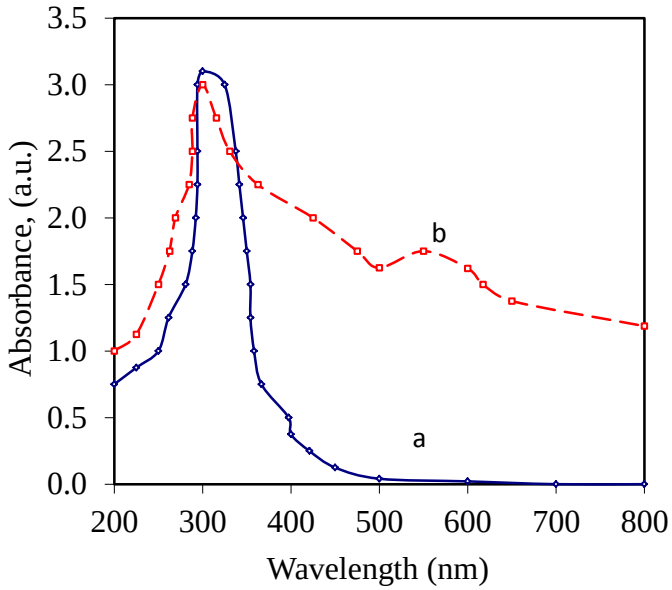

Figure 3.22 : UV-vis spectra recorded for $HAuCl_4$(aq), 200 ppm Au^{3+}, pH 3 control (a) before exposure to bacterial cells and (b) after 48 hours exposure and 3 hours osmotic lysis of bacterial cell wall by sonication of cells.

3.4. TEM analysis of bacterial cells before and after exposure to metal ions

The observation of Au nanoparticles by TEM (Figure 3.23) verifies the formation of Au nanoparticles by biosorption which is in good agreement with previous reports by Konishi et al. (Konishi, Tsukiyama et al. 2006; Konishi, Tsukiyama et al. 2007). TEM of cobalt nanoparticles gives unambiguous evidence for possible production of bio-nanoparticles by biological process. TEM images of bacteria exposed to Co^{2+} however show the occurrence of biogenic nanoparticles to be smaller. To date there has been very little report of cobalt bio-nanoparticles in the literature at large. As evident in Figure 3.23 far more nanoparticles are observed for Au^{3+} systems in comparison to the Co^{2+} system. Possibility due to different reduction mechanisms, i.e. specific

dissimilatory mechanism with Au^{3+} and the unspecific resistance mechanism for Co^{2+} systems, no nano-particles were observed for iron solutions since the reduction mechanism is expected to involve Fe^{3+} reduction to Fe^{2+}.

Though we are unable to carry out further qualitative analysis of the precipitates formed, these results have some consistency with previous investigations. At higher magnifications of *S. putrefaciens* cells after exposure, it was observed that most of the gold and cobalt precipitates were localized between the cell wall and the plasma membrane with some of gold and cobalt precipitates observed to be extracellular (Figure 2.23). This further reinforces reports of extracellular nucleation and agglomeration by Konishi et al. of gold nanoparticles formed at low pH 2 (Konishi, Tsukiyama et al. 2007).

Further investigation was carried with the gold metal assay and dead cells. Table 1 shows that up to 49%, 749 mg-Au^{3+}/g-cells of the gold metal ions can be removed by deactivated dead cells after a 24 hours contact time. Samples were also taken from these assays and TEM analysis performed as before. Figure 3.24a-e show that nano-particles were formed by inactivated cells for Au^{3+} located on the outer surface of bacterial cells but none were observed for the Co^{2+} assays. Also we noted that fewer nano-particles were observed for the dead cells in comparison to live cells.

Envelope profiles of *S. putrefaciens* prior to interaction with aqueous metal ion solution Figure 3.23a and Figure 3.25a are representative of Gram-negative bacteria concentrated in 0.9% NaCl(aq) pH 5.6. Cells are rod shaped approximately 0.5 μm wide and 2 μm long. Figure 3.25b show the corresponding image of cells after exposure to Co^{2+} solution with pH 3. Images show cell morphology to be considerably more irregular with reduced cell length and a decrease in the thickness of the polymeric fringe which is consistent with work carried out by Gaboriaud et al. (Langlet, Gaboriaud et al. 2008) using AFM and TEM imagery.

Their investigation demonstrated significant changes to the surface properties with a decrease in softness of the most external layers which is of particular interest to this study as it is associated with the biosorption of metal ions by the LPS outer leaf of the outer cell membrane layer of the bacterial cell wall. This thinning of the LPS was

reported to be in part due to the effect of pH on the hydrophilic/hydrophobic nature of the cell envelope. Solutions of low pH induce thinning and a reduction in softness of both the periplasm and polymeric layer which presumably would be due to the repulsive behaviour of intermolecular forces leading to a decrease in void spaces between the cytoplasm and the outer membrane and hence a significant change in the bacterial surface properties as is demonstrated in our investigations. This could have significant effects on the biosorption processes. Caution is required as the damage to the cell envelope may be significant over an extended period of time and thus biosorption of metal ions by the outer leaf of the cell lipopolysaccharide layer occurs by an amalgamation of biotic and/or abiotic biosorption and/or dissimilatory and resistance redox bio-reduction processes.

From the morphology of bacterial cells in Figure 3.25b it must be considered that at low pH, as is the case in this study, transformation may be due to biological artefacts rather than animate living cells, i.e. attention is required when describing the process as biotic. Cell lyses at low pH would cause the cell to burst and release biological electro-active enzymes such as cytochrome-c which reduce the metal ions into the surrounding solution. Thus the biosorption and bioreduction of metal ions could be occurring by abiotic processes by inactive lyses cells. Alternatively the reduction could be a biotic reaction by enzymes within the cell envelope such as cytochrome-c, the reduced metal product then released later by the cell lyses at low pH.

It is expected that different mechanisms are indeed involved for the complete bioreduction of these metal ions and that this would suggest that for Co^{2+} the process is a strictly biotic resistance mechanism while that for gold is a biotic dissimilatory, (Konishi, Tsukiyama et al. 2006; Konishi, Tsukiyama et al. 2007), abiotic and non-enzymatic for de-activated heat-treated bacterial solutions. Metal ions can also be adsorbed and reduced by a pure chemical process involving the bacterial surface and external biological artefacts.

Recently similar reports of biogenic nanoparticles by de-activated cells have also been reported by De Corte et al. (De Corte, Hennebel et al. 2011), where the nanoparticles were only formed when in the presence of an electron donor such as H_2 or formate. Amino acids and glutathione could also have a role in the metal's reduction (Nies 1999;

De Corte, Hennebel et al. 2011). They postulated a mechanism involving the formation of an Au(I)-Sulphide complex based upon investigation of gold nanoparticles produced by cyanobacteria (Lengke, Fleet et al. 2006). Here the intermediate Au(I)-S species is further reduced to Au(0) particles by hydrogen in solution, the source of sulphur being amino acids and glutathione in bacterial cells. The role of the de-activated bacterial biomass is as a catalyst, providing an interfacial surface for the interaction of gold anions with reducing agents such as hydrogen in solution.

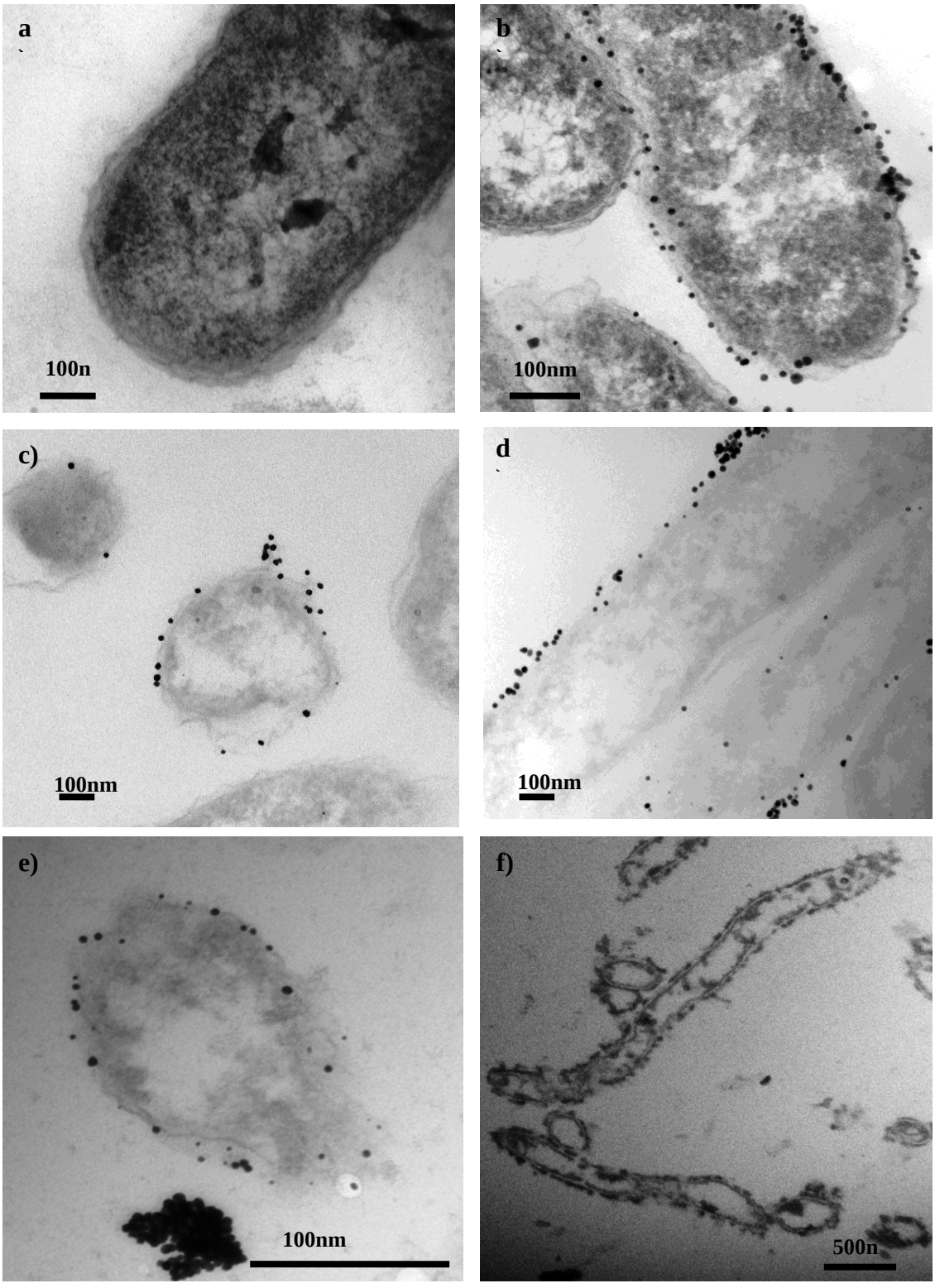

Figure 3.23 : TEM images of *S. putrefaciens* before and after exposure to aqueous $HAuCl_4$(aq), $CoSO_4$(aq) and $Fe(NO_3)_3$(aq) solution at pH 3 after 24 hours. (a) Cells before exposure (stained). (b) Cells after exposure to 170 ppm Au^{3+} (stained). (c-d) S. *putrefaciens* of cells after exposure to 170 ppm Au^{3+} (un-stained). (e) Cells after

exposure to 195 ppm Co^{2+} (un-stained). (f) Cells after exposure to 200 ppm Fe^{3+} (stained).

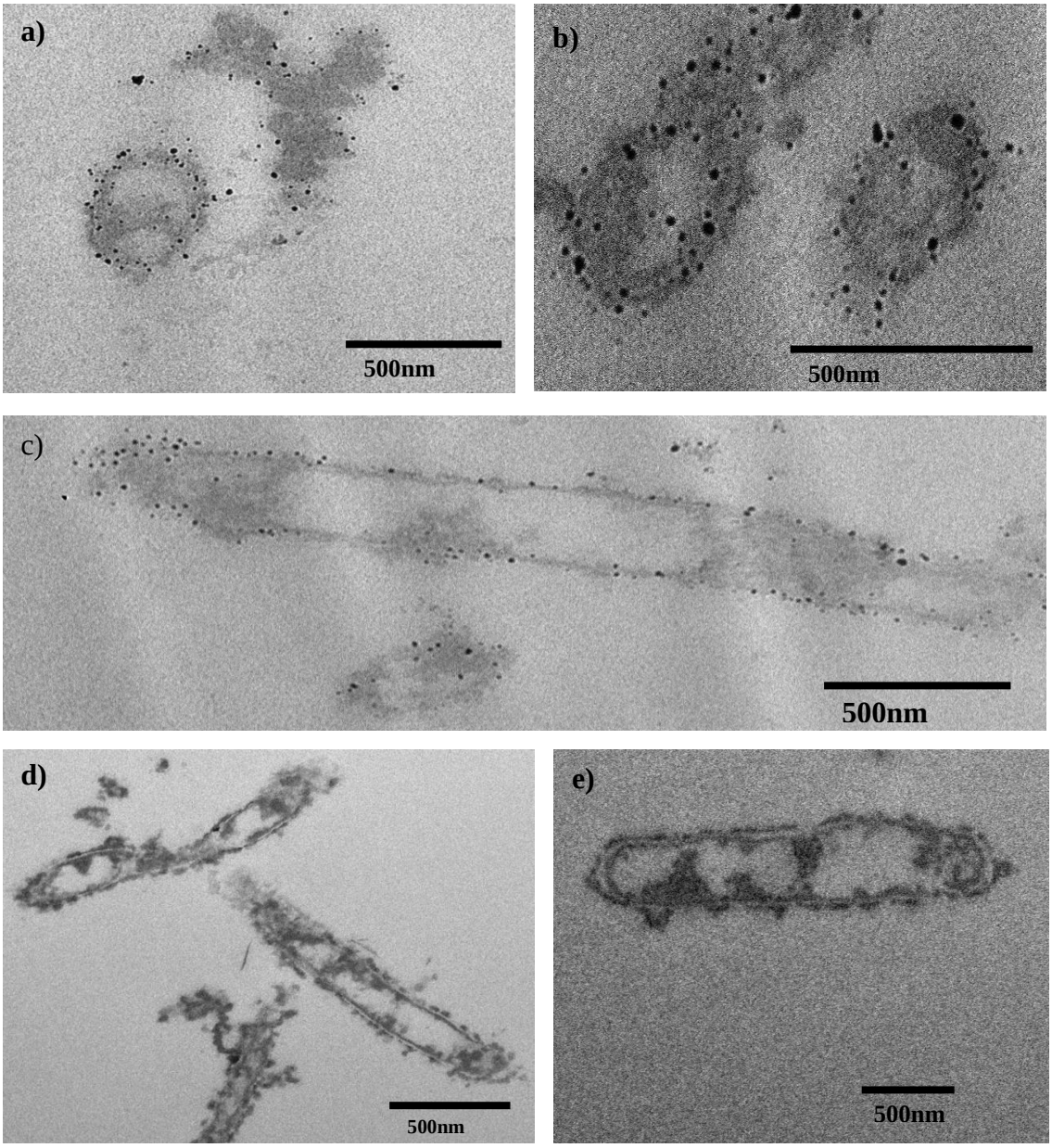

Figure 3.24 : TEM images of deactivated *S. putrefaciens* before and after exposure to aqueous $HAuCl_4$(aq) and $CoSO_4$ solution at pH 3 after 24 hours. (a-c) Cells after exposure to 200 ppm Au^{3+} (un-stained). (d-e) Cells after exposure to 200 ppm Co^{2+} (un-stained).

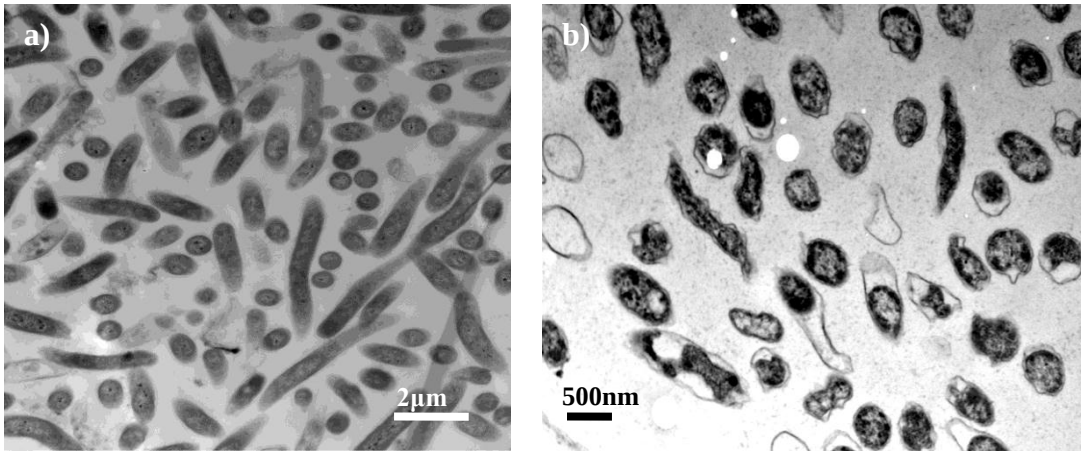

Figure 3.25 : TEM images of *S. putrefaciens* before and after exposure to aqueous $CoSO_4$(aq) solution at pH 3.

3.5. Conclusions

We here have demonstrated the ability to remediate cobalt, iron and gold metal ions by *S. putrefaciens* with an outlook as a green methodology for metal remediation and recovery. The results show the biosorption of the metal ions to be a fast process with TEM evidence of zero-valent biogenic nanoparticle production and hence simultaneous bioreduction by initially active cells for Au^{3+} and Co^{2+}, and both initially active as well as deactivated cells for Au^{3+}.

To our best knowledge this is the first visual unambiguous evidence of significant intra and extracellular cobalt bio-nanoparticles by dissimilatory bacterial cells and further evidence of nanoparticles produced by dead dissimilatory bacterial cells.

The low pH where these events occur is striking and extends the range of condition for the viability of bacterial cells and the interaction of the bacterial cell envelope and metal ions. The results gave good correlations with the Langmuir isotherm model and parameters showed that Co^{2+} ions had the highest affinity to the bacterial cells in comparison to Au^{3+} and Fe^{3+} ions. Fundamental thermodynamic analysis showed the biosorption reactions to be spontaneous, with more negative Gibbs free energy values for the removal of gold ions followed by iron and cobalt.

The pseudo second order model shows satisfactory application to metal assays and diffusion analysis of film and intra-particular diffusion coefficients show that intra-particular diffusion to be the rate determining step for the overall sorption process.

References

*Ahmad, A., S. Senapati, et al. (2003). "Extracellular Biosynthesis of Monodisperse Gold Nanoparticles by a Novel Extremophilic Actinomycete, Thermomonospora sp." Langmuir **19**(8): 3550-3553.*

*Aksu, Z. and H. Gülen (2002). "Binary biosorption of iron(III) and iron(III)-cyanide complex ions on Rhizopus arrhizus: modelling of synergistic interaction." Process Biochemistry **38**(2): 161-173.*

*Anushree, M. (2004). "Metal bioremediation through growing cells." Environment International **30**(2): 261-278.*

Atkins, P. W. (2001). The elements of physical chemistry : with applications in biology. New York, W.H. Freeman.

*Bhatnagar, A., A. K. Minocha, et al. (2010). "Adsorptive removal of cobalt from aqueous solution by utilizing lemon peel as biosorbent." Biochemical Engineering Journal **48**(2): 181-186.*

*Chen, C. and J. Wang (2010). "Removal of Heavy Metal Ions by Waste Biomass of Saccharomyces Cerevisiae." Journal of Environmental Engineering **136**(1): 95-102.*

Crank, J. (1979). The mathematics of diffusion, Clarendon Press.

*De Corte, S., T. Hennebel, et al. (2011). "Biosupported Bimetallic Pd–Au Nanocatalysts for Dechlorination of Environmental Contaminants." Environmental Science & Technology **45**(19): 8506-8513.*

*Deplanche, K. and L. E. Macaskie (2008). "Biorecovery of gold by Escherichia coli and Desulfovibrio desulfuricans." Biotechnology and Bioengineering **99**(5): 1055-1064.*

*Deplanche, K., R. D. Woods, et al. (2008). "Manufacture of stable palladium and gold nanoparticles on native and genetically engineered flagella scaffolds." Biotechnology and Bioengineering **101**(5): 873-880.*

*Febrianto, J., A. N. Kosasih, et al. (2009). "Equilibrium and kinetic studies in adsorption of heavy metals using biosorbent: A summary of recent studies." Journal of Hazardous Materials **162**(2-3): 616-645.*

Freundlich, H. (1906). Ueber die Adsorption in Lösungen.

Helfferich, F. G. (1995). Ion exchange, Dover Publications.

*Ho, Y. S. and G. McKay (1999). "Pseudo-second order model for sorption processes." Process Biochemistry **34**(5): 451-465.*

*Khoo, K. M. and Y. P. Ting (2001). "Biosorption of gold by immobilized fungal biomass." Biochemical Engineering Journal **8**(1): 51-59.*

*Konishi, Y., T. Tsukiyama, et al. (2006). "Intracellular recovery of gold by microbial reduction of AuCl4− ions using the anaerobic bacterium Shewanella algae." Hydrometallurgy **81**(1): 24-29.*

*Konishi, Y., T. Tsukiyama, et al. (2007). "Microbial deposition of gold nanoparticles by the metal-reducing bacterium Shewanella algae." Electrochimica Acta **53**(1): 186-192.*

*Krishnan, K. A. and T. S. Anirudhan (2008). "Kinetic and equilibrium modelling of cobalt(II) adsorption onto bagasse pith based sulphurised activated carbon." Chemical Engineering Journal **137**(2): 257-264.*

*Langlet, J., F. Gaboriaud, et al. (2008). "Impact of Chemical and Structural Anisotropy on the Electrophoretic Mobility of Spherical Soft Multilayer Particles: The Case of Bacteriophage MS2." Biophysical Journal **94**(8): 3293-3312.*

*Langmuir, I. (1918). "THE ADSORPTION OF GASES ON PLANE SURFACES OF GLASS, MICA AND PLATINUM." Journal of the American Chemical Society **40**(9): 1361-1403.*

*Lengke, M. F., M. E. Fleet, et al. (2006). "Morphology of Gold Nanoparticles Synthesized by Filamentous Cyanobacteria from Gold(I)−Thiosulfate and Gold(III)−Chloride Complexes." Langmuir **22**(6): 2780-2787.*

*Loferer-Krossbacher, M., J. Klima, et al. (1998). "Determination of bacterial cell dry mass by transmission electron microscopy and densitometric image analysis." Appl Environ Microbiol **64**(2): 688-694.*

*Mamba, B. B., N. P. Dlamini, et al. (2009). "Biosorptive removal of copper and cobalt from aqueous solutions: Shewanella spp. put to the test." Physics and Chemistry of the Earth, Parts A/B/C **34**(13-16): 841-849.*

*Mohan, D. and K. P. Singh (2002). "Single- and multi-component adsorption of cadmium and zinc using activated carbon derived from bagasse—an agricultural waste." Water Research **36**(9): 2304-2318.*

*Mukherjee, P., S. Senapati, et al. (2002). "Extracellular Synthesis of Gold Nanoparticles by the Fungus Fusarium oxysporum." ChemBioChem **3**(5): 461-463.*

*Mulvaney, P. (1996). "Surface Plasmon Spectroscopy of Nanosized Metal Particles." Langmuir **12**(3): 788-800.*

*Nies, D. H. (1999). "Microbial heavy-metal resistance." Applied Microbiology and Biotechnology **51**(6): 730-750.*

*Norland, S., M. Heldal, et al. (1987). "On the relation between dry matter and volume of bacteria." Microbial Ecology **13**(2): 95-101.*

*Poots, V. J. P., G. McKay, et al. (1978). "Removal of Basic Dye from Effluent Using Wood as an Adsorbent." Journal (Water Pollution Control Federation) **50**(5): 926-935.*

*Selatnia, A., M. Z. Bakhti, et al. (2004). "Biosorption of Cd2+ from aqueous solution by a NaOH-treated bacterial dead Streptomyces rimosus biomass." Hydrometallurgy **75**(1–4): 11-24.*

*Selatnia, A., A. Boukazoula, et al. (2004). "Biosorption of Fe3+ from aqueous solution by a bacterial dead Streptomyces rimosus biomass." Process Biochemistry **39**(11): 1643-1651.*

*Stookey, L. L. (1970). "Ferrozine---a new spectrophotometric reagent for iron." Analytical Chemistry **42**(7): 779-781.*

*Veglio, F. and F. Beolchini (1997). "Removal of metals by biosorption: a review." Hydrometallurgy **44**(3): 301-316.*

*Volesky, B. (2001). "Detoxification of metal-bearing effluents: biosorption for the next century." Hydrometallurgy **59**(2-3): 203-216.*

Chapter 4: Bioelectrochemical experimentation: electrochemical analysis of reaction thermodynamics with and without live bacterial cells

Chapter 4: Bio-electrochemical experimentation: electrochemical analysis of reaction thermodynamics with and without live bacterial cells

4.1. Introduction

Figure 4.1 gives an overview of the complexity of the electron transfer reactions occurring at a polarised electrode substrate surface consisting of a number of consecutive steps in the overall process of electron transfer at a charged interface.

Current density vs. potential *(i/E)* relationship where analysed to determine electron transfer reactions occurring at various potentials for metal ion species in electrolyte solutions. Quantitative analysis of individual reaction at equilibrium conditions were investigated using the Nernst equation (Bockris and Reddy 1970). Evaluation of these parameters gave a quantitative analysis for the elucidation of metal ion electronation processes occurring at the surface of the electrified electrode substrate.

Linear sweep voltammetry using slow scan rates of 0.010 V/s where used to determine reversible potentials for specified metal ion reduction reactions under investigation. Linear sweep voltammetry using faster scan rates (> 0.050 V/s) were also carried out for some systems for further reification of possible reaction mechanisms from current peaks analysis. Electrolytes where un-buffered and systems where not degassed of oxygen as representative of "real" mine waters and industrial effluents.

A systemic approach has been taken here with preliminary electrochemical analysis carried using Pt and Au RDE's as a basis for analysis using graphite electrodes with and without the addition of bacterial cells. Platinum and gold commonly used metallic solid electrodes for cathodic processes under investigation here. Due to the relatively high overpotentials requited for hydrogen evolution (Sawyer et al., 1995). Preliminary experimentation with Pt and Au RDE's was carried out in Na_2SO_4(aq) background electrolyte for cobalt and iron systems and in a HCl(aq) matrix for gold systems. Further experimentation with graphite electrodes was carried out in NaCl(aq) background electrolytes for cobalt and iron systems.

Graphite as an electrode substrate is a cheaper alternative to noble metal substrates and has favourable physical-chemical properties of high specific surface area, good fluid

permeability and compressibility, chemical inertness and good electrochemical conductivity (McCreery 2008). Reports of direct and indirect electron transfer of bacterial cells with electrified carbon substrates are well documented (Gregory, Bond et al. 2004) making it an ideal solid conducting material in bioelectrochemical systems of significance here.

Our experimentation has focused upon changes in the thermodynamics in the presence of bacterial cells evaluated upon changes in reversible potentials of metal ion electronation and electrodeposition. This quantified with a reduction in the Gibbs free energy (ΔG) of electronation reactions leading to remediation of dissolved metal ions, evaluated in this chapter by an overall savings in the minimum energy requirements with and without the addition of our representative electroactive bacterial cells.

Bioelectrochemical process for water purification of nitrate (Ghafari, Hasan et al. 2008), perchlorate (Thrash, Van Trump et al. 2007) and uranium (Gregory and Lovley 2005) by the interplay of electro-active bacteria and electrified graphite electrodes is a proven concept. There are also well documented reports regarding the phenomena of the bio-electrocatalytic (Hill and Higgins 1981) ability of electroactive bacteria with a plethora of research papers focused upon the anodic chamber where bacterial cells motivate their degradation via electro-oxidation of organic material to produce electrons which travel to the cathodic chamber usually with O_2 reduced to H_2O in bio-electrochemical systems such as microbial fuel cells (Bretschger, Cheung et al. 2010).

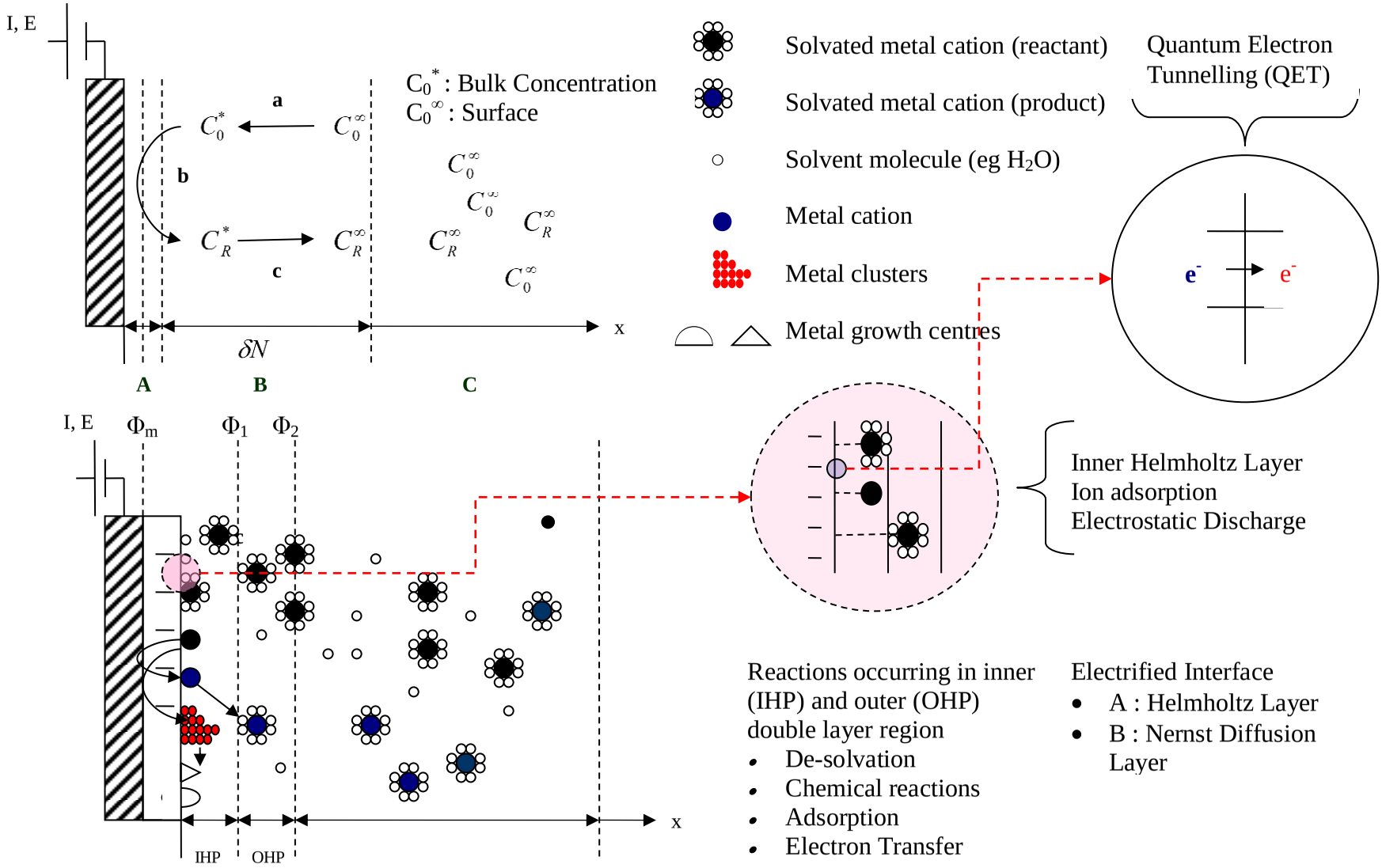

Figure 4.1 : Overview of reaction mechanism electrochemical process of metal ions species on Pt and Au RDE's and G10 graphite electrodes.

As with the biosorption processes investigated in chapter 3, *Shewanella putrefaciens* were applied here as a model dissimilatory electro-active bacterium. Genomic analysis (Fredrickson, Romine et al. 2008) of the Shewanella strain have shown that the Shewanella genus share a suite of cytrochrome electroactive protein enzymes which are responsible for the transfer of electrons from the inner to the outer membranes where they are accessible to electrodes, metal ions and electron mediators. Recent findings regarding the *Shewanella* genus (Shi, Richardson et al. 2009) and bacterial strain *Shewanella putrefactions* (Marsili, Baron et al. 2008) have been reported to produce their own in situ electron-mediators such as flavin molecules and membrane vesicles which contain multi-heam cytrochrome enzymes (Gorby, McLean et al. 2008) which demonstrate redox reactivity towards metal ions and radionuclide's (Kano and Ikeda 2000).

Remediation of metal ions by biosorption and bio-reduction processes have been evaluated in chapter 3. This chapter further investigates influences of bacteria upon electrodeposition reactions as a complementary strategy of this thesis's investigation. An all-encompassing theoretical investigation regarding the combination of these for the enhancement of metal remediation would also require theoretical experimentation upon reaction kinetics and mass transfer of respective reaction "bottlenecks" (rating determining steps) and modelling of simultaneous microbiological, and electrochemical processes occurring.

4.2. Materials and methods

These electrochemical characterisation experiments were performed using an H-Cell, (Figure 4.2). The anolyte and catholyte sections were separated by a glass frit and each filled with 50 ml of electrolyte solution under study. The glass H-cell was submerged in 0.1 M nitric acid water bath overnight and prior to experimentation washed with 0.1 M nitric acid followed by copious amounts of triple distilled water.

Preliminary experiments potentials were measured against a saturated calomel reference electrode (SCE) placed approximately 10 mm from the RDE via a Luggin. Bioelectrochemical experiments were carried out with Ag/AgCl reference electrode. All potentials are reports vs. the Ag/AgCl reference electrode.

Figure 4.2 : (a) Glass H-Cell.

A Sycopel Scientific Au and Pt rotating disc electrode (RDE) (Figure 4.3) embedded in a Teflon holder with a disc area of 0.385 cm^2 was used as the working electrode for preliminary voltammetric analysis. The rotating disc electrodes where polished with fine silica paper and washed with 1 M nitric acid followed by triple distilled water. A platinised titanium sheet of area 0.2 cm x 0.2 cm was used as a counter electrode.

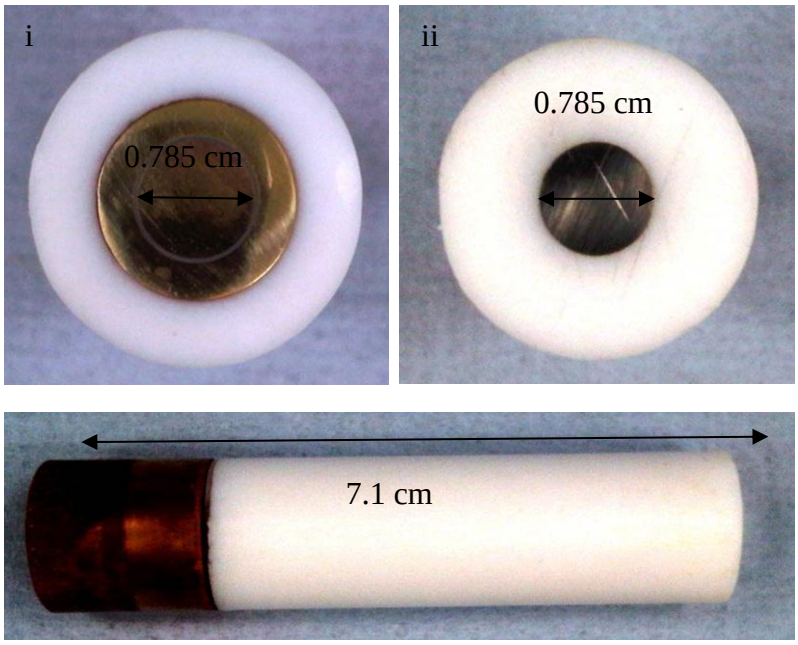

Figure 4.3 : Gold (i) and platinum (ii) rotating disc electrode.

Graphite electrodes (Figure 4.4) were used for all bio-electrochemical reduction experiments. G10 graphite electrodes of 1 x 1 x 1 cm (A = 6 cm^2) (Ralph Coidan ltd)

connected with water tight fittings to 0.1 mm stainless steel wires and sealed with conductive stainless steel epoxy (Sigma-Aldrich). The electrical resistance of the connections were less than 1 Ω (≈ 0.25 Ω). The reactor and auxiliaries were soaked in disinfectant followed by 1 M HNO_3(aq) and rinsed thoroughly with de-ionized water. Graphite electrodes were polished with fine grit paper and sonicated in deionised water to remove debris, soaked overnight in 1 M HNO_3(aq) to remove metal deposits and other contaminates followed by washing in ethanol to remove organic substances and stored in deionised water to saturate the electrodes and force out air pockets.

The graphite and Ag/AgCl reference electrode where held in place using plastic holders as illustrated by Figure 4.4 which were machined to have a snug fit into the mouth of the H-cell. The reference electrode was positioned to be no less than 1-2 mm from working electrode surface to reduce the potential drop between the reference electrode tip and surface of working electrode.

The top of the plastic holder was fitted with a rubber stopper and crimp sealed which did not allow gas leakage in or out of the reactor. The holder for the counter electrode was held in place with a clamp just above the mouth of the anodic chamber to allow exchange of atmospheric O_2(g) with the solution.

a : Graphite electrodes
b : Reference electrode
c : Glass H-Cell
d : Electrode holder (top View)
e : Electrode holder (side View)

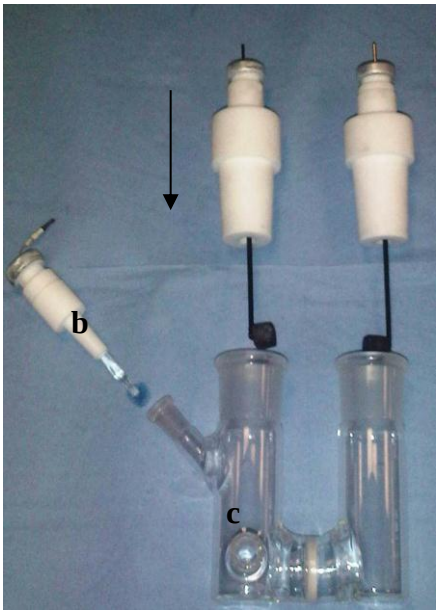

Figure 4.4 : Bioelectrochemical experimental set up.

Bacterial cells where added to the solution using sterile needles. An identical protocol was followed for culturing bacteria as described in chapter 3. For all experiments bacterial concentrations where 1 x 10^{10} CFU/ml.

The measurement of the solution pH and conductivity was performed using an Electrochemical analytical meter (SevenMulti, manufactured by Metter-Toledo GmbH).

4.2.1. Electrolyte preparation [1][2][3]

4.2.1.1. Preliminary experimentation with Pt and Au Rotating disc electrodes

Solutions were prepared from analytical grade reagents (Fisher Scientific) or standard solutions of Spectrosol grade (VWR) and made up in de-ionised water. Electrolyte solutions of 1 x 10^{-3} M Au^{3+} were made with 1000 mg/l standard solutions of Au^{3+} from Spectrosol (VWR), by adding 49 ml of the standard solution to 250 ml flask and filling and to the mark with de-ionised water. Aqueous electrolyte solutions of Co^{2+} and SO_4^{2-} were prepared (Figure 3.4) with concentrations of 30, 300 and 3000 ppm Co^{2+} species and SO_4^{2-} as the base electrolyte by dissolving the required amount of $CoSO_47H_2O$(s) and Na_2SO_4(s) in a 1000 ml volumetric flask, amounts of which are summarised in Table 4.1.

---

[1] (Au^{3+}) : 1 g/L Au^{3+} standard solution (SS). 0.049 L SS = 0.049 L x 1 g/L = 0.049 g Au^{3+} 0.049 g Au^{3+} / 0.250 L / 196.67 g/mol = 1 x 10^{-3} M Au^{3+}

*[2] (Co^{2+}) : 0.143 g $CoSO_4.7H_2O$ / 281.68 g/mol = 5.08x 10^{-4} mol Co^{2+} 5.08x 10^{-4} mol Co^{2+}/ 1L x 58.93 g Co^{2+} / mol **X** 1000 mg/g = 30 mg/L (SO_3^{2-}) : (1) SO_4^{2-} from $CoSO_4.7H_2O$ = 0.143 g / 281.68g/ mol /1 L **X** 96g SO_4^{2-}/ mol = 0.0487 g (2) SO_4^{2-} required from $Na_2SO_4.5H_2O$ = 3.5 g/L – 0.0487 g/L / 96 g SO_4^{2-}/mol = 0.0360 mol/L (3) Amount of Na_2SO_4 required = 0.0360 mol/L **X** 322.19 g $Na_2SO_4.10H_2O$ / mol **X** 1 L= 11.619 g $Na_2SO_4.5H_2$. Similar procedures for 300 and 300 ppm Co^{2+} solutions.*

*[3] (Fe^{3+}) : 0.875 g $Fe_2(SO_4)_3.7H_2O$(s) / 489.66 g/mol = 1.787 x 10^{-3} mol $Fe_2(SO_4)_3.7H_2O$ 1.787 10^{-3} mol $Fe_2(SO_4)_3.7H_2O$ **X** 2= 3.574 x 10^{-3} mol Fe^{3+} 3.574 x 10^{-3} mol Fe^{3+}/ 1 L **X** 55.85 g Fe^{3+}/ mol **X** 1000 mg/g = 200 mg/L (SO_3^{2-}) : (1) SO_4^{2-} from $Fe_2(SO_4)_3.7H_2O$ = 0.875 g / 489.66 g/mol **X** 3 mol SO_4^{3-}/mol / 96g SO_4^{2-}/mol / 1 L= 0.51 g/L (2) SO_4^{2-} required from $Na_2SO_4.10H_2O$ = 3.5 g/L – 0.51 g/L / 96g SO_4^{2-}/ mol = 0.031 M (3) Amount of Na_2SO_4 required = 0.031 mol/L **X** 322.19 g $Na_2SO_4.5H_2O$ / mol **X** 1 L= 10.047 g $Na_2SO_4.5H_2O$*

System Concentrations				Mass Required / g	
	Co^{2+}		SO_4^{2-}		
ppm	mol/dm^3	ppm	mol/dm^3	$Co.SO4.7H_20$	Na_2SO_4
30	5.08×10^{-4}	3500	3.64×10^{-2}	0.143	11.619
300	5.08×10^{-3}	3500	3.64×10^{-2}	1.43	10.100
3000	5.08×10^{-2}	4887	5.09×10^{-2}	14.3	0

Table 4.1 : Summary of system concentrations of Co^{2+} and SO_4^{2-}.

An aqueous electrolyte solution of $Fe^{3+}$and SO_4^{2-} was prepared with concentrations of 3.581×10^{-3} M (200 ppm) Fe^{3+} species and 3.64×10^{-2} M (3500 ppm) SO_4^{2-} by dissolving 0.878 g of $Fe_2(SO_4)_3(H_2O)_5$(s) and 10.047 g of $Na_2SO_4.5(H_2O)$(s) in distilled water with a total volume of 1000 ml. Concentrations were chosen from levels reported in literature vis-à-vis acid mine drainage (Feng, Aldrich et al. 2000). Measured pH and conductivities are summarized in Table 4.2 and electrolyte solutions displayed in Figure 4.5.

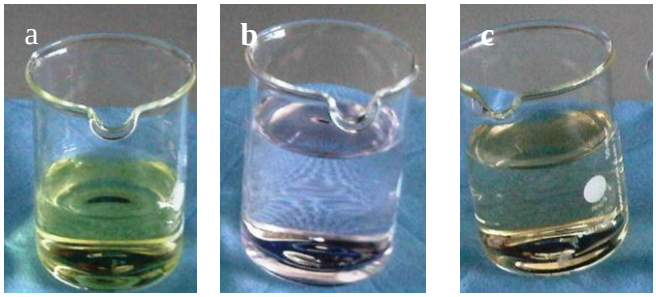

Figure 4.5: (a) Gold (Au^{3+}), (b) cobalt (Co^{2+}) and (c) iron (Fe^{3+}) and solution of 200 ppm concentration.

Species	Complex	$[M^{n+}]$	pH	κ mS/cm
Au^{3+}	$HAuCl_4$	197 ppm	1.46	36.00
Co^{2+}	$CoSO_4$	300 ppm	3.77	4.73
Fe^{3+}	$Fe_2(SO_4)_3$	200 ppm	2.72	5.77

Table 4.2: Measured conductivities and pH of electrolytes.

4.2.1.2. Bioelectrochemical experimentation with graphite electrodes

Bioelectrochemical experimentation with cobalt and iron metal ions where carried out with 0.9% NaCl as the base electrolyte which is the medium which the bacteria where concentrated and stored in upon growth. Solutions were prepared from analytical grade reagents supplied by Fisher Scientific International Company or standard solutions from Spectrosol and solutions made up from deionised water. Aqueous electrolyte solutions of 200 ppm Co^{2+} and Fe^{3+} were made from their sulphate salts and 0.9% NaCl(aq) base electrolyte by the addition 0.954 g $CoSO_4.7H_2O$(s) (M_r = 281.1 g)) and 0.9 g of NaCl(s) and 0.877 g $Fe_2(SO_4)_3.7H_2O$(s) (M_r = 489.96 g) and 0.9 g NaCl(s) in a 1000 ml beaker filling close to the mark, the pH adjusted with 1 M NaOH(aq) or 1 M HNO_3(aq), transferred to a 1000 ml conical flask and filled to the mark with triple distilled water.

Aqueous electrolyte solutions of 200 ppm Au^{3+} were prepared with 1000 mg/l standard solutions of $HAuCl_4$(aq) in 2 M HCl(aq) base electrolyte matrix using Spectrosol grade standard solutions (VWR). A volume of 50 ml of standard solutions was added to a 250 ml flask filled close to the mark, altering the solution to pH by the addition of 1 M NaOH(aq) or 1 M HNO_3(aq) and completely filling to the mark with triple distilled water. Experiments, electrolyte compositions, pH and conductivities are summarised in Table 4.3.

Species		[C_0] ppm	Experiment	κ mS/cm	pH	Base electrolyte
Au^{3+}	$HAuCl_4$(aq)	200	i ii	35.2	2	in 2 M HCl(aq) matrix
Co^{2+}	$CoSO_4$(aq)	200		24.7	2	in 0.9% NaCl(aq)
Fe^{3+}	$Fe_2(SO_4)_3$(aq)	200	i	42.7	2	in 0.9% NaCl(aq)

Table 4.3 : Bio-electrochemical electrolytes and experimental groups and their measured conductivities and pH's.

4.2.1.3. Ohmic drop correction

All potentials were corrected for ohmic resistance due to the uncompensated potential drop in the electrolyte between the tip of the Luggin capillary or reference electrode and the working electrode surface (Oelßner, Berthold et al. 2006) using eq^{n} 4.1 and eq^{n} 4.2. Where E_a is the observed potential and E_p is the applied voltage of working electrode, R_u is the resistance (ohms), z (cm) is the distance between the Luggin capillary and working electrode, κ (mS/cm) is the electrolyte conductivity and r (cm) is the radius of the working electrode.

$$E_P = E_a - iR_u \qquad (4.1)$$

$$R_u = \frac{z}{2\pi\kappa r^2} \qquad (4.2)$$

4.2.2. Thermodynamics - Qualitative evaluation of system

For an electrode reaction such as that described by eq^{n} 2.38 the reversible potential can be described by eq^{n} 2.38. Where both the reduction of O and the oxidation of R are occurring at equal rates. A rudimentary analysis of *i/E* polarization phenomena with observation of current with variation of anodic and cathodic potentials was applied. With a comparison of theoretical reversible potentials E_r from slow scan voltammograms, with standard equilibrium potentials E^0_e and calculated Nernst potentials E_e using eq^{n} 2.39 (Table 4.4), for a qualitative indication of which species in our system are being deposited in respect to applied potential.

$$O + ne^- \rightleftharpoons R \qquad (2.38)$$

$$E_e = E_e^\theta + \frac{RT}{nF}\ln\left[\frac{C_O}{C_R}\right] \equiv E_r \qquad (2.39)$$

Table 4.4 describes the standard electrode potentials E^0_e for various reactions which may occur in respective noble metal and graphite electrode interface systems containing Au^{3+}, Co^{2+} and Fe^{3+} metal ions and bacterial cells such as *Shewanella putrefaciens* CN32 as reported by Bard, Parsons et al. (Bard, Parsons et al. 1985), Madigan et al (Madigan and Brock 2009) and Fricke et al. for the Cytrochrome OmCB (Fricke,

Harnisch et al. 2008) and Alessandro (Carmona-Martinez, Harnisch et al. 2011) for Cytrochrome OmCA and MtrC, implicated as key protein enzymes for electron transfer mechanisms by bacteria. Nernst potentials E_e calculated for possible redox electroreduction, electrodeposition and proton and water reduction reactions for known concentrations of $AuCl_4^-$, Co^{2+} and H^+ are also summarised in Table 4.4.

For the Fe^{3+}/Fe^{2+} redox couple concentrations of Fe^{2+} were approximated as 1x 10^{-8} M. As applied in eq^n 3.5 Ln(M^0) and Ln(H_2) can be taken as unity, hence the Nernst equilibrium potentials can be described by eq^n 4.4 - eq^n 4.8 expressed in reference to a standard hydrogen electrode and Ag/AgCl electrode.

The Nernst equation corrects for non-standard conditions and thus gives a more valid comparison of equilibrium (reversible) potentials where electroreduction reactions occur. For other redox reactions such as $AuCl_2^-/Au^0$ and Co^{3+}/Co^{2+} only standard potentials could be used as concentrations of $AuCl_2^-$ and Co^{2+} are unknown in respective systems.

$$AuCl_4^-(aq) + 3e^- \rightleftharpoons Au \qquad (4.4)$$

$$E_{1.1} / V \text{ vs. SHE} = 1.002 + 0.00856 \ln (AuCl_4^-)$$

$$E_{1.1} / V \text{ vs. Ag/AgCl} = 0.805 + 0.00856 \ln (AuCl_4^-)$$

$$Co^{2+}(aq) + 2e^- \rightleftharpoons Co \qquad (4.5)$$

$$E_{3.3} / V \text{ vs. SHE} = -0.277 + 0.0128 \ln (Co^{2+})$$

$$E_{2.1} / V \text{ vs. Ag/AgCl} = -0.474 + 0.0128 \ln (Co^{2+})$$

$$Fe^{3+}(aq) + e^- \rightleftharpoons Fe^{2+} \qquad (4.6)$$

$$E_{2.1} / V \text{ vs. SHE} = 0.770 + 0.0257 \ln (Fe^{2+} \approx 1x10^{-8}) + 0.0257 \ln (Fe^{3+})$$

$$E_{2.1} / V \text{ vs. Ag/AgCl} = 0.573 + 0.0257 \ln (Fe^{2+} \approx 1x10^{-8}) + 0.0257 \ln (Fe^{3+})$$

$$2H^+(aq) + 2e^- \rightleftharpoons H_2 \qquad (4.7)$$

$$E_4 / V \text{ vs. SHE} = 0 + 0.0128 \ln (H^+)$$

$$E_4 / V \text{ vs. Ag/AgCl} = -0.197 + 0.0128 \ln (H^+)$$

$$2H_2O\ (l) + 2e^- \rightleftharpoons H_2 + 2OH^-(aq) \qquad (4.8)$$

E_5 / V vs. SHE = -0.830 + 0.0128 ln (H_2O)

E_5 / V vs. Ag/AgCl = -1.027 + 0.0128 ln (H_2O)

Pourbaix diagrams discussed in chapter 2 in relation to metal ion speciation can also be used to determine potential windows for metal ion electronation reactions. Changes in pH by bacterial cells could cause metal ions to precipitate or in cause changes in revisable potentials with changes in pH. Figure 4.6 and Figure 4.7 summaries Pourbaix diagrams gives thermodynamic information upon reversible potentials for metal ion electronation and electrodeposition reactions of interest. As shown in Figure 4.6 changes in pH up to 8 would have no effects upon the potential window for electrodeposition of gold and cobalt.

Ferric iron is stable in pH's up to 2.5 after which it forms a dissolved $Fe(OH)^{2+}$ species which reduce the potentials required for the Fe^{3+}/Fe^{2+} electronation reaction. Therefore any changes in reversible potentials for Fe^{3+} electronation with bacterial cells may be due to increases in pH by bacterial activity. As shown in Figure 4.7 changes in pH up to 6 should have no effects upon the potential window for electrodeposition of iron as for cobalt and gold systems.

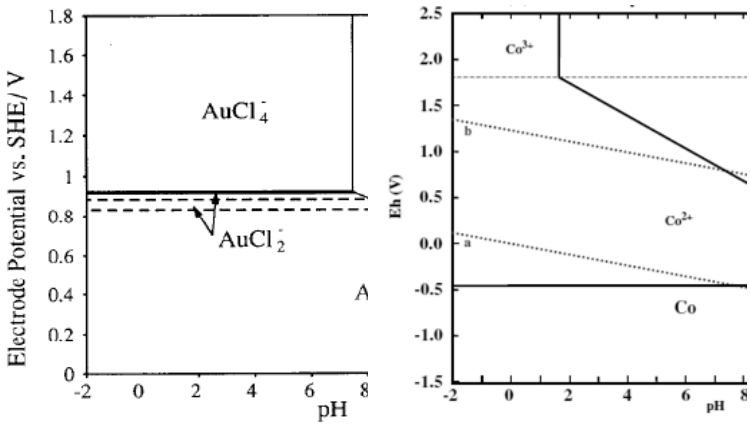

Figure 4.6 : Potential-pH diagram for $Au^{3+}$and Co^{2+} metal ion systems described in chapter 2 as described by Kelsall et al. (Kelsall, Welham et al. 1993) for gold and Chivot et al. (Chivot, J et al. 2008) for colbalt.

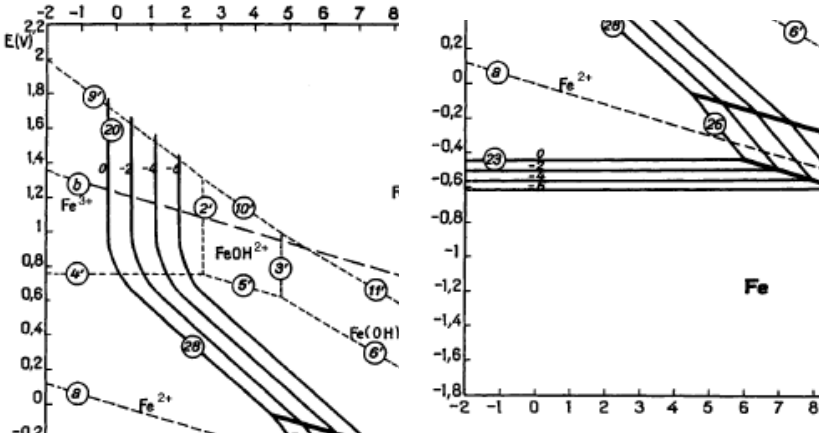

Figure 4.7 : Potential-pH diagram for and Fe^{3+} metal ion systems described in chapter 2, reproduced from Pourbaix (Pourbaix 1966).

Half-Reaction	Reference	Reaction	n	$[M^{n+}]$ or $[H^+]$ ppm (mg/L)	Standard Potential E_e° V vs. SHE	Standard Potential E_e° V vs. Ag/AgCl	Nernst Potential E_e V vs. SHE	Nernst Potential E_e V vs. Ag/AgCl
$AuCl_4^- + 3e^- \rightleftharpoons Au + 4Cl^-$	(Bard, Parsons et al. 1985)	R1.1	3	$[AuCl_4^-] = 200$	1.002	0.805	0.938	0.741
$AuCl_4^- + 2e^- \rightleftharpoons AuCl_2^- + 2Cl^-$		R1.2	2	$[AuCl_4^-] = 200$	0.926	0.729	0.830	0.633
$AuCl_2^- + 2e- \rightleftharpoons Au$		R1.3	2	-	1.154	0.957	-	-
$Co^{2+} + 2e^- \rightleftharpoons Co$		R2	2	$[Co^{2+}] = 200$	-0.277	-0.474	-0.350	-0.547
$Fe^{3+} + e^- \rightleftharpoons Fe^{2+}$		R3.1	1	$[Fe^{3+}] = 200$	0.770	0.573	-	-
		R3.1	1	$[Fe^{3+}] = 200$, $[Fe^{3+}] \approx 1 \times 10^{-8}$ M	0.770	0.573	0.323	0.126
$Fe^{2+} + 2e^- \rightleftharpoons Fe$		R3.2	2	-	-0.410	-0.607	-	-
$2H^+ + 2e^- \rightleftharpoons H_2(g)$ - pH0		R4.1	2	$[H^+] = 1008$	0.000	-0.197	0.000	-0.197
$2H^+ + 2e^- \rightleftharpoons H_2(g)$ - pH1		R4.2	2	$[H^+] = 100.8$	0.000	-0.197	-0.030	-0.227
$2H^+ + 2e^- \rightleftharpoons H_2(g)$ - pH2		R4.3	2	$[H^+] = 10.08$	0.000	-0.197	-0.059	-0.256
$2H^+ + 2e^- \rightleftharpoons H_2(g)$ - pH3		R4.4	2	$[H^+] = 1.008$	0.000	-0.197	-0.089	-0.286
$2H_2O(l) + 2e^- \rightleftharpoons H_2(g) + 2OH^-(aq)$		R5	2	-	-0.830	-1.027	-	-
Cytrochrome a ox/red	(Fricke, Harnisch et al. 2008)	R6.1	1	-	0.390	0.193	-	-
Cytrochrome c ox/red		R6.2	1	-	0.250	0.053	-	-
Ubiuinone ox/red		R6.3	2	-	0.110	-0.087	-	-
Cytrochrome b ox/red		R6.4	1	-	0.035	-0.162	-	-
Cytrochrome *OmCA and MtrC*		R6.5	1	-	-0.008	-0.200	-	-
Cytrochrome OmCB		R6.6	1	-	-0.190	-0.387	-	-
$O_2 + 2H^+ + 2e^- \rightleftharpoons H_2O_2$	(Bard, Parsons et al. 1985)	R7	2	-	0.650	0.453	-	-
$O_2 + 4H^+ + 4e^- \rightleftharpoons H_2O$		R8	4	-	1.230	1.033	-	-
$Cl_2 + 2e^- + \rightleftharpoons 2Cl^-$	(E 1984)	R9	2	-	1.393	1.196	-	-
$NO_3^- + 2e^- + 2H^+ \rightleftharpoons NO_2^- + H_2O$		R10	1	-	0.835	0.638	-	-

Table 4.4 : Reported standard potentials (E_e^0) and calculated Nernst potentials E_e for possible reactions occurring for the various systems in question.

4.2.3. Experimental procedure

Preliminary voltammetry experimentation with Pt and Au RDE's were carried with a single rotating rate for quantitative and qualitative elocution of reversible potentials for respective electronation reactions. Further upon linear sweep voltammetry with bacterial cells were conducted in un-stirred solutions with graphite electrodes. After each scan, the electrolyte was stirred with a magnetic stirrer and the working electrode polarized at a potential of +1.00 V vs. Ag/AgCl until initial OCP's were re-established for the metal ion solution under investigation. This was taken as a sufficient indicator that system conditions were re-established. For a typical experiment 50 ml of electrolyte under investigation was added to the glass cell followed by 10 ml of bacterial cells of 1 x 10^{10} CFU/ml concentrations using sterile syringes in the proximity of a burning blue Bunsen flame and mixed for a few seconds to homogenise the solution.

4.3. Qualitative evaluation electrochemical reaction without bacterial cells upon on Pt and Au metal and G10 graphite electrodes

In perspective, mine waters and industrial effluents would contain a consortium of anions and cations (Brown, Barley et al. 2002) which could be an influence on the speciation of metal cations and influence mechanisms of electronation reactions.

Cyclic voltammetry was carried out of background electrolytes used for preliminary experimentation with noble electrodes and carbon based graphite electrodes to establish solvent potential windows of the electrolyte and for further comparison of cyclic voltammograms of electrolytes with metal ions.

Electrolytes were not buffered or degased of oxygen as the aim of this investigation was to be representative of mine waters and industrial effluents and in keeping with Green Chemistry paradigm where no chemicals are added and processes carried out at room temperature.

4.3.1. Background electrolyte cyclic voltammetry for experimentation with Au and Pt RDE's

Figures 4.8 to 4.9 describe cyclic voltammograms with scan rates of 0.010 V/s of Na_2SO_4(aq) and HCl(aq) electrolytes, used as background electrolytes for experiments with Pt and Au electrodes. Scans where carried out from open circuit potential scanned negative to -1.5 V, the scan reversed to +1.5 V and cycled back to open circuit potential. Potential limits of -1.5 and +1.5 V where chosen as all metal ion electrochemical reactions for metal ion reduction of Au^{3+}, Co^{2+} and Fe^{3+} analysed lay well within these limits.

Figure 4.8 illustrates voltammograms for a Pt electrode in 2 M HCl, reflecting the acidic nature of the electrolyte. Small currents less than -0.050 mA/cm^2 are observed from open circuit potentials of ≈ 0 V which would correspond to proton reduction and further drop after -0.8 V corresponding to further proton reduction. On the reverse scan a small rise in current from 0.2 V would correspond to hydrogen oxidation of any hydrogen adsorbed upon the surface oxide layer. Ohmic resistance is shown on the forward scan from potentials of 0 V. No cathodic current is observed on the reverse scan for adsorbed oxygen reduction (R7 and R8) which would be consistent with the low concentrations of dissolved oxygen in electrolyte and high overpotentials required for oxygen reduction. The voltammograms for the Au electrode in 2 M HCl display ohmic resistance behaviour, with little current observed for hydrogen evolution. This is consistent with large overpotentials required hydrogen evolution on Au electrode in comparison to Pt electrodes (Sawyer, Sobkowiak et al. 1995).

Figure 4.9 illustrates voltammograms for Au and Pt electrodes in 3.5 g/L Na_2SO_4(aq) of ohmic resistance on the forward and reverse scans with little or no hydrogen evolution on the negative scan or oxygen reduction on the reverse anodic scan observed.

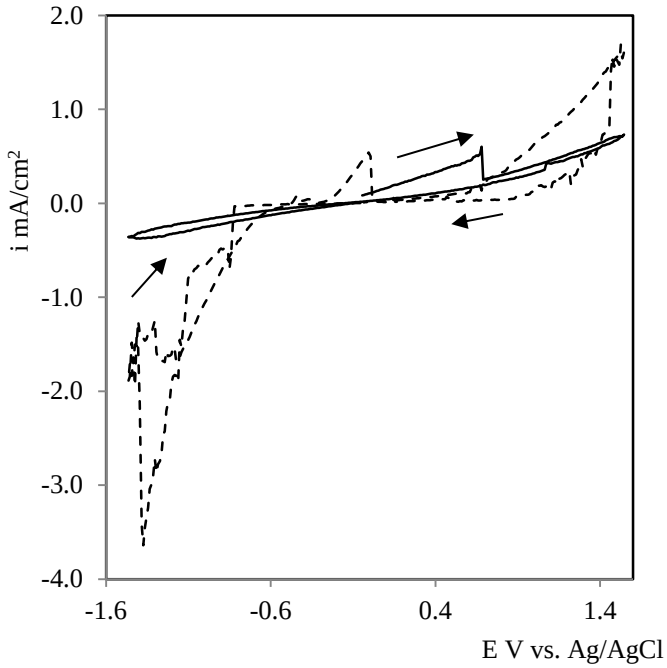

Figure 4.8 : Cyclic voltammogram (S = 0.010 V/s) for 2 M HCl on Au (─) and Pt (--) RDE at 25°C.

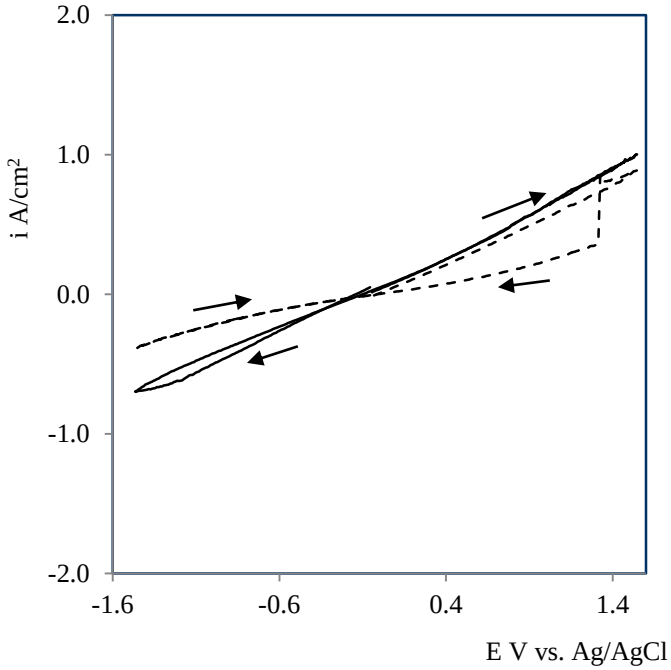

Figure 4.9 : Cyclic voltammograms (S = 0.010 V/s) for 3.5 mg/L Na_2SO_4 (aq) on Au (─) and Pt (--) RDE at 25°C.

4.3.2. Background electrolyte voltammograms for experimentation with graphite electrodes

Background electrolytes were changed for experimentation with graphite electrodes, further cyclic voltammetry using slow scan rate of 0.010 V/s were carried out with 0.9% NaCl(aq) as the background electrolyte which is the aqueous medium in which our bacterial cells were re-suspended, after concentration from cultured nutrient tryptic soya broth and 0.1 M HNO_3(aq) reflecting the acid nature of our metal ion electrolytes.

Voltammograms of solutions of 0.9% NaCl(aq) are illustrated in Figure 4.10. A cathodic reduction current from potentials of 0.5 V is observed for oxygen adsorption and reduction to H_2O_2 and H_2O described by R7 and R8 in Table 4.4; similar currents are observed by Guenbour et al. (Guenbour, Iken et al. 2006). Higher cathodic currents for oxygen reduction on graphite electrode compared to noble Pt and Au electrodes would be due to dissimilar surface chemistry of the electrode with reports of high oxygen absorption upon graphite electrodes (Guenbour, Iken et al. 2006).

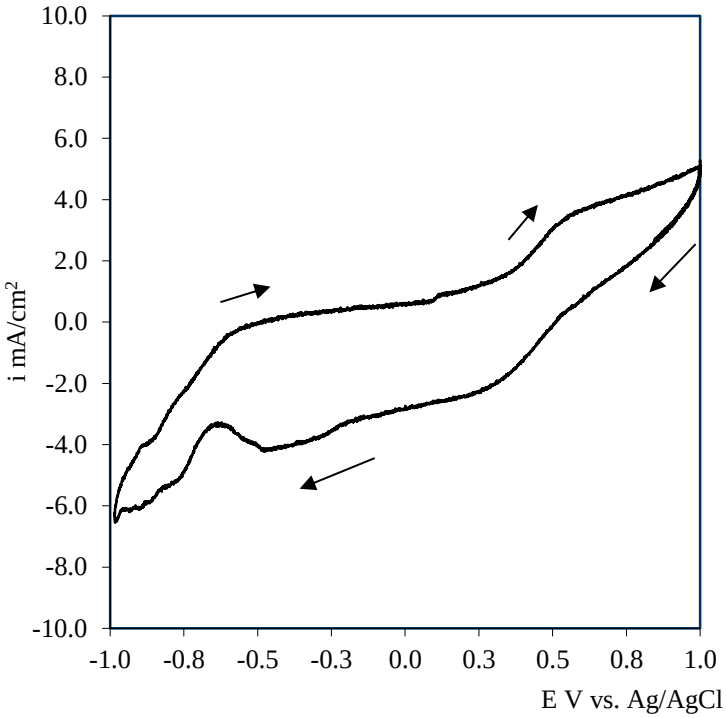

Figure 4.10 : Cyclic voltammograms (S = 0.010 V/s) for solutions of 0.9% NaCl(aq) on G10 Graphite electrode at 25°C pH =5.8, κ = 16.57 mS/cm.

The possibility of chloride oxidation to chorine gas has also been taken into account as for electrolytes with 0.9% NaCl. Chloride evolution would occur only for potentials greater than 1.196 V from reported standard potentials *Ee*° vs. Ag/AgCl and investigation by Janssen (L.J.J 1974).

Figure 4.11 illustrate cyclic voltammogram of 0.1 M HNO_3(aq) as an illustration of the acidic nature of electrolyte. On the reversible scan the second oxidation peak at 0.612 V would be due to nitrite oxidation NO_2^-/NO_3^-. 1 M nitric acid was used to set pH of electrolyte baths. Usually only 1- 5 ml was required so nitrate concentration in electrolyte baths can be deemed negligible. A considerably higher proton (R4.1) cathodic current is evident in comparison to noble metal substrates. No cathodic current corresponding to oxygen adsorption and reduction is evident. Two anodic peaks are observed, which would be associated with adsorbed hydrogen oxidation and desorption from the electrode surface. No cathodic current for O_2 reduction is observed.

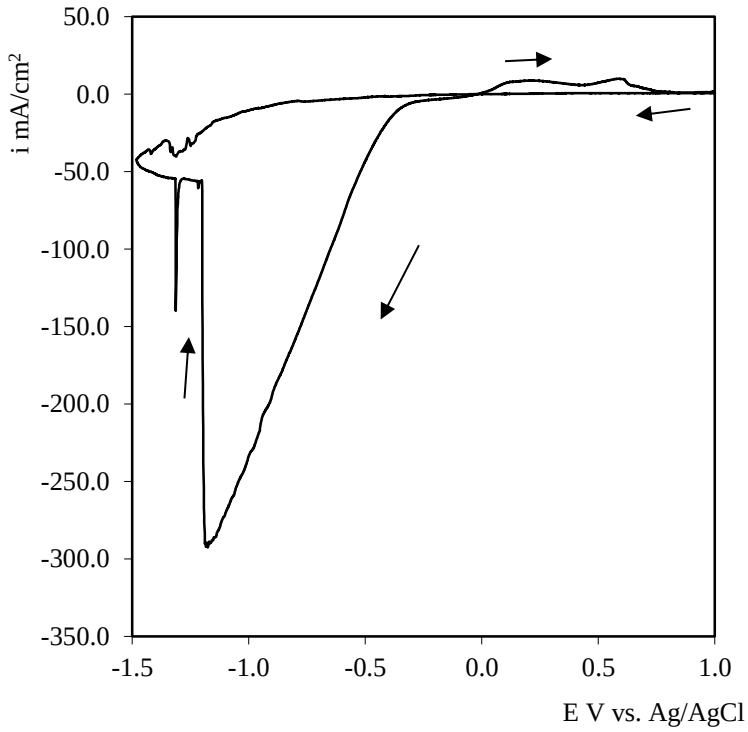

Figure 4.11 : Cyclic voltammogram (*S* = 0.010 V/s) for solutions of 0.1 M HNO_3(aq) on G10 Graphite electrode at 25°C, pH = 2.

4.3.3. Solvent potential windows : Electrode limits for Pt, Au and graphite electrodes in specified supporting electrolyte and pH

The voltage "window" of the range of accessible potentials will be limited on the positive side by the oxidation of the electrode material, for example platinum and gold oxidation to metal ions and metal oxides in the electrolyte. Or oxidation of the supporting electrolyte, distilled water by formation of molecular or chemisorbed oxygen from water. On the negative side our window is limited by reduction of the supporting electrolyte or solvent, in all our systems being hydrogen evolution (Sawyer, Sobkowiak et al. 1995). Cyclic voltammetry of electrodes were conduced within this window. With scans between +1.0 V and -1.0 V, this from background scans can be deemed within the solvent potential limits, namely water reduction to molecular hydrogen on the negative side and water oxidation on the positive side.

4.3.4. Electrochemical analysis of carbon electrodes and bacterial cells in NaCl(aq) supporting electrolyte

Figure 4.12 describes the cyclic voltammogram of *Shewanella putrefaciens* in 0.9% NaCl(aq). Scans were made after 1 hr addition of 10 ml 1 x 10^{10} CFU/ml bacterial cells added to a 0.9% NaCl electrolyte. Observed open circuit potentials were 0.062 V after 1 hr addition of bacterial cells. Two anodic peaks P1 (-0.346 V) and P2 (+0.058 V) were observed which would be indicators of electron donation by "in situ" bacterial electron mediators or electroactive enzymes located within the outer cell wall of bacterial cells. The anodic peaks of redox system P1 would most likely correspond to outer membrane cytrochrome-c proteins as reported illumined by Fricke et al. (Fricke, Harnisch et al. 2008) who applied linear sweep voltammetry to investigate the electron transfer of *G. sulfurreducens* biofilms and report a major electron transfer redox system around -0.376 V vs. Ag/AgCl which they concluded would most likely correspond to outer membrane c-cytrochrome FerB closely related to OmCB, based on reports of isolated and electrochemically analysed 89 kDa cytrochrome-c FerB of *G. sulfurreducens* by Magnuson et al. (Magnuson, Isoyama et al. 2001). P2 would also correspond well to cytochrome-c (R6.2) type protein systems with similar potentials reported by Wang et al. (Wang, Li et al. 2002) who investigated the direct electrochemistry of cytrochrome-c on glassy carbon electrode and Baron et al. (Baron, LaBelle et al. 2009) who conducted

electrochemical measurements of electron transfer kinetics of *Shewanella oneidensis* MR-1.

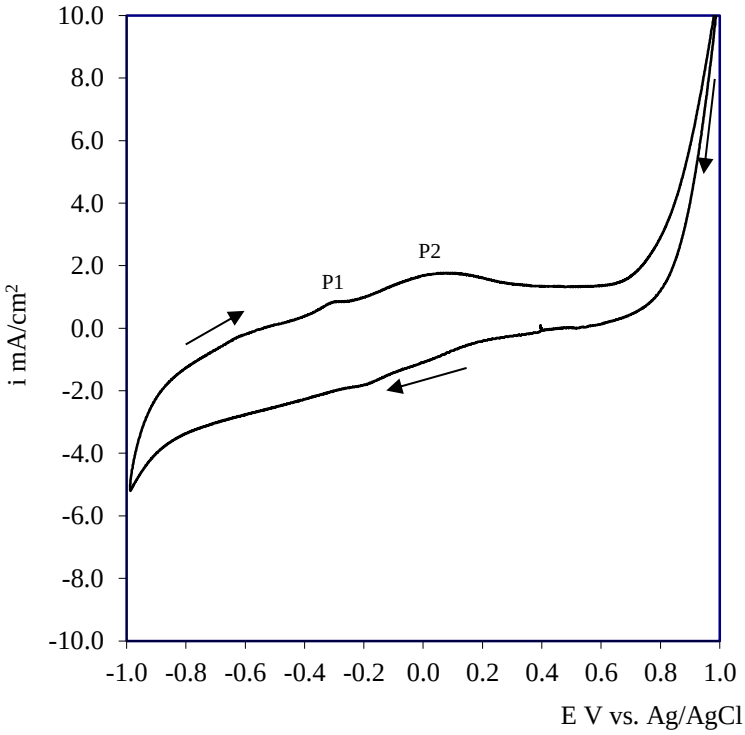

Figure 4.12 : Cyclic voltammogram (S = 0.010 V/s) for solution containing 10 ml of 1 x 10^{10} CFU/ml *S. putrefaciens* cells on an G10 Graphite electrode at 25°C from solutions of 0.9% NaCl(aq).

These metal reductive cytrochrome protein enzymes would be key components located in outer cell membrane or released by living or deactivated bacterial cells in the biosorption and bio-reduction of metal ions in solution. In chapter 3 we further proved that live cells were able to bio-reduce and bio-nucleate gold and cobalt metal ions and deactivated bacterial cells were also able to bio-nucleate gold metal ions. This presumably occurs by redox protein enzymes located on the surface of bacterial biomass or released actively or passively by cell lyses into the surrounding solution or other non-enzymatic reaction mechanisms.

4.3.5. Electrochemical analysis of the electrodeposition of gold from electrolytes without bacterial cells

Linear sweep voltammetry with a Pt rotating disc electrode was used to study Au deposition from 1 M $HAuCl_4$ (aq) solution. Figure 4.13 describes a linear sweep voltammogram using slow scan rates of 0.010 V/s. Open circuit potentials of ≈ 0.605 V were observed. On a negative-potential scan from 1.2 V a limiting currents is observed from 0.4 V which would correspond well to redox couple R1.1 of $AuCl_4^-/Au^0$ gold electrodeposition with a cathodic current from potentials of 0.605 V vs. Ag/AgCl. This compares well with previous reports by Harrison and Thompson (Harrison and Thompson 1975) and Diaz et al. (Diaz, Kelsall et al. 1993) who investigated the kinetics of Au^{3+}/Au depositions in aqueous chloride electrolytes and Bond et al. (M. Bond, Kratsis et al. 1997) who investigated a comparison of gold reduction in dilute aqua regia of 0.1 M HCl(aq) and 0.32 M HNO_3(aq). The anodic current which would be associated with oxygen evolution from potentials of 1.2 V illustrated in Figure 4.13(a) appears abnormal, with the scan initially going positive before returning negative. This may be due to ohmic drop correction causing the potentials at high currents to become irregular.

On the reverse scan for the linear sweep voltammogram described by Figure 4.13b a cathodic crossover branch was observed with a potential (E_c) of 0.605 V which further validates the reaction mechanism, were this crossover potential would be equivalent to the metal ion/metal redox couple equilibrium reversible potential applied by Soto et al. (Soto, Arce et al. 1996). On the back scan fluctuations in signal power is observed around potentials of 1.0 V which could be due to environmental noise (Sawyer, Sobkowiak et al. 1995).

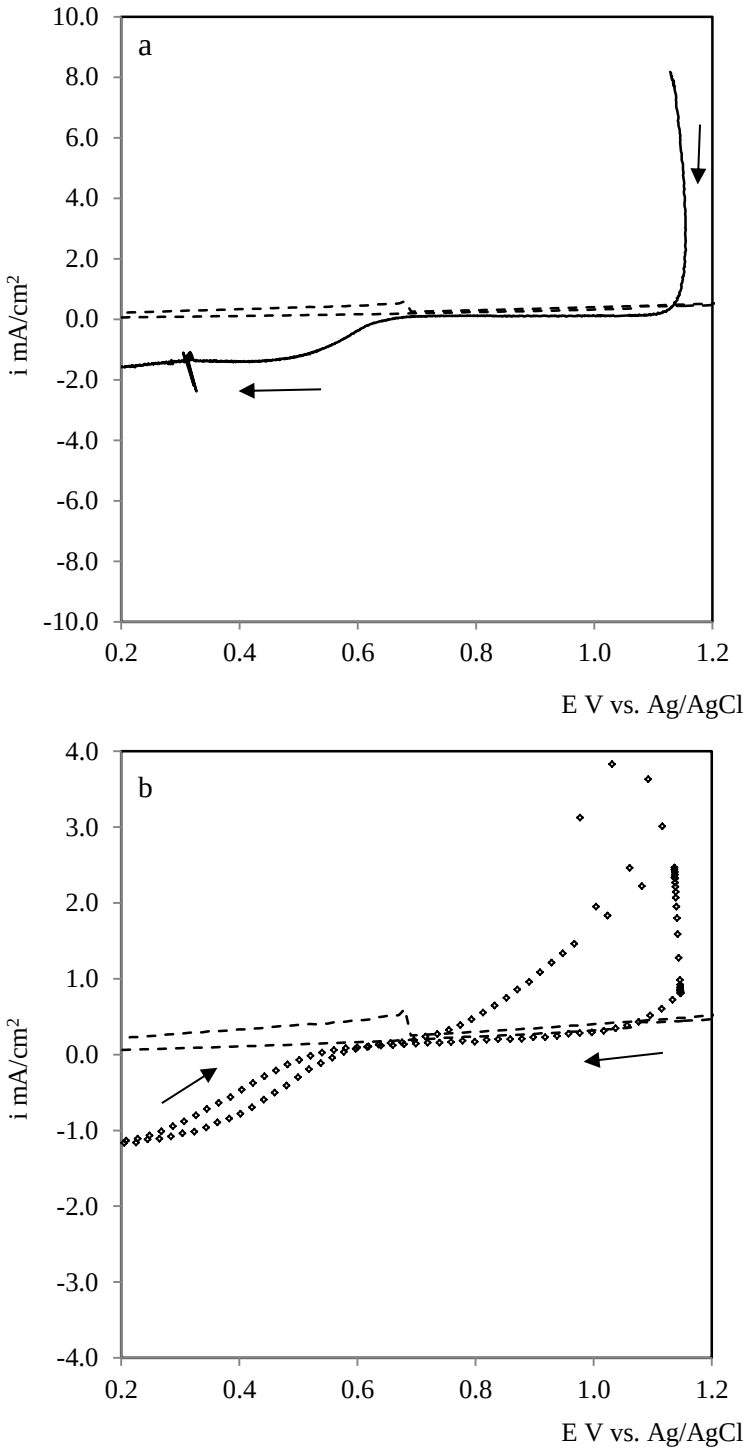

Figure 4.13 : (a) Linear sweep voltammograms (S = 0.001V/s) for Au^{3+} reduction on a Pt RDE (ω = 1500 rpm) at 25 °C from 1 x 10^{-3} M $HAuCl_4$ (aq), pH 1.46 and κ = 36 mS/cm. (b) Cyclic voltammogram (S = 0.020 V/s) for Au^{3+} reduction on a Pt RDE (ω = 1800 rpm) at 25 °C from 1 x 10^{-3} M $HAuCl_4$, pH = 1.46 and κ = 36 mS/cm. Background cyclic voltammograms (---) from Figure 4.8 also shown for comparison.

Figure 4.14 exemplifies cyclic voltammograms for Au^{3+} electrolyte with graphite electrodes without bacteria with open circuit potentials ≈ 0.6 V vs. Ag/AgCl. Two reduction shoulders are observed crossing the potential axis from potentials of 0.618 V which would be consistent with gold electrodeposition by $AuCl_3^-$ reduction. A further reduction is observed at potentials of 0.025 V of proton reduction and the co-deposition of a hydrogen rich metallic phase.

On the reverse sweep a further sharp increase in current from potentials of 0.074 V would correspond to dissolution of the co-deposited hydrogen rich phase preceding the dissolution of the bulk. A further rise is observed post potentials of 0.648 V with two peaks recorded at 0.730 V and 0.938 V. Similar peaks were described for gold nucleation on Pt RDE by Diaz et al (Diaz, Kelsall et al. 1993). Reverse potentials E_r observed for gold electrodeposition upon Pt RDE and graphite for the electrolyte in our system are summarised in Table 4.5 for later comparison of changes when bacterial cell are added to the electrolyte bath.

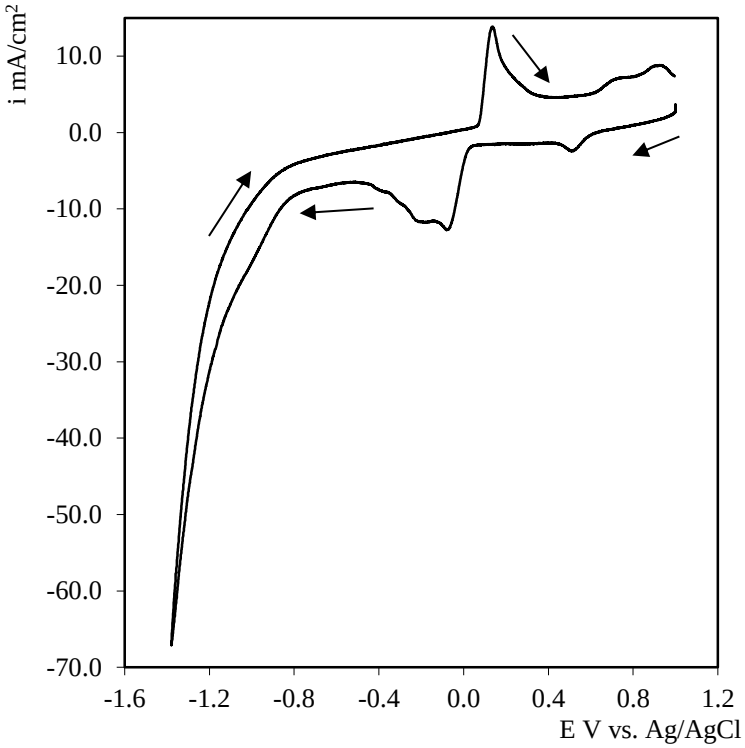

Figure 4.14 : Cyclic voltammograms (S = 0.010 V/s) for Au^{3+} reduction on an G10 graphite electrode at 25°C from 200 ppm Au^{3+} in 2 M HCl(aq) matrix, pH = 2, κ = 35.2 mS/cm.

Reaction	Electrode Substrate	Electrolyte	E_r V vs. Ag/AgCl
$AuCl_4^- + 3e^- \rightleftharpoons Au + 4Cl^-$	Au RDE	197 ppm Au^{3+} in 2 M HCl(aq) matrix pH 1.45, κ 36 mS/cm	0.605
$AuCl_4^- + 3e^- \rightleftharpoons Au + 4Cl^-$	G10 Graphite	200 ppm Au^{3+} in 2 M HCl(aq) matrix pH 2, κ 35 mS/cm	0.601

Table 4.5 : Summary of observed reversible potentials (E_r) observed for Au^{3+} electrodeposition on Pt and G10 graphite electrodes.

4.3.6. Electrochemical analysis of the electrodeposition of cobalt from electrolytes without bacterial cells

The deposition of cobalt was initially studied for systems containing 300 ppm Co^{2+} in sulphate base electrolyte, pH 3.77. Figure 4.15 shows the resultant cyclic voltammogram using gold RDE as the working electrode at room temperature. The cathodic current increases slightly from -0.155 V and further increases after potentials of -0.450 V and -1.150 V. During the reverse scan an anodic current is observed preceding potentials of -0.45 V.

Following theoretical predictions the reversible potentials (E_r) of various potentials observed from voltammograms with slow scans (0.010 V/s) should correspond to the standard reversible potentials and calculated Nernst potentials E_e summarised in Table 4.4. Upon analysis of Figure 4.15 one can deduce that the increase in cathodic current potentials from -0.155 V to -0.489 V correspond to the H^+/H_2 proton reduction reaction R4, less than -0.489 V corresponding to the progress of the $Co^{2+/}Co$ deposition reaction R2 and from potentials of -1.097 V from the H_2O/H_2 reaction R5. On the reverse scan a small cathodic current less than 0.01 mA/cm^2 is observed from hydrogen evolution and an increase in anodic current positive of -0.489 V which would correspond to the dissolution of cobalt from the surface of the Au RDE. Similar potentials and current densities regarding Co^{2+} deposition have been reported for similar systems (Bertazzoli

and Sousa 1997; Abd El Rehim, Abd El Wahaab et al. 1998; Jeffrey, Choo et al. 2000; Dulal, Charles et al. 2004).

The decrease in cathodic current on the forward scan from potentials of -0.638 V and -0.974 V could be due to an increase in pH on the surface leading to the precipitation of $Co(OH)_2$, blocking the surface of the electrode or the formation of a co-deposited hydrogen rich metallic phase which could occur at slower rates with a reduced observed current. The reduction of oxygen and evolution of hydrogen could also cause a reduction in pH in the Helmholtz inner layer which could also lead to a passivation of electrode surface as described by eq^n 4.9.

$$Co^{2+} + OH^- \rightarrow Co(OH)_2 \qquad (4.9)$$

Jeffrey et al. (Jeffrey, Choo et al. 2000) report cobalt deposition to occur by a preceding chemical reaction (c.e.e) mechanism via a cobalt hydroxide complex described by eq^n 4.10-4.12. For solutions of 0.050 M Co^{2+} the rate determining step was deemed the electronation of the CoOH species adsorbed in the inner Helmholtz layer.

$$Co^{2+} + H_2O \rightarrow CoOH^+(ads) + H^+ \qquad (4.10)$$

$$CoOH^+(ads) + e^- \rightarrow CoOH(ads) \qquad (4.11)$$

$$CoOH(ads) + H^+ + e^- \rightarrow Co + H_2O\ (RDS) \qquad (4.12)$$

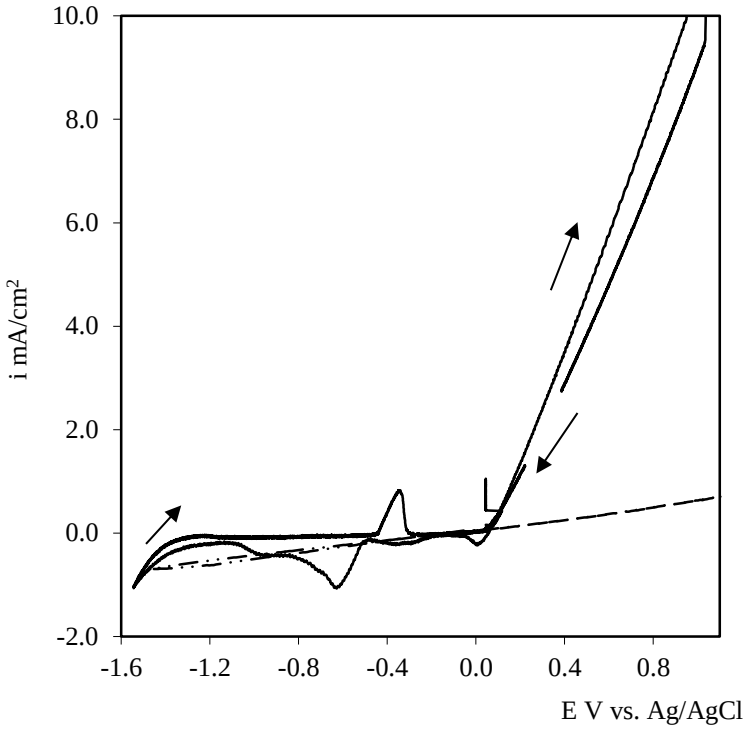

Figure 4.15: Cyclic voltammograms (S = 0.001 V/s). For Co^{2+} reduction on an Au RDE at 25°C from 5.09 x 10^{-3} M (300 ppm) Co^{2+} + 3.65 x 10^{-2} M (3500 ppm) SO_4^{2-}, pH = 3.77 and κ = 4.73 mS/cm. Background cyclic voltammograms (---) from Figure 4.9 also shown for comparison.

Figure 4.16 exemplifies cyclic voltammetry for Co^{2+} species in 0.9% NaCl electrolyte with graphite electrodes without bacteria. Preliminary cyclic sweeps with faster scan rates (0.100 V/s) for cobalt electrolytes were carried out with reducing inversion potentials. The appearance and disappearance of current peaks can here be used as indicator of electronation reactions occurring.

Following each sweep, the working electrode was polarised at +1.045 V and the electrolyte stirred to strip metal deposits from the surface of the electrode until open circuit potentials were observed. The anodic peak that corresponds to cobalt stripping became less prominent for reverse sweep potentials greater than -1.045 V. This would be due to less cobalt deposited on the electrode surface and so less stripped. Thus one can conclude that Co^{2+} electrodeposition requires overpotentials less cathodic than -1.045 V for significant cobalt deposition on G10 graphite electrodes. Two anodic peaks are observed for potentials greater than -1.045 V which would most likely correspond to

the dissolution of different cobalt phases as concluded by Soto el al. (Soto, Arce et al. 1996).

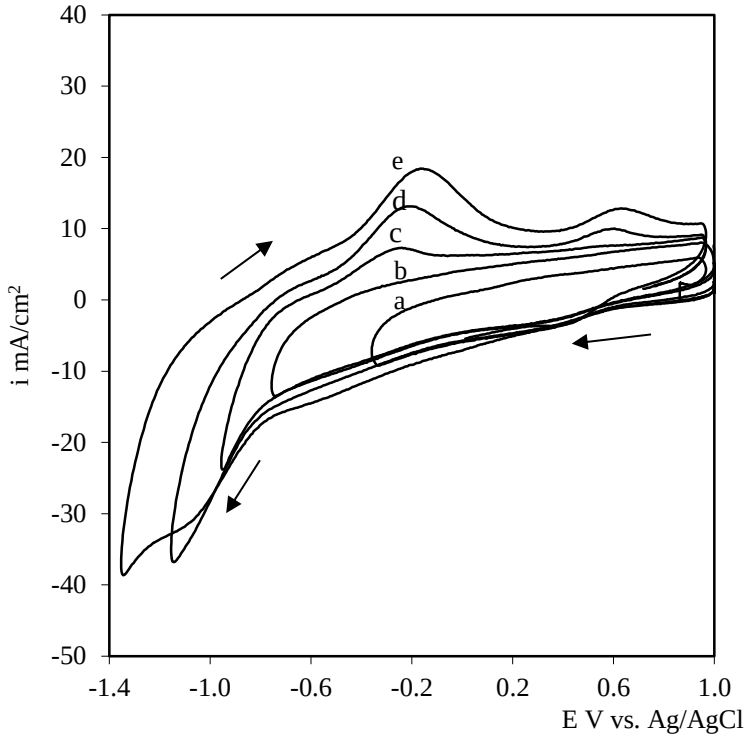

Figure 4.16 : Cyclic voltammograms (S = 0.100 V/s) for Co^{2+} reduction on an G10 graphite electrode at 26°C from 200 ppm Co^{2+} + 0.9% NaCl(aq), pH = 2, κ = 24.7 mS/cm.

Figure 4.17 describes cyclic voltammograms, carried out with slow scans of 0.010 V/s in solutions containing 200 ppm Co^{2+} in 0.9% NaCl upon graphite electrodes. Open circuit potentials on clean electrodes were ≈ 0.600 V which decreased to 0.050 V after a few scans presumable due to a reduction of dissolved oxygen molecules in solution. The voltammogram shows a cathodic current associated with absorbed O_2(g) reduction from potentials of 0.490 V, a further reduction current beyond potentials of 0 V from proton reduction and a further reduction there upon from water reduction. From reported standard potentials and previous experimentation of Co^{2+} electrodeposition on Au RDE one would expect electrodeposition of cobalt from solution, post potentials of ≈ -0.500 V. Therefore the cathodic reduction current from cobalt deposition is masked by simultaneous proton reduction.

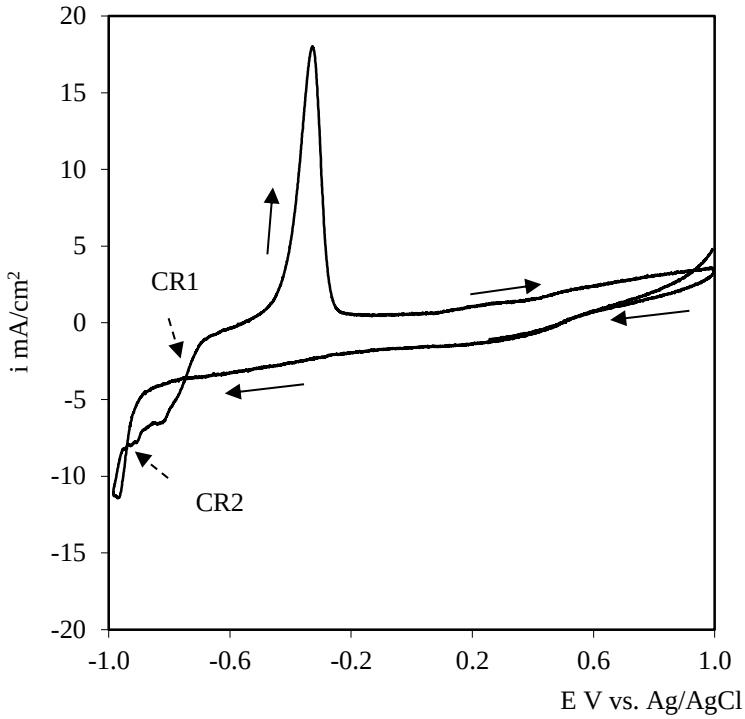

Figure 4.17 : Cyclic voltammograms (S = 0.010 V/s) for Co^{2+} reduction on an G10 graphite electrode at 25°C from 200 ppm Co^{2+} + 0.9% NaCl(aq) pH = 2, κ = 3.07 mS/cm.

On the reverse sweep two cathodic crossovers which are indicative of the formation of new phases by nucleation processes, are observed. CR1 at -0.924 nominated as the nucleation overpotential in imitation of analysis described by Soto et al. (Soto, Arce et al. 1996) and Rios-Reyes et al. (Rios-Reyes, Mendoza-Huizar et al. 2010). The potential cross over -0.743 V nominated as the overcrossing potential with similar values reported by Soto et al. of -0.700V for cobalt electronucleation onto Glassy Carbon electrode from ammonium chloride solutions (Soto, Arce et al. 1996). A sharp rise in anodic current is observed after potentials -0.577 V which would correspond to cobalt stripping from the electrode surface.

Following theoretical predictions the overcrossing potential would correspond to the reversible potential (E_r) of the Co^{2+}/Co redox couple (Soto, Arce et al. 1996), with a significant negative shift in reversible potentials and thus an increase in the energy requirements of the electronation phase transformation reaction on graphite substrates compared to previous experimentation with noble metals such as gold as summarised in Table 4.6.

Reaction	Electrode Substrate	Electrolyte	E_r V vs. Ag/AgCl
$Co^{2+} + 2e^- \rightarrow Co$	Au RDE	200 ppm Fe^{3+} in 3500 ppm Na_2SO_4(aq) pH 2.77, κ = 5.77 mS/cm	-0.489
$Co^{2+} + 2e^- \rightarrow Co$	G10 – Graphite	200 ppm Fe^{3+} + 0.9% NaCl (aq) pH 2 κ = 3.07 mS/cm	-0.743

Table 4.6 : Summary observed reversible potentials (E_r) for Co^{2+} reduction on Au RDE and G10 graphite electrodes.

4.3.7. Electrochemical analysis of the electrodeposition of iron from electrolytes without bacterial cells

The electron transfer of Fe^{3+}/Fe^{2+} electronation has been reported to occur by no adsorbed intermediates wherein no ligand transfer between the reactants and the electrode surface occurs (Harinipriya and Sangaranarayanan 2004). Figure 4.16 describes linear voltammograms of Fe^{3+} reduction on an Au RDE at 25°C from 200 ppm Fe^{3+}. The measured open circuit potential observed prior to experimentation for the system is -0.05 V. One would expect this open circuit potential to be closer to the 0.6 V as for the standard potential of the Fe^{3+}/Fe^{2+} couple (Angell and Dickinson 1972) described by eq^n 4.13. Calculated Nernst reversible potentials of 0.126 V which accounts for low concentration of the ferrous Fe^{2+} ($\approx 1 \times 10^{-8}$ M) species, goes some way to account for the significant negative shift. Furthermore Fe^{3+} ions in sulphate medium can form a series of species such as $FeSO_4^+$, $Fe(SO_4)_2^-$ and $Fe(SO_4)_3^{2-}$ (Samec and Weber 1977; Langmaier, Trojánek et al. 1999) describe by eq^n 4.14a-c. These charge carrying species travel to the inner Helmholtz layer of electrode surface and are reduced as described by eq^n 4.14a-c. Also blocking of the electrode surface by SO_4^{2-} by preferential adsorption may play a role (Bockris, Mannan et al. 1968) reducing the area available to the Fe^{3+} cation involved in the electronation reactions. Reversible potentials of $\approx$ 0.05 V for this redox couple have also been reported Dew et al. (Dew and Phillips 1985) for systems similar to ours, thus we have reasoned that the majority of the cathodic current produced from 0.05 to -0.15 V is from the Fe^{3+}/Fe^{2+} (R.3.1) redox couple.

$$Fe(H_2O)_6^{3+} + e^- \rightarrow Fe(H_2O)_6^{2+} \quad (4.13)$$

$$Fe^{3+} + SO_4^{2-} \rightarrow FeSO_4^+ \quad (4.14a)$$

$$Fe^{3+} + 2SO_4^{2-} \rightarrow Fe(SO_4)_2^- \quad (4.14b)$$

$$Fe^{3+} + 3SO_4^{2-} \rightarrow Fe(SO_4)_3^{3-} \quad (4.14c)$$

$$FeSO_4^+ + e^- \rightarrow FeSO_4 \quad (4.15a)$$

$$Fe(SO_4)_2^- + e^- \rightarrow Fe(SO_4)_2^{2-} \quad (4.15b)$$

$$Fe(SO_4)_3^{3-} + e^- \rightarrow Fe(SO_4)_3^{4-} \quad (4.15c)$$

From comparison of Standard E_e^0 and Nernst E_e in Table 4.4 with observed E_r for various electronation reaction one can reason that the further decrease in current density is from H^+/H_2 (R.4) redox couple and that from -0.45 to -1.15 V from Fe^{2+}/Fe (R.3.3) iron electrodeposition.

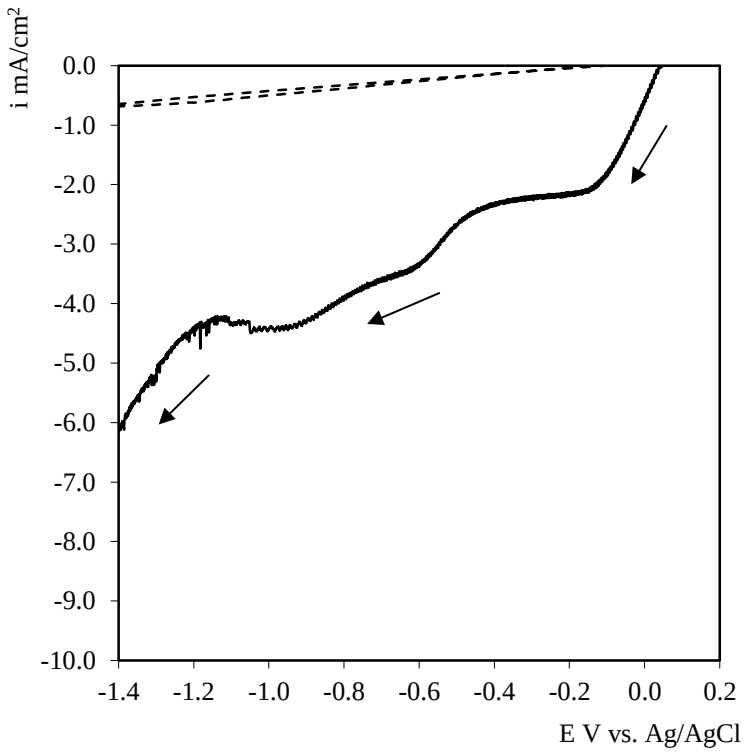

Figure 4.18 : Linear sweep voltammograms (S = 0.001V/s) for Fe^{3+} reduction on an Au RDE (ω = 1800 rpm) at 25°C from 5.38 x 10^{-3} M $Fe_2(SO_4)_3(H_2O)_5$, pH = 2.72 and κ = 5.77.

Background cyclic voltammograms (---) from Figure 4.9 also shown for comparison.

Similar reversible potentials for iron deposition were reported by Bockris et al. (Bockris, Mannan et al. 1968) who investigated the deposition and dissolution of iron from ferrous electrolytes of various pH's. They report a mechanism of iron deposition from $FeSO_4$(aq) electrolytes to be similar to that for Co deposition involving a c.e.e reaction mechanism as described by eq^n 4.16 - 4.18.

$$Fe^{2+} + H_2O \rightarrow FeOH^+_{(ads)} + H^+ \quad (4.16)$$

$$FeOH^+_{(ads)} + e^- \rightarrow FeOH_{(ads)} \quad (4.17)$$

$$FeOH^+_{(ads)}\ H^+ + e^- \rightarrow Fe + H_2O \quad (4.18)$$

Fe^{3+} systems with graphite were carried out in 0.9% NaCl base electrolyte as for cobalt. Figure 4.19a is the first cyclic scan on a clean electrode from open circuit potentials of 0.500 V and Figure 4.19b is the subsequent second scan. A reduction current is observed around -0.400 V on the first scan which would correspond well to the iron electrodeposition reaction Fe^{2+}/Fe (R3.2). On the second scan this reduction current is masked but a crossover cathodic branch observed around potentials of -0.500 V. This cathodic crossover would correspond to the reversible potential Fe^{2+}/Fe as for cobalt systems described previously. Scan 2 displayed a strong cathodic current from 0.600 V which corresponds well to the Fe^{3+}/Fe^{2+} reduction couple (R3.1). Two anodic peaks are observed with corresponding potentials of 0.214 V and 0.605 V for both scan 1 and 2. The first peak would correspond to adsorbed molecular and atomic hydrogen oxidation and the second from the Fe^{2+}/Fe^{3+} oxidation couple.

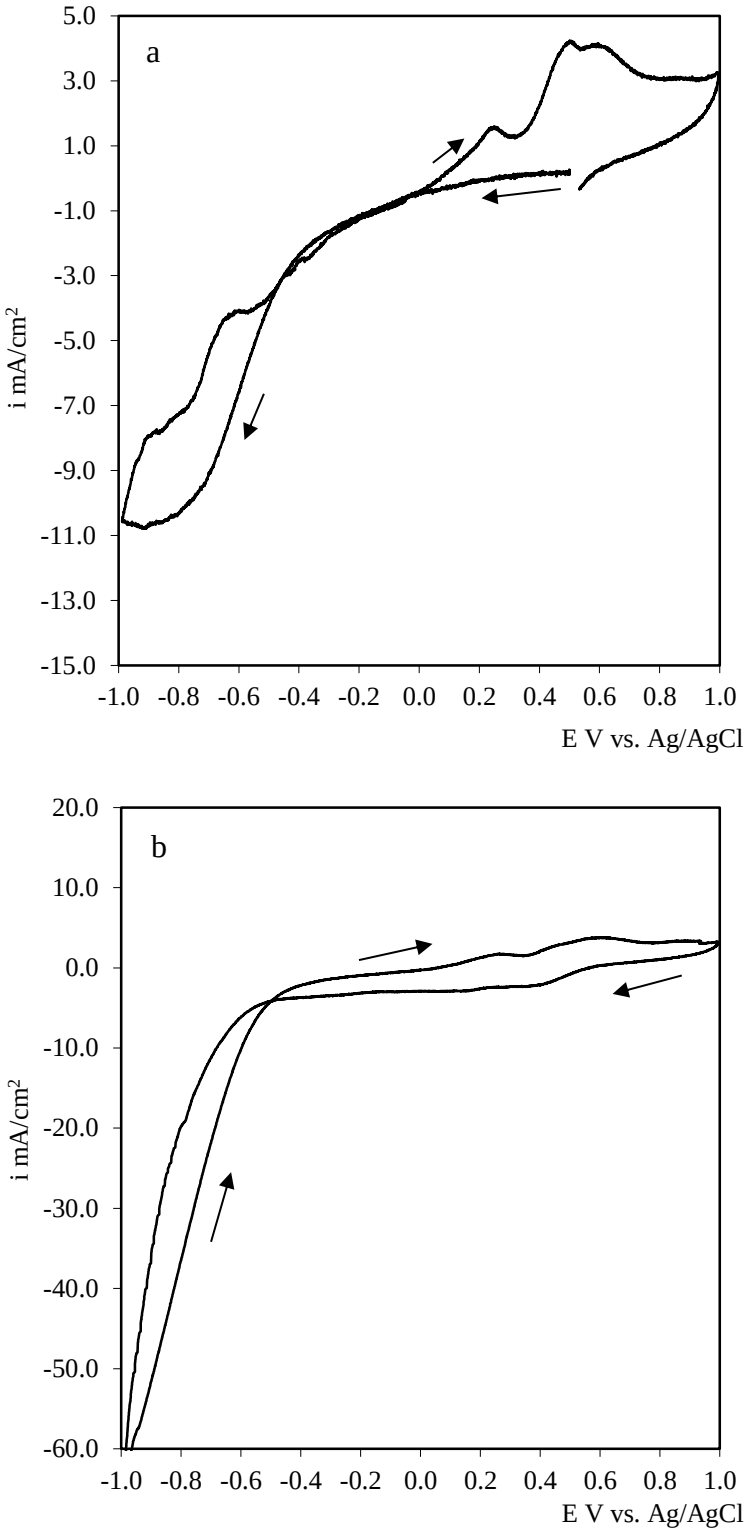

Figure 4.19 : Cyclic voltammograms for Fe^{3+} reduction on an G10 graphite electrode (S = 0.010 V/s) at 25°C from 200 ppm Fe^{3+} + 0.9% NaCl(aq), pH = 2, κ = 24.7 mS/cm. (a) Scan 1 (b) Scan 2.

Reaction	Electrode Substrate	Electrolyte	E_r V vs. Ag/AgCl
$Fe^{3+} + e^- \rightarrow Fe^{2+}$	Au RDE	200 ppm Fe^{3+} in 3500 ppm Na_2SO_4(aq)	0.045
$Fe^{2+} + 2e^- \rightarrow Fe$		pH 2.77, κ = 5.77 mS/cm	-0.456
$Fe^{3+} + e^- \rightarrow Fe^{2+}$	G10 - Graphite	200 ppm Fe^{3+} + 0.9% NaCl(aq)	0.600
$Fe^{2+} + 2e^- \rightarrow Fe$		pH 2 κ = 42.7 mS/cm	-0.670

Table 4.7 : Observed reversible potentials (E_r) taken from *i/E* voltammograms for Fe^{2+} reduction on Au RDE and G10 graphite electrodes.

4.4. Qualitative evaluation electrochemical reaction with bacterial cells upon graphite electrodes

Figures 4.20 – 4.23 give representative voltammograms of graphite electrodes with representative metal ion electrolytes with the addition of 10 ml of 1 x 10^{10} CFU/ml *Shewanella putrefaciens* bacterial cells. As discussed in chapter 3, bacterial cells act as biosorbent of metal ions spontaneously. The addition of cells would cause a decrease in metal ion concentration by biosorption and therefore one would expect a negative shift of reversible potentials as predicted by the Nernst equation, eq^n 4.19.

$$dE = E_{e,b} - E_{e,a} = \frac{RT}{nF} \ln\left[\frac{C_{O,b}}{C_{O,a}}\right] \qquad (4.19)$$

Using the pseudo second order model which in chapter 3 was shown to be a good model for biosorption of gold, cobalt and iron metal ions, we estimated the amount of metal ions which would be removed from solution and adjusted predicted values of the Nernst equation for representative redox reactions. q_e was estimated using the Langmuir equation using values of q_{max} and b quantified in chapter 3. Table 4.8 summarises the parameters used, calculated concentrations of metal ions in solution and changes in Nernst reversible potentials. For all metal ion electronation reactions, a reduction in metal ion concentration would cause a negative shift in reversible potential and hence an increase in the overall Gibbs free energy of the process.

	Langmuir			Pseudo-2nd Order Equation					
	q_{max}	b	q_e	k_2	C_o	C_t	t		dE_e
	mg/g	L/mg	mg/g	g /mg min^{-1}	mg/L	mg/L	min	Reaction	V
Au	769	0.178	737	8.16×10^{-5}	200	140	30	$AuCl_4^- + 3e^- \rightleftharpoons Au + 4Cl^-$	-0.003
Co	25000	0.001	1190	2.00×10^{-3}	200	49	30	$Co^{2+} + 2e^- \rightleftharpoons Co$	-0.018
Fe	1429	0.002	341	3.00×10^{-4}	200	178	10	$Fe^{2+} + 2e^- \rightleftharpoons Fe$	-0.001

Table 4.8 : Respective shifts in the Nernst potential upon changes in metal ion concentrations by biosorption of metal ions based on analysis described in chapter 4.

4.4.1. Electrochemical analysis of the electrodeposition of gold from electrolytes with bacterial cells

Figure 4.20 illustrates 2 examples of linear sweep voltammograms using slow scan rates of 0.010 V/s with and without 10 ml bacteria suspensions of $1x10^{10}$ CFU/ml. Scans were made after 30 minutes of addition of bacterial cells. As is evident in the scans there is a positive shift in reversible potentials where the current crosses the potential axis when bacterial cells are added to the solution.

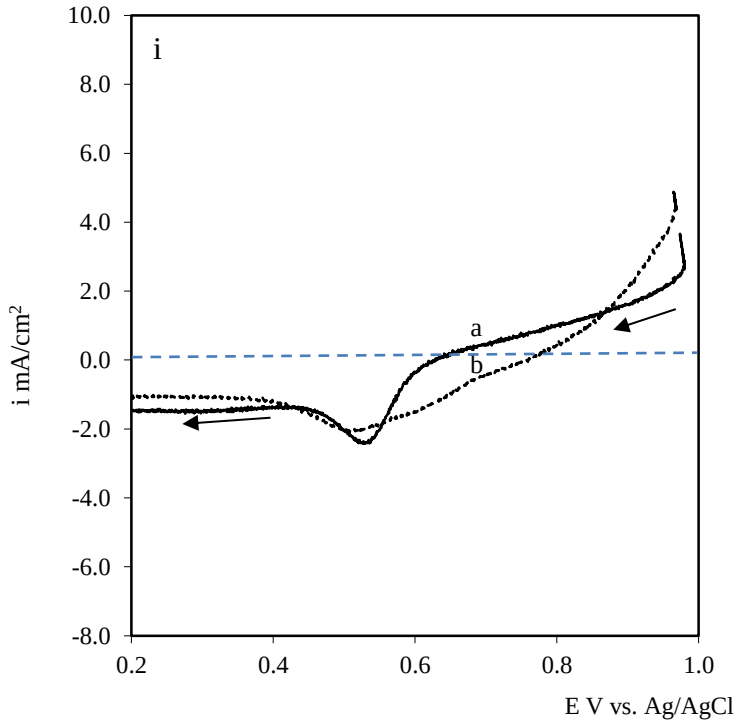

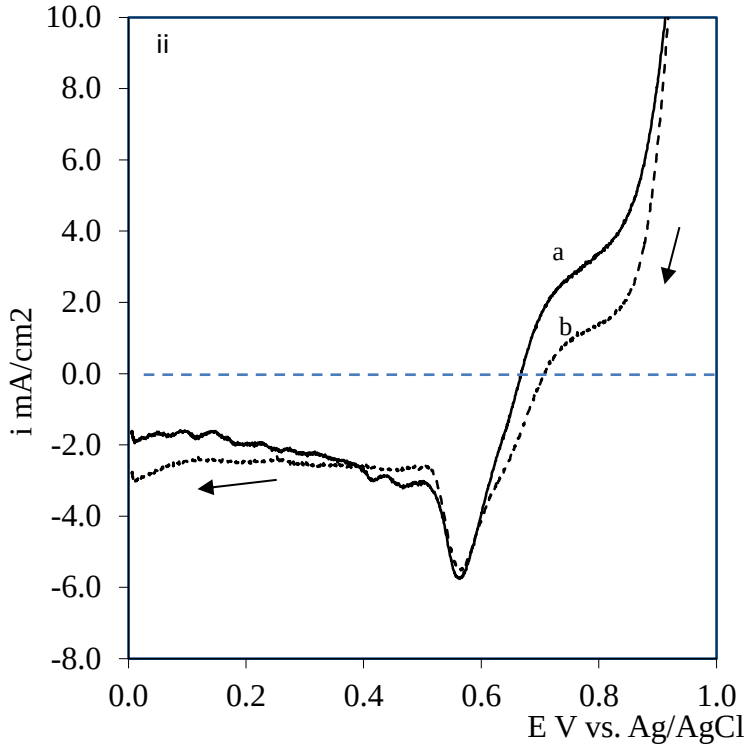

Figure 4.20 (i-ii) : Linear sweep voltammograms (S = 0.010 V/s) for Au^{3+}reduction on an G10 graphite electrode at 25°C from 200 ppm Au^{3+} in 2M HCl matrix pH = 2, κ = 35.2 mS/cm.

(a) without cells (b) with 10 ml $1x10^{10}$ CFU/ml bacterial cells for two typical experimentations.

This would suggest a change in thermodynamics of the gold electrodeposition reaction (R1.1) with a reduction in the overall reaction Gibbs free energy. Which we would infer, is due to bacterial and bacterial component interactions with the electrode surfaces. A positive shift is thus conclusive evidence that bacterial cells or bacterial components reduce the energy requirements of reactions as positive shift would point to a reduction in Gibbs free energy for heterogeneous electrodeposition.

There are also changes in the shape of the curve proceeding gold electrodeposition reversible potentials. Evidently the gradient of scans is steeper when bacterial cells are added to the solution. This is indicative of a change in the kinetic behaviour of the electron transfer reaction, i.e. an increase in the kinetic rate. Further Tafel analysis (discussed in chapter 5) of voltammograms would be needed to investigate influence of bacterial cells on reaction mechanisms and bacterial bio-catalysis of electrodeposition reactions.

4.4.2. Electrochemical analysis of the electrodeposition of cobalt from electrolytes with bacterial cells

Figure 4.21 illustrates the cyclic voltammograms using slow scan rates of 0.010 V/s for cobalt solutions without (a) and with (b) 10 ml of 1 x 10^{10} CFU/ml bacterial cells taken before the addition of cells and after 30 minutes of their addition. The voltammogram shows high resistance which would be due to the relatively low conductivity of the electrolyte. A high resistance may distort linear sweep voltammograms thereby confounding interpretation regarding current-potential behaviour. However it still allows one to analyse changes in shapes of voltammograms and note peaks to determine where electronation reactions are occurring.

As the deposition of cobalt occurs simultaneously with hydrogen evolution, changes in reverse potentials could not be directly evaluated but changes in the electrodeposition thermodynamics can be qualified using cathodic crossover branches which would correspond to electroreduction reverse potentials as described by Soto et al. (Soto, Arce et al. 1996). Voltammetry experiments without cells those taken after 30 minutes addition show negative cathodic crossovers C_a and C_b of -0.734 V and -0.736 V respectively. This would suggest that bacteria do not influence thermodynamics of the process with negligible changes in reversible potentials. A rationalization for negligible shifts in reversible potentials of cobalt, when compared to gold systems, may be that base metal cations such as cobalt Co^{2+} are not reduced by cells for dissimilatory reasons. Thus different protein enzymes are likely to be employed which may not have an effect on reaction thermodynamics for cobalt in comparison to gold experimentation.

The magnitude of the cobalt dissolution peaks are also significantly reduced as illustrated by Figure 4.21, with a peak current densities of 0.0069 A/cm^2 and 0.0179 A/cm^2 with and without bacterial cells in the electrolyte bath. This would suggest that bacteria reduce the amounts of cobalt electrodeposited on the surface of the electrode and influence reaction kinetics. This may be due to bacterial coverage of the electrode surface, obstructing cobalt ion mass transport to the electrified interface.

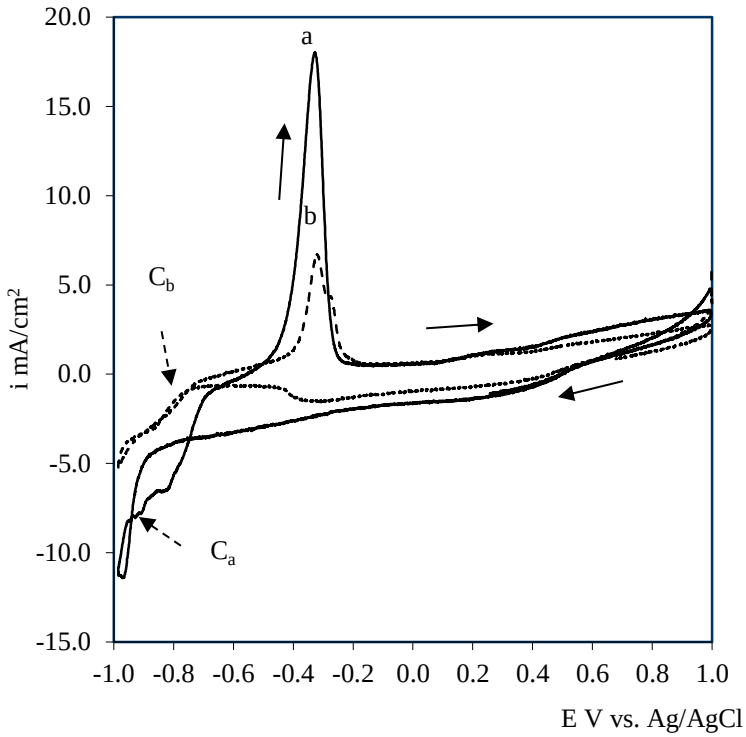

Figure 4.21 : Cyclic voltammograms (S = 0.010 V/s) for Co^{2+} reduction on G10 graphite electrode at 25°C from 200 ppm Co^{2+} + 0.9% NaCl(aq), pH = 2, κ = 24.7 mS/cm (a) without bacteria cells (b) scan taken after 30 minutes addition 10 ml of 1x 10^{10} CFU/ml.

4.4.3. Electrochemical analysis of the electrodeposition of iron from electrolytes with bacterial cells

Figure 4.22 illustrates cyclic voltammograms for ferrous sulphate systems with the addition of bacterial cells. As with gold systems, there is a positive shift in reversible potentials for the ferric ion reduction described by the Fe^{3+}/Fe^{2+} redox couple, this pointing to a possible change in the thermodynamics of this redox couple for iron in sodium chloride electrolytes when bacteria are added to the electrolyte bath.

This could also be due to a rise in pH of solution by bacterial processes leading to the formation of ionic hydroxide species and a reduction in the potential window as discussed previously from Pourbaix analysis. A positive shift would suggest less energy is required to overcome the barrier to heterogeneous electroreduction leading to electrodeposition of ferric metal ions with the addition of bacterial cells as with gold electrodeposition and is influencing the concentration of metal ions located at the

electrical interface. Further theoretical investigation would be required in buffered solutions. If the process is due as with gold to bacterial interaction then we would infer that similar bacterial protein enzymes or bacterial artefacts could be implicated for this shift in reversible potentials of Fe^{3+} and $AuCl_4^-$ species.

Also evident in Figure 4.22, higher limiting currents with bacteria for ferric ion reduction is observed. For potentials of 0.2 V vs. Ag/AgCl, limiting currents of -1.457 A/cm^2 and -1.026 A/cm^2 for electrolytes with and without bacterial cells are observed. This would suggest that bacteria influence mass transfer of metal ionic species to the electrode surface. It is unclear how and why bacteria influence ionic mass transport to the electrode surface. Further Levich analysis of limiting currents for Fe^{3+} electronation using RDE's could be applied to determine bacterial influence on diffusion phenomena regarding metal ion mass transfer through the Nernst diffusion layer (see Figure 4.1).

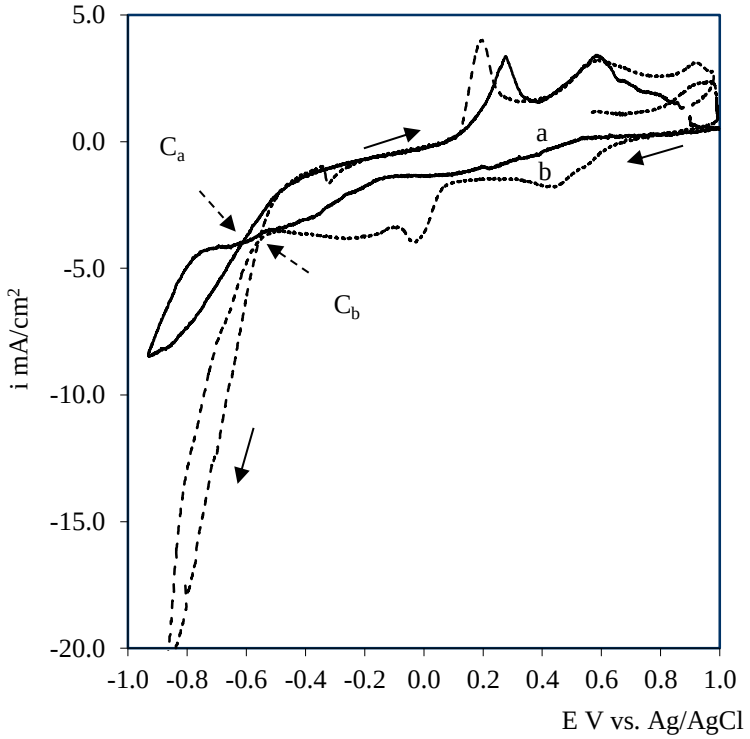

Figure 4.22 : Cyclic voltammograms for Fe^{3+} reduction on G10 graphite electrode (S = 0.010 V/s) at 26°C from 200 ppm Fe^{3+} + 0.9% NaCl(aq), pH = 2, κ = 42.7 mS/cm.
(a) Without bacterial cells, (b) with 10 ml 1x10^{10} CFU/ml bacterial cells (scan made after 10 minutes after addition of cells).

As for cobalt solution the revisable potentials for Fe^{2+}/Fe iron deposition can be evaluated using cathodic cross over branches. A cross over branch was observed at -0.602 V which would correspond to Fe^{2+}/Fe redox reversible potential. When bacteria were added to the electrolyte, a positive shift in cathodic crossover was observed at 0.042 V. This may be due to an increased concentration of Fe^{2+} reduced by bacterial cells, although conclusive evidence would require further extensive investigation.

4.5. Discussion

Electrochemical analysis of metal ion reduction and deposition has been investigated here by using Au, Pt and graphite electrode substrates in acidic electrolytes containing Au^{3+}, Co^{2+} and Fe^{3+} metal cations. With quantitative analysis with bacteria cells added to the solution and empirical observation of respective slow scan voltammograms applied for examination of any changes in thermodynamics of metal ion electronation reactions. Our aim being to conclude upon possible savings in energy requirements of electronation reactions by the addition of bacterial cells.

Iron and gold systems with bacteria show a significant shift in reversible potentials for $AuCl_4^-/Au$ and Fe^{3+}/Fe^{2+} and Fe^{2+}/Fe redox couple. To the contrary negligible influence on revisable potentials for Co^{2+} electrodeposition is observed evaluated with cathodic crossovers. This apparent dichotomy we would further hypothesize is due to dissimilative artefacts and bacterial components such as cytrochrome-c and redox mediators which bio-reduce metal ions such as Fe^{3+} an Au^{3+} as described in chapter 3 as part of dissimilative mechanisms and may also reduce energy requirements of respective electrochemical electronation phenomena. Another possibility as illuminated in Figure 4.23, could be that bacteria increase the surface concentrations of metal ions in the charge interface region, involving biosorption and bio-desorption mechanisms. Where there is an elevated concentration of metal ions adsorbed upon the outer lipopolysaccharide membrane leaf of the outer cell membrane, by bacteria respiring upon the electrode surface and desorbed when in close enough proximity of charged interface region by inner galvanic potential forces.

A basis of quantitative comparison of energy requirements for metal mediation by electrodeposition of metal ions can be evaluated by eq^n 2.32 and 2.33, based on water oxidation (H_2O/O_2 E^a_e = 1.11 V)[4] occurring in the anodic chamber of the electrode, which does not limit the overall process. Although in reality overpotentials would be applied to speed up reactions and further engineering design would need to take into account potential losses; values here are given only to put the present analysis in some overall relative perspective. As summarised in Table 4.9 there was a 36% reduction in

[4] E_a (H_2O/O_2) = 1.229 – 0.05916 pH; E_a = 1.229 – (0.05916 x 2) = 1.111

the Gibbs free energy requirements for gold electrodeposition, insignificant changes for cobalt systems and 11% reduction for ferric iron electrodeposition.

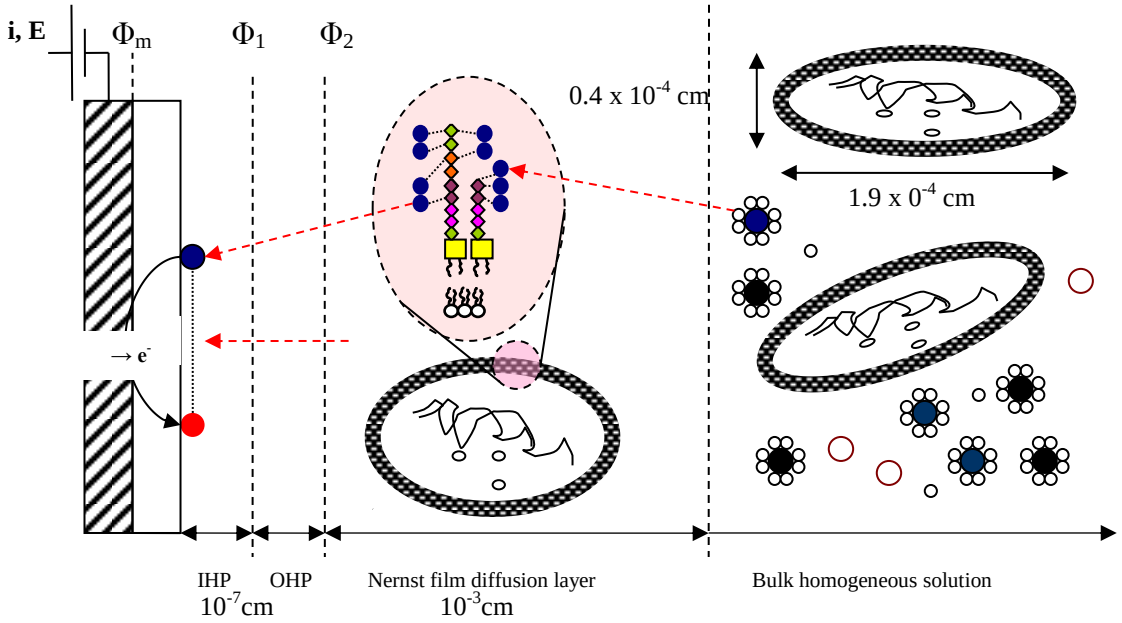

Figure 4.23: Biological mediated metal ion transport and electronation reaction mechanisms.

$$\Delta G = -nFE^{e}{}_{cell} \qquad (2.32)$$

$$E^{e}{}_{CELL} = E^{a}_{e} - E^{c}_{e} \qquad (2.33)$$

		R1 Cathodic E^c_e	R2 Cathodic E^c_e	Anodic E^a_e	E_{cell} $E^a_e - E^c_e$	n	ΔG kJ/mol	% Change
R1 : $AuCl_4^- + 3e^- \rightleftharpoons$ Au	i.a	0.618		1.11	-0.492	3	142	-36%
	i.b	0.749		1.11	-0.361		104	
	ii.a	0.668		1.11	-0.442		128	-9%
	ii.b	0.706		1.11	-0.404		117	
R2 : $Co^{2+} + 2e^- \rightleftharpoons Co$	a	-0.733		1.11	-1.843	2	356	0%
	b	-0.743		1.11	-1.853		358	
R3.1 : $Fe^{3+} + e^- \rightleftharpoons Fe^{2+}$	a	0.496	-0.634	1.11	-2.358	3	683	-11%
R3.2 : $Fe^{2+} + 2e^- \rightleftharpoons Fe$	b	0.668	-0.574	1.11	-2.126		615	

Table 4.9 : Calculated Gibbs free energy requirements for various electrodeposition reactions with and without bacterial cells.

4.6. Conclusions

This study would conclude that live bacteria added to the electrolyte bath have significant changes in reaction thermodynamics of metal cation reduction of Fe^{3+} and electrodeposition for $AuCl_4^-$ ionic species. This based on linear sweep voltammetry experimentation of our metal electrolytes with a reduction in Gibbs free energy of metal cation reduction as part of remediation strategies. Upon analysis of Pourbaix diagrams we would state that changes in gold electrodeposition potential is unaffected by pH up to 8 and therefore indirect changes of system pH by bacterial cell would not be the cause. That for iron is speculative and would require further experimentation as Fe^{3+} forms ionic $Fe(OH)^{2+}$ species with increases of pH greater than 2.5 which would have an effect upon electronation thermodynamics.

These metal species are proven to be biosorbed and utilized by electroactive Gram-negative bacteria as electron accepters as part of metabolic respiration described in previous investigation and investigated in chapter 3. It would follow that relational protein enzymes or in situ bio-fabricated electron mediators could be implicated in the changes in reaction thermodynamics especially for gold systems. Further experimentation would be required for the determination of respective reaction mechanism and bacterial influence. This experimentation does show significant changes to gold electrodeposition and further experimentation is warrant for the development of bioelectrochemical science and prospective technological engineering.

Imminent experimentation upon effects of bacteria upon electronation kinetics would be a natural progression upon investigation here as would investigation on mass transfer of metal ions in the presence of bacterial cells. Theoretical aspects of which are outlined in concluding chapter 5.

References

*Abd El Rehim, S. S., S. M. Abd El Wahaab, et al. (1998). "Electroplating of cobalt from aqueous citrate baths." Journal of Chemical Technology & Biotechnology **73**(4): 369-376.*

*Angell, D. H. and T. Dickinson (1972). "The kinetics of the ferrous/ferric and ferro/ferricyanide reactions at platinum and gold electrodes: Part I. Kinetics at bare-metal surfaces." Journal of Electroanalytical Chemistry and Interfacial Electrochemistry **35**(1): 55-72.*

Bard, A. J., R. Parsons, et al. (1985). Standard potentials in aqueous solution. New York, M. Dekker.

*Baron, D., E. LaBelle, et al. (2009). "Electrochemical Measurement of Electron Transfer Kinetics by Shewanella oneidensis MR-1." Journal of Biological Chemistry **284**(42): 28865-28873.*

*Bertazzoli, R. and M. d. F. P. Sousa (1997). "Studies of the electrodeposition of cobalt on a vitreous carbon electrode." Journal of the Brazilian Chemical Society **8**: 357-362.*

*Bockris, J. O. M., R. J. Mannan, et al. (1968). "Dependence of the Rate of Electrodic Redox Reactions on the Substrate." The Journal of Chemical Physics **48**(5): 1898-1904.*

Bockris, J. O. M. and A. K. N. Reddy (1970). Modern electrochemistry : an introduction to an interdisciplinary research. New York, Plenum Press.

*Bretschger, O., A. C. M. Cheung, et al. (2010). "Comparative Microbial Fuel Cell Evaluations of Shewanella spp." Electroanalysis **22**(7-8): 883-894.*

Brown, M., B. Barley, et al. (2002). Minewater treatment : technology, application and policy. London, IWA.

*Carmona-Martinez, A. A., F. Harnisch, et al. (2011). "Cyclic voltammetric analysis of the electron transfer of Shewanella oneidensis MR-1 and nanofilament and cytochrome knock-out mutants." Bioelectrochemistry **81**(2): 74-80.*

Chivot, J, et al. (2008). New insight in the behaviour of Co-H[2]O system at 25-150 °C, based on revised Pourbaix diagrams. Kidlington, ROYAUME-UNI, Elsevier.

*Dew, D. W. and C. V. Phillips (1985). "The effect of Fe(II) and Fe(III) on the efficiency of copper electrowinning from dilute acid Cu(II) sulphate solutions with the chemelec cell: Part I. Cathodic and anodic polarisation studies." Hydrometallurgy **14**(3): 331-349.*

*Diaz, M. A., G. H. Kelsall, et al. (1993). "Electrowinning coupled to gold leaching by electrogenerated chlorine: I. Au(III)□Au(I) / Au kinetics in aqueous Cl2/Cl− electrolytes." Journal of Electroanalytical Chemistry **361**(1–2): 25-38.*

*Dulal, S. M. S. I., E. A. Charles, et al. (2004). "Dissolution from electrodeposited copper–cobalt–copper sandwiches." Journal of Applied Electrochemistry **34**(2): 151-158.*

*E, Y. (1984). "Electrocatalysts for O2 reduction." Electrochimica Acta **29**(11): 1527-1537.*

*Feng, D., C. Aldrich, et al. (2000). "Treatment of acid mine water by use of heavy metal precipitation and ion exchange." Minerals Engineering **13**(6): 623-642.*

*Fredrickson, J. K., M. F. Romine, et al. (2008). "Towards environmental systems biology of Shewanella." Nat Rev Micro **6**(8): 592-603.*

*Fricke, K., F. Harnisch, et al. (2008). "On the use of cyclic voltammetry for the study of anodic electron transfer in microbial fuel cells." Energy & Environmental Science **1**(1): 144-147.*

*Ghafari, S., M. Hasan, et al. (2008). "Bio-electrochemical removal of nitrate from water and wastewater—A review." Bioresource Technology **99**(10): 3965-3974.*

*Gorby, Y., J. McLean, et al. (2008). "Redox-reactive membrane vesicles produced by Shewanella." Geobiology **6**(3): 232-241.*

*Gregory, K. B., D. R. Bond, et al. (2004). "Graphite electrodes as electron donors for anaerobic respiration." Environmental Microbiology **6**(6): 596-604.*

*Gregory, K. B. and D. R. Lovley (2005). "Remediation and Recovery of Uranium from Contaminated Subsurface Environments with Electrodes." Environmental Science & Technology **39**(22): 8943-8947.*

*Guenbour, A., H. Iken, et al. (2006). "Corrosion of graphite in industrial phosphoric acid." Applied Surface Science **252**(24): 8710-8715.*

*Harinipriya, S. and M. V. Sangaranarayanan (2004). "Estimation of exchange current density for ferric/ferrous reaction at electrode surfaces—influence of ionic desolvation and dipolar adsorption." Journal of Colloid and Interface Science **273**(1): 247-255.*

*Harrison, J. A. and J. Thompson (1975). "The kinetics of gold deposition from chloride solution." Journal of Electroanalytical Chemistry and Interfacial Electrochemistry **59**(3): 273-280.*

*Hill, H. A. O. and I. J. Higgins (1981). "Bioelectrocatalysis." Philosophical Transactions of the Royal Society of London. Series A, Mathematical and Physical Sciences **302**(1468): 267-273.*

*Jeffrey, M. I., W. L. Choo, et al. (2000). "The effect of additives and impurities on the cobalt electrowinning process." Minerals Engineering **13**(12): 1231-1241.*

*Kano, K. and T. Ikeda (2000). "Fundamentals and Practices of Mediated Bioelectrocatalysis." Analytical Sciences **16**(10): 1013-1021.*

*Kelsall, G. H., N. J. Welham, et al. (1993). "Thermodynamics of Cl-H2O,Br-H2O, I-H2O, Au-Cl-H2O, Au-Br-H2O and Au-I-H2O Systems at 298 K." Journal of Electroanalytical Chemistry **361**(1-2): 13-24.*

*L.J.J, J. (1974). "The mechanism of the chlorine evolution on different types of graphite anodes during the electrolysis of an acidic NaCl solution." Electrochimica Acta **19**(6): 257-265.*

*Langmaier, J., A. n. Trojánek, et al. (1999). "Kinetics of the ferric/ferrous electrode reaction on Nafion®-coated electrodes." Journal of Electroanalytical Chemistry **469**(1): 11-17.*

*M. Bond, A., S. Kratsis, et al. (1997). "Comparison of the Gold Reduction and Stripping Processes at Platinum, Rhodium, Iridium, Gold and Glassy Carbon Micro- and Macrodisk Electrodes." Analyst **122**(10): 1147-1152.*

Madigan, M. T. and T. D. Brock (2009). Brock biology of microorganisms. San Francisco, CA, Pearson/Benjamin Cummings.

*Magnuson, T. S., N. Isoyama, et al. (2001). "Isolation, characterization and gene sequence analysis of a membrane-associated 89 kDa Fe(III) reducing cytochrome c from Geobacter sulfurreducens." Biochem J **359**(Pt 1): 147-152.*

*Marsili, E., D. B. Baron, et al. (2008). "Shewanella secretes flavins that mediate extracellular electron transfer." Proceedings of the National Academy of Sciences **105**(10): 3968-3973.*

*McCreery, R. L. (2008). "Advanced Carbon Electrode Materials for Molecular Electrochemistry." Chemical Reviews **108**(7): 2646-2687.*

*Oelßner, W., F. Berthold, et al. (2006). "The iR drop – well-known but often underestimated in electrochemical polarization measurements and corrosion testing." Materials and Corrosion **57**(6): 455-466.*

Pourbaix, M. (1966). Atlas of electrochemical equilibria in aqueous solutions. Oxford, New York, Pergamon Press.

*Rios-Reyes, C., L. Mendoza-Huizar, et al. (2010). "Electrochemical kinetic study about cobalt electrodeposition onto GCE and HOPG substrates from sulfate sodium solutions." Journal of Solid State Electrochemistry **14**(4): 659-668.*

*Samec, Z. and J. Weber (1977). "The effect of the double layer on the rate of the Fe3+/Fe2+ reaction on a platinum electrode and the contemporary electron transfer theory." Journal of Electroanalytical Chemistry and Interfacial Electrochemistry **77**(2): 163-180.*

Sawyer, D. T., A. Sobkowiak, et al. (1995). Electrochemistry for Chemists, Wiley.

*Shi, L., D. J. Richardson, et al. (2009). "The roles of outer membrane cytochromes of Shewanella and Geobacter in extracellular electron transfer." Environmental Microbiology Reports **1**(4): 220-227.*

*Soto, A. B., E. M. Arce, et al. (1996). "Electrochemical nucleation of cobalt onto glassy carbon electrode from ammonium chloride solutions." Electrochimica Acta **41**(16): 2647-2655.*

*Thrash, J. C., J. I. Van Trump, et al. (2007). "Electrochemical Stimulation of Microbial Perchlorate Reduction." Environmental Science & Technology **41**(5): 1740-1746.*

*Wang, J., M. Li, et al. (2002). "Direct Electrochemistry of Cytochrome c at a Glassy Carbon Electrode Modified with Single-Wall Carbon Nanotubes." Analytical Chemistry **74**(9): 1993-1997.*

`

Chapter 5: Summary, conclusions and outlook

`

Chapter 5: Summary, concluding remarks and outlook

5.1. Summary of findings and conclusions

This research aims for the benign application of chemical engineering principles and paradigms with a green chemistry philosophy for social value in the remediation and recovery of precious and toxic metal ions by the collaboration and application of microbial and electrochemical phenomena. Our modest investigation aims firstly a sincere evaluation and conceptualization of bioelectrochemical metal cation remediation strategies. In hope a stepping stone to future engineering development and progression of the scientific state of art.

The potential for the collaboration of these two fields is immense as reviewed in chapter 1 and one would still feel that the academic community have only scratched the surface of the vast complexities of the symbiotic interactions and their modelling of such interfacial phenomena discussed in chapter 2. We hope that the foundations have been laid here for future application especially for the relatively un-developed application of bioelectrochemical systems for inorganic waste water treatment.

A summary of key findings of empirical experimentation of microbiological and bio-electrochemical metal ion remediation is given here with an eye for further investigation.

5.1.1. Microbiological biosorption of metal ions

Figure 5.1 gives a review of microbiological biosorption processes and possible mechanism hypothesized for microbiological experiments in chapter 3. Microbiological biosorption of metal ions were shown to be thermodynamically spontaneous with the overall adsorption process bottlenecked by the transport of metal ions through the cell membrane as evaluated by quantitative analysis of diffusion coefficients for intraparticular diffusion and film diffusion. The biosorption process was shown to be fast with up to 60% of the gold metal ions removed. With evidence of biogenic

`

nanoparticles formation located in the bacterial cell wall with active and deactivated cells for gold and initially active cells for cobalt.

5.1.2. Bio-electrochemical remediation of metal ions

For a more micro-analytical molecular understanding of the reaction mechanisms an electrochemical study would need to be combined with experimental data from a molecular biology and metabolomics. This study does however provide a macro-analytical understanding of overall changes in thermodynamics of Au^{3+}, Co^{2+} and Fe^{2+} electronation and electrodeposition in aqueous effluents of low pH upon electrified G10 graphite electrodes. Our results show significant positive shifts in the gold electrodeposition revisable potentials with reduction in Gibbs free energy and savings in energy.

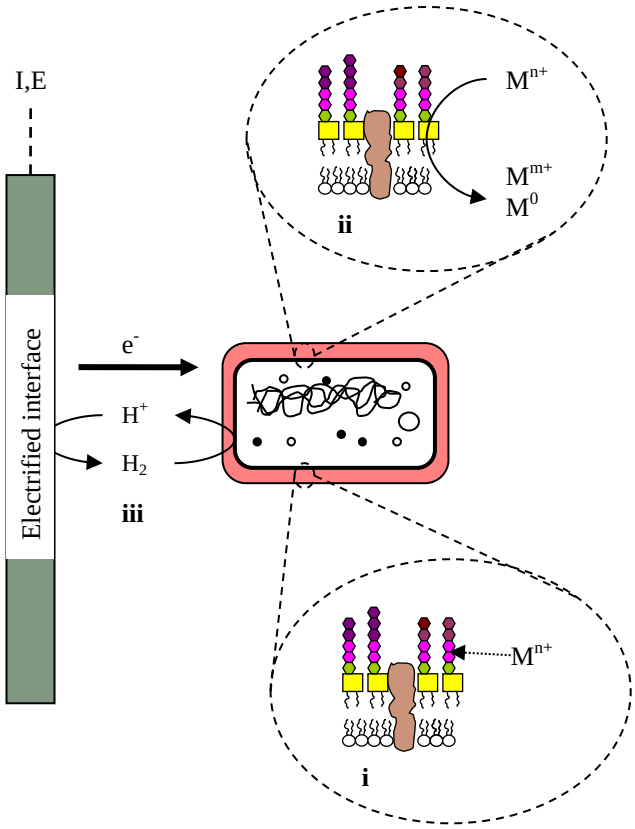

(i) Biosorption
The biosorption of metal ions has been shown to be a fast and thermodynamically a favourable reaction

(ii) Bio -reduction
Microbiological reduction of metal ions is confirmed for gold and cobalt ions. Further investigation is required in the value and recovery of biogenetic nanoparticles in the growing field of nanotechnology

(iii) In-situ electron donor
The "concept" of applying carbon substrates as electron donors to respiring heterogeneous (grown as biofilm on electrode) and homogeneous (dissolved in solution) bacterial cells have been formulated here for inorganic waste water treatment. Further experimentation is required for engineering operating conditions and design of bioelectrochemical reactor for such a purpose

Figure 5.1 : Microbiological remediation summary.

`

The key step forward would be the evaluation of bacterial growth and sustenance upon charged electrode substrates (applied as dissimilative electron donors) with the simultaneous electrodeposition and biosorption of metal ions.

Further modelling and comparison with empirical experimentation of such process would be useful but complicated with a multitude of reactions occurring for given electrolyte pH, conductivity, agitation and composition. A basic strategy outlined by eq^{n} 5.1 – 5.3, electrodeposition of metal ion "C_i" would be a function of applied current (or potential) and initial reacting species concentrations, eq^{n} 5.1. Bacterial biosorption is a function of initial metal ion concentrations, eq^{n} 5.2, and bacterial concentrations based upon bacterial respiration by electron donors C_d (such as the electrode or electrochemical hydrogen evolution) and electron acceptors C_a (such as oxygen or metal ions) described by eq^{n} 5.3. A structured model of dual-limitation kinetics as developed by Bae and Rittmann (Bae and Rittmann 1996) may be applicable. Also the toxic effects of metal ions on microbial viability must also be taken into account as discussed in chapter 3.

$$\frac{dc_i}{dt} = f(I, C_{i,0}) \qquad (5.1)$$

$$\frac{dq_i}{dt} = f\left(\frac{dX}{dt}, C_{i,o}\right) \qquad (5.2)$$

$$\frac{dX}{dt} = f(C_a, C_d) \qquad (5.3)$$

Economical and practical judgement upon application of such a system would be based upon time, power and practical usage and maintenance of specific electroactive bacterial communities.

Our results show up to 36% reduction in the Gibbs free energy requirements for gold metal electrodeposition which could lead to a reduction in power requirements and cost. This with the simultaneous biosorption and bioreduction of gold anions described in chapter 3 with up to 60% removal efficiency from un-buffered solutions of pH 3 and the production of biogenic nanoparticles by *Shewanella putrefaciens*.

`

The technology for the remediation and recovery of metal ions from low concentration to acceptable standards is burdened by high costs and inefficiencies in these systems due largely to mass transfer issues and side reactions such as hydrogen evolution. Where the two processes are employed in sequence, we conclude would be a cost effective green alternative. Here, electrochemical remediation of effluents carried out to acceptable concentrations for live bacteria cells to further purify the water to acceptable regulatory discharge standards in a separate biosorption unit.

The green chemistry application of inorganic waste water as raw materials for biogenic nanoparticle fabrication and metal recycling is of significant value especially if the process is able to hold to the green chemistry ethos. A possible design of such a bioelectrochemical systems could use three dimensional electrodes, where high surface area per unit volume is required as would be the case for dilute metal ion contaminated effluents below 500 ppm (Walsh and F 2001).

A summary of bioelectrochemical remediation summaries is given in Figure 5.2.

`

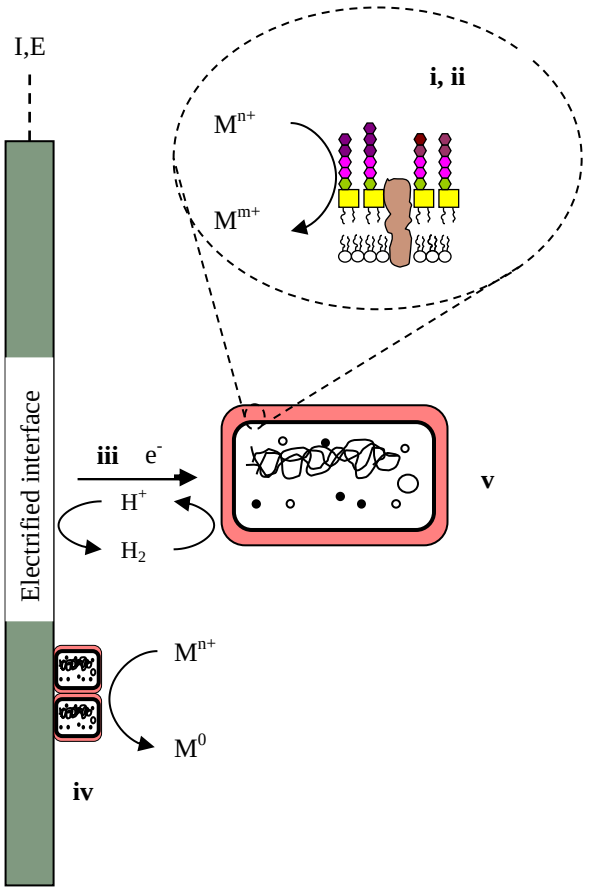

(i) Enhanced remediation
We would hypothesize the enhanced metal ion remediation of metal ions could by the simultaneous (and symbiotic) biosorption and bio-reduction of metal ions by electroactive gram negative bacteria and simultaneous electrodeposition of metal ions. Further experimental investigation would be consequential and further bio-electrochemical reactor engineering operation and design and efficiency

(ii) Reduction in energy requirements of metal ion electronation
The addition of bacterial cells has shown to reduce energy requirements for iron (Fe^{3+}/Fe^{2+}) and gold (Au^{3+}/Au) reduction with possible savings in power and cost

Figure 5.2 : Bioelectrochemical remediation summaries.

5.2. Further work

A review of the previous investigations biosorbtion and bioelectroremediation of metal ions, findings of preliminary electrochemical, microbiological and bioelectrochemical experimentation of inorganic wastewater has been given. Bioelectrochemical experimentation is by no way comprehensive but proved fruitful for further investigation of concepts, ideas and hypothesises which would be of scientific and engineering merit and of some subservient contribution and value in reducing the polluting affliction of inorganic waste water effluents upon the beautiful planet we inhabit.

To add to the conclusion formed with concurrent questions asked in reply giving a bearing for future investigation. Alternative explorations are described further in relation to green nanoparticle fabrication, innovative microbial fuel cells designs,

`

further analysis of bacterial effects upon electronation reaction mechanisms and kinetics and bio-electronucleation phenomena.

5.2.1. Biogenic nanoparticle production

Microbiology offers a greener route to the production of nanoparticles of growing interest due to their unusual and exotic optical, chemical and photochemical and electronic properties (Mandal, Bolander et al. 2006). Most techniques are capital intensive, inefficient in energy and material, require the usage of organic and inorganic toxic chemicals and extremities of temperature and pressure (Lloyd, Byrne et al. 2011). Microbiology could provide inspiration to a greener (cleaner, non-toxic, environmentally benign) process. Biogenic gold nanoparticles are produced (see Figure 5.3) by the live and deactivated bacterial strain *Shewanella putrefaciens* in accord with previous reports in the growing academic scientific community (Suresh, Pelletier et al. 2011). The elucidation of biochemical pathways of metal ion reduction would be imperative in the rational development of nanoparticle synthesis. Our experimentation has shown biotic and abiotic fabrication of nanoparticles in un-buffered aqueous solutions of low pH.

There is growing interest also in bio-nanofabrication for application in a variety of areas (Wen-Tso 2006). Precious metal ions such as platinum $PtCl_6^{2-}$ (Konishi, Ohno et al. 2007) and palladium Pd^{2+} (Windt, Aelterman et al. 2005) have been singled out, with numerous catalytic applications such as the dehalogenation reduction and dehydrogenation reactions for the treatment of soils and ground water (Hennebel, De Gusseme et al. 2009). Biogenic magnetic iron contains nano-crystals first discovered by Blackmore (Blakemore 1975) in 1975, with demonstrated applications as biosensors (Blakemore 1975). The biosynthesis of silver nanoparticles by various Ag-resistance bacteria (Slawson, Van Dyke et al. 1992; Klaus-Joerger, Joerger et al. 2001; Zhang, Li et al. 2005) and fungi (Mukherjee, Ahmad et al. 2001; Ahmad, Senapati et al. 2003) has also been studied recently with particular consideration to their applications as an antimicrobial agent (De Gusseme, Sintubin et al. 2010).

`

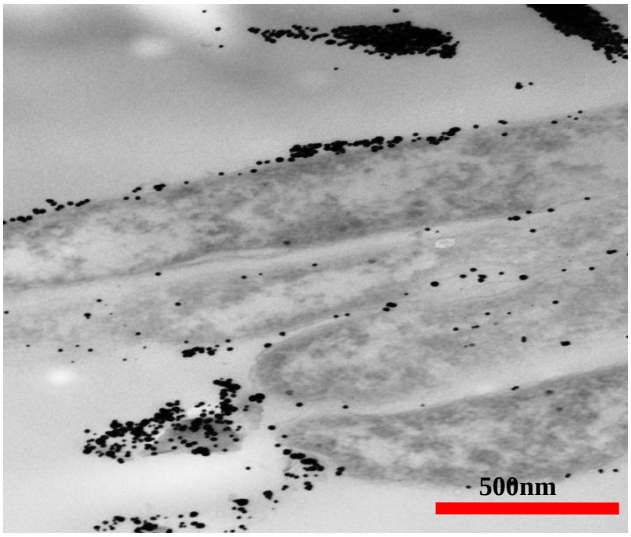

Figure 5.3 : Biogenic gold nanoparticles formation from solutions of 1 mM $HAuCl_4$ containing 10 ml of $1x10^{10}$ CFU/ml *Shewanella putrefaciens*.

A change in focus of a product driven process for the fabrication of biogenic particles brings a new perception in the application of bioelectrochemical systems, as of yet unexplored, especially for the in-situ respiration of cells using electrified carbon substrates. The selection of the best microbial candidate for a specified biogenic product of characteristic dimensions and composition would be the key starting point for the optimization of operating conditions (such as pH, ionic strength, mixing speed of solution, inoculum size), in relation to microbial growth and microbial redox transformation building upon the growing scientific foundations of our knowledge of participating enzymes and biochemical components located within the cell and upon the surface of the cell membrane (bio-charge transfer) interface. The harvesting of biogenic nanoparticles would also require consideration depending upon location (extra or intracellular precipitated nanoparticles), where physicochemical treatments or enzymatic lyses could be applied.

5.2.2. Innovative microbial fuel cell for inorganic waste water treatment

A logical and innovative progression would be the combination of cathodic bio-electrochemical metal ion remediation and recovery with anodic organic waste water oxidation, where the anodic bio-oxidation process would provide the electron supply to the cathode. The application of a MFC to drive a cathodic BER process has been

`

demonstrated by Clauwaert et al. (Clauwaert, Rabaey et al. 2007) in regard to nitrification processes. The application of metal ion reduction with metal ions such as Fe^{3+} and MnO_2 mediators in the electron transport terminal oxygen electron acceptor has also been demonstrated (ter Heijne, Hamelers et al. 2006). The concept of bioelectrochemical reactors has been advocated here for the remediation of dilute metal-ion contaminated effluents. As verified by chapter 3, the biosorption of metal ions by electroactive dissimilative bacteria is a fast process with possible recovery of the biogenetic metal nanoparticles produced. Also the reduced energy requirements for electrodeposition with the application of bacterial cells as part of bioremediation strategies of metal ions has been proven for gold and iron systems in chapter 4. Novel electrode materials and (macro/micro/nano) topographies (see Figure 5.4) would also be an interesting area of investigation.

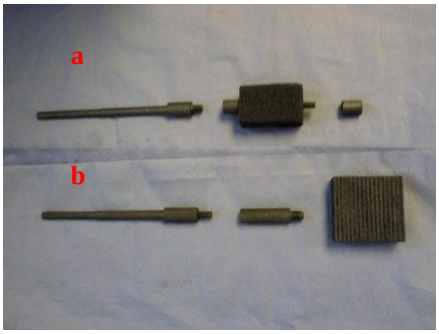

Figure 5.4 : (a) Porous graphite electrodes such RVC could be an excellent electrode substrate in bioelectrochemical systems, (b) graphite electrodes with ridged surfaces could further support bacterial biofilm growth.

This investigation was unable to evaluate metal remediation in microbial fuel cells systems with anodic oxidation and remediation of organic material but we would recommend such an investigation.

5.2.3. Investigation in changes in electronation reaction mechanisms and bio-electrocatalysis of electron transfer reactions by bacterial cells

The experimentation was only able to evaluate changes electronation thermodynamics in “real” systems containing no buffer and un-degassed. A worthwhile scientific continuance of this research would be to study changes in reaction mechanisms in “ideal” systems where pH is controlled and effects of dissolved oxygen and various ions

`

is taken into account. Reaction mechanisms of various electronation leading to electrodeposition of metal ions can be found in chapter 2. Also the Butler Volmer equation gives valuable information in regards to reaction kinetics of electronation reactions in the presence of bacterial cells with possible application of bacteria as bio-electocatalysisyts.

Eq^{n} 2.58 describes the general description of the Butler-Volmer equation which is valid for a multistep overall electrodiotic reaction in which there may be more electron transfers other than the rate determining step illustrated in Figure 5.5 (Bockris and Reddy 1970; Bockris and Nagy 1973).

$$i = i_o\left[\exp\left[\frac{\alpha_a F\eta}{RT}\right] - \exp\left[\frac{-\alpha_c F\eta}{RT}\right]\right] \qquad (2.58)$$

Eq^{n} 2.59 – 2.60 described the relation between the symmetry factor and transfer coefficient where the rate determining step (RDS) reaction occurs υ times as part of the overall reaction involving $\vec{\gamma}$ reaction steps preceding and $\overleftarrow{\gamma}$ steps preceding the RDS. With "*N*" reaction steps in the overall reaction mechanism and "*r*" electrons transferred in the rate determining step.

$$a_c = \frac{\overleftarrow{\gamma}}{v} + r\beta \qquad (2.59)$$

$$a_a = \frac{N - \vec{\gamma}}{v} + r\beta \qquad (2.60)$$

The Tafel plot of η vs. Log(i) described by eq^{n} 2.62 from slow scan linear sweep voltammetry can also be used to describe small deviations (the low potential field approximation) from equilibrium potentials (typically 0.050 V < $|\eta|$ < 0.100 V) for catholic and anodic reactions and be used for elocution of the Tafel Slope related to charge transfer mechanisms.

$$Log(|-i|) = Log(i_0) - \frac{\eta}{\lambda} \qquad (2.62)$$

`

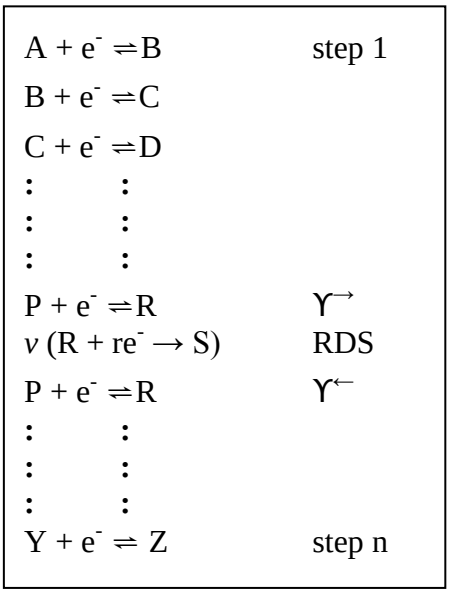

Figure 5.5 : Multi-step electron transfer reaction.

The gradient of the Tafel plot therefore can be used as analytical tool for evaluation of the rate determining step for a given charge transfer reaction occurring in the inner Helmholtz layer of our electrified interface. For example, the mechanisms of gold electrodeposition can summarized in Table 5.1, which involves three steps in the overall reaction (Harrison and Thompson 1973) and would give Tafel slope of 120, 60 or 25 depending upon which reaction step is rate limiting. Changes in the gradient of Tafel slope would therefore give some indication of bacterial influence upon metal ion electronation reaction mechanism.

	RDS			Gold ($AuCl_4^-$) electrodeposition	Reference
	1	2	3		
γ	0	1	2	$MCl_3^- \rightarrow MCl_{3(ads)}$	*(Harrison and Thompson 1973)*
r	0	2	1	$MCl_{3(ads)} + 2e^- \rightarrow MCl_{(ads)} + 2Cl^-$	
ν	1	1	1		
α	0.5	1	2.5	$MCl_{(ads)} + e^- \rightarrow M + Cl^-$	
∂Log lil / $\partial\eta$	120	60	25		

Table 5.1 : Butler-Volmer parameters estimated for electrodeposition by 3 electron transfer to gold metal cations in chloride electrolytes.

`

The Butler Volmer equation is based on the Arrhenius equation where the rate constant for the cathodic or anodic current described by eq^{n} 5.4 and eq^{n} 5.5. Where $\Delta G_c^{0\#}$ is the Gibbs free energy of activation, h is the Planck Constant, k_B is the Bolzmann constant.

The exchange current density i_0 (A/cm^2) is a key parameter in the evaluation of catalytic reactions occurring at an electrified interface and key to the evaluation of the kinetic enhancements by initially electroactive bacterial solutions. Eq^{n} 5.6 gives definition of i_0 which can be further simplified to eq^{n} 5.7.

$$\vec{k} = \frac{k_B T}{h}\left[\exp\frac{-\Delta\vec{G}_e^{0\#}}{RT}\right] \tag{5.4}$$

$$\overleftarrow{k} = \frac{k_B T}{h}\left[\exp\frac{-\Delta\overleftarrow{G}_e^{0\#}}{RT}\right] \tag{5.5}$$

$$\frac{k_B T}{h} FC_R\left[\exp\frac{-\Delta\overleftarrow{G}_e^{0\#}}{RT}\right]\left[\exp\frac{\alpha_a F\Delta\varphi_e}{RT}\right] = i_o = \frac{k_B T}{h} FC_R\left[\exp\frac{-\Delta\vec{G}_e^{0\#}}{RT}\right]\left[\exp\frac{-\alpha_c F\Delta\varphi_e}{RT}\right] \tag{5.6}$$

$$F\overleftarrow{k}C_R\left[\exp\frac{-\beta F\Delta\varphi_e}{RT}\right] = i_o = F\vec{k}C_o\left[\exp\frac{-\beta F\Delta\varphi_e}{RT}\right] \tag{5.7}$$

Extensive electrochemical investigation of iron electrodeposition using Tafel analysis has been described by Bockris et al. (Bockris, Drazic et al. 1961). Their experimentation investigate the rate of disposition and dissolution of iron for systems of varying Fe^{2+} concentration, pH and presence of a range on anions, with elocution of reaction mechanisms and associated rate determining steps. This would be an exciting scientific basis for further understanding the bacterial cells and bacterial artefacts influence upon electronation reaction of metal ions and further engineering of bioelectrochemical systems.

`

5.2.4. Bio-electro-nucleation

Further investigation upon bacterial influence upon nucleation processes would also be of scientific interest and possible technological potential where bacteria dissolved or attached to electrode may influence metal nucleation mechanisms.

The mechanism of electronucleation and growth can be determined from the analysis of time current transients accomplished by the application of a step potential from open circuit potentials. There are several detailed descriptions of the potentiostatic current transients during three-dimensional nucleation for diffusion control based on investigations by Hills, Schiffrin and Thompson (Hills, Schiffrin et al. 1974). Theoretical models described by Scharifker (Scharifker and Mostany 1984) have been effectively applied to gold electrocrystallization from a thiosulphate-sulfite electrolyte as reported by Sorbi and Roy (Sobri and Roy 2005). Three-dimensional nucleation under diffusion control can be determined from experimentally measured current transients and reduced to a dimensionless form by plotting I^2/I^2_m versus $(t/t_m)^2$, where I_m and t_m relate to minimum current and time measurements from the chronoamperometric polarisations. The mechanism of nucleation can be determined by comparing experimental and theoretical plots of instantaneous mechanisms described by eq^n 5.8 or progressive mechanisms described by eq^n 5.9.

$$\frac{I^2}{I_m^2} = \frac{1.9542}{t/t_m}\left[1-\exp\left(-1.2564(t/t_m)\right)\right]^2 \qquad (5.8)$$

$$\frac{I^2}{I_m^2} = \frac{1.2254}{t/t_m}\left[1-\exp\left(-2.3367(t/t_m)^2\right)\right]^2 \qquad (5.9)$$

`

5.3. General Conclusions on Hypotheses'

Hypothesis 1*: Electroactive microorganisms have novel application in the remediation and recycling of toxic and precious metals ions from aqueous effluent streams.*

We would conclude they do, illustrated with microbial biosorption and bioreduction reactions as part of green chemistry philosophy for the remediation of metal ion contaminated waste waters and recovery of valuable biogenic by-products.

Hypothesis 2*: An enhancement of contaminated remediation processes can be achieved by the alliance of electrochemical and microbiological phenomena*

A number of symbiotic strategies has been conceptualised, building upon fundamental investigation discussed here upon changes in electronation thermodyanmics, we would state that there is huge scope for the application of bioelectrochemical systems for metal contaminated waste water treatment.

`

5.4. And finally…

This thesis gives an amalgamation of bio-electrochemical phenomena in relation to metal ion remediation strategies formed upon foundations of electrochemical electronation reactions at an electrified interface with metal ionic species located in proximity of the Helmholtz inner layer; and microbiological biosorption and bio-reduction of metal ions as part of dissimilatory and redox resistance mechanisms. The future seems bright for the collaboration of these bio-physical-chemical process in bioelectrochemical systems for the remediation and recovery of precious and toxic metal ions from aqueous effluents of low pH and low metal ion concentration.

The key concept here is the interplay of bacterial cells which respire upon electrified carbon substrates as electron donors by direct and indirect mechanisms. These bacterial cells are thus employed as bio-sorbents and possible bio-nano-factories for the recovery of high value metallic bio-genetic-particles. Bacterial cells in this study have also been shown to reduce energy requirements for the respective gold electrodeposition and electroremediation processes. We were unable to evaluate simultaneous bioelectrocatalysis of heterogeneous electrodeposition reactions although further investigation is warranted with the Shewanella genus and alternative species and strains active in acidic mine waters (Johnson and Hallberg 2003).

Furthermore in light of the monumental advances at present in the genetic engineering of bacterial cells to express required phenotypes, it is possible to (a) customise nature in the over-expression of the consortia of protein enzymes, electron-mediators and nanowires reviewed in this thesis and implicated in the direct or indirect electron transfer with solid conducting electrode interfaces and electron transfer and/or bioaccumulation of metal ionic species, and (b) surface engineer cell surface properties and architecture, therefore armouring cells to biosorb metal ions (Kuroda and Ueda 2011) and allow growth in electrolytes of low pH containing toxic ionic species.

`

References

*Ahmad, A., S. Senapati, et al. (2003). "Extracellular Biosynthesis of Monodisperse Gold Nanoparticles by a Novel Extremophilic Actinomycete, Thermomonospora sp." Langmuir **19**(8): 3550-3553.*

*Bae, W. and B. E. Rittmann (1996). "A structured model of dual-limitation kinetics." Biotechnology and Bioengineering **49**(6): 683-689.*

*Blakemore, R. (1975). "Magnetotactic bacteria." Science **190**(4212): 377-379.*

*Bockris, J. O. M., D. Drazic, et al. (1961). "The electrode kinetics of the deposition and dissolution of iron." Electrochimica Acta **4**(2–4): 325-361.*

*Bockris, J. O. M. and Z. Nagy (1973). "Symmetry factor and transfer coefficient. A source of confusion in electrode kinetics." Journal of Chemical Education **50**(12): 839.*

Bockris, J. O. M. and A. K. N. Reddy (1970). Modern electrochemistry : an introduction to an interdisciplinary research. New York, Plenum Press.

*Clauwaert, P., K. Rabaey, et al. (2007). "Biological Denitrification in Microbial Fuel Cells." Environmental Science & Technology **41**(9): 3354-3360.*

*De Gusseme, B., L. Sintubin, et al. (2010). "Biogenic Silver for Disinfection of Water Contaminated with Viruses." Applied and Environmental Microbiology **76**(4): 1082-1087.*

*Harrison, J. A. and J. Thompson (1973). "The reduction of the aquachloro complexes of rhodium." Journal of Electroanalytical Chemistry and Interfacial Electrochemistry **43**(3): 405-413.*

*Hennebel, T., B. De Gusseme, et al. (2009). "Biogenic metals in advanced water treatment." Trends in Biotechnology **27**(2): 90-98.*

*Hills, G. J., D. J. Schiffrin, et al. (1974). "Electrochemical nucleation from molten salts—I. Diffusion controlled electrodeposition of silver from alkali molten nitrates." Electrochimica Acta **19**(11): 657-670.*

*Johnson, D. B. and K. B. Hallberg (2003). "The microbiology of acidic mine waters." Research in Microbiology **154**(7): 466-473.*

*Klaus-Joerger, T., R. Joerger, et al. (2001). "Bacteria as workers in the living factory: metal-accumulating bacteria and their potential for materials science." Trends in Biotechnology **19**(1): 15-20.*

*Konishi, Y., K. Ohno, et al. (2007). "Bioreductive deposition of platinum nanoparticles on the bacterium Shewanella algae." Journal of Biotechnology **128**(3): 648-653.*

*Kuroda, K. and M. Ueda (2011). "Molecular design of the microbial cell surface toward the recovery of metal ions." Current Opinion in Biotechnology **22**(3): 427-433.*

`

*Lloyd, J. R., J. M. Byrne, et al. (2011). "Biotechnological synthesis of functional nanomaterials." Current Opinion in Biotechnology **22**(4): 509-515.*

*Mandal, D., M. Bolander, et al. (2006). "The use of microorganisms for the formation of metal nanoparticles and their application." Applied Microbiology and Biotechnology **69**(5): 485-492.*

*Mukherjee, P., A. Ahmad, et al. (2001). "Fungus-Mediated Synthesis of Silver Nanoparticles and Their Immobilization in the Mycelial Matrix: A Novel Biological Approach to Nanoparticle Synthesis." Nano Lett **1**(10): 515-519.*

*Scharifker, B. R. and J. Mostany (1984). "Three-dimensional nucleation with diffusion controlled growth: Part I. Number density of active sites and nucleation rates per site." Journal of Electroanalytical Chemistry and Interfacial Electrochemistry **177**(1–2): 13-23.*

*Slawson, R. M., M. I. Van Dyke, et al. (1992). "Germanium and silver resistance, accumulation, and toxicity in microorganisms." Plasmid **27**(1): 72-79.*

*Sobri, S. and S. Roy (2005). "Gold Electrocrystallization from a Spent Thiosulfate-Sulfite Electrolyte." Journal of the Electrochemical Society **152**(9): C593-C599.*

*Suresh, A. K., D. A. Pelletier, et al. (2011). "Biofabrication of discrete spherical gold nanoparticles using the metal-reducing bacterium Shewanella oneidensis." Acta Biomaterialia **7**(5): 2148-2152.*

*ter Heijne, A., H. V. M. Hamelers, et al. (2006). "A Bipolar Membrane Combined with Ferric Iron Reduction as an Efficient Cathode System in Microbial Fuel Cells†." Environmental Science & Technology **40**(17): 5200-5205.*

Walsh and C. F (2001). Electrochemical technology for environmental treatment and clean energy conversion. Research Triangle Park, NC, ETATS-UNIS, Pure and applied chemistry.

*Wen-Tso, L. (2006). "Nanoparticles and their biological and environmental applications." J Biosci Bioeng **102**(1): 1-7.*

*Windt, W. D., P. Aelterman, et al. (2005). "Bioreductive deposition of palladium (0) nanoparticles on Shewanella oneidensis with catalytic activity towards reductive dechlorination of polychlorinated biphenyls." Environmental Microbiology **7**(3): 314-325.*

*Zhang, H., Q. Li, et al. (2005). "Biosorption and bioreduction of diamine silver complex by Corynebacterium." Journal of Chemical Technology & Biotechnology **80**(3): 285-290.*

Appendix A2

Appendix A2.1: Gibbs free energy

Work (*W*): Transfer of energy which achieves/utilizes uniform motion to the surrounding.
Heat (*Q*): Transfer of energy which achieves/utilizes disorderly motion to the surrounding.
Gibb Energy (*G*): The maximum amount of non-expansive work that can be extracted from the system undergoing a change at constant temperature and pressure. Can also be defined as the total change in entropy of the system at constant temperature.
Internal Energy (*U*): Sum of all the kinetic and potential contributions to the energy of all the atoms, ions, and molecules in the system.
Enthalpy (*H*): Measure of heat at constant pressure.
Entropy (*S*): Measure of disorder.

The second law of thermodynamics (Atkins 2001) states that the entropy of the universe tends to increase and a spontaneous reaction would be one where the total entropy of a process increases where the total entropy is defined by eq^{n} A2.1 which takes into account the system and surrounding entropy. For a process which occurs at constant pressure (*P*) and temperature (*T*) the total change in entropy of the surroundings can be described by eq^{n} A2.2, substitution into eq^{n} A2.3 and rearrangement give us our definition of the change in Gibbs free energy of our system eq^{n} A2.4.

Gibbs free energy therefore gives us a method to describe the total change of the entropy of the system and its surroundings at constant pressure and temperature and a measure of spontaneity of the reactions. Where a decrease in Gibbs free energy (and increase in total entropy) would occur for a thermodynamically spontaneous reaction as illustrated by Figures A2.1 and A2.2 and vice versa for an un-spontaneous reactions with corresponding decrease in the total entropy of the system and surrounding and increase in Gibbs free energy.

$$\Delta S_{total} = \Delta S + \Delta S_{sur} \qquad \text{(A2.1)}$$

$$\Delta S_{sur} = \frac{(q)_{rev}}{T} = -\frac{\Delta H}{T} \qquad \text{(A2.2)}$$

$$\Delta S_{total} = \Delta S - \frac{\Delta H}{T} \qquad \text{(A2.3)}$$

$$\Delta G = -T\Delta S_{total} = \Delta H - T\Delta S \qquad \text{(A2.4)}$$

Gibbs free energy not only gives a qualification of the spontaneous nature of a reaction but also a quantitative measure of the maximum amount of non-expansive work (any work arising from the non-expansion of the system) that can extracted from a spontaneous system or non-expansive work which would be required to drive the process in a system.

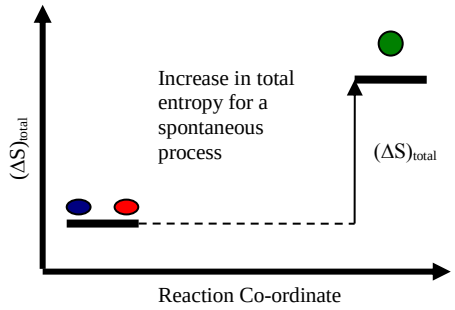

Figure A2.1: Change in entropy for a spontaneous reactions.

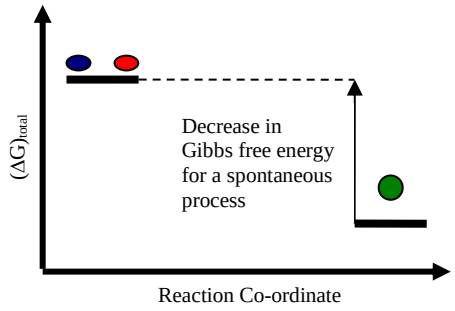

Figure A2.2: Change in entropy for a spontaneous reactions.

From eq^{n} A2.4 substitution of eq^{n} A2.5 for enthalpy (ΔH) change at constant pressure and change in internal (ΔU) energy eq^{n} A2.6 gives us the expression described by eq^{n} A2.7. Further substitution of our definitions of heat and work, where *w'* is defined as non-expansive work and $p_{ex}\Delta V$ expansive work and rearrangements leads to expression eq^{n} A2.10 which is valid for processes taking place at constant temperature and pressure.

$$\Delta H = \Delta U + p\Delta V \quad \text{(A2.5)}$$

$$\Delta U = q + w \quad \text{(A2.6)}$$

$$\Delta G = q + w + p\Delta V - T\Delta S \quad \text{(A2.7)}$$

$$q = T\Delta S \quad \text{(A2.8)}$$

$$w = w' - p_{ex}\Delta V \quad \text{(A2.9)}$$

$$\Delta G = q + w' - p_{ex}\Delta V + p\Delta V - T\Delta S \quad \text{(A2.10)}$$

For a revisable process eq^{n} A2.35 can be further simplified with expressions for heat transfer for a reversible process q_{rev} is defined by eq^{n} A2.8 and setting p_{ex} to p as justified for a reversible expansion process leads to eq^{n} A2.10, where cancelling of the 1st, 3rd, 4th and 5th terms gives us our derivation of the *w'* eq^{n} A2.11. The non-expansive work done during a reversible reaction is the maximum amount of non-expansive work such as electrical work in electrochemical cells or the synthesis of ATP from ADP for microbial respiration.

$$\Delta G = T\Delta S + w' - p\Delta V + p\Delta V - T\Delta S \quad \text{(A2.11)}$$

$$\Delta G = w' \quad \text{(A2.12)}$$

Appendix A2.2: Sorption isotherms

The sobrtion metal ion uptake can described by eq[n] A2.38 where :

$$q = (C_o - C_t)\frac{V}{M_c} \qquad \text{(A2.13)}$$

Langmuir Isotherm (Langmuir 1918) first described by Langmuir in 1918 who considered adsorbion as a chemical phenomenon and although does not shed light on mechanistic aspects of the adsorption, does give information on the maximum adsorption capabilities such as q_{max}, based on the following assumptions:

- sorption is redistricted to the monolayer
- there is a fixed number of adsorption sites
- all adsorption sites are uniform
- there is no interaction between sorbed species

The adsorption of *M* by a adsorbent *S* forming *MS* can be described by eq[n] A2.14, with respective equation for the rate of adsorption and desorption described by eq[n] A2.15 and A2.16, with the overall rate of adsorbed r described by eq[n] A2.17.

$$M + S = MS \qquad \text{(A2.14)}$$

$$r_A = k_A[M][S] \qquad \text{(A2.15)}$$

$$r_{-A} = k_{-A}[MS] \qquad \text{(A2.16)}$$

$$r = k_A[M][S] - k_{-A}[MS] \qquad \text{(A2.17)}$$

Rearrangement of eq[n] A2.17 leads to eq[n] A2.18 gives an expression for the equilibrium constant *K*.

$$\frac{k_A}{k_{-A}} = \frac{[MS]}{[M][S]} = K \qquad \text{(A2.18)}$$

Substitution of S_t described by eq^n A2.19 into eq^n A2.20 which expresses the total number of sorption sites.

$$[S_t] = [S] + [MS] \tag{A2.19}$$

$$K[S_t] - K[MS] = \frac{[MS]}{[M]} \tag{A2.20}$$

Rearrangement of which, leads to the Langmuir isotherm eq^n A2.21 equivalent to eq^n A2.22 – A2.23 where S_t (or q_{max}) represents the maximum number of sorption sites and b (or K) is an expression for the equilibrium constant and related to reaction thermodynamics.

$$[MS] = \frac{S_t K[M]}{1 + K[M]} \tag{A2.21}$$

$$q_e = \frac{q_{\max} b[C_e]}{1 + b[C_e]} \tag{A2.22}$$

$$\frac{1}{q_e} = \frac{1}{q_{\max}} + \frac{1}{(q_{\max} b)C_e} \tag{A2.23}$$

The Freudlich Isotherm described by eq^n A2.24 and A2.25 has been historically presented as an empirical equation with limited ability in interpretation of the Freudlich constants K_F and n although some attempts have been made in derivation of the Freundlich adsorption isotherm frovm kinetics by Skopp (Skopp 2009).

$$q_e = K_F (C_e)^{1/n} \tag{A2.24}$$

$$Ln(q_e) = Ln(K_F) + \frac{1}{n} Ln(C_e) \tag{A2.25}$$

Appendix A2.3: Biosorption kinetics

The amount of metal ions sorbed q can be defined by eq^{n} A2.26 where C_o is the initial concentration of metal ions, C_t is the concentration at time t, V is the volume of the electrolyte

$$q = (C_o - C_t)\frac{V}{M_c} \tag{A2.26}$$

The pseudo-first order model of Lagergren can be described by eq^{n} A2.27. Integration and rearrangement of this for the boundary conditions $t = 0$, $q_t = q_0$ and $t = t$, $q = q_t$ leads to a form of the Langergan equation described by eq^{n} A2.29.

$$\frac{dq_t}{dt} = k_1(q_e - q_t) \tag{A2.27}$$

$$\int_{q_{0(t=0)}}^{q_f\,(t=t_f)} \frac{1}{(q_e - q_t)} dq_t = k_1 \int_{t=o}^{t=t} dt \tag{A2.28}$$

$$Log(q_e - q_t) = Log(q_e) - \frac{k_1}{2.303} t \tag{A2.29}$$

The pseudo-second order model described by eq^{n} A2.30, separation of variables and integration of eq^{n} A2.31 with the boundary conditions $t = 0$, $q_t = q_0$ and $t = t$, $q = q_t$ leads to eq^{n} A2.32 where the initial rate v_0 can be described by eq^{n} A2.33.

$$\frac{dq_t}{dt} = k_2(q_e - q_t)^2 \tag{A2.30}$$

$$\int_{q_{0(t=0)}}^{q_f\,(t=t_f)} \frac{1}{(q_e - q_t)^2} dq_t = k_1 \int_{t=o}^{t=t_f} dt \tag{A2.31}$$

$$\frac{t}{q_t} = \frac{1}{q_e} + \frac{1}{q_e^2 k_2 t} \tag{A2.32}$$

$$v_o = k q_e^2 \tag{A2.33}$$

The inter-particular diffusion model of Weber and Morris can be described by eq^{n} A2.34. taking logarithm of gives eq^{n} A2.35.

$$q_t = k_{id} t^{0.5} \quad \text{(A2.34)}$$

$$Log(q_t) = Log(k_{id}) + 0.5 Log(t) \quad \text{(A2.35)}$$

Appendix A2.4: Microbiological diffusion processes

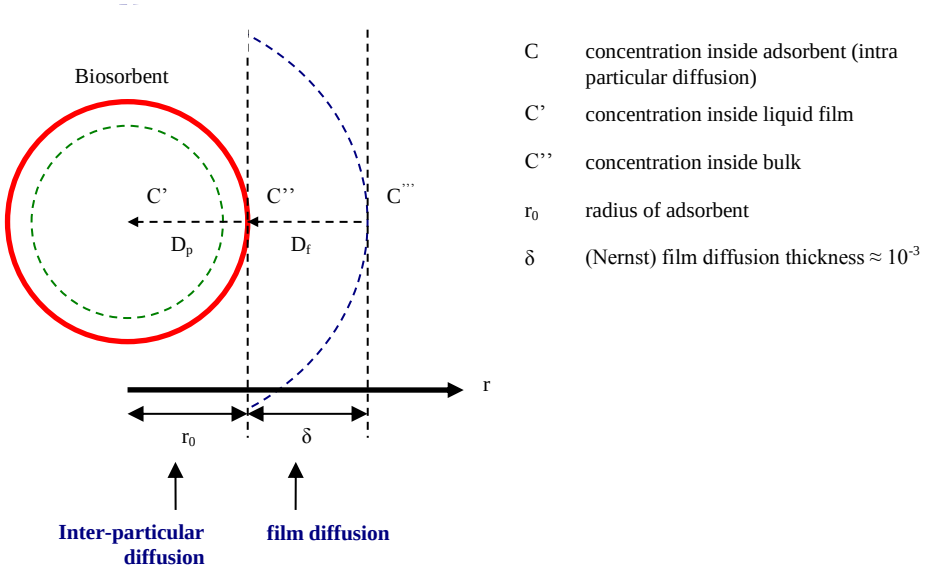

Figure A2.3: Modelling of bacterial biosorption interface.

Biological models for film and particular diffusion are based upon the assumption that adsorbents are specifical and adapted and replicated from deviations given by Helfferich (Helfferich 1995) and Cranks (Crank 1975).

As observed in TEM imagery (described in chapter 3) bacterial cells are rod shaped. A crude approximation was made that on a macro level bacterial cells can be treated as spherical. From average measure of bacterial cell dimensions of length (*l*) 1.833 µm x width (*w*) 0.422 µm. An average volume can be determined as 0.242 μm^3 using eq^n A2.36. An approximate value of r_0 can be calculated for our crude approximation using eq^n A2.37, an expression for the volume of a sphere.

$$V_b = [(w^2 \times \frac{\pi}{4})(l - w) + (\pi \times \frac{w^6}{6})] \quad \text{(A2.36)}$$

$$V_s = \frac{4}{3}\pi r_o^3 \quad \text{(A2.37)}$$

Inter particular rate limitation

Diffusion processes can usually be described by Flicks 1st and 2nd law of diffusion (eqn A2.38 – A2.39). This mathematical theory of diffusion was defined by Crack, as given in his text The Mathematic of Diffusion (Crank 1975) as :

> "…based upon the hypnosis that the rate of mass transfer of diffusing substance through unit area of a section is proportional to the concentration gradient measured normal to the section."

$$J_A = -D_p \, grad C_A' \tag{A2.38}$$

$$div J_A = -\frac{\partial C_A'}{dt} \tag{A2.39}$$

Inter particular rate limitation can be described eqn A2.40 for systems with spherical geometry with a constant diffusion coefficient. Eqn A2.40 can be solved with the initial and boundary conditions given in Table A2.1.

$$\frac{\partial C_{A'}}{dt} = D_p \left[\frac{\partial^2 C_{A'}}{dr^2} - \frac{2}{r} \frac{\partial C_{A'}}{dr} \right] \tag{A2.40}$$

Initial condition
$r > r_0,\ t = 0,\ C_A'(t) = 0$
$0 \le r \le r_0,\ t = 0,\ C'(t) = C_A'$

Boundary condition:
$r > r_0,\ t > 0,\ C_A'(t) = 0$

Table A2.1: Initial and boundary conditions for eqn A2.40.

The infinite boundary condition applied here which assumes that for a particle diffusion limited rate the concentration *C''* at the bead surface is the same as the bulk which implies negligible resistance across the film/adsorbent interphase.

Application of the Laplace transform to eq^{n} A2.40 and application of the initial and boundary conditions leads to eq^{n} A2.41, where *U(t)* is an expression for the fractional attainment of equilibrium and depends on the magnitude of $D_p t/r_0$

$$U(t) = 1 - \frac{6}{\pi^2} \sum_{n=1}^{\infty} \frac{1}{n^2} \left[- \frac{D_p t \pi^2}{r_0^2} \right] \quad \text{(A2.41)}$$

$$U(t) = \frac{m'^{0}_{A} - m'_{A}(t)}{m'^{0}_{A} - m'^{\infty}_{A}} \quad \text{(A2.42)}$$

$$U(t) = 1 - \frac{m'_{A}(t)}{m'^{0}_{A}} \quad \text{(A2.43)}$$

Application of the Vermeulen approximation (Vermeulen 1953) to eq^{n} A2.43 leads to eq^{n} A2.44. The substitution of the half life $t_{1/2}$ for which *U(t)* = 0.5 leads to eq^{n} A2.45 and eq^{n} A2.46, a relation for the particle diffusion coefficient.

$$U(t) = \left(1 - \exp \frac{D_p \pi^2 t^{1/2}}{r_0^2} \right) \quad \text{(A2.44)}$$

$$t^{1/2} = 0.030 \left[\frac{r_p^2}{D_p} \right] \quad \text{(A2.45)}$$

$$D_p = 0.03 \left[\frac{R_p^2}{t^{1/2}} \right] \quad \text{(A2.46)}$$

Film diffusion limitation

Film diffusion rate limitation rate laws can be derived based on the following assumptions:

- Bio-sorbents are spherical and uniform in size
- Inter-diffusion can be assumed quasi-stationary
- One dimensional diffusion

A rate can be derived upon the above assumptions and the quasi-stationary flux can be derived from eq^{n} A2.38 described by eq^{n} A2.47 leading to eq^{n} A2.48 from the material balance of the reaction. The equilibrium condition at the interface can be described by eq^{n} A2.49. Combination of eq^{n} A2.47 and eq^{n} A2.48 gives eq^{n} A2.50.

$$J_A = D_f \frac{C_A^{''} - C_A^{'''}}{\delta} = D_f \frac{\Delta C_A}{\delta} \qquad \text{(A2.47)}$$

$$-\frac{dm_i^{'}}{dt} = AJ_A \qquad \text{(A2.48)}$$

$$\frac{C_A^{'}}{C_A^{''}} = \frac{C^{'}}{C^{'''}} \qquad \text{(A2.49)}$$

$$-\frac{dC_A^{''}}{dt} = \frac{3}{r_0}\frac{C^{'''}}{C^{'}} J_A \qquad \text{(A2.50)}$$

Eq^{n} A2.50 can be solved once again with application of Laplace transform and the initial and boundary conditions given in Table A2.2. The initial condition corresponding to uniform initial concentration C_i' in the adsorbent and none in the solution. The boundary condition based on the infinite boundary condition. The solution of eq^{n} A2.51 leads to eq^{n} A2.52.

Initial condition
$r = r_0,\ t = 0,\ C^{''} = \frac{C_A^{'0} C^{'''}}{C^{'}}$
$r \geq r_0 + \delta,\ t = 0,\ C_i(r) = 0$
Boundary condition : Infinite solution volume
$r > r_0 + \delta,\ t > 0,\ C_A'''(r,t) = 0$

Table A2.2: Initial and boundary conditions for eq^{n} A2.69.

Where *U(t)* is shown to depend only on the magnitude of $DCt/r_0\delta C'$. The substitution of the half life $t_{1/2}$ for which *U(t)* = 0.5 leads to eq^n A2.106, a relation for the particle diffusion coefficient.

$$U(t) = 1 - \exp\left(-\frac{3D_f t\pi^2 C_A^{'''}}{r_0 \delta\, C_A^{'}} \right) \tag{A2.51}$$

$$D_f = 0.230\left[\frac{r_o\, \zeta}{t^{1/2}} \frac{q_e}{C_0} \right] \tag{A2.52}$$

Webster Morris adsorption model

It is possible to deduce an average diffusion coefficient from the initial gradient of the sorption curve when plotted against the square route time as (Crank 1975) described by equation A2.53 and equivalent to the Webber Morris model for absorption A2.54.

$$\frac{q_t}{q_\infty} = 12\left[\frac{Dt}{\pi\, d_p^{\,2}} \right]^{1/2} \tag{A2.53}$$

$$q_t = k_{id} t^{1/2} \tag{A2.54}$$

Eq^n A2.54 is based upon the diffusion of species in a spear and is based on the deviation by Cranks (Crank 1975).

Substitution of *u* described by eq^n A2.55 leads equation eq^n A2.56.

$$u = C_A r_0 \tag{A2.55}$$

$$\frac{\partial u}{dt} = D\left[\frac{\partial^2 u}{dr^2} \right] \tag{A2.56}$$

Solution of eq^n A2.56 for the given initial and boundary conditions summarised in Table A2.3 leads to eq^n A2.57. Where C_1 is the constant concentration at the surface of the sphere and the initial concentration C_0.

The concentration at the centre is given by the limit as $r \rightarrow 0$, leading to eq^{n} A2.58, with the total amount of diffusing substance entering or leaving the spear is given by eq^{n} A2.59 and the corresponding solution for small times described by eq^{n} A2.60 and eq^{n} A2.61.

Upon which it is possible to deduce the average diffusion coefficient from the initial gradient of the sorption curve when plotted against $t^{1/2}$. Equation A2.61 for the initial stages of adsorption can be approximated by eq^{n} A2.62, equivalent to the Webber Morris eq^{n} A2.54.

Initial condition
$t = 0, 0 < r < r_0, u = rf(f)$

Boundary condition : Infinite solution volume
$t > 0, r = 0, u = 0$
$t > 0, r = r_0, u = r_0 C_1$

Table A2.3: Initial and boundary conditions for eq^{n} A2.111.

$$\frac{C-C_0}{C_1-C_0} = 1 - \frac{2r_0}{\pi r}\sum_{n=1}^{\infty}\frac{(-1)^n}{n} Sin\left(\frac{n\pi r}{r_0}\right)\exp\left(\frac{-Dn^2\pi^2 t}{r_0^2}\right) \qquad \text{(A2.57)}$$

$$\frac{C-C_0}{C_1-C_0} = 1 - 2\sum_{n=1}^{\infty}\frac{(-1)^n}{n}\exp\left(\frac{-Dn^2\pi^2 t}{r_0^2}\right) \qquad \text{(A2.58)}$$

$$\frac{M_t}{M_\infty} = 1 - \frac{6}{\pi^2}\sum_{n=1}^{\infty}\frac{1}{n}\exp\left(\frac{-Dn^2\pi^2 t}{r_0^2}\right) \qquad \text{(A2.59)}$$

$$\frac{C-C_1}{C_0-C_1} = \frac{r_0}{r}\sum_{n=1}^{\infty}\left(erfc\,\frac{(2n+1)}{2(Dt)^{1/2}} - erfc\,\frac{(2n+1)a+r}{2(Dt)^{1/2}}\right) \qquad \text{(A2.60)}$$

$$\frac{M_t}{M_\infty} = 6\left(\frac{Dt}{r_0^2}\right)^{1/2}\left(\pi^{(-1/2)} + 2\sum_{n=1}^{\infty} ierfc\left(\frac{na}{2(Dt)^{1/2}}\right)\right) - \frac{3Dt}{r_0^2} \qquad \text{(A2.61)}$$

$$\frac{M_t}{M_\infty} = 12\left(\frac{Dt}{\pi r_0^2}\right)^{1/2} \qquad \text{(A2.62)}$$

Appendix A2.5: The ferrozine assay

The determination of soluble Fe^{3+} and Fe^{2+} ions in solution before and after exposure to bacterial cells was determined using the ferrozine (3-(2-Pyridyl)-5,6-diphenyl-1,2,4-triazine-p,p′-disulfonic acid monosodium salt hydrate) reagent (see Figure A2.4) as chelating agent (Vermeulen 1953; Stookey 1970; Dawson and Lyle 1990; Riemer, Hoepken et al. 2004) .

The assay involves the ferric to ferrous reduction step using hydroxylamine hydrochloride as a reducing agent in a HEPES buffer followed by reacting with ferrozine to form a stable, intensively magenta coloured species. The intensity can be quantified using UV adsorption spectroscopy and calibrated to ionic iron concentrations of 1- 50 ppm.

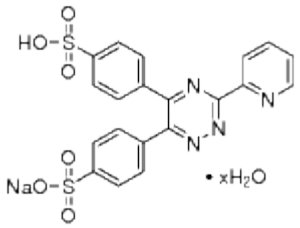

Figure A2.4 : Chemical formulae of ferrozine reagent.

All solutions where prepared from distilled water using 0.05% wt/wt ferrozine (M_r = 492.47 g/mol, Sigma-Aldrich $C_{20}H_{13}N_4NaO_6S_2 \cdot xH_2O$,) prepared in 50 mM HEPES (M_r = 238.30, Sigma-Aldrich 4-(2-Hydroxyethyl)piperazine-1-ethanesulfonic acid, N-(2-Hydroxyethyl)piperazine-N′-(2-ethanesulfonic acid)) buffer. The ferric ion was reduced using a saturated solution of hydroxylamine hydrochloride (M_r = 69.49 g/mol, Sigma-Aldrich $H_2NOH.HCl$).

Simples where taken from microbiological samples, filtered with 0.2 µm filter paper and diluted x 4 with distilled water. 0.1 ml of this was mixed by vortex with 0.1 ml of hydroxylamine/HCl in 1.5 ml eppendorf cup and incubated for 30 minutes for the ferric to ferrous iron reduction step. 20 µm of this solution was transferred to a new eppendorf cup containing 200 µm ferrozine/HEPES solution. 1 ml of distilled water added to the eppendorf and the resulting solution mixed by vortex and transferred to 1.5 UV curvets

and ultra-violet adsorption at 562 nm measured. Before each experiment of iron biosorption assays, a calibration was conduced using Fe^{3+} (M_r = 241.86, 1000 mg/L in 0.5 M HNO_3 SpectrosoL solutions VWR) standards of 50 ppm, 25 ppm, 5 ppm and 1 ppm.

Figure A2.5 and Figure A2.6 illustrate example calibrations of A_{562nm} with iron standard solutions.

Figure A2.5 : Calibration assay for Fe^{3+} using the ferrozine assay.

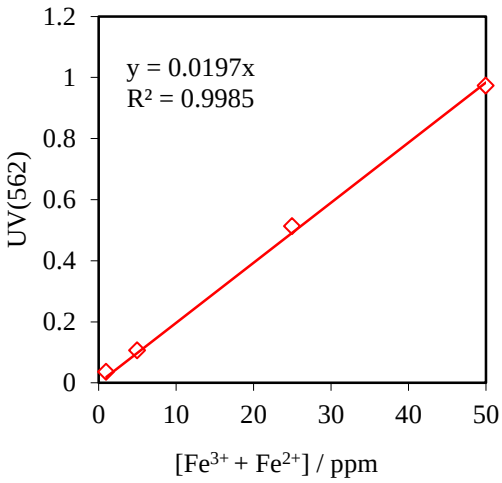

Figure A2.6: Calibration graph correlating Fe^{3+}.

References

Atkins, P. W. (2001). The elements of physical chemistry : with applications in biology. New York, W.H. Freeman.

Crank, J. (1975). The mathematics of diffusion. Oxford, Eng, Clarendon Press.

*Dawson, M. V. and S. J. Lyle (1990). "Spectrophotometric determination of iron and cobalt with Ferrozine and dithizone." Talanta **37**(12): 1189-1191.*

Helfferich, F. G. (1995). Ion exchange, Dover Publications.

*Langmuir, I. (1918). "THE ADSORPTION OF GASES ON PLANE SURFACES OF GLASS, MICA AND PLATINUM." Journal of the American Chemical Society **40**(9): 1361-1403.*

*Riemer, J., H. H. Hoepken, et al. (2004). "Colorimetric ferrozine-based assay for the quantitation of iron in cultured cells." Analytical Biochemistry **331**(2): 370-375.*

*Skopp, J. (2009). "Derivation of the Freundlich Adsorption Isotherm from Kinetics." Journal of Chemical Education **86**(11): 1341.*

*Stookey, L. L. (1970). "Ferrozine---a new spectrophotometric reagent for iron." Analytical Chemistry **42**(7): 779-781.*

*Vermeulen, T. (1953). "Theory for Irreversible and Constant-Pattern Solid Diffusion." Industrial & Engineering Chemistry **45**(8): 1664-1670.*

Appendix A3

Appendix 3.1 : TEM procedure

Figure A4.1 and A4.2 gives a pectoral representation of sample preparation protocol for TEM analysis as described in chapter 3.

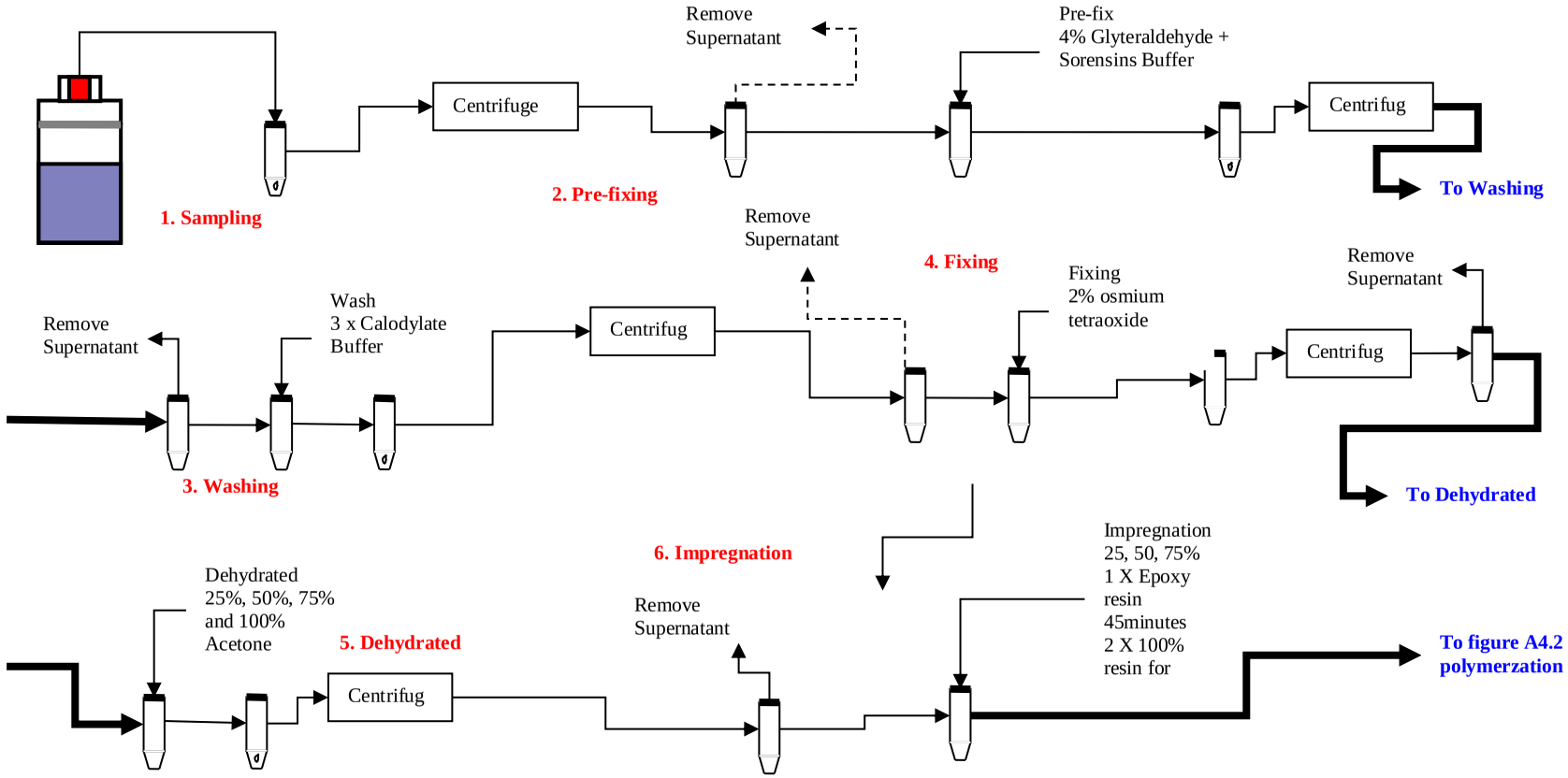

Figure A3.1 : Procedure for TEM sample processing preparation.

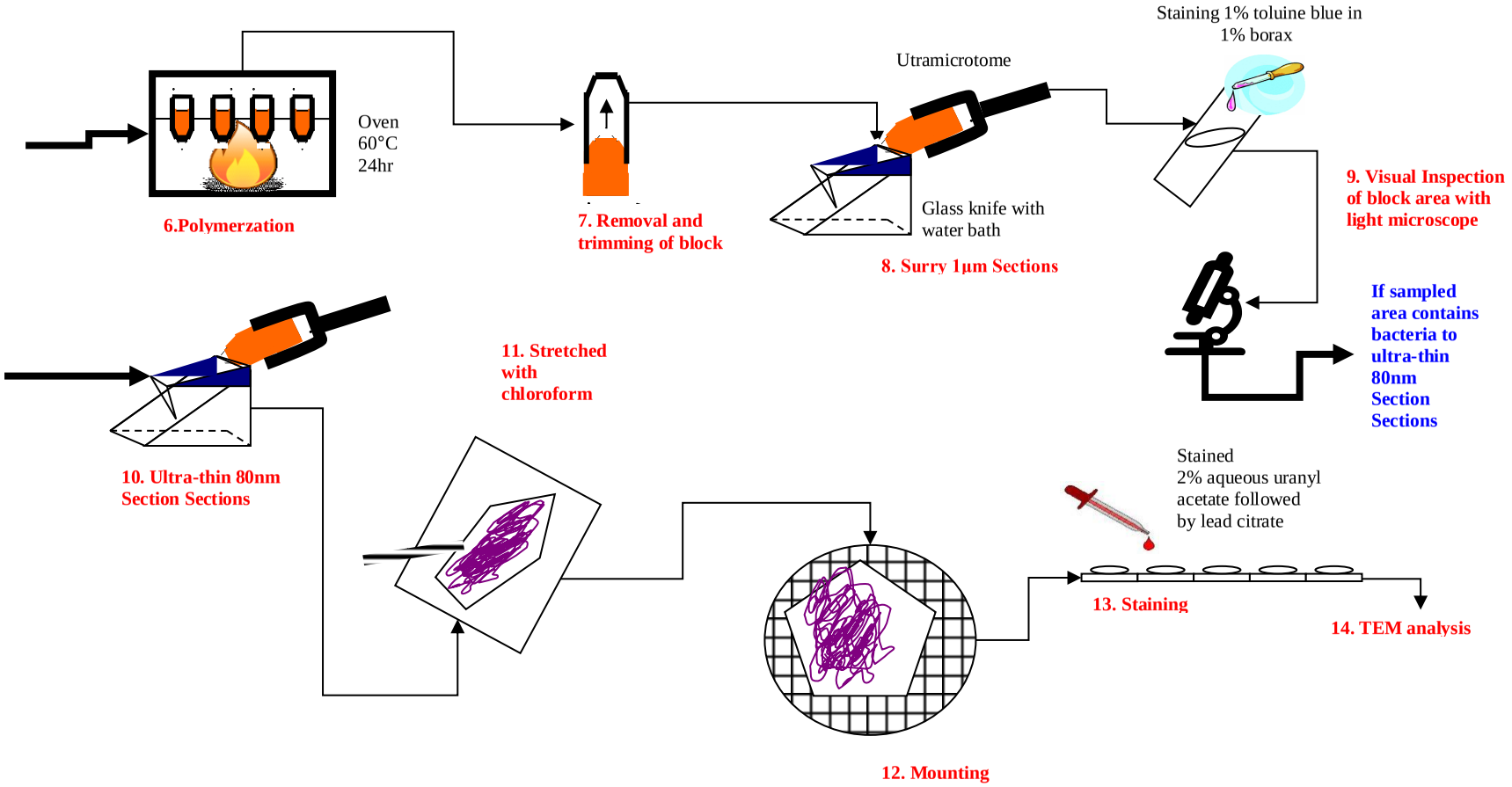

Figure A3.2 : Procedure for TEM sample processing preparation (continued from A4.1).